ADSORPTION OF HEAVY METAL IONS AND DYES FROM AQUEOUS SOLUTIONS BY USING LAPLAP PURPUREUS (DOLICHOS BEAN) STEM POWDER AS BIOSORBENT

A thesis submitted to

BHARATHIDASAN UNIVERSITY

for the award of the degree of

DOCTOR OF PHILOSOPHY

IN

CHEMISTRY

By

G. BHARATHIDASAN,

(Ref.No. 29337/PhD.K2/Chemistry/Part-Time/October 2016)

Under the guidance of

Dr. N. Mani, M.Sc., Ph.D.,

Assistant Professor



P.G AND RESEARCH DEPARTMENT OF CHEMISTRY

A.V.V.M. SRI PUSHPAM COLLEGE (Autonomous)

(Affiliated to Bharathidasan University)

POONDI-613 503, THANJAVUR DISTRICT TAMILNADU, INDIA

MARCH 2022



PG and Research Department of Chemistry, A.V.V.M. Sri Pushpam College (Autonomous), (Affiliated to Bharathidasan University, Tiruchirappali.), Poondi-613503, Thanjavur-District, Tamilnadu, INDIA.

.....

Dr.N. MANI, M.Sc., Ph.D.,

Date:

Assistant Professor

CERTIFICATE

This is to certify that the thesis entitled ADSORPTION OF HEAVY METAL IONS AND DYES FROM AQUEOUS SOLUTIONS BY USING LAPLAP PURPUREUS (DOLICHOS BEAN) STEM POWDER AS BIOSORBENT submitted to Bharathidasan University, Tiruchirappalli, for the award of the degree of DOCTOR OF PHILOSOPHY IN CHEMISTRY, embodies the result of the bonafide research work carried out by G. BHARATHIDASAN, under my guidance and supervision in the P.G and Research Department of Chemistry, A. Veeriya Vandayar Memorial Sri Pushpam College (Autonomous), Poondi, Thanjavur District, Tamil Nadu, India.

I further certify that no part of the thesis has been submitted anywhere else for the award of any degree, diploma, associateship, fellowship or other similar titles to any candidate.

Research Advisor

DECLARATION

I do hereby declare that this work has been originally carried out by me under the

supervision of Dr. N. MANI, Assistant Professor, Department of Chemistry, A Veeriya

Vandayar Memorial Sri Pushpam College (Autonomous), Poondi, Thanjavur district,

Tamil Nadu, Affiliated to Bharathidasan University, Tiruchirapalli - 620 024 and this

work has not been submitted elsewhere for any other degree.

Place: Poondi, 613 503.

(G. BHARATHIDASAN)

Research Scholar

Date:



PG and Research Department of Chemistry, A.V.V.M Sri Pushpam College (Autonomous), Poondi – 613 503. Thanjavur District. Tamilnadu, India

CERTIFICATE OF PLAGIARISM CHECK

1	Name of the Research Scholar	G. BHARATHIDASAN
2	Course of Study	Ph.D., CHEMISTRY
3	Title of the Thesis	ADSORPTION OF HEAVY METAL IONS AND
		DYES FROM AQUEOUS SOLUTIONS BY
		USING LAPLAP PURPUREUS (DOLICHOS
		BEAN) STEM POWDER AS BIOSORBENT
4	Name of the Research	Dr. N. MANI
	Supervisor	
5	Department / Institution /	PG and Research Department of Chemistry,
	Research Centre	A.V.V.M Sri Pushpam College (Autonomous),
		Poondi – 613503 Thanjavur District.
		Tamilnadu, India
6	Acceptable Maximum Limit	20%
7	Percentage of similarity of	9%
	Content identified	
8	Software Used	Urkund
9	Date of Verification	09.03.2022

Report on plagiarism check item with % of similarity attached

Signature of the Research Supervisor

Signature of the Candidate

Curiginal

Document Information

Analyzed document All Chapters (G. Bharathidasan).docx (D129848838)

Submitted 2022-03-09T11:31:00.0000000

Submitted by Srinivasa ragavan S
Submitter email bdulib@gmail.com

Similarity 9%

Analysis address bdulib.bdu@analysis.urkund.com

Sources included in the report

Sour	ces included in the report		
w	URL: https://cyberleninka.org/article/n/373030 Fetched: 2020-06-03T12:02:52.5030000	88	6
w	URL: https://vlab.amrita.edu/?brch=190&cnt=1∼=606⊂=2 Fetched: 2021-10-30T11:53:42.8430000	88	2
w	URL: http://www.ijaema.com/gallery/170-ijaema-may-3958.pdf Fetched: 2022-03-09T11:32:18.1170000	88	84
w	URL: https://pennstate.pure.elsevier.com/en/publications/removal-of-perchlorate-by-synthetic-organosilicas-and-organoclay-Fetched: 2022-03-09T11:33:41.3030000	88	1
w	URL: https://www.deswater.com/DWT_articles/vol_192_papers/192_2020_271.pdf Fetched: 2022-03-09T11:32:53.8330000	88	8
w	URL: https://iwaponline.com/jwrd/article/9/3/249/66946/Comparative-study-of-the-adsorption-capacity-of Fetched: 2019-11-02T09:51:03.7300000	88	1
w	URL: http://ijghc.com/download_frontend.php?id=393&table=Green%20Chemistry Fetched: 2022-03-09T11:32:24.2100000	88	45
w	URL: https://www.oatext.com/pdf/FNN-2-112.pdf Fetched: 2020-07-23T19:47:28.9270000	88	8
W	URL: https://1library.net/document/q06jo09q-removal-hexavalent-chromium-aqueous-low-cost-adsorbent-aavns.html Fetched: 2020-07-12T08:43:25.4170000	88	2
w	URL: https://www.scirp.org/html/10-9401317_5741.htm Fetched: 2021-11-29T13:12:42.0530000	88	3
w	URL: https://slidetodoc.com/3-rd-international-colloquium-energy-and-environmental-protection/Fetched: 2022-03-09T11:33:12.0930000	88	1
w	URL: http://tailieu.tv/tai-lieu/isotherms-thermodynamics-and-kinetics-of-rhodamine-b-dye-adsorption-on-natural-diato-pham-dinh-du-42886/ Fetched: 2022-03-09T11:33:08:3570000	88	5

ACKNOWLEDGEMENTS

I am extremely grateful and indebted to Professor Dr. N. Mani, M.Sc., Ph.D., Assistant Professor, Department of Chemistry, A Veeriya Vandayar Memorial Sri Pushpam College (Autonomous), Poondi, for his valuable guidance to me and his excellent supervision, co-ordination and continuous encouragement throughout the study period.

I express my sincere thanks to (late) Sriman K. Thulasiah Vandayar, Former Secretary and Correspondent, A Veeriya Vandayar Memorial Sri Pushpam College (Autonomous) Poondi, Thanjavur, for giving me the golden opportunity to undertake the Ph,D programme in the College of excellence.

I express my sincere thanks to President and Secretary & Correspondent for their support to fulfil the Ph.D. Programme.

I am very grateful to Dr.R.Sivakumar, Principal, A.V.V.M. Sri Pushpam College (Autonomous), Poondi, Thanjavur, for his permission to use the laboratory facilities.

I would like to thank to Dr.S.Kumaravel, Dean of Science, A.V.V.M. Sri Pushpam College (Autonomous), Poondi, Thanjavur, for his permission to use the laboratory facilities.

I wish to express my thanks to Doctoral Committee Members Dr. S. Raja Mohamed, Associate Professor (Retd), Khadir Mohideen College, Adirampattinam, Thanjavur Dt, Dr. G.Vishnuvardhanaraj, Assistant Professor, A.V.V.M. Sri Pushpam College (Autonomous), Poondi, Thanjavur, Dr. C.Pragathiswaran, Assistant Professor, Dept. of Chemistry, Periyar EVR College, Tiruchirappalli, for their enthusiastic encouragement in bringing out this thesis in a successful manner.

I thank most sincerely Dr. V. Nandhakumar, Associate Professor and Co-ordinator, Department of Chemistry, A.V.V.M. Sri Pushpam College (Autonomous), Poondi, Thanjavur, for his help and keen interest.

I am also thankful to Dr. N. Nagarajan, Associate Professor of Ancient Science, Tamil University, Thanjavur, Dr. G.Sakthivel SASTRA University, Thanjavur, Dr.D.Tamilvendan, Manager in QC, Indian Oil Corporation Ltd Salem Laboratory, for their timely support.

I am very much thankful to all the staff and non-teaching staff members, Department of Chemistry, A.V.V.M. Sri Pushpam College (Autonomous), Poondi, for their timely help and valuable support.

I like to thank all my fellow research scholars, under the guidance of my supervisor for their help then and there. I thank to Dr. K. Mohamed Faisal and Dr.K.Ramesh for their continuous support throughout my research work.

I express my heartfelt thanks to my parents Mr.P. Ganesan and Shrimathi.G.Parvathi, my wife P. Rajeshwari and my dear Children B.Tamilmozhi, B.Tamilvizhi and B.Amithran, my brother G. Parthasarathy and family, my sister G.Banumathi Loganathan all family members and friends M.Muruganantham, VAO, Dr.G.Pukalarasan, Dr.S.Saivaraj, Dr.A.Elavarasan who have raised my energy in toughest times.

Lastly, I offer my regards to many people who have helped me at various stages of my work then and there needed. This work would not be possible without their help.

CONTENTS

Chapter No	Content	Page No
1 INTRO	ODUCTION	
1.1	A description of the problem of water pollution	1
1.2	Industrial wastewater treatment	2
1.3	Necessity for removal of heavy metal ions and dyes from the	3
	environment	
1.4	The conventional technique for removal of heavy metal ions	4
	and dyes	
	1.4.1 Coagulation-flocculation	5
	1.4.2 Membrane separation	6
	1.4.3 Electrochemical Method	6
	1.4.4 Ion exchange	6
	1.4.5 Solvent extraction	7
1.5	Adsorption	8
	1.5.1 Physical adsorption	8
	1.5.2 Chemical adsorption	9
	1.5.3 Biosorption	10
	1.5.4 Mechanism of Biosorption	11
1.6	Various Adsorbent onto Adsorption Studies	11
	1.6.1 Creature Adsorbent	12
	1.6.2 Soil Adsorbent	12
	1.6.3 Ash Adsorbent	12
	1.6.4 Lignin Adsorbent	13
	1.6.5 Activated carbon	13
1.7	Heavy metal ions and dyes	14
	1.7.1 Copper	14
	1.7.2 Chromium	15
	1.7.3 Nickel	17
	1.7.4 Bismark Brown R	18

		1.7.5 Malachite Green	19
		1.7.6 Methyl Orange	20
II	OBJE	CCTIVES AND SCOPE OF THE PRESENT WORK	21
III	REVI	EW OF LITERATURE	25
	3.1	Adsorption of heavy metal ions by Biomaterials	25
	3.2	Adsorption of dyes by Biomaterials	36
IV	MAT	ERIALS AND METHODS	
	4.1	Experimental Method	47
		4.1.1 Pant collection	47
		4.1.2 Plant Details	47
		4.1.3 Preparation of Laplap pupureus Stem Powder (LPSP)	48
		as an adsorbent	
		4.1.4 Preparation of Copper [Cu (II) ion] solution	48
		4.1.5 Preparation of Chromium [Cr (VI) ion] solution	48
		4.1.6 Preparation of Nickel [Ni (II) ion] solution	48
		4.1.7 Preparation of Bismark Brown R Dye Solution	49
		4.1.8 Preparation of Malachite Green Dye Solution	49
		4.1.9 Preparation of Methyl Orange Dye Solution	49
	4.2	Sorption Studies	49
		4.2.1 Batch experiment method	49
	4.3	Adsorption Isotherms	51
		4.3.1. Langmuir isotherm model	51
		4.3.2. Freundlich Isotherm	52
	4.4	Adsorption Kinetics	52
		4.4.1 The Pseudo first-order model	53
		4.4.2 The Pseudo second-order model	54
	4.5.	Thermodynamic parameters	55
\mathbf{V}		RESULTS AND DISCUSSION	
	5.1	REMOVAL OF COPPER (II) IONS FROM AQUEOUS	57
		SOLUTION USING LPSP	
		5.1.1 Effect of pH on adsorption of copper (II) ions	57
		5.1.2 Effect of biosorbent dosage on adsorption of copper(II)	58
		ions	

	5.1.3 Effect of contact time on adsorption of Copper (II) ions	58
	5.1.4 Effect of Initial Concentration for Copper (II) ions on	59
	adsorption	
	5.1.5. Adsorption Isotherms	59
	5.1.5.1. Langmuir isotherm model	59
	5.1.5.2. Freundlich Isotherm	60
	5.1.6. Adsorption Kinetics	61
	5.1.6.1 The Pseudo first-order model	61
	5.1.6.2 The Pseudo second-order model	62
	5.1.7. Thermodynamic parameters	62
	5.1.8. FTIR Spectrum of LPSP before and after adsorption	63
	of Cu (II) metal ions	
	5.1.9. X-Ray Diffraction of LPSP before and after	63
	adsorption of Cu (II) metal ions	
	5.1.10. SEM Analysis for Copper (II) Ions on Adsorption	64
5.2	Removal Of Chromium (Vi) Ions From Aqueous Solution	77
	Using LPSP	
	5.2.1 Effects of pH on Chromium (VI) ion adsorption	77
	5.2.2 Effects of LPSP dose on Chromium (VI) ions	77
	Adsorption	
	5.2.3 Effects of taction time on Chromium (VI) ions	78
	adsorption	
	5.2.4 Effects of various Concentrations on Chromium (VI)	78
	ions adsorption	
	5.2.5 Effects of temperature on Chromium (VI) ions	79
	adsorption	
	5.2.6 Adsorption Isotherm Models	79
	5.2.6.1. Langmuir isotherm model	80
	5.2.6.2 Freundlich Isotherm	81
	5.2.7 Kinetic Study	82
	5.2.7.1. The Pseudo first-order model	82
	5.2.7.2. The Pseudo second-order model	83
	5.2.8 Thermodynamic parameters	84

	5.2.9. FT-IR spectrum of LPSP before and after adsorption	85
	of Cr (VI) metal ions	
	5.2.10. X-Ray Diffraction of LPSP before and after adsorption	85
	of Cr (VI) metal ions	
	5.2.11. SEM Analysis for LPSP before and after adsorption	86
	of Cr (VI) metal ions	
5.3.	Removal of Nickel (II) Ions From Aqueous Solution Using	100
	5.3.1 Effect of pH for Nickel (II) ions on adsorption	100
	5.3.2 Effect of Biosorbent dosage for Nickel (II) ions on	101
	Adsorption	
	5.3.3 Effect of contact time for Nickel (II) ions on adsorption	101
	5.3.4 Effect of Initial Concentration for Nickel (II) ions on	102
	adsorption	
	5.3.5 Adsorption Isotherm Models	102
	5.3.5.1. Langmuir isotherm model	103
	5.3.5.2 Freundlich Isotherm	104
	5.3.6 Kinetic Study	105
	5.3.6.1. The Pseudo first-order model	105
	5.3.6.2. The Pseudo second-order model	105
	5.3.7. Thermodynamic parameters	106
	5.3.8. FTIR Spectrum for LPSP on before and after	107
	adsorption of Ni (II) metal ions	
	5.3.9 X-Ray Diffraction analysis for LPSP on before and	108
	after adsorption of Ni (II) metal ions	
	5.3.10 SEM Analysis for LPSP on before and after	108
	adsorption of Ni (II) metal ions	
5.4	Removal of Bismark Brown R dye from aqueous solution	121
	using LPSP	
	5.4.1 Effect of pH for BBR dye from aqueous solution onto	121
	adsorption using LPSP	
	5.4.2 Effect of biosorbent dose for BBR dye from aqueous	122
	solution onto adsorption using LPSP	
		122

	5.4.3 Effect of contact time for BBR dye from aqueous	
	solution onto adsorption using LPSP	123
	5.4.4 Effect of Initial concentration for BBR dye from	
	aqueous solution onto adsorption using LPSP	124
	5.4.5 Adsorption Isotherm Studies	124
	5.4.5.1. Langmuir Isotherm	125
	5.4.5.2. Freundlich Isotherm	125
	5.4.6 Kinetics Studies	125
	5.4.6.1. Pseudo First order	126
	5.4.6.2. Pseudo Second order	126
	5.4.5 FT-IR spectra of Laplap purpureus stems powder	
	after BBR dye adsorption	127
	5.4.6 XRD Analysis for LPSP adsorbent before and after	
	BBR dye on adsorption	127
	5.4.7. Scanning Electron Microscope Analysis for BBR dye	
	on LPSP before and after adsorption	
5.5	Adsorption of Malachite Green dye on Laplap purpureus	138
	stems powder (LPSP)	
	5.5.1 Effect of pH on adsorption of Malachite Green dye	138
	5.5.2 Effect of Biosorbent (LPSP) dose on adsorption of	138
	Malachite Green dye	
	5.5.3 Effect of contact time for adsorption of Malachite	139
	Green dye	
	5.5.4 Effect of Initial concentration on adsorption of	139
	Malachite Green dye	
	5.5.5 Adsorption Isotherm	140
	5.5.5.1 Langmuir Isotherm	140
	5.5.5.2 Freundlich Isotherm	141
	5.5.6. Adsorption Kinetic Studies	141
	5.5.6.1 Pseudo First order	141
	5.5.6.2 Pseudo Second order	142
	5.5.7 FT-IR spectra of LPSP before and after adsorption of	
	MG dye	143

	LIST OF PUBLICATIONS	
	REFERENCES	
VI	SUMMARY AND CONCLUSIONS	169
	of methyl orange dye	
	5.6.9. SEM Analysis for LPSP before and after adsorption	159
	adsorption of methyl orange dye	
	5.6.8 XRD pattern analysis for LPSP before and after	158
	methyl orange dye	
	5.6.7 FT-IR spectra of LPSP before and after adsorption of	158
	5.6.6.2 Pseudo Second order	157
	5.6.6.1 Pseudo First order	157
	5.6.6. Adsorption Kinetic Studies	156
	5.6.5.2 Freundlich model of adsorption Isotherm	156
	5.6.5.1 Langmuir Isotherm	155
	5.6.5 Adsorption Isotherm	155
	dye onto adsorption using LPSP	
	5.6.4 Effect of Initial dye concentration for methyl orange	154
	adsorption using LPSP	
	5.6.3 Effect of contact time for methyl orange dye onto	154
	adsorption using LPSP	
	5.6.2 Effect of biosorbent dose for methyl orange dye onto	153
	using LPSP	
	5.6.1 Effect of pH for methyl Orange dye onto adsorption	153
	using LPSP	
5.6	Adsorption of Methyl Orange dye from aqueous solution	153
	before and after adsorption of MG dye	143
	5.5.8 Scanning Electron Microscope Analysis for LPSP	

LIST OF TABLES

Table	T:41.	Page
No	Title	No
4.1.	R _L Values and Types of Isotherm	51
5.1.1.	Effect of pH in Cu (II) ions adsorption, Time 50 min, Volume of Cu (II)	64
	solution 50 mL, Concentration of Cu (II) 150mg/L, Biosorbent Dose 200 mg	
	and Temperature 30°C.	
5.1.2	Effect of Biosorbent (LPSP) dose in Cu (II) ions adsorption, Time 50 min,	65
	pH 7, Volume of Cu (II) ions solution 50 mL, Concentration of Cu (II)	
	150mg/L and Temperature 30°C.	
5.1.3	Effect of Contact Time in Cu (II) ions adsorption, pH 7, Volume of	65
	Cu (II) solution 50 mL, Biosorbent Dose 200 mg, Concentration of	
	Cu (II) 150mg/L and Temperature 30°C.	
5.1.4	Effect of initial Concentration of Cu (II) ions in adsorption, pH 7,	66
	Volume of Cu (II) ions solution 50 mL, Biosorbent Dose 200 mg, Time	
	50 min and Temperature 30°C.	
5.1.5	Percentage of Cu (II) metal removal in various initial concentration on	66
	LPSP biosorbent	
5.1.6	Langmuir and Freundlich isotherm parameters for the adsorption of	67
	Cu (II) on <i>LPSP</i>	
5.1.7	Dimensionless Separation factor (R _L) for the adsorption of Cu (II) on	67
	LPSP	
5.1.8	Kinetics parameter for the adsorption of Cu (II) onto LPSP	68
5.1.9	Thermodynamic parameters for the adsorption of Cu (II) on LPSP	69
5.1.10	Comparative study of adsorbent capacity in Langmuir constant	69
	$q_{max} \ (mg/g)$ of various biosorbent for Copper (II) ions.	
5.2.1	Effects of pH for Chromium (VI) ion on adsorption, Time 50 min,	86
	Volume of Cr (VI) ions solution 50 mL, Concentration of Cr (VI)	
	150 mg/L, Biosorbent Dose 200 mg and Temperature 35°C.	
5.2.2	Effects of LPSP dose for Chromium (VI) ions on adsorption, Time	87
	50 min, pH 7, Volume of Cr (VI) ions solution 50 mL, Concentration	
	of Cr(VI) ions solution 150mg/L and Temperature 35°C.	

5.2.3	Effects of taction time for Chromium (VI) ions on adsorption,	87
	Biosorbent dose 200 mg, pH 7, Volume of Cr (VI) ions solution	<i>.</i>
	50 mL, Concentration of Cr (VI) ions solution 150mg/L and	
	Temperature 35°C.	
5.0.4	-	00
5.2.4	Effects of various Concentrations of Chromium (VI) ions on	88
	adsorption, Biosorbent dose 200 mg, Time 50 min, pH 7, Volume of	
	Cr (VI) ions solution 50 mL, and Temperature 35°C.	
5.2.5	Effects of various Temperature for Chromium (VI) ions on adsorption,	88
	Concentrations of Chromium (VI) ions solution 150 mg/L, Biosorbent	
	dose 200 mg, Time 50 min, pH 7, and Volume of Cr (VI) ions solution	
	50 mL.	
5.2.6	Percentage of Cr (VI) metal removal in various initial concentration on	89
	LPSP biosorbent	
5.2.7	Langmuir and Freundlich isotherm parameters for the adsorption of	89
0.2.7	Cr (VI) on LPSP	0)
5 2 0	` '	00
5.2.8	Dimensionless separation factor (RL) for the adsorption of Cr (VI) on	90
	LPSP	
5.2.9	Kinetic parameters for the adsorption of Cr (VI) ions on <i>LPSP</i>	90
5.2.10	Thermodynamic parameters for the adsorption of Cr (VI) ions on LPSP	91
5.2.11	Comparative study of adsorbent capacity for Cr (VI) metal ions on	91
	Langmuir constant q _{max} (mg/g) by various biosorbent.	
5.3.1	Effect of pH for Ni(II) ions on adsorption, Time 50 min, Volume of	109
	Ni(II) ions solution 50 mL, Concentration of Ni(II) 150mg/L,	
	Biosorbent Dose 200 mg and Temperature 30°C.	
5.3.2	Effect of Biosorbent (LPSP) dose for Ni(II) ions on adsorption, Time	109
	50 min, pH 7, Volume of Ni(II) ions solution 50 mL, Concentration of	
	Ni(II) ions solution 150mg/L and Temperature 30°C.	
5.3.3		110
3.3.3	Effect of Contact Time for Ni(II) ions on adsorption, pH 7, Volume of	110
	Ni(II) ions solution 50 mL, Biosorbent Dose 200 mg, Concentration of	
	Ni(II) ion solution 150mg/L and Temperature 30°C.	

5.3.4	Effect of Ni(II) ion solution Concentration, pH 7, Volume of Ni(II) ions solution 50 mL, Biosorbent Dose 200 mg, Time 50 min and	110
	Temperature 30°C.	
5.3.5	Percentage of Ni(II) metal removal in various initial concentration on	111
	LPSP biosorbent	
5.3.6	Langmuir and Freundlich isother parameters for the adsorption of	111
	Ni(II) ions on LPSP biosorbent	
5.3.7	Dimensionless separation factor (R _L) for adsorption of Ni(II) ions on	111
	LPSP Biosorbent.	
5.3.8	Kinetic parameter for adsorption of Ni(II) ions onto LPSP Biosorbent	112
5.3.9	Thermodynamic parameter for adsorption of Ni(II) ions on LPSP	113
5.3.10	Comparative study of adsorbent capacity for Ni(II) metal ions on	113
	Langmuir constant q _{max} (mg/g) by various biosorbent.	
5.4.1	Effect of pH for BBR dye uptake, Time 50 min, Biosorbent dose	128
	300 mg, Volume of BBR dye solution 50 mL, Initial dye concentration	
	200 mg/L and Temperature 30°C.	
5.4.2	Effect of Biosorbent dose for BBR dye uptake, Time 50 min, pH 8,	128
	Volume of BBR dye Solution 50 mL, Initial dye concentration	
	200 mg/L and Temperature 30°C	
5.4.3	Effect of contact time for BBR dye uptake, pH 8, volume of BBR dye	129
	solution 50 mL, Biosorbent dose 300 mg, Initial dye concentration	
	200 mg/L and Temperature 30°C.	
5.4.4	Effect of Initial dye concentration for BBR dye uptake, Time 50 min,	129
	pH 8, Volume of BBR dye Solution 50 mL, Biosorbent dose 300 mg	
	and Temperature 30°C.	
5.4.5	Langmuir and Freundlich model parameters	130
5.4.6	Pseudo-first-order and second order kinetic parameters	130
5.5.1	Effect of pH for MG dye adsorption, Time 50 min, Biosorbent weight	144
	300 mg, Volume of dye solution 50 mL, Initial dye concentration	
	200 mg/L and Temperature 30°C.	

5.5.2	Effect of Biosorbent dose on MG dye adsorption, Time 50 min, pH 8,	144
	Volume of dye Solution 50 mL, Initial dye concentration 200 mg/L and	
	Temperature 30°C.	
5.5.3	Effect of contact time on MG dye adsorption, pH 8, volume of dye	145
	Solution 50 mL, Biosorbent weight 300 mg, Initial dye concentration	
	200 mg/L, Temperature 30°C.	
5.5.4	Effect of Initial dye concentration on MG dye adsorption, Time	145
	50 min, pH 8, Volume of dye Solution 50 mL, Biosorbent weight 300	
	mg and Temperature 30°C.	
5.5.5	Langmuir and Freundlich adsorption isotherm parameters for MG dye	146
	on LPSP	
5.5.6	Pseudo-first-order and Pseudo-second-order kinetic parameters for MG	146
	dye on LPSP	
5.6.1	Effect of pH in MO dye, Time 30 min, Adsorbent weight 300 mg,	159
	Volume of MO dye solution 50 mL, Initial dye (MO) concentration	
	200mg/L and Temperature 30°C.	
5.6.2	Effect of biosorbent (LPSP) dose in MO dye, Time 30 min, pH 3,	160
	volume of MO dye solution 50 mL, Initial dye (MO) concentration	
	200mg/L and Temperature 30°C	
5.6.3	Effect of contact time in MO dye, pH 3, volume of MO dye solution	160
	50 mL, Initial dye (MO) concentration 200mg/L and Temperature 30°C	
5.6.4	Effect of Initial dye concentration in MO dye, pH 3, Time 30 min,	161
	volume of MO dye solution 50 mL and Temperature 30°C.	
5.6.5	Langmuir and Freundlich model parameters for MO dye	161
5.6.6	Pseudo-first-order and second order kinetic parameters for MO dye	161

LIST OF FIGURES

Figure	T:41-	Page
No	Title	No
1.1	Structure of Bismark Brown R Dye	18
1.2	Structure of Malachite Green Dye	19
1.3	Structure of Methyl Orange Dye	20
4.1.	Laplap purpureus Plant and its stem powder	47
5.1.1	Effect of pH in Cu (II) ions adsorption, Time 50 min, Volume of Cu (II)	70
	solution 50 mL, Concentration of Cu (II) 150mg/L, Biosorbent Dose	
	200 mg and Temperature 30°C.	
5.1.2	Effect of Biosorbent (LPSP) dose in Cu (II) ions adsorption, Time	70
	50 min, pH 7, Volume of Cu (II) ions solution 50 mL, Concentration of	
	Cu (II) 150mg/L and Temperature 30°C.	
5.1.3	Effect of Contact Time in Cu (II) ions adsorption, pH 7, Volume of	71
	Cu (II) solution 50 mL, Biosorbent Dose 200 mg, Concentration of	
	Cu (II) 150mg/L and Temperature 30°C.	
5.1.4	Effect of initial Concentration of Cu (II) ions in adsorption, pH 7,	71
	Volume of Cu (II) ions solution 50 mL, Biosorbent Dose 200 mg, Time	
	50 min and Temperature 30°C.	
5.1.5	Langmuir Isotherm plot for adsorption of Cu (II) metal Ions on LPSP	72
5.1.6	Freundlich Isotherm plot for adsorption of Cu (II) metal Ions on LPSP	72
5.1.7	Pseudo first order plot for adsorption of Cu (II) metal Ions on LPSP	73
5.1.8	Pseudo second order plot for adsorption of Cu (II) metal Ions on LPSP	73
5.1.9	FTIR images of LPSP before and after adsorption of Cu (II) metal ions.	74
5.1.10.	XRD images of LPSP before and after adsorption of Cu (II) metal ions	75
5.1.11	SEM images of LPSP before and after adsorption of Cu (II) metal ions	76
5.2.1	Effects of pH for Chromium (VI) ion on adsorption, Time 50 min,	92
	Volume of Cr (VI) ions solution 50 mL, Concentration of Cr (VI) ions	
	solution 150 mg/L, Biosorbent Dose 200 mg and Temperature 35°C.	
5.2.2	Effects of Biosorbent (LPSP) dose for Chromium (VI) ions on	92
	adsorption, Time 50 min, pH 7, Volume of Cr (VI) ions solution 50 mL,	
	Concentration of Cr(VI) ions solution 150mg/L and Temperature 35°C.	

5.2.3	Effects of taction time for Chromium (VI) ions on adsorption, Biosorbent	93
	dose 200 mg, pH 7, Volume of Cr (VI) ions solution 50 mL,	
	Concentration of Cr(VI) ion solution 150mg/L and Temperature 35°C.	
5.2.4	Effects of initial Concentrations of Chromium (VI) ions solution on	93
	adsorption, Biosorbent dose 200 mg, Time 50 min, pH 7, Volume of	
	Cr (VI) ions solution 50 mL, and Temperature 35°C.	
5.2.5	Effects of Temperature for Chromium (VI) ions on adsorption,	94
	Concentrations of Chromium (VI) ions 150 mg/L, Biosorbent dose	
	200 mg, Time 50 min, pH 7, and Volume of Cr (VI) ions solution 50 mL.	
5.2.6	Langmuir adsorption Isotherm plot for adsorption of Cr (VI) metal Ions	94
	on LPSP	
5.2.7	Freundlich adsorption Isotherm plot for adsorption of Cr (VI) metal Ions	95
	on LPSP	
5.2.8	Pseudo first order kinetic model plot for adsorption of Cr (VI) metal Ions	95
	on LPSP	
5.2.9	Pseudo second order kinetic model plot for adsorption of Cr (VI) metal	96
	Ions on LPSP	
5.2.10	FTIR analysis of LPSP before and after adsorption of Cr (VI) metal Ions	97
5.2.11	XRD Pattern of LPSP before and after adsorption of Cr (VI) metal ions	98
5.2.12	SEM image of LPSP before and after adsorption of Cr (VI) metal ions	99
5.3.1	Effect of pH on adsorption of Ni(II) ions, Time 50 min, Volume of Ni(II)	114
	ions solution 50 mL, Concentration of Ni(II) ions solution 150mg/L,	
	Biosorbent Dose 200 mg and Temperature 30°C.	
5.3.2	Effect of Biosorbent dose (LPSP) on adsorption of Ni(II) ions solution,	114
	Time 50 min, pH 7, Volume of Ni(II) ions solution 50 mL, Concentration	
	of Ni(II) ions solution 200mg/L and Temperature 30°C.	
5.3.3	Effect of Contact Time for Ni(II) ions solution on adsorption, pH 7,	115
	Volume of Ni(II) ions solution 50 mL, Biosorbent Dose 200 mg,	
	Concentration of Ni(II) ions solution 200mg/L and Temperature 30°C.	
5.3.4	Effect of initial Concentration for Ni(II) ions solution on adsorption,	115
	pH 7, Volume of Ni(II) ions solution 50 mL, Biosorbent Dose 200 mg,	
	Time 50 min and Temperature 30°C.	

5.3.5	Langmuir adsorption Isotherm model for removal of Ni(II) metal ions	116
	using LPSP	
5.3.6	Freundlich adsorption Isotherm model for removal of Ni(II) metal Ions	116
	using LPSP	
5.3.7	Pseudo First order model for removal of Ni(II) metal Ions using LPSP	117
5.3.8	Pseudo second order model for removal of Ni(II) metal Ions using LPSP	117
5.3.9	FTIT Analysis for adsorption of Ni(II) metal ions on before and after	118
	using LPSP	
5.3.10	XRD Pattern for adsorption of Ni(II) metal ions on before and after using	119
	LPSP	
5.3.11	SEM Analysis for adsorption of Ni(II) metal ions on before and after	120
	using LPSP	
5.4.1	Effect of pH for BBR dye uptake, Time 50 min, Biossorbent dose	131
	300 mg, Volume of BBR dye solution 50 mL, Initial dye concentration	
	200 mg/L and Temperature 30°C.	
5.4.2	Effect of Biosorbent dose for BBR dye uptake, Time 50 min, pH 8,	131
	Volume of BBR dye Solution 50 mL, Initial dye concentration 200 mg/L	
	and Temperature 30°C.	
5.4.3	Effect of contact time forBBR dye uptake, pH 8, volume of Solution	132
	50 mL, Biosorbent dose 300 mg, Initial dye concentration 200 mg/L,	
	Temperature 30°C.	
5.4.4	Effect of Initial dye concentration for BBR dye uptake, Time 50 min,	132
	pH 8, Volume of Solution 50 mL, biosorbent dose 300 mg and	
	Temperature 30°C.	
5.4.5	Langmuir isotherm plot of Bismark Brown R dye using Laplap	133
	purpureus plant stem powder at 30°C.	
5.4.6	Freundlich isotherm plot of Bismark Brown R dye using Laplap	133
	purpureus plant stem powder at 30°C.	
5.4.7	Pseudo first order plot for adsorption of Bismark Brown R dye using	134
	Laplap purpureus plant stem powder.	
5.4.8	Pseudo second order plot for adsorption of Bismark Brown R dye using	134
	Laplap purpureus plant stem powder	

using Laplap purpureus plant stem powder 5.4.10 XRD images of before and after adsorption of Bismark Brown R dy using Laplap purpureus plant stem powder. 5.4.11 SEM images of before and after adsorption of Bismark Brown R dy	
using Laplap purpureus plant stem powder.	
	e 137
5.4.11 SEM images of before and after adsorption of Bismark Brown R dy	e 137
using Laplap purpureus plant stem powder.	1
5.5.1 Effect of pH on adsorption of MG dye, Time 50 min, Biosorbent weigh	nt 147
300 mg, Volume of dye solution 50 mL, Initial dye concentration	n
200 mg/L and Temperature 30°C.	
5.5.2 Effect of Biosorbent dose on adsorption of MG dye, Time 50 min	n, 147
pH 8, Volume of dye Solution 50 mL, Initial dye concentration 200 mg/	L
and Temperature 30°C.	
5.5.3 Effect of contact time on adsorption of MG dye, pH 8, volume of dy	e 148
Solution 50 mL, Biosorbent weight 300 mg, Initial dye concentration	n
200 mg/L, Temperature 30°C.	
5.5.4 Effect of Initial concentration on adsorption of MG dye, Time 50 min	n, 148
pH 8, Volume of dye Solution 50 mL, Biosorbent weight 300 mg an	d
Temperature 30°C.	
5.5.5 Langmuir adsorption isotherm plot for Malachite Green dye usin	g 149
Laplap purpureus plant stem powder	
5.5.6 Freundlich adsorption isotherm plot for Malachite Green dye usin	g 149
Laplap purpureus plant stem powder.	
5.5.7 Pseudo first order plot for Malachite Green dye using Laplap purpurer	s 150
plant stem powder.	
5.5.8 Pseudo second order plot for Malachite Green dye using Lapla	p 150
purpureus plant stem powder	
5.5.9 FT-IR Analysis for LPSP before and after adsorption of MG dye	151
5.5.10 Scanning Electron Microscope Analysis for LPSP before and after	er 152
adsorption of MG dye.	
5.6.1 Effect of pH in MO dye, Time 30 min, Adsorbent weight 300 mg	g, 162
Volume of MO dye solution 50 mL, Initial dye (MO) concentration	n
200mg/L and Temperature 30°C.	

5.6.2	Effect of biosorbent (LPSP) dose in MO dye, Time 30 min, pH 3,	162
	volume of (MO) dye solution 50 mL, Initial dye (MO) concentration	
	200mg/L and Temperature 30°C.	
5.6.3	Effect of contact time in MO dye, pH 3, volume of MO dye solution 50	163
	mL, Initial dye (MO) concentration 200mg/L and Temperature 30°C.	
5.6.4	Effect of Initial dye concentration in MO dye, pH 3, Time 30 min,	163
	volume of MO dye solution 50 mL and Temperature 30°C.	
5.6.5	Langmuir isotherm plot for Methyl Orange dye using Laplap purpureus	164
	plant stem powder	
5.6.6	Freundlich isotherm plot for Methyl Orange dye using Laplap purpureus	164
	plant stem powder	
5.6.7	Pseudo first order plot for Methyl Orange dye using Laplap purpureus	165
	plant stem powder	
5.6.8	Pseudo second order plot for Methyl Orange dye using Laplap purpureus	165
	plant stem powder.	
5.6.9	FT-IR Analysis for LPSP before and after adsorption of MO dye	166
5.6.10	XRD pattern for LPSP before and after adsorption of MO dye	167
5.6.11	SEM Analysis for LPSP before and after adsorption of MO dye	168

LIST OF ABBREVIATIONS

FTIR Fourier Transform Infrared Spectroscopy

XRD X-ray diffraction

SEM Scanning Electron Microscope

LPSP Laplap Purpureus Stem Powder

BBR Bismark Brown R

MG Malachite Green

MO Methyl Orange

 q_t The amount of metal ion/dye adsorbed at time t (mg/g)

C_i The Initial Concentration of metal ion/dye (mg/L)

C_t The metal ion/dye adsorbed at time t (mg/L)

m The mass of the biosorbent (g)

C_f Final concentration of metal ion/dye (mg/L)

C_e Equilibrium constant of metal ion/dye (mg/L)

The equilibrium concentration (mg/L)

qe The amount of metal ion/dye adsorbed at equilibrium (mg/g)

The amount of metal ion/dye adsorbed on per unit weight sorbent (mg/g)

 q_{max}/q_{m} The constant related to maximum adsorption capacity (mg/g)

b The Langmuir constant related to energy of adsorption

R_L Dimensionless separation factor

K_f The Freundlich constant related to adsorption capacity (mg/g)

1/n The sorption intensity (mg/L)

K₁ Rate constant of pseudo first order adsorption (g.mg⁻¹.mn⁻¹)

t constant time (min)

K₂ rate constant of pseudo second order adsorption (g.mg⁻¹.mn⁻¹)

 ΔG° Free energy change of sorption process (KJ/mol)

*K*_o Equilibrium constant

T Temperature (${}^{\circ}C$)

R Universal gas constant

 ΔH° Standard heat/enthalpy changes of the sorption (KJ/mol)

 ΔS° Entropy change of sorption (KJ/mol)

CHAPTER-I

INTRODUCTION

Water quality is a major problem for humanity since it is inextricably related to human life. Water supply and civilization are practically synonymous, according to the history of civilization [1]. Water shortages caused by climatic changes have caused the extinction of several towns and civilizations. Consequently, water has been dubbed the "elixir of life". Water is a universal solvent and a major component of all living organisms, as is widely known. Water availability and scarcity have an impact on the distribution and quantity of plants, animals, and human being. Man's direct and indirect activities have recently disrupted this delicate balance. Hundreds of thousands of waste chemical auxiliaries have been released into the environment. The natural distribution of heavy metals in the environment on land, in rivers, lakes, and seas have been disrupted by human activities. Several other heavy metals have been proven to accumulate in food chains and to be hazardous to aquatic and terrestrial species even at extremely low quantities, shortly after the Minamata disease was discovered in Japan [2].

1.1 A description of the problem of water pollution

Water pollution arises due to the release of industrial effluents are a main distress in growing countries. Usually, either unused or untreated industrial waste waters are being released to the natural environment. This industrial effluents act as major water pollutants. The most of the important category of pollutants derived from dyes, which are organic in nature and they are in the industrial effluents discharged from various industries like food, pharmaceutical, textiles, cosmetics, paper, leather, rubber and plastics industries. Synthetic dyes are being produced on large amount than

the natural dyes and are regularly used in textile industries, due to their wide-ranging of application; the synthetic dyes can causes serious environmental problem and severe health risks. The dyes may be discharged into water bodies is toxic to aquatic species as well as human beings, due to the presence of an aromatic nature or heavy metal in their structure, which causes many healthiness troubles such as nausea, hemorrhage and ulceration [3,4].

1.2 Industrial wastewater treatment

Wastewater treatment used to describe the mechanisms and processes applied to clean up industrial waste water before it is discharged into the environment or recycled. Most industries bring some wet waste, but in the developed nation, recent trends have been to reduce or recycle this waste during the production process. Although many industries have moved away from using wastewater, others are still reliant on it.

The different types of contaminated wastewater necessitate various approaches to removing the contaminants.

- i) Sedimentation
- ii) Oxidation
- iii) Floatation
- iv) Membrane filtration
- v) Ultra filtration
- vi) Electrochemical treatment
- vii) Biological treatment
- viii) Chemical precipitation

1.3 Necessity for removal of heavy metal ions and dyes from the environment

It is the most important to remove the metal ions and dyes from industrial effluents before the expulsions into the natural water bodies to meet up National Regulatory Standards as well as save the public healthiness and other living things in the environment as well as globe.

Pollutants are deposited in sediments as a result of the incessant release of industrial, domestic, and agricultural wastes into the water bodies. Heavy metals, for example, are pollutants that endanger public health once they enter the food chain. Heavy metals, unlike most organic pollutants, cannot be destroyed via biodegradation. Heavy metal deposition in fish, shellfish, mussels, sedimentary rocks, and other aquatic ecosystem components has been documented across the world [5]. Massive quantities of certain heavy metal ions can be toxic due to direct metal action, inorganic salts, or organic compounds from which the metal can easily be separated or introduced into the cell. Metal exposed can happen in a variety of situations, especially in an industrial plant. Accidents can result in acute, high-level exposure in some environments.

However at low concentrations, some heavy metals are toxic to aquatic organisms. Heavy metals contamination in water and aquatic life, such as fish, necessitates ongoing monitoring and surveillance because these elements do not degrade and tend to biomagnifying in humans via the food chain. Metals like copper, nickel, and chromium are also found in dyes and colour pigments. Metals are difficult to remove from wastewater and may evade the sewage treatment system's capabilities. Furthermore, the unutilized dyes and colour ejected in dyeing vat effluent interferes with light transmission in the water bodies receiving the effluent. As a result, heavy metals must be eliminated from aquatic life.

Similarly, dyeing industry's effluents are among the most challenging to treat into fresh water, because of their sedimentation, turbidity, poisonous components and its color. In which, the color is the major contaminant for visible to the naked eye. Dyes may possibly to reduce photosynthesis in aquatic life due to reduced sun light penetration, and they may also be toxic to some aquatic species due to the presence of metal ions, dyes and aromatics nature in their structure. Dyes are generally synthetic and have a complex of aromatic molecular configuration, making them more stable and complicate to degrade. Anionic dyes are direct, acid, and reactive dyes; cationic dyes are basic dyes; and non-ionic dyes are disperse dyes.[6,7]

The chromophores are covered by anionic and non-ionic dyes, they have mostly azo or anthroquinone variety. Toxic amines are formed in the effluent due to the reductive cleavage of azo linkages. Because of their fused aromatic structures, anthraquinone-based dyes are more resistant to degradation and thus, remain retained the colours in wastewater. Reactive dyes are generally composed of an azo-based chromophore combined with various reactive groups, such as vinyl sulphone, chlorotriazine, trichloropyrimidine, and difluorochloropyrimidine. They vary from most other dyes in that they form covalent bonds with textile fibers like cotton. They are widely used in the textile industry due to their advantageous properties of bright colour, washing fastness, simple application techniques, and low energy consumption. Water soluble reactive and acid dyes are troubling because they pass unaffected through the conventional treatment system, posing issues.[8,9,10]

1.4 The conventional technique for removal of heavy metal ions and dyes

The conventional technique for the removal of heavy metal ions and dyes from industrial effluents including coagulation, precipitation, distillation, filtration,

flocculation, oxidation, floatation, ion exchange, solvent extraction, evaporation, batch adsorption. However, the uses of these treatment processes have been found to be sometime restricted, due to expensive, cost of operation is high and the potential creation of secondary pollutants. Additionally, such processes may be unsuccessful or very expensive when the initial heavy metal ions concentrations are in the range of 10-100 mg/L. In current years, environmentally benign biosorption methods have been studied widely utilizing biomass as a biosorbent for removal of heavy metal ions and dyes from the polluted wastewater.

1.4.1 Coagulation-flocculation

Coagulation-flocculation method have been carried out by several researchers for the purification of organic substances, trace element, heavy metals and dyes from industrial effluents. In the early stages of the coagulation-flocculation procedure, aluminium sulphate has been used as coagulant by Egyptians and Romans. In recent years, the coagulation-flocculation method have employed for fine particle agglomerate and the conversion of big particles from colloids for minimizing turbidity and also reduces other inorganic, organic pollutants from the effluents. This method is comprised by two different steps:

- A) Mixing dispersed coagulant in effluent for treatment of violent agitation, and
- B) Formation of well defined floccules from dispersed coagulant by the gentle agitation.

At last, the floccules have allowed for settlement and then separated as sludge when treatment waste water allowed to consequent treatment process for release into water bodies.[11-14]

1.4.2 Membrane separation

The membrane separation method have been studied as a convenient for the removal of unwanted inorganic elements from industrial waste water. In this method, amalgamation of membrane was introduced in 1980's for selectively adsorb and effectively improve the separation performance during the process. When the industrial waste water flows through the membrane, the functional group of the active sites interacts with the pollutants to separate effluents from waste water with a high rate of adsorption capacity due to very closer contact distance between the pollutant of water and active sites of membrane. Particularly, the major active site of the functional groups could be affix with the contaminants while exudation of waste water across the membrane. [15,16]

1.4.3 Electrochemical Method

An electrochemical process have been used widely for the removal of heavy metals and dyes from industrial effluents. Specifically, it was utilized to separate ores in the mining industry via electro-refining for many years, and it also been used to recover copper metal from pickle liquors. The electrochemical method has been used to recover metals from metal plating tanks for the past 25-30 years. In this method, a direct current is passed between cathode plates and an insoluble anode in aqueous containing metal ions. The positively charged metal ions stick to the negatively charged cathodes, appearing a metal deposit that can be stripped away and recovered. [17]

1.4.4 Ion exchange

Ion exchange is a reversible interchange on water treatment process, commonly applied for waste water treatment to removing dealkalization, denitrification, deionization. The ion exchange material like resin, beads or granules contains

permanent insoluble anions, kept electrically neutral by replaceable sodium cation. Especially, the softening of drinking water may be achieved by ion exchange procedure is carried by a strong acid cationic exchanger of the R-Na form. In this method the ion exchangers are packed in columns of sizes matching to the flow rate of the water to be treated. Generally, at the final stage of the softening process of water the Ca²⁺ and Mg²⁺ ions were retained while an effluent contains sodium salts.

$$2R$$
-Na + (Ca,Mg) (HCO₃)₂ \rightarrow R₂ (Ca,Mg) + 2NaHCO₃

Similarly, the removal of unwanted elements and heavy metal ions by this method, and also the ion exchanger can be regenerate corresponding to the element present in the effluent.

1.4.5 Solvent extraction

Liquid-Liquid extraction is also commonly referred as solvent extraction. This is the process of removing/separating of hazardous metal ions from sludge and industrial sediments by basis of their relative solubility. In this method, a solvent - a fluid (selective complexing agent) is helps to dissolve another substance, but it does not destroy any other compounds. When, the phenomenon occurs over the course of two different immiscible (liquids that do not dissolve in one another) phases while put together. It may be possible due to differ their liquid polarity. The sequence of the phases, whether a specific liquid is on top or on the bottom, is identified by its density. Solvent extraction is used across multiple industries depending upon the industries, including used in petrochemical refining industries. Especially, it can be beneficial for hazardous waste generators, hence solvent extraction ultimately reduces the quantity of hazardous waste from effluent.[18]

1.5 Adsorption

Adsorption is stand for competency of the solid substance to attract the other surfaces of the molecules of gas or solution at which they are in contact by the external surface or internal surface (walls of capillaries or crevices) of solids or by the surface of liquids. Solids that are used to adsorb gases or dissolved substances are called adsorbents; the adsorbed molecules are generally represented as the adsorbate. The best example of an outstanding adsorbent is the charcoal utilized on gas masks to take out the fatal impurities from the industrial effluents or a stream of air. It can be describe as the adsorption meant by the adhesion of atoms, ions, biomolecules or molecules of gas, liquid, or dissolved solids to a surface by creates a thin film of the adsorbate (the molecules or atoms being accumulated) on the surface of the adsorbent [19, 20].

Adsorption, like as surface tension, is a consequence of surface energy. In a bulk phase, all the bonding (i.e., ionic, covalent, or metallic) requirements of the constituents atoms of the materials are filled by other atoms in the bulk phase. On the other hand, atoms on the surface of the adsorbent are not completely surrounded by the other adsorbent atoms and as a result can attract adsorbates. The proper nature of the bonding depending upon the nature of the species involved, but the adsorption process was commonly classified as physisorption (i.e., weak vander waals forces) or chemisorption (i.e., covalent bonding). It may also be takes place by electrostatic force of attraction [21]. Adsorption, either physical or chemical adsorption may be in nature.

1.5.1 Physical adsorption

If the forces of attraction presented between adsorbate and adsorbent by physical forces, the adsorption is called as physisorption or physical adsorption. In physical adsorption, the electron distributions of adsorbate molecules undergo some

distortion in mutual proximity; though, the electrons maintain their association with their original nuclei. This category of adsorption is also known as physisorption or vander waals adsorption. It can be simply reversed by heating or decreasing the pressure. Physical Adsorption is similar to the gas condensation in liquids and the force of pull between solid adsorbents and adsorbed molecule is dependent on the physical or vander Waals. There is no chemical specificity for physical adsorption, a gas that tends to be adsorbed to a solid when the temperature is low enough or the gas pressure is high enough.

1.5.2 Chemical adsorption

If the forces of attraction existing between adsorbate particles and the active sites of specific surface location on adsorbent material are almost of the same strength as chemical bonds, the adsorption was known as chemical adsorption. This type of adsorption was also called chemisorption or Langmuir adsorption. In chemical adsorption, gases molecules are held to a solid surface by chemical forces that are specific for each surface and each gas molecule. Chemical adsorption take place generally at higher temperatures than those at which physical adsorption occurs; moreover, chemical adsorption is normally a slower process than physical adsorption and, like most chemical reactions, frequently involves the energy of activation. Chemisorption is possible only on clean active sites unlike as physisorption, when the adsorbate can't make direct contact for long time with the surface of adsorbent, chemisorption is making a single layer process. Predominantly, chemisorption is applied to determine the number of existing active sites for increase the rate of chemical reactions. Additional properties can includes the reduction or oxidation on temperature at which catalysts becomes active, strength of definite types of active sites, or capacity of materials to perform after the reduction/oxidation cycles. The

chemisorption occurs on all surfaces of active site, if their temperature and pressure conditions are favorable.

1.5.3 Biosorption

Biosorption can be explained by a simple physicochemical method concerning a metabolic passive binding of metal ions (biosorbate) on the surface of a biologically-originating biosorbent [22]. The use of plant derived materials includes chemical and biological removal. The reversible quick procedure involves the ion-binding process in water solutions in a wide variety of interactions on the surface of the biosorbent[23]. The benefits of this process include simple operation without additional chemical requirements, low sludge production, low operating costs and high efficiency that otherwise constitute the major constraints for most conventional technology[24]. Biosorption, even at diluted concentrations, can remove contaminants and is of particular relevance for heavy metal removal, due to toxicity. Biosorbents for a biosorption process can be used for microorganisms (live and dead) and other byproducts of industry and agriculture. The first step of the biosorption is to suspend biosorbent in the biosorbate solution (metal ions/dyes). Equilibrium is achieved after incubation for a specific time interval. The enriched metal biologic is separated at this stage [24].

The biosorption process is advantageous because of its reversible characteristics, no needs of chemicals, a one-stage, fast-ranging process, it contains no danger of toxic effects, and it enables an intermediate concentration of metal ions in balance and is not metabolized [25]. The biosorption capacity (mg/g) can be determined by the amount of adsorbete (matal ion/dyes) biosorbed per unit weight of the biosorbent.

1.5.4 Mechanism of Biosorption

A complex process involving the binding of sorbate on biosorbent is the biosorption mechanism. Many natural materials may be applied as biosorbents that involve bonding, chelation, reduction, precipitation, and complexation in biosorption of metal ions and dyes by physical (electrostatic interaction or vander Waals force of attraction). Biosorbents have a chemical/functional body that can attract metal ions and dyes, the functional group of biosorbent such as amine, amide, imidazole, thioethyl, sulphonate, carbonyl, carboxyle, phosphodiester and phenolic, phenolic and imina groups, which can be control and characterization of these mechanisms. The chemical, stereochemical, and coordination characteristics of metal ions like molecular weight, ionic radius, and oxidation state of the targeted metal species; properties of the biosorbent, that is, the structure and nature (in case of microorganism: living/ nonliving); type of the binding site (biological ligand); the process parameters like pH, temperature, concentration of sorbate and sorbent, and other competing metal ions/dyes; and availability of the binding sites. These combined effects of the above parameters influence the metal/dye speciation (the formation of new forms of metal ions/dye as a result of occurs biosorption). [26, 27]

1.6 Various Adsorbent onto Adsorption Studies

In recent years different types of adsorbents have been using for the study to removal of heavy metals and dyes from industrial waste water for the purpose of unpolluted water releasing from industries. In water treatment process, selection of adsorbent is the most important theme because of expected good adsorption capacity, availability low cost, and regeneration. Hence, various natural adsorbent materials have been studied for the separation of metal ions and dyes.

1.6.1 Creature Adsorbent

Prawn shell waste powder derived from medium of aqua culture forming to removed malachite green[28], egg shell powder made from the source of houses and restaurants waste for methylene blue[29], flakes of chitosan obtained by fishery wastes to take out acid yellow dye [30], Cu⁺² ions removed via utilization of oxide coated egg shell powder [31], and activated sheep bone was used for removal of Hg⁺² [32] have been studied due to free/low cost, locally availability, good adsorption ability and regeneration.

1.6.2 Soil Adsorbent

Commercially purchased ball clay has used onto adsorption due to its adhesives property to remove Cd⁺² ions from aqueous solution [33], natural clay adsorbent acts as a negative charge character for the removal for positive charge of methylene blue dyes [34], the negative charge of octahedral repeat layer of kaolinite obtained from local clay due to these property removes methyl orange [35], removal of basic blue 41 applicable due to their presence of silica phase was strongly attached on brick grains [36], adsorption of dissolved Cu⁺², Zn⁺² by iron oxide-coated sand provides stable and efficient for adsorption [37].

1.6.3 Ash Adsorbent

Fly ash material is a physically powerful and inexpensive natural sorbent to heavy metal ions and dyes by reason of its surface morphological charge. Consequently, fly ash either functioning as a single or in amalgamation with photo catalysts is a composite substrate capable for concurrently removing heavy metal ions and dyes. Large number of regulated surface areas essential one to develop the effectiveness of the method. Standardized surface energy and crystalline structure of

raw fly ash can be modified. The morphological structure of surfactants can be controlled by increase the size of pore for the adsorbent substance as well as increases the length of surfactant's tail and temperature of post-synthesis.[38].

1.6.4 Lignin Adsorbent

Lignocellilose (Latin lignum = wood) biopolymers strengthen the cell wall of plants and consist of main components: cellulose and hemicelluloses form a framework in which lignin in incorporated as a king of connector, thus solidifying the cell wall. Lignin have a three-dimensional structure and partialy random amorphous phenolic polymer network, it is naturally produced in the cell walls of higher plants. The cell wall lignification makes plants resistant to wind and pests. Lignin, complex oxygen-containing organic polymer that with cellulose, forms the chief constituents of wood. It is second to cellulose as the most abundant Earth, A secondary metabolite, lignin is concentrated in the cell walls of wood and makes up 24-35 percent of the oven-dry weight of softwoods and 17-25 percent of hardwoods. Most importantly, lignin derivatives can confer high environmental benefits due to high adsorption capability of their mechanism, stability, biocompatibility and abundance in the plant kingdom. It is a renewable raw material, currently almost exclusively used for generating energy, although it could also be used for removing heavy metal ions and dyes from various industrial effluents [39].

1.6.5 Activated carbon

It is a carbonaceous substance such as lignite, coal, and petroleum pitch. Activated carbon is an inert solid adsorbent material generally used to remove dissolved contaminants from industrial wastewater and process gas-phase streams. It can be produced as an activated carbon source material using hot gases. Activated

carbon has porous on its surface with the active binding sites, inexpensive and readily available for uses as adsorbents in adsorption, furnishing a large surface area to remove contaminants from various industrial effluents. It has more numbers of useful surface areas per gram than any other materials available for physical adsorption. This method is effective in removing certain organic compounds like chlorine, fluorine in drinking water and dyes, heavy metal ions from wastewater [40].

1.7 Heavy metal ions and dyes

1.7.1 Copper

Copper is an essential trace mineral which needs very small amount to human body it is normally bonded to proteins structure in our body, which is healthy. Sometimes copper doesn't bind to human proteins and is known as unbound or free and it will be causes for unhealthy and toxicity. When the copper toxicity acquired as an inherited it is called as Wilson's disease. Acquired copper toxicity can come from a few various sources like eating copper salts (copper sulphate) form on unused cooking or food storage items like pots, pans and inside water pipes. If copper salts form in water pipes, it will generates contaminate water.

The copper toxicity gets from eating in excess of copper-rich food or nutritional supplements. Ingest the toxicity of copper produces by drinking an acidic beverage or eating food stored in a copper container for an extended period. Lot of copper can be fatal to human being, the large amounts of copper ingesting through human skin, it leads to severe toxicity in internal organs of the human body, especially in brain, liver, and lungs. The two main symptoms of it nausea and vomiting and other such as diarrhea, muscular convulsion, anemia, jaundice, fever, bodily chills, pain in the abdominal area, lack of urine, and metallic taste in our mouth.

Copper (II) ions have the tendency of bioaccumulation, persistency, nonbiodegradability and toxicity in nature [41-43]. The Copper (II) ions accumulation is causes for brain, pancreas, heart and skin diseases in human body [44]. The divalent state of Copper (II) is the most toxic and it is widely used in manufacturing of various metallic alloys and electrical tools. Particularly, most of the Copper (II) ion waste originates from electrical and semi-conductor industries, manufacturing of fungicides, ore refining and antifouling paints and also that waste released from mining, agricultural materials, disposal of electrical wiring waste, electroplating operation, welding, treating on sewage and plumbing. The excessive Copper contaminated in drinking water sources that can be harmful and causes for vomiting, diarrhea, abdominal pain, tachycardia and also causes for stomach upset, ulcer, mental retardants, liver and brain damages [45-47]. Commonly, toxicity of Copper arises from eating food materials and drinking water or an excess of copper enriched in breathing air. The acute toxicity of copper leads to anemia, intravascular hemolytic, acute liver and acute renal failure with tubular damage, shock coma and death and its mild conditions results like diarrhea, vomiting and nausea [48-50].

1.7.2 Chromium

Chromium is utilized in assemble of cars, pottery, glass, and linoleum. Exposure to too much chromium leads to lungs and respiratory tract illness and kidney diseases. In addition, excess exposure to chromium metal may also cause to gastrointestinal symptoms, like as diarrhea and vomiting, often with blood. Symptoms may causes to rigorous water-electrolyte disorders, increased mild acidity of blood and body tissues, and/or insufficient blood flow to its tissues resulting in shock. Lesions on the kidneys, liver, and muscular layer of the heart (myocardium) may also develops.

Chromium has been used enormously in various industries particularly likes textiles, metal finishing work, electroplating technique, leather tanning, production of stainless steel, preparation of chromate, dyes making for plastics, wood and manufacturing of paint, pigments and chemicals [51-53]. Chromium metal exists in the form of its trivalent (Cr (III)) or hexavalent (Cr (VI)) in the environment. The species of Chromium metal act as a highly toxic in the biological system like carcinogen, teratogen and mutagen [54, 55]. Especially, the oxidation state of Chromium (VI) has more poisonous character than Chromium (III) to human health [56]. The hexavalant Chromium is almost quite soluble in water over the entire range of pH, hence it easily contaminates in the environment [57]. Moreover, Cr (III) metal converted into more carcinogenic and mutagenic character by the conversion of oxidized under certain conditions due to some bacteria in the environment [58]. It causes to liver damage, edemas, pulmonary congestion, skin allergies and cancer on human beings by prolonged exposure of Chromium metal species, but the recommended limits of chromium in potable water is 0.05 mg/ L [59,60]. Even though, Chromium (III) metal is needed 50-200 mg per day to human body for the utilization of fat, protein and sugar [61]

The heavy metal chromium is exhibits as two stable oxidation states like Cr(III) and Cr(VI). The Cr(VI) state is of particular concern because this form is hazardous to health. Chromium metal is released into the natural water bodies from various industries like electroplating, leather tanning, cement industries, steel industries, and photography. Adverse effects of hexavalent form of chromium causes for skin irritation, dermatitis and ulcer formation. Over exposure to Cr(VI) leads to liver damage, pulmonary congestion and edema. Particularly, inhalation of Cr(VI) can causes for perforation of mucous membranes of the nasal septum as result coughing,

wheezing, and shortness of breath. Even though, the recommended limits of chromium in potable water is 0.05 mg/ L [60].

1.7.3 Nickel

Nickel is common in jewelry; nickel allergy is most often associated with earrings and other body-piercing jewelry containing nickel. If the person work in an occupation that constantly exposes to nickel, high risk may be developing allergy than someone doesn't work in the metal industries. Additionally, people have regular exposure to nickel as doing "wet work" consequently it causes either sweat or frequent contact with water. It is possibly more to develop nickel allergy. These people may incorporate bartenders, people who have works in certain food industries and domestic cleaners and other people may have an increased risk of nickel allergy for metalworkers, tailors and hairdressers.

Nickel compounds widely using in various industrial process like non-ferrous metal, paint formulation, electroplating, mineral processing, battery manufacturing, porcelain enameling, copper sulfate preparation and stream-electric power plants are leading to high concentration in aquatic environment [62]. Mainly Nickel (II) generated from petroleum refining, plating factory waste water released to natural ecosystem and drinking for long time of Ni (II) polluted water will causes lungs and nervous problem [63]. Nickel carbonyl compound is a carcinogenic and it can be easy for absorption of skin at an atmosphere in the concentration of 30 mg/L for half an hour, which is leads to lethal [64]. Nickel (II) ion is one of the micronutrient for human, animals and plants. However, its high level concentration can causes toxic like skin allergies, pulmonary fibrosis, respiratory tract cancer [65-67], bone problems, dermatitis (itching of Ni), which is most frequently effect by exposure of nickel through the coins and jewelry.

Especially, higher concentration of nickel leads to cancer in lungs, nose and bone [68, 69]. Moreover, headache, nausea, dizziness, vomiting, chest pain, dry cough, tightness in the chest, shortness breathing, rapid breathing, cyanosis and extreme weakness [70, 71].

1.7.4 Bismark Brown R

Bismark Brown R commonly called as Basic Brown-4 is a cationic basic diazo dye. It is widely utilizing in dyeing of synthetic fibers, cotton, coloring in paper, pulp, wool, leather, rubber and plastic industries. Discharge of these dye waste water contaminating in environmental ecological system leads to harmful effects. Bismark Brown R is characterized due to the presence of one or more azo group (-N=N-) forms bridges between the aromatic rings, hence it produces harmful to human health. It is contacts for short time or prolonged with eyes and skin causes for severe irritation with redness appearance at the sites of contact. It produces irritation of gastrointestinal with nausea, diarrhea, vomiting, soreness and redness of throat and mouth by ingestion. On inhalation it causes for irritation of throat with a feeling of chest tightness and may leads to wheezing and coughing. It is also carcinogenic for human being and aquatic species [72-74] IUPAC name of Bismark Brown R is 4-[[3-[(2,4-diamino-5-methyl phenyl)diazenyl]-4-methylphenyl]diazenyl]-6-methylbenzene-1,3-diamine;dihydro chloride.

$$H_2N$$
 H_3C
 N^2N
 CH_3
 CH_3
 CH_3

Figure: 1.1 Structure of Bismark Brown R Dye

1.7.5 Malachite Green

Malachite green is a basic dye and it has been utilized largely in dyeing for leather, silk, wool, jute and including in distilleries [75]. It also using in aquaculture, animal husbandry and commercial fish hatchery as a therapeutic agent for antifungal. Similarly, it is utilizing as an antiseptic and fungicidal for human being [76]. It is highly toxic for flora and fauna, and it stimulus risk of cancer and also act as a liver tumor-developing agent. MG dye has mutagenic and carcinogenic effects by its aquatic activities [77, 78]. The aqueous form of MG dye in water bodies on ecosystem which causes for damage to kidneys, gills, liver, intestines, gonads and particularly, gonadotrophic cells on oceanic animals and also causes for irritation in digestive system of human by consuming sea food. The direct contact of MG dye with eye will leads to permanent injury for human eyes, likewise contact with skin causes irritation with redness and pain [79,80]. Particularly, MG dye is used for external purposes as an antiseptic, antibacterial, and anti protozoan agent, but it is an oral application that is hazardous and carcinogenic by the presence of nitrogen [81]. The reduced form of MG dye is leucomalachite green (LMG) (a metabolite) might persist in edible aquatic organism, the intake of these organisms which leads to toxic in human beings for extension of time periods [82]. The crystalline form of MG dye belongs to triphenylmethane dyes. It is very dangerous and have highly cytotoxic characters to the mammalian cells and also act as aprovital role for liver tumar-enhancing agent [83, 84].

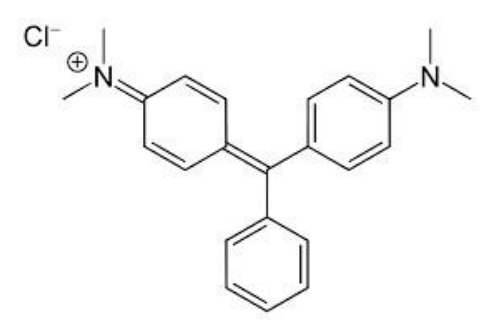


Figure: 1.2 Structure of Malachite Green Dye

1.7.6 Methyl Orange

Generally, the Methyl Orange dye is a mono azo group of dye due to -N=Npresence on MO dye and it has low biodegradability in the environment. It is used in various laboratories like textiles, paper, printing, pharmaceutical, food and commercial products and it poses toxic property towards aquatic species [85, 86]. Methyl Orange dye is an anionic character molecules, it is a nitrogen compound structure. Therefore, it acts as an azo-dye that leads to allergies and hypersensitivity [87]. In methyl Orange basic form, a hydrogen ion (H⁺) is lost from -N=N- bridge between the rings and the electrons utilized for binding the hydrogen neutralize the positively charge on the terminal nitrogen, hence it has no longer able to π -bond [88]. MO is a water-soluble azodye and it is used as an acid-base indicator in laboratory [89]. It is entering the body via ingestion metabolizes into aromatic amine by intestinal microorganisms. MO dye is generating cancer by the production of aromatic amines through the liver reductive enzymes catalyze the reductive cleavaging of the azo linkage [90, 91]. The Reactive MO dye ($C_{14}H_{14}N_3NaO_3S$) structure.

Figure: 1.3 Structure of Methyl Orange Dye

CHAPTER-II

OBJECTIVES AND SCOPE OF THE PRESENT WORK

OBJECTIVES

The main objectives of this research work is to evaluate the discharge of the heavy metal ions and the textile dyes from synthetic aqueous solution by adsorption technique utilizing widely obtainable economically cheap agricultural waste biosorbent is an alternative to commercial adsorbents.

The specific objectives of the present research investigations are

- ➤ To develop Biosorbent from *Laplap purpureus* (Dolichos Bean) stems as an agricultural waste material.
- > To optimize different experimental parameters to obtain as an efficient Biosorbent.
- To evaluate the adsorbing character of the prepared Biosorbent with the adsorbates like heavy metal ions such as Copper II, Chromium VI and Nickel II and Bismark Brown R, Malachite Green and Methyl Orange dyes.
- ➤ To study the effect of various parameters of the adsorption process such as initial pH, Biosorbent dose, contact time, initial adsorbate concentration and temperature by adsorption of selected adsorbates through the proper batch mode of sorption studies.
- > To fit the equilibrium data with adsorption isotherms to interpret the type of adsorption.
- ➤ To screen the kinetic features of the adsorption process by various kinetic models such as Legergran and Ho.

- ➤ To study the thermodynamic parameters like Free energy change, Enthalpy change, Entropy change and Heat of adsorption process to determine the mechanism of the adsorption.
- ➤ To confirm the projected mechanisms by FT-IR, XRD and SEM analytical techniques.

SCOPE OF THE PRESENT WORK

The several methods have been constructed for the treatment of contaminated waters for long years. The various important methods are conducting includes coagulation, chemical precipitation, ion exchange, floatation, membrane filtration, reverse osmosis, oxidation and biological treatment. However, among these treatment methods, indigenous applications and advantages of some mechanisms were observed. In which, adsorption is most favored one due to its simplicity of design, low cost, easy to operate, time aspect, intensive to toxic substance and reliability.

In recent trend the selection of new adsorbent is great attention for the removal of heavy metal ions and cationic-anionic dyes from the industrial wastes in order to reduce processing cost, some of the investigations currently focused on the application of cost free adsorbents, clay materials, by-products, and biosorbents. Biosorbent was prepared from agriculture waste of home garden and widely available plant waste, offers as cost free bio-adsorbent for conventional treatment of industrial effluents.

Adsorption utilizing biosorbent has become a best alternative method for the purification of the industrial effluents with heavy metal ions and cationic-anionic dyes. An adsorption is the process of mass transfer by physical or chemical interactions between the substances from effluent with binding surface of the solid adsorbent. In the

presence of large binding surface areas, better adsorption capacity and surface reactive adsorption by biosorbent can discharge organic and inorganic pollutants from industrial waste water.

The above informations promoted us to attempt in the present work, only one biosorbent derived from *Laplap purpureus* plant stems dried by direct sun light. The biosorbent (LPSP) used for the possibility to abate with few heavy metal ions and cationic-anionic dyes from aqueous solution. The selected plant is utilized for the preparation of biosorbent is cultivated throughout the world in home garden and agriculture lands are available in more. Amongst the different kind of organic and inorganic pollutants from the heavy metal ions and dyes that are leads to harmful affect to human beings and other terrestrial animals, aquatic animals in general. The selected heavy metal ions like Cu (II), Cr (VI) and Ni (II) ions are due to their biologically significant transition metal ions for animals and human wellbeing. Among the largest quantity of various metal ions are disposed to environmental stream from the manmade and industrial activities. The dyes Bismark Brown R, Malachite Green and Methyl Orange are employed in this study as these dyes find an important place on printing and dyeing in textile industries.

All inclusive objectives of the present endeavors were to study the kinetic and thermodynamic characteristics of adsorption for three metal ions, such as Cu (II), Cr (VI) and Ni (II) and three dyes viz. BBR, MG and MO by low cost biosorbent LPSP with an aim to separate some split of pollutants by the mechanism of adsorption technique, such a study would certainly be useful in the identification of low cost adsorbent material for the adsorption treatment to the wastewaters. In addition, its mechanism aspects will act as the instrument for handling with effectively to such

material. The batch equilibrium method was employing for the adsorption. A complete study of the initial pH, adsorbent dose, contact time, temperature between the adsorbent and adsorbate and initial dye concentration on the adsorption technique have been analyzed on the basis of results of equilibrium, kinetic and thermodynamic studies, a reliable mechanism for the adsorption technique have been recommended. The recommended mechanisms have been good supported by spectral characterizations like as FT-IR, XRD and SEM analysis.

CHAPTER - III

REVIEW OF LITERATURE

This chapter deals with scrutinize of earlier explorations reported in the publications where biomass and varieties of agricultural waste materials have been utilized to eliminate harmful heavy metal ions and deleterious dyes from aqueous solutions. In recent time the numerous researchers have explored the possibility of this attitude.

3.1 Adsorption of heavy metal ions by Biomaterials

Mamatha et al, [92] have been reported for the removal of copper metal ions by using Pongamia pinnata tree bark powder and it was prepared by the method of sundried for 3 days then dried at 80°C in hot air oven and allowed to pulverized to make powder in the particle size of 225 μm. The bark powder further washed with double distilled water after that dried at 60°C for 8 hours. The batch mode of adsorption parameters like pH (2 - 8), concentration of metal ions (10 -100 mg/L), adsorbent concentration (2-10 g/L) and contact time (20, 40, 60, 80, 100 and 120 min), were studied. Adsorption isotherms were analyzed such as Langmuir, Freundlich and Tempkin isotherms to understand the distribution of metal ions between the liquid phase and sorbent. The adsorption kinetic models also studied like pseudo first order, pseudo second order and Elovich models for the adsorption of solute from liquid solution. It was concluded that the optimum pH was 5.8, adsorbent dose was 10 g/L and contact time 2 hours.

Ju Okoli et al, [93] investigated the removal efficiency of toxic heavy metals Cr (IV) by using low cost adsorbents like Coconut husks (ACNH) and Palm kernel fiber (APKF) were prepared by dried in oven at 80°C for 24 hours separately. The removal capacities were found on various parameters such as effect of contact time and effect of initial concentration by the formula for metal uptake was $q_e = V (C_i - C_e) / m$. The adsorption kinetic models like pseudo first order, pseudo second order and adsorption isotherms such as Langmuir and Freudlich models were studied. It was concluded that the Freudlich model was better fit for the adsorption of Cr (IV) by ACNH likewise Langmuir model ($R^2 = 0.941493$) was better fitted for adsorption of Cr (IV) by APKF.

Brahmaiah T et al, [94] utilized rice straw powder as low cost adsorbent made by cut into small segments and washed with distilled water and then dried for 24 hours in an oven after that it was ground as fine powder and then treated with 240 mL of NaOH solution then dried at 100°C for 24 hours in oven. Batch adsorption experiments were carried out by various pH, adsorbent dose, initial Chromium concentration and contact time. The amount of heavy metal ions adsorbed on adsorption was determined by the formula of % Adsorption = C_i - C_f / C_i × 100. Adsorption kinetic parameters like pseudo first order, pseudo second order studied to define the adsorption kinetics about heavy metal ions. It was reported that Legargren pseudo second order model was well fitted for both untreated and treated rice straw adsorbent.

Rehab et al, [95] studied removal efficiency of Cu (II) with peanut hulls powder, it was prepared by first washed with tap water to remove soil, dirt and dust particles and further washed with distilled water and then dried at 60° C in oven for 48 hours, after that grinded into powder, which were separated to various sizes like $<250 \mu m$, $250 \mu m$, 0.3 mm, 0.4 mm and 0.8 mm. The separated powders were applied on various adsorption processes without any other physical or chemical treatment.

The solution of Cu (II) ions made up of 1000 mg of CuSO₄ dissolved in distilled water of 1 liter. The different adsorption parameters were studied such as effect of adsorption time, effect of particle size distribution, effect of dosage, effect of solution temperature and effect of solution pH and initial Concentration. Adsorption isotherm parameters were analyzed to determine the capacity of the adsorption, such as Langmuir and Freundlich adsorption isotherms. Adsorption kinetics also studied like pseudo first order, pseudo second order and intra particle diffusion models. SEM, TGA, XRD, FTIR and BET were analyzed. It was concluded that the Langmuir model was fitted with adsorption data and pseudo second order model was provided a good correlation, it was assumed that the rate-controlling steps might be chemisorption between the adsorbate and adsorbent.

Sadeek et al, [96] utilized three different biosorbents like rice husk, palm leaf and water hyacinth (Nile rose) were prepared by washed with distilled water then dried for 3 days at 50°C, after that the biosorbents were ground and sieved to get the particle size in between 0.5 and 1 mm. The stock solutions such as Cu (II), Co (II) and Fe (II) were made from copper nitrate (Cu(NO₃)₂ 6H₂O), cobalt nitrate (Co(NO₃)₂ 6H₂O) and (FeCl₃ 6H₂O) by dissolving deionized water. The various factors were affecting in adsorption of heavy metals like effect of immersion time (30, 60, 120, 180 and 240 min), effect of pH (7 and 9), effect of initial metal ions concentration and effect of biosorbents chemical structures. Adsorption isotherms such as Lagnmuir and Freundlich models were analyzed and it was reported that the Langmuir model had high correlation (R² above 0.999). The q_{max} values of biosorption capacity for Cu (II) ions like 285.7, 217.4 and 181.8 mg/g in the order of rice husk, palm leaf and water hyacinth. The adsorption kinetics were examined to find the efficiency of the

adsorption mechanisms, such as pseudo first order, pseudo second order, intra particle diffusion models and also differential thermal analysis was studied.

Sami Guiza [97] used Cellulose waste orange peel (CWOP) for biosorption of Cu (II) ions from its salt solution of copper sulphate (CuSO₄ 5H₂O). The adsorbent material was prepared by sliced and crushed then allowed for sieved to get the size of particles was 500 μm. The stock solution of Cu (II) was made by dissolving in double distilled water. The different adsorption parameters were carried like effect of stirring (N = 200 rev/min), effect of initial concentration (10, 20 and 30 mg/L) and effect of cellulose waste orange peel mass (m = 0.6, 1.0 and 1.2 g). The adsorption isotherms and thermodynamic models were carried by Langmuir isotherm constant (K_L). It was concluded that CWOP was pH dependent for adsorption of Cu (II) ions at pH 5. Freundlich isotherm was better with adsorption capacity of Cu (II) ions 63 mg/g. The R_L value of Langmuir isotherm well between 0-1 and spontaneous and exothermic during the thermodynamic study of adsorption of Cu (II) metal ions.

Fouad Krika et al, [98] studied cork biomass as adsorbent for the removal of cadmium metal ions from the solution of Cadmium nitrate (Cd (NO₃).4H₂O) was dissolved by using distilled water. The cork biomass sieved in various diameters of $d_1 < 0.08$; $0.08 < d_2 < 0.1$; $0.1 < d_3 < 0.16$ and $0.16 < d_4 < 0.2$ mm. The batch adsorption experiments were done and the amount of adsorbed metal ions determined by the equation of $q_e = (C_o - C_e)$. V/m. Similarly, the percentage of removal was calculated in the formula of R(%) = $(C_o - C_e)$ 100 / C_o . The effects of contact time (10, 20, 30, 40, 50, 60, 70, 80, 90 and 100 min), particle size (between 0.05 and 0.2 mm), pH (2 to 6) and the biosorption isotherms like Langmuir and Freundlich were studied adsorption kinetics such as pseudo first order, pseudo second order and also

thermodynamic parameters were carried out. It was reported that the cork biomaterial was acceptable for the sorption of toxic metal ions. The equilibrium data of adsorption well fitted with Langmuir and the pseudo second order kinetic model was better for adsorption of cadmium ions. The negative value of ΔG^o referred as spontaneous nature in thermodynamic studies.

Abdunnaser et al, [99] utilized Fava Beans for removal Pb^{2+} , Cd^{2+} and Zn^{2+} ions from aqueous solution. The adsorbent material washed by tap and distilled water and then dried at 80° C- 100° C in oven for 36 to 48 hours. After that, the sample was grinded in mortar and allowed to 250-500 μ m on sieves. The stock solution was made up of 1000 mg/L to get Pb^{2+} , Cd^{2+} and Zn^{2+} ions solution separately and 0.1 M of HCl (or) 0.1 M of NaOH were used to adjusted the pH value. The basic adsorption parameters were studied such as effects of pH, contact time, adsorbent weight and heavy metal ions concentrations. The adsorption capacity for Fava beans in the order of $Pb^{2+}(100\%) > Cd^{2+}(92.86) > Zn^{2+}(36.86)$ in 2 gram of adsorbent dose.

Cheraghi et al, [100] studied the feasibility of sesame waste as biosorbent for Cd (II) ions removal on batch adsorption process. The adsorption kinetics, adsorption isotherms models were carried out and SEM, Energy-Dispersive X-ray (EDX) and FTIR also analyzed. It was concluded that the equilibrium of adsorption possible within 30 min and it followed both kinetic models in the order of Lagergren first order < pseudo second order kinetic models in adsorption process. The best particle size for biosorption was 210 μ m. The optimum value of pH was found as 6. The adsorption isotherms were investigated that Langmuir model was best fitted. The maximum of adsorption (Q_{max}) obtained (84.74mg/g). Desorption and reusability also studied as a

result the biomass for the sesame waste considered to commercial level for the adsorption removal of Cd (II) ions.

Gupta vikal et al [101] prepared adsorbent from green algae by washed with double distilled water several time for remove unwanted particles on surface of the green algae, after that the material was introduced in water bath for 24 hours. The 1000 mg/L of stock solution made from 2.876 g of KMnO₄ dissolved in double distilled water and to maintain the pH values 0.1 N H₂SO₄ and 0.1 N of NaOH solutions were prepared. Adsorption experiments were studied like effect of concentration of MnO₄ ions (100, 200, 300, 400, 500, 600, 700 and 800 mg/L) and effect of contact time (3, 6, 18, 24 and 48 hours). The adsorption isotherms parameters like Langmuir and Freundlich models were studied both were fitted with its adsorption data. It was concluded that the adsorption efficiency mainly depending up on the operating variables like concentration of permanganate ions and contact time.

Mohamed Chiban et al [102] used *C. rhizome* and *W. frutescens* for removal of As (V) on adsorption process. The plant parts like leaves and stems were studied in air conditioning for a week, and then cut into small segments, then washed with double distilled water and again dried for 24 hours at 35°C. After drying, the materials were grounded to obtain fine powder. The stock solution of arsenate (As (V)) prepared from 4.164 g of sodium arsenate (Na₂HAsO₄.7H₂O) dissolved in double distilled water. Adsorption experiments have analyzed to calculate the percentage and amount of arsenate ions adsorbed by the formulas like, % removal = $(C_i - C_t / C_i) \times 100$ and $Q_t = C_i - C_t / m \times v$. Adsorption isotherms like Langmuir, Freundlich and Temkin models were studied. Thermodynamic parameters were analyzed like Gibbs free energy (ΔG°) , enthalpy (ΔH°) and entropy change (ΔS°) . It was reported that the maximum

arsenate ions removed at pH 8.0. The % of removal efficiency of arsenate for both dried plants in the order of 91% (3.64 mg/g) for *C. rhizoma* and 72% (2.99 mg/g) for *W. frutescens*. All isotherms models were fitted with equilibrium data and it was observed that endothermic and spontaneous process for both plants adsorbent materials by thermodynamic studied.

Ali et al, [103] derived the biomass adsorbent from cultural collection and it was washed with deionized water then dried at 80°C in oven for overnight. The derived biomass was grinded well to get the particles size of 100 µm by using standard metal sieve. The stock solution of cadmium was made from 1.630 g of cadmium chloride (CdCl₂) dissolved in deionized water. Various batch adsorption processes were carried out such as effect of pH (3, 4, 5, 6, 7, 8 and 9), biomass dose (0.25, 0.5, 0.75, 1.0, 1.5 and 2.0 g), effect of temperature (18, 26, 37 and 45°C), contact time (30, 60, 90 and 120 min) and initial concentration of Cd (40, 60, 100, 150 and 200 mg/L) were studied. Adsorption equilibrium isotherms like Langmuir and Freundlich models were analyzed to find the quantity of Cd metal ions adsorbed. It was concluded that the dry biomass of *S. Plantensis* depending on different parameters. The optimum conditions for Cd metal ions removal by pH 8, biomass 2 g, incubation at 26°C, contact time 90 min and Cd concentration 60 mg/L. The experimental data fitted with the Langmuir model and *S. Plantensis* dry biomass had potential removal efficient for Cadmium metal ions.

Mohamed et al, [104] used marine green algae (*Ulva lactuca*) powder had utilized as adsorbent for the removal of Cd²⁺ ions. Different adsorption factors were carried out such as pH (2, 3, 4, 5, 5.5, 6, 7 and 8), biomass amount (0.05, 0.1, 0.2 and 0.4 g), initial Cd²⁺ concentration and biomass adsorbent character studied like SEM, FTIR were analyzed and also biosorption of isotherm models, desorption of Cd²⁺ metal

ions have been studied. It was reported that the pH 5.5 chose as the compromised level for removal percentage, 0.1 g of biosorbent weight was got highest percentage of removal and Cd²⁺ ions concentration from 7 and 10 mg/L have more efficient with 30°C was optimum temperature. The biosorption of equilibrium data were fitted as very well for Langmuir and Freundlich isotherm models and the FTIR spectrum have confirmed the biomass functional groups. The desorption studies suggested that the regeneration was possible to reuse for adsorption of Cd²⁺ ions. Finally, concluded that the *U. lactuca* can utilized as eco-friendly biosorbent to remove Cd²⁺ ions from its aqueous solutions.

Sadia Waseem et al, [105] studied the removal efficiency of Pb (II) and Cd (II) by *A. nilotica* leaves. It was prepared by washed with distilled water and dried in sunlight and followed dried at 50°C in an electrical oven. Then the biomass grounded as powder using electrical grinder and sieved to get 100 µm of particle size for using in the process of adsorption. The Cd (II) and Pb (II) stock solutions were prepared by dissolving 1000 mg/L of Cd(NO₃)₂.4H₂O and Pb(NO₃)₂ respectively. The batch adsorption experiments have done to find the adsorption behavior of Cd (II) and Pb (II) metal ions. Adsorption isotherms, kinetic models and thermodynamic parameters also studied, as a result it was concluded that it was followed Langmuir and Freundlich models, the adsorption process found to be spontaneous and endothermic and the adsorption kinetics followed pseudo second order model.

Fatima Ouadjeniu et al [106] investigated the removal efficiency of Cu(II), Cd(II) and Cr(III) by using dam silt powder material in the size of 75 μm. The 1000 ppm of stock solutions of Cd(II), Cu(II) and Cr(III) were prepared by dissolved in 1 liter of deionized water in 2.368 g of C₄H₆CdO₄.2H₂O₇, 3.8 g of Cu(NO₃)₂ 3H₂O and

5.124~g of CrCl $_3$ 6H $_2$ O respectively. The batch adsorption processes have been studied and adsorption isotherms models like Langmuir, Freundlich, Langmuir-Freundlich and Dubinin-Radushkevich (R-D) models. It was reported that maximum metal ions sorption capacity in the order of Cr(III) (26.31~mg/g) > Cu(II) (11.76~mg/g) > Cd (0.35~mg/g) by the dam silt powder.

Ali et al [107] studied the removal of copper metal ions from its aqueous solutions by using micro algae (Cyanobacterium) *S. plantensis* biomass was collected from its culture medium and allowed to rinse with deionized water for the removal of residual alkalinity. After that, it was dried at room temperature in an oven for 24 hours and then at 80°C for 12 hours. The dried biomaterial was grinded to obtain the powder in the size of 0.45µm. The 1000 ppm of copper metal ions stock solution prepared by 2.51 g of CuSO₄5H₂O salt was dissolved by using 1 liter of deionized water. The various required concentration of copper solutions were made by dilution and the initial pH was adjusted with dilute solution of HCl and NaOH. The batch biosorption studies have carried out like effects of biomass dose (1.5, 1.0, 0.75, 0.5, 0.25, 0.2, 0.150, 0.100, 0.050, 0.025 and 0.02 g), contact time (30, 60, 90, 120, 150 and 180 min), temperature (20, 26, 37, 45, 55 and 60°C), pH (2, 3, 4, 5, 6, 7, 8, 9 and 10) and initial concentration of copper (10, 40, 50, 60, 100, 150 and 200 mg/L). It was concluded that the dried biomass had high efficient for removing 90.6% of copper ions within 90 minutes with an eco-friendly process.

Hassan Rezaei [108] used *Spirulina sp.* for the removal of chromium metal ions from its aqueous solution. The biomass was obtained from cultural crops and it was dried at 60°C for 24 hours in an oven and then sieved to get less than 1mm. The initial pH of chromium metal solution was altered by using 0.1 M of HNO₃ and 0.1 M of

NaOH solutions. The adsorption of chromium metal ions was significantly affected by various adsorption parameters. The adsorption equilibrium isotherms, kinetic modeling have been studied and additionally FTIR and SEM studies were analyzed to find the properties of adsorbent biomass. It was reported that the optimum pH was 5 and temperature was 25°C for the removal of chromium metal ions by the biomass of *Spirulina sp.* The biosorption followed both isotherms, but the Freundlich model was better with $R^2 = 0.997$ than the Langmuir model. The R_L values indicated that it was favorable (0 < R_L < 1) adsorption between adsorbent and adsorbate. The FTIR revealed that the presence of NH and OH groups with carbonyl group represented the presence of amino acid in the biosorbent. The SEM clearly exhibited the biosorption of chromium metals by biomass.

Suresh Kumar Halnor [109] investigated the adsorption removal of chromium (IV) metal ions by $Syzygium\ cumini$ plant leaves (SCLP). The plant leaves dried and made as powder form and then it was washed, filtered and followed by treating with 0.1N HCl for 30 min and then washed with water then dried in hot air oven at 100° C. The stock solution of Cr (IV) was obtained from potassium dichromate. It was concluded that the adsorption of Cr (IV) ions using SCLP depends upon pH, initial concentration and adsorbent dose. The maximum adsorption capacity occurred in 1gram of dose and pH 2. The R_L ($R_L = 0.000476$) values of adsorption isotherms indicated that the adsorption was favored.

Akbar Esmaeili et al, [110] have been studied that the *G. corticata* (red marine macroalgae) and *S. glaucescens* (brown algae) were utilized for the removal of Hg (II) ions from its aqueous solutions. These collected two algae were rinsed more times by using tap water for removal of sand and dirt particles. The biomass dried on sun light

for 5 days and then ground to get the particle size of 0.5 -1 mm. The experimental stock solution of Hg²⁺ was made by using deionized water to dissolve 0.37 g of Hg(CH₃COO)₂3H₂O. The various kind of basic parameters were examined and then adsorption isotherms and also adsorption kinetic models have been analyzed. It was concluded that the adsorption equilibrium data was correlated with Freundlich model for both adsorbent biomass and that the biomass of *S. glaucescens* followed by first order, similarly *G carticata* biomass obeyed second order by the kinetics studies observed.

Khairia et al [111] utilized cortexes of banana, tangerine and kiwi used as biosorbent powders were derived in different size of particles after the treatment of 0.5 N strength of NaOH. The adsorption capacity could be calculated by the equation of $q_e = P_o - P_e / W \times V$ and the percentage of metal removal was Obtained by $(P_o - P_e) / P_o \times 100$. It was concluded that the alkalinization have been created as an active surface area with negative sites, that was used to binding with heavy metal ions. The optimum pH was 6.0 in adsorption of heavy metal ions likes Cd^{2+} , Cr^{3+} and Zn^{2+} for all three fruit cortexes. The experimental results reported that the three heavy metal ions were fitted very well with Langmuir equation and it was followed pseudo second order model by adsorption kinetic studied.

Sfaksi et al, [112] examined the adsorption efficiency of cork waste for the removal of Cr (VI) metal ions by batch adsorption methods like particle size effect (d: 0.16 < d < 0.2; 0.1 < d < 0.16; and <math>d < 0.08 mm) pH effect (1, 2, 3, 4 and 5), initial Cr(VI) concentration (0.5 – 500 mg/L) and temperature (25, 35 and 45°C). The BET have been analyzed to measure the surface area of the cork waste and FTIR studies indicated clearly about the complex nature of the cork waste. The adsorption

equilibrium and kinetic models were studied to determine the adsorption capacity. It was concluded that the pH was most influence on Cr (VI) ions adsorption with cork biosorbent. The maximum adsorption (97%) of Cr (VI) occurred between the pH 2.5 and 3.0 and the multilayered of adsorption was formed by the confirmation study of adsorption kinetic mechanisms.

Adsorption of dyes by Biomaterials

Nowadays a huge number of biosorbents have been utilized to removal of dyes, such as *Daucus carota* [113] studied carrot leaves and stems powder have been used after washed and dried in hot air oven at 60°C respectively. The size of the particles 100-150 µm of materials utilized for the possibility to remove the cationic dyes like methylene blue (MB) and malachite green (MG). Different batch adsorption experiments were carried out to explored by carrot leaves powder (CLP) and carrot stems powder (CSP) onto methylene blue and malachite green in order to understand the adsorption process, Lagergran's pseudo firs order, Ho's pseudo second order model and Weber-Morris intra particle diffusion models were analyzed to observe the experimental data, as a results pseudo second order and intra particle diffusion models were best described about adsorption process and the thermodynamic studies indicated that it were spontaneous, exothermic and physical in nature on adsorption process in the order of CLP-MB > CSP-MB > CLP-MG > CLP-MG.

The biosorbent of *Kappaphycus alvarezii* (EKA), *Gracilaria salicornia* (EGS) and *Gracilaria edulis* (EGE) [114] were obtained from seaweed by ethanol activation. The EKA, EGS and EGE were utilized to find the removal efficiency onto Rhodamine B (RB) in aqueous solution. Biosorption experiments were done likes biosorbent dose (0.025 - 0.15 g), initial concentration of RB (10 - 50 mg/L) and contact time (up to

120 min). The supernatant solutions was filtered from biosorbent and then their concentration determined by UV-Visible spectrophotometer. The biosorption equilibrium and kinetic models were analyzed, as a result Langmuir model has higher adsorption properties for ethanol activated biosorbents such as 112.35 (EKA), 105.26(EGS) and 97.08 mg/g(EGE) compared to raw biosorbents 9.84(KA), 11.03 (GS) and 8.96 mg/g (GE). Biosorption of kinetic model concluded that the pseudo second order model was better fit for Rhodamine B dye.

Solanum tuberosum plant wastes [115] were studied potato leaves powder (PLP) and potato stems powder (PSP) have been prepared by washed double distilled water for remove dust impurities. Leaves were dried in room temperature, subsequently in hot air oven at 60° C and then the stems were boiled for 45 min in the presence of double distilled water to separate the fibers then dried in oven at 60° C to make as powder for both cases, in the range of particles size between 100-150 μ m. The stock solutions of methylene blue (MB) and malachite green (MG) dyes made up of 1000 mg/L for both case by dissolved in double distilled water. It was reported that the adsorption of MB and MG onto PSP and PLP preferred at pH higher than pH_{pzc} by the determination of pH_{pzc} and studied the kinetic data of adsorption fitted with pseudo second order and intra particle diffusion models. The adsorption equilibrium data were matched with Langmuir and Freundlich models and the capacities of the various systems on adsorption in the order of PLP-MB (52.6 mg/g) > PSP-MB (41.6 mg/g) > PLP-MG (33.3 mg/g) > PSP-MG (27.0 mg/g). Thermodynamic study also explored that it was exothermic, spontaneous and physical in nature.

Haloxylon recurvum stems [116] has been studied, the plant stems were used as a potential biosorbent for the removal of Methylene Blue dye. In this studied, for the

method of preparation of biosorbent, their stems were cut into small segments and then thoroughly washed by tap water for eliminate unwanted dirt, after that dried stems pieces ground by a domestic grinder. In which no chemical or physical treatment followed for the preparation of biosorbent. The initial and final solutions in the each adsorption experimental samples were analyzed by UV-Visible Spectrophotometer for the consideration of sorption occurred by the biomass. The various parameters of adsorption were carried out like effect of pH (2-12), effect of biomass dose (1-10 g/L), effect of contact time (10-350 min) and effect of temperature (290-350 K). It was concluded that it follows Pseudo first order kinetics studied.

Cucumis sativus fruit peel [117], were used raw and chemically treated fruit peel prepared with the addition of Con.H₂SO₄ for 12 hours, and it was sucked in 2% of NaHCO₃ to neutralized. The various parameters such as initial dye concentration, the solution of pH and contact time to obtain the percentage of removal for crystal violet and rhodamine B dyes were conducted. It was concluded that the adsorption equilibrium data were fitted with Langmuir isotherm model and adsorption kinetic model data shown that it was follows the pseudo second order kinetic model exhibited as chemisorptions process.

Coconut coir dust [118] investigated the removal of cationic dye Methylene Blue by adsorprion using Coconut (*Cocus nucifera L.*) coir dust as adsorbent in the range of particle size between 50 to 100 µm for that preparation of adsorbent the coir dust dried at 60°C in oven for 24 hours, further no other chemical treatment for this adsorbent preparation. The adsorption process have been studied as a function of pH from 2-10 adjusted by using 0.1M of NaOH or 0.1 M of H₂SO₄. It was reported that it obeys pseudo second order model by the studied of adsorption equilibrium kinetic

models. It was also concluded that the adsorption process is endothermic and spontaneous in nature by thermodynamic analysis.

Sumanjit Kaur et al, [119] studied the efficiency adsorption of Congo Red dye by Charcoals of Ground Nut and Eichhornia prepared in the method of dried in oven after that a batch adsorption system was carried out through the various parameters like effects of contact time, pH, temperatures, biosorbent dose, Ionic strength, and Initial dye concentrations. The pseudo first order, pseudo second order and Intra particle diffusion models were analyzed to determine the adsorption kinetics as a results reported that it follows pseudo second order model with R^2 =0.99 and more over the adsorption capacity also increases when increasing temperature, it was observed to be 117.6 and 56.8 mg/g Ground Nut Charcoal and Eichhornia Charcoal viz. at 318 K. The equilibrium data was fitted with Freundlich model by the heterogeneous in nature.

Sumanjit Kaur et al, [120] explored that the adsorbent materials Ground Nut and *Eichhornia* Charcoals were prepared by washed with tap water and then washed with double distilled water for removal of suspended impurities, soil, and dust particles after that dried in oven without free excess of air. The charcoals were sieved to remove the coarse particles and to get charcoals in the size of 70-75 μ for both charcoals. The different adsorption parameters were applied to evaluate the adsorption efficiency of charcoals for Basic Blue 9 dye. The Langmuir adsorption isotherm was highly favored by the values of R_L <1 and it was follows pseudo second order kinetic model for the adsorption of Basic Blue 9 dye by the evidence of q_e and R^2 values.

Wood apple shell [121] studied the wood apple shells (*Limonia acidissima*) used as a low cost adsorbent to analyze the removal efficiency of malachite green dye in the form of aqueous solution by the effect of various variables, adsorbent dosage,

initial dye concentration, pH, contact time and temperature were ascertained to investigate the optimal conditions of experiments. The Langmuir adsorption isotherm model was good fitted with 80.645 mg/g than the Freundlich model. The thermodynamic adsorption was concluded that it was demonstrated as a spontaneous and endothermic in nature on biosorption processes and also FTIR, SEM have analyzed to confirmed the malachite green dye adsorption of wood apple shells and observed various surface morphology of the biosorbent.

Casuarina equisetifolia Needle [122], were studied the needle was utilizing after dried in oven at 80°C. The stock solution of Methyl Violet 2B was prepared by dissolving 1 g in 1 liter of distilled water. The various parameters were done such as effects of contact time (10-240 min), initial dye concentration (10,50 and 100 mg/L), pH medium (2-10) and temperature (30,40, 50 and 60°C) for find out the optimizing conditions and calculated the amount, percentage of adsorption by the standard formula $q_e = (C_i - C_e) \text{ V/m}$ and $\% = (C_i - C_e) \times 100\% \text{ /C}_i$ respectively. Thermodynamic variables were investigated like the Gibbs free energy (ΔG°), enthalpy (ΔH°) and entropy (ΔS^{o}). The adsorption isotherm models were also done like Langmuir, Freundlich equations used to describe the removal efficiency of Methyl Violet 2B in sorption process. The adsorption kinetic parameters like pseudo first order, pseudo second order and Weber-Morris Intra particles diffusion were studied to explain the mechanism of the sorption process. It was concluded that Langmuir isotherm and pseudo second order were best fitted in the experimental data with highest adsorption capacity $q_{max} = 164.99$ mg/g. Thermodynamic study exhibited that the sorption was endothermic, spontaneous and physical in nature.

Bengal gram seed husk [123] Seed Husk of Bengal gram thoroughly washed with de-ionized water for the removal of dirty matter and then the dried husk materials was ground to get desired particle size to found the removal efficiency of Seed Husk of Bengal gram by using Congo Red, Direct Turquise Blue 86 and Direct Black 38 dyes.

Saw dust [124] were investigated the adsorption of tartrazine dye by oven treated saw dust for 24 hours at 110°C without any other modifications. The various batch adsorption methods were analyzed such as effect of pH, effect of initial concentration and contact time. The FT-IR study was confirmed the functional groups on the adsorbent and the surface morphology of the saw dust adsorbent by Scanning Electron Microscope analysis. The kinetic parameters of the adsorption also studied like pseudo first order, pseudo second order and Intra particle diffusion model. It was concluded that it follows pseudo second order model. The thermodynamic parameters ΔG° , ΔH° and ΔS° were examined, the value of ΔH° indicated that the removal process was endothermic in nature.

Adejumoke et al, [125] used raw *Irvingia gabonensis* (dika nut) and con.H₂SO₄ treated form of dika nut were studied for the uptake of cationic dye rhodamine B from aqueous solution by dissolving 1 g of rhodamine B in 1000 cm³ of de-ionized water. Batch adsorption was carried out like initial pH, initial dye concentration, adsorbent dosage and temperature. The Langmuir, Freundlich, Temkn and Dubinin-Radushkevich adsorption isotherms were fitted with the adsorption data. Pseudo second order kinetic model of adsorption was better fits for both raw and acid treated adsorbent with respect to the rhodamine B dye adsorption.

Wycliffe Chisutia Wanyonyi et al, [126] were used *Eichhornia Crassipes* (Water hyacinth) as a biomass for the removal of Congo Red from aqueous solution, no chemical treatment for the preparation of biomass. Batch adsorption was studied and also various parameters such as effects of contact time, adsorbent dosage, initial dye concentration and particle size. The results concluded that Freundlich adsorption isotherm model was better fit with high correlation coefficients ($R^2 = 0.923$) than the Langmuir model, multilayer of adsorption occurred by Freundlich adsorption isotherm. The $R^2 = 0.99$ value of pseudo first order kinetic model was confirmed the rate of adsorption.

Kalaiselvi et al, [127] were studied the removal efficiency of Crystal Violet dye by rhizome of *Acorus calamus*. The biosorbent was prepared by washed with tap water and then distilled water after that dried in sun light, subsequently dried in oven at 100°C for 6 hours without any other pretreatment for Crystal Violet biosorption. Different parameters were carried like that effect of biosorbent dosage (50-250 mg/L), effect of pH (2-10), effect of contact time (10-120 min) and initial dye concentration (5-20 mg/L). Biosorption isotherms were studied such as Langmuir, Freundlich, Tempkin, Dubinin-Radushkevich and Harkin-Jura isotherms and also done biosorption kinetics parameters like pseudo first order, pseudo second order and Intra-Particle diffusion models. It was reported that the optimum percentage of removal occurred in range of pH is greater than 7 and the thermodynamics of biosorption indicated as an endothermic process in adsorption of Crystal Violet by the biosorbent rhizome of *Acorus calamus*.

Satish Patil et al, [128] studied various agricultural wastes were utilized in the adsorption of methylene blue dye like Tamarind fruit shell powder (TFSP), Chiku leaf powder (CLP), Coconut coir pith (CCP) and Toor plant leap powder (TPLP) were prepared without chemical treatment. Various parameters carried out with the help of oscillator in 230 rpm at 303 K. The adsorption kinetic models and the Langmuir adsorption isotherm also done in terms of dimensionless constant separation factor, RL (RL = $1/(1+bC_0)$). The reported of the experiments were shown that the adsorption capacities of methylene blue exhibited in the order of CCP > CLP > TPLP > TFSP.

Binglu Zhao et al, [129] were used cationic surfactant-modified and natural peanut husk were utilized as adsorbent for removal of light green dye. A batch mode of adsorption were applied to found the adsorption capacities on modified peanut husk like effect of contact time, solution pH, temperature, concentration of NaCl and CaCl₂ and Light green dye concentration were performed on adsorption. FT-IR and XRD patterns also analyzed as a results observed that the aliphatic carbon content derived from CBP (cationic surfactant hexadecylpyridium bromide) in modified peanut husk (MPH) to adsorb anionic light green and no obvious difference between NPH and MPH by study of XRD pattern. It was concluded that the adsorption was favored in pH 2-4. The pseudo first order and Elovich models done in the kinetic process and Langmuir model was better fitted with the equilibrium data at 303 K and the capacity of the adsorption up to 146.2 + 2.4 mg/g with adsorption process was spontaneous exothermic in nature by the thermodynamic studied. It was promoted us to investigate the removal of dyes from aqueous solution by using natural bio waste material as adsorbent.

Zulkarnain Chaidir et al, [130] investigated the removal efficiency of methyl orange dye from aqueous solution by durian fruit (*Durio Zibethinus Murr.*) seeds in order to find out low cost biosorbent prepared. The biosorbent powder activated by using 0.01 N of HCl acid for one hour and then several times washed to get neutral pH of biosorbent. The various parameters of adsorption were done at different pH of the solution, initial concentration, biosorbent mass, agitation rate, contact time and temperature were studied to obtained the adsorption capacity of the biosorbent using the formula was $Q = (C_0-C_e)$ V/m and also done FTIR and SEM analysis investigated that the functional groups like O-H, C-H and C-O were involved on biosorption and the heterogeneous surface becomes changed as homogeneous, it was demonstrated that the interaction has been done between biosorbent with methyl orange respectively.

Shaik Karimulla et al [131] used bio-sorbent from *Thespesia populanea* and *Pongamia pinnata*'s leaves and stems were cut, rinsed with tap water and subsequently washed with distilled water then dried in direct sun light. The dried biomaterials were grinded as powder to get particle size of < 75 µ and then treated on oven at 105°C that ashes were applied to study the removal of methyl orange by various parameters such as time of equilibrium, effect of pH, optimum equilibration time, sorbent concentration, interfering ions. It was reported that the bio-sorbent extracted the methyl orange dye at pH 3 of polluted water and optimized the maximum removal amount of methyl orange by physicochemical parameters and also investigated that divalent and trivalent co-anions on the fivefold structure of biosorbent more interfering with extraction of dye than the monovalent anions.

Paul Egwuonwu et al [132] investigated the adsorption efficiency of various trees bark like Neem tree, Mango tree and Locust bean tree barks were utilized onto methyl orange and methyl red dyes. The tree barks powder were prepared by washed up to till no colour in the washed water and then bark materials dried at 105-110°C in an air oven for 24 hours after that ground as fine powder by using mixer grinder. The particles screened as 150-212 μm were named as Mango bark powder (MBP), Neem bark powder (NBP) and Locust bean powder (LBP). The batch adsorption were carried like different temperature (303, 308, 313, 318 and 323 K), dye initial concentration (1×10⁻³ - 5×10⁻³ mg/L), pH (2-9) and adsorbent dose (0.5, 1.0, 1.5, 2.0 and 2.5 g) to get equilibrium isotherms. It was concluded that the adsorptive characters like MBP was best for both dyes adsorption, LBP was better than NBP for methyl red, but LBP and NBP were same in adsorptive character for methyl orange, hence LBP and LBP were used an interchangeable material for methyl orange dye adsorption.

Date Palm Fiber [133] were studied to examine the removal of malachite green dye by the date palm fibres (DPF) waste materials were cut, ground and sieved in the size of \leq 63 μ m. The batch adsorption experiments were carried out by using 100 rpm of orbital shaker at 25°C, the adsorbed solutions were separated by using Whatman filter paper (125 mm), dye uptake was measured with the help of spectrophotometer to find out the percentage of dye (MG) removal. It was revealed that the Langmuir and Freundlich isotherms were analyzed for the adsorption equilibrium data and pseudo second order model was better matched than pseudo first order model by the kinetic studied.

Lotus leaf [134] examined to evaluated for the elimination efficiency of malachite green dye on lotus leaf, it was prepared by dried first at room temperature

and then dried at 60°C for 6 hour with the help of hot air oven. The dried leaves ground as powder for using on adsorption process. The malachite green hydrochloride ($C_{23}H_{26}N_2Cl$) was prepared by dissolving in distilled water. The desired concentrations of experimental solutions were derived by successive dilutions. The effect of various experimental conditions were conducted to find out the amount of malachite green dye adsorbed per gram of lotus leaf and also percentage of removal using the formulas of $q_e = V$ ($C_o - C_e$)/m and $R\% = (C_o - C_e / C_o) \times 100$ % respectively. It was reported that the adsorption equilibrium data were better fitted with Koble-Corrigan, Redlich-Peterson and Langmuir isotherm models. The monolayer of adsorption was observed with the removal efficiency of 125.3 mg/g at 316 K and it followed pseudo second order model. The process of adsorption was spontaneous and endothermic in nature and it was suggested that lotus leaf act as an effective inexpensive adsorbent.

Potato peel [135] were investigated the cationic-malachite green dye sorption efficiency were found by potato peel biosorbent, and also done some operational parameters like initial dye concentration (5, 10, 20, 30, 40, 50 mg/L), biosorbent weight (0.25, 0.35, 0.50, 0.75, 1.00 g), pH (2, 4, 8), stirring speed (0, 100, 200, 400, 800 rpm), temperature (25, 35, 45°C), ionic strength in NaCl (0, 0.25, 2.00g) and particle size (0.18-0.50, 0.50-1.25, 1.25-2.00 mm) were studied at constant temperature 25°C other than temperature study. The sorption of kinetic and equilibrium data were analyzed by non-linear method, that was concluded that the Redlich-Peterson model was better than Langmuir model and pseudo-*n*th order was best fitted than pseudo first order and pseudo second order. Potato peel biosorbent can be used as an alternative material to commercially high cost adsorbent.

CHAPTER-IV

MATERIALS AND METHODS

4.1 Experimental Method

4.1.1 Pant collection

Laplap purpureus plant stems (LPSP) were collected from local home garden after harvest at Sevvaypatti village, Karambakudi taluk, Pudukkottai district, Tamil Nadu in India.

4.1.2 Plant Details



Figure: 4.1. Laplap purpureus Plant and its stem powder

Botanical Name : Laplap pupureus

Family : Fabaceae

English Name: Dolichos Bean

Tamil Name : Banthal Avarai

Used Part : Stem

4.1.3 Preparation of Laplap pupureus Stem Powder (LPSP) as an adsorbent

The plant stems were cut into small segments, thoroughly washed with tap water to remove unwanted dirt, sand impurities and then washed by distilled water after that followed by dried in direct sun light for five days. The dried plant stems were ground as fine powder by utilizing domestic grinder and screened to separate the particles of $<90~\mu m$ by using manual (Jeyant Test Sieves) sieves. These separated powder particles were kept in good conditioned air tight plastic bottle for further uses in adsorption studies.

4.1.4 Preparation of Copper [Cu (II) ion] solution

The stock solution of 1000 mg/L of Cu (II) was prepared by dissolving with 1000 mg of measured amount of copper (II) sulphate penta hydrate (CuSO₄.5H₂O) in double distilled water. The Experimental stock solution was diluted for the desired initial concentration.

4.1.5 Preparation of Chromium [Cr (VI) ion] solution

The stock solution of 1000 mg/L of Cr (VI) was prepared by dissolving with 1000 mg of measured amount of chromium sulphate pentahydrate (CrSO₄.5H₂O) in double distilled water. The Experimental stock solution was diluted for the desired initial concentration.

4.1.6 Preparation of Nickel [Ni (II) ion] solution

The stock solution of 1000 mg/L of Ni (II) was prepared by dissolving with 1000 mg of measured amount of nickel ammonium sulphate hexahydrate (Ni(NH₄)₂(SO₄)₂.6H₂O) in double distilled water. The Experimental stock solution was diluted for the desired initial concentration.

4.1.7 Preparation of Bismark Brown R Dye Solution

The Himedia grade of Bismark Brown R dye stock solution was prepared by precisely weighed 1000 mg of Bismark Brown R dye dissolved in 1000 ml of double distilled water. The experimental dye solution was obtained by diluting the stock solution in precise proportions to required initial dye concentrations.

4.1.8 Preparation of Malachite Green Dye Solution

The Himedia grade of Malachite Green dye stock solution was prepared by accurately weighed 1000 mg of Malachite Green dye dissolved in 1000 ml of double distilled water. The experimental dye solution was obtained by diluting the stock solution in accurate proportions to desired initial dye concentrations.

4.1.9 Preparation of Methyl Orange Dye Solution

The A.R. grade of Methyl Orange dye stock solution was prepared by dissolving accurate quantity of 1000 mg of Methyl Orange dye dissolve in 1000 ml double distilled water. The experimental solution was obtained by diluting the stock solutions to the designed initial dye concentrations.

4.2 SORPTION STUDIES

4.2.1 Batch experiment method

Batch experiment method has chosen due to its reliability and simplicity. The batch experiments were performed using 250 ml of Erlenmeyer flasks by taking 50 mL of aqueous solution of dyes and metal ions in Erlenmeyer flasks and predestined amount of biosorbent was introduced in each flasks.

The various experiments have conducted like pH, biosorbent dose, contact time, initial concentration and temperature with individual variable. The experiments were

carried by mechanical shaker machine in 360 rpm for desired time, after that the remaining concentration of supernatant sample solutions were filtered by using Whatman No.40 filter paper to remove the biosorbent and adsorption progress was observed by lambda 35 UV-Visible Spectrophotometer at λ_{max} 420 nm, 620 nm and 500 nm wave length of maximum absorbance for Bismark Brown R, Malachite Green and Methyl Orange dyes respectively and UV-Spectrometer, Systronic PC based double beam Spectrophotometer (2202) was used for Cu (II) (590 nm), Cr (VI) (580 nm) and Ni (II) (460 nm) ions. The dyes and metal ions concentration retained by LPSP biosorbent phase was calculated from the following equation;

$$q_t = (C_i - C_t)V/m$$

Where,

 q_t = The amount of metal ion / dye adsorbed (mg/g) at time t,

 C_i = The initial metal ion / dye concentration (mg/L),

 C_t = The metal ion / dye adsorbed (mg/L) at time t,

V = The volume of solution (mL),

m = The mass 0f the biosorbent (g),

Where, t is equal to contact time of equilibrium, $C_t = C_e$, $q_t = q_e$, then the quantity of metal ions / dyes were calculated by using the above equation.

The percentage of dyes and metal ions removal were calculated from the following equation.

Percentage of Removal =
$$C_i - C_f / C_i \times 100$$

Where,

C_i = Initial Concentration of metal ions/dyes solutions,

 C_f = Final Concentration of metal ions/dyes solutions.

4.3. Adsorption Isotherms

4.3.1. Langmuir isotherm model

The Langmuir isotherm model (Langmuir, 1918) studied about saturated monolayer formation for solute on the surface of the adsorbent [136]. The linear term of Langmuir isotherm model was used in the form

 $C_e/q_e = 1/q_mb + C_e/q_m$

C_e = Equilibrium constant of metal ions/dyes (mg / L),

q_e = The amount of metal ions/dyes adsorbed at equilibrium (mg/g),

 q_m = The constant related to maximum adsorption capacity (mg/g),

b = The Langmuir constant related to energy of adsorption.

From the equation of the linear plot of C_e/q_e versus C_e should be a straight line. It exhibits that adsorption follows the Langmuir isotherm model. The constant q_m and b can be derived from slope and intercept of the plot. The shape of the Langmuir adsorption isotherm can be expressed by dimensionless separation factor, R_L [137, 138]. The R_L values give an idea about the nature of the adsorption process as given below (Table – 4.1).

Table-4.1: R_L Values and Types of Isotherm

R _L values	Adsorption
$R_{L} > 1$	Un favourable
$R_L = 1$	Linear
$0 < R_L < 1$	Favourable
$R_{L} = 0$	Irreversible

4.3.2. Freundlich Isotherm

The metal ions/dye molecules distribution between the solid phase and liquid phase can be explained by means of the Freundlich isotherm model (Freundlich, 1906) [139]. The familiar equation the Freundlich isotherm model is specified on the basis of heterogeneous surface is,

$$q_e = k_f C_e^{1/n}$$

and the linearized form of equation is,

$$\log q_e = \log k_f + 1/n \log C_e$$

Where,

q_e = The amount of metal ions/dyes adsorbed on per unit weight of sorbent (mg/g)

 K_f = The Freundlich constant, which is correlated to calculate of adsorption capacity (mg/g).

1/n = The sorption intensity (mg/L).

 C_e = The equilibrium concentration (mg/L).

Linear plots of log q_e vs log C_e . The K_f and 1 / n values can be derived from the slope and intercept respectively. If value of 1/n lies in between 1 to 10, the linearity of Freundlich plot recommends the formation of multilayer of metal ions/dyes on the biosorbent surface. The Freundlich adsorption coefficients K_f of metal ions/dyes on biosorbent LPSP can find in mg/L from the values of 1/n and K_f .

4.4 Adsorption Kinetics

Adsorption model of kinetic equation have been applied to analysis the experimental data to investigate about mechanism of the adsorption potential rate controlling steps like as mass transfer and then chemical reaction. The transition

properties of batch adsorption process were examined by means of pseudo-first-order and pseudo-second-order.

4.4.1 The Pseudo first-order model

The pseudo-first-order rate expression is described by the equation:

$$dq_t/d_t = k_1(q_e-q_t)$$

Where,

k₁ is the rate constant of pseudo first order adsorption (g.mg⁻¹.mn⁻¹),

qe is metal ion/dyes adsorbed at equilibrium per unit of sorbent (mg/g),

qt are dyes/metal ions adsorbed (mg/g).

The integrated form of above equation becomes as

$$\log (q_e - q_t) = \log(q_e) - (k_{1/2.303})t$$

The adsorption coefficient along with equilibrium capacity can be find out from the linear plot $\log (q_e - q_t)$ versus time (t) indicates a straight line of slope $(k_{1/2.303})$ and an intercept of $\log (q_e)$ [140]. However, if q_e from intercepts does not equal to the equilibrium of the metal ions/dyes uptake, then the reaction is not be as first-order, even though if the plot have high correlation coefficient with experimental values. The correlation coefficient and calculated equilibrium uptake q_e not equivalent to the experimental value of q_e suggesting that as insufficiency of the pseudo-first-order kinetic model to fit well the kinetic data.

4.4.2 The Pseudo second-order model

The pseudo-second-order rate expression based on the sorption capacity of solid phase is generally expressed [141] as

$$dq_t/d_t = k_2(q_e-q_t)^2$$

Where, k₂ is the rate constant of second order adsorption (g.mg⁻¹.min⁻¹), For the same boundary condition the integrated form of the above equation becomes,

$$t/q_t = 1/k_2 q_e^2 + 1/q_e(t)$$

where,

t = contact time (min)

q_e = the amount of metal ion/dye adsorbed at equilibrium (mg/g)

 q_t = the amount of metal ion/dye adsorbed at any time (mg/g)

 $k_2\,$ = The pseudo-second-order from the slope and intercept of the plots of (t/qt) $\label{eq:k2} \mbox{versus t.}$

The pseudo- second- order rate constant k_2 values and correlation coefficient (r^2) values can be determined by the plots. The reasonable degree of agreement between the calculated values and experimental values were found in the pseudo-first-order model compared with pseudo-second-order model.

4.5. Thermodynamic parameters

Thermodynamic parameters such as standard free energy (ΔG°), standard enthalpy change (ΔH°) and standard entropy change (ΔS°) were calculated by means of equilibrium constant change (K_0) with temperature (T). The free energy change can be verified by the following equation [142].

$$\Delta G^{\circ} = -RT \ln Ko$$

Where,

 ΔG° = free energy change of sorption process (kJ/mol),

K_o = equilibrium constant,

T = temperature in (K),

R = universal gas constant.

The free energy change may be represented in terms of enthalpy change of sorption as a function of temperature as follows

$$\Delta G^{\circ} = \Delta H - T\Delta S$$

The adsorption coefficient K_0 can be derived by combined and rearranging above represented two Equations.

$$ln K_0 = \Delta H^{\circ} / RT + \Delta S^{\circ} / R$$

Where,

 ΔH° = standard heat changes of the sorption (KJ/mol).

 ΔS° = entropy change of sorption (KJ/mol).

The standard enthalpy and entropy changes values are calculated from the slope and intercept of linear plot lnK_0 versus 1/T. Thermodynamic parameter values are derived from the above equation for the adsorption of metal ions/dyes on adsorbent. The negative values of free energy changes ΔG° prove the spontaneous nature of sorption of metal ions/dyes on adsorbent and the positive values of ΔH° prove the sorption process of an endothermic nature. The positive values of ΔS° to be evidence for increased randomness at solid - solution interface during the sorption of metal ions/dyes on the adsorbent.

CHAPTER-V

RESULTS AND DISCUSSION

5.1 Removal of Copper (Ii) Ions From Aqueous Solution Using LPSP

5.1.1 Effect of pH on adsorption of copper (II) ions

The effect of pH of the solution is the main factor that directs the adsorption of metal ions on surface of the biosorbent (LPSP) material. The adsorption ability can be attributed at specific pH for the chemical form of heavy metals in the solution. (i.e. Pure ionic metal form or metal hydroxyl form). Additionally, by reason of different functional groups on the biosorbent surface, at which grow to be as active sites for the metal binding at a particular pH, the effect of pH on adsorption can vary substantially. So, an increase in pH may leads to an increase or decrease in the adsorption, as a result different optimum pH values dependent upon the kind of adsorbent. To study the effect of pH on the percentage of removal of Cu (II) ions, the solution pH were varied from 2 to 10 by adding 1N HCl and 1N NaOH to the stock solution, agitation speed 360 rpm, Volume of Cu (II) ions solution 50 mL, pH 7, Temperature 30°C, Time 50 minutes, Cu (II) ions concentration 150 mg/L were constant.. The adsorption of Cu (II) increases upto pH 7, it may be caused by increases the negative charges of the biosorbent surface, its responds to increases the Cu (II) metal binding when increases the pH. However, at the lowered pH the adsorption of Cu (II) metal ions also lowered due the presence of hydrogen ions (H⁺) on biosorbent surface repulsive with Cu (II) metal ions during the adsorption [143,144]. On other hand, when the pH>7 the adsorption of metals are decreases due to occupation of OH ions on the adsorption sites, which hinder the further approach of Cu(II) ions towards the biosorbent surface. From the investigational results, the optimal pH range of adsorption for the Cu (II) ions is 7 as shown in table-5.1.1., and figure-5.1.1.

5.1.2 Effect of biosorbent dosage on adsorption of copper (II) ions

The biosorbent dose is an important variable in metal uptake on adsorption. The effect of biosorbent dose was investigated by varying from 50 to 250 mg, agitation speed 360 rpm, Volume of Cu (II) ions solution 50 mL, pH 7, Temperature 30°C, Time 50 minutes, Cu (II) ions concentration 150 mg/L were constant. The biosorbent dosages have removal efficiency on the adsorption of Cu (II) ions by LPSP are represented in table-5.1.2., and figure-5.1.2. It is exhibited that when the adsorbent dose increases with increase the removal efficiency of Cu (II) ions. This is due to contact surface areas increased with increasing of biosorbent dose. It was more possible for Cu (II) ions onto be adsorbed on adsorption sites and so the adsorption efficiency increased [145]. Therefore, the whole studies are carried out by the biosorbent dosage of 200 mg.

5.1.3 Effect of contact time on adsorption of Copper (II) ions

In batch adsorption process, contact time is one of the most important factors. In the experimental parameters like contact time (10 to 80 minutes), Temperature (30°C), pH 7, adsorbent dose 200 mg, initial copper ion concentration 150 mg/L and agitation speed (360 rpm) were kept constant. It was exposed that the percentage of removal for copper (II) ions increases with increasing contact time up to 50 min and remained constant until 80 min. The maximum removal efficiency was occurring within first 50 min. It was inferred that the contact time influenced the biosorption of Cu (II) ions by biosorbent (LPSP) from aqueous solutions. Therefore, it was noted that the biosorption of Cu (II) ions was very rapid and reaches maximum biosorption within 50 min of contact time, after that the process of biosorption slow because during the

initial stage of Cu (II) ions biosorption a large number of vacant surface area were available compared to that in later stages, which are represented in table-5.1.3., and figure-5.1.3 [146].

5.1.4. Effect of Initial Concentration for Copper (II) ions on adsorption

To study the effect of initial Cu (II) ions on the adsorption level varying concentration (50 to 250 mg/L) under the constant temperature (30°C), pH 7, agitation speed (360 rpm), contact time 50 minutes and 200 gm of adsorbent dose. The removal efficiency for effect of initial Cu (II) ions concentration was obtained from the experimental data which are represented in figure-5.1.4., and table-5.1.4. It shows that when increasing initial Cu (II) ion concentration, the removal efficiency of copper (II) ions decreases. In lower concentration of Cu (II) ions, the number of metal ions less than the available adsorption surface area of the biosorbent. Therefore, Cu (II) ions are easily adsorbed on vacant surface area in lower concentration. On the other hand, as the Cu (II) ions concentration increases, the vacant surface area are filled up and no further adsorption occurs because of saturation of vacant surface area of biosorbent [147].

5.1.5. Adsorption Isotherms

5.1.5.1. Langmuir isotherm model

The Langmuir isotherm model studied about saturated monolayer formation for solute on the surface of the adsorbent [136]. The linear term of Langmuir isotherm model was used in the form

$$C_e/q_e = 1/q_m b + C_e/q_m$$
 (5.1.1)

 C_e = Equilibrium constant of metal ions (mg / L),

 q_e = The amount of metal ions adsorbed at equilibrium (mg/g),

 q_m = The constant related to maximum adsorption capacity (mg/g),

b = The Langmuir constant related to energy of adsorption (L/mg).

From the equation of the linear plot of C_e/q_e versus C_e should be a straight line. It exhibits that adsorption follows the Langmuir isotherm model. The constant q_m (118.76 to 250.63 mg/g) and b (0.0923 to 0.0614 L/mg) can be derived from slope and intercept of the plot (figure - 5.1.5) and the values are shown in table.5.1.6. Furthermore, q_{max} of the LPSP is 118.76 mg/g was compared with the previous studies, which are represented in table – 5.1.10. The shape of the Langmuir isotherm can be expressed by dimensionless factor, R_L [137, 138]. The R_L values give an idea about the nature of the adsorption process, If $R_L > 1$ unfavorable adsorption, $R_L = 1$ linear adsorption, $0 < R_L < 1$ favorable adsorption, $R_L = 0$ irreversible adsorption. In Cu (II) ions removal, the R_L values were 0 to 1 for the present investigation as given in table - 5.1.7. The results point outs the Langmuir isotherms model fitted well for the chosen adsorbate-adsorbent system for the removal of Cu(II) metal ions.

5.1.5.2. Freundlich Isotherm

The metal ions distribution between the solid phase and liquid phase can be explained by means of the Freundlich isotherm model [139]. The familiar equation for the Freundlich isotherm model is specified as

$$\log q_e = \log k_f + 1/n \log C_e$$
 (5.1.2)

Where,

q_e = Amount of Cu (II) ions adsorbed on per unit weight of sorbent (mg/g),

 K_f = The Freundlich constant, which is correlated to calculate of adsorption capacity (mg/g).

1/n = Sorption intensity (mg/L),

C_e = Equilibrium concentration (mg/L).

Linear plots drawn between log q_e versus log C_e . The K_f and 1 / n values can be derived from the slope and intercept respectively and the values are represented in

table.5.1.6. When 1/n lies between 1 to 10 values, the linearity of Freundlich plot recommends the formation of multilayer of Cu (II) on the adsorbent surface. The Freundlich adsorption coefficients K_f of Cu (II) on biosorbent LPSP was found to be 2.5061 to 5.3210 mg/L from the values of 1/n and K_f indicates that LPSP is a beneficial adsorbent in the removal of Cu (II) ions.

5.1.6. Adsorption Kinetics

Adsorption model of kinetic equation have been applied to analysis the experimental data to investigate about mechanism of the adsorption potential rate controlling steps like as mass transfer and then chemical reaction. The transition properties of batch adsorption process were examined by means of pseudo-first-order and pseudo-second-order.

5.1.6.1 The Pseudo first-order model

The pseudo first-order kinetic model expression by the equation:

$$dq_{t}/d_{t} = k_{1}(q_{e}-q_{t})$$
 (5.1.3)

Where,

 k_1 = is the rate constant of first order adsorption (g.mg⁻¹.mn⁻¹),

q_e = is Cu (II) adsorbed at equilibrium per unit of sorbent (mg/g),

 $q_t = is Cu (II) adsorbed at time (mg/g)$.

The integrated form of equation (5.1.3) becomes

$$\log (q_e - q_t) = \log(q_e) - (k_{1/2.303})t$$
 (5.1.4)

A plot log $(q_e$ - $q_t)$ versus (t) indicates a straight line of slope $(k_{1/2.303})$ and an intercept of log (q_e) .[140]

The reasonable degree of agreement between the calculated values and experimental values were found and show in table 5.1.8. pseudo-first-order model compared with pseudo-second-order model. The correlation coefficient for the

adsorption of Cu (II) was found very high ($r^2 = 0.99$) for pseudo-first-order model. This value indicates that, the adsorption capacities (q_e) calculated values is very close to the experimental adsorption capacity (q_e) in pseudo first order, hence the sorption of Cu (II) ions on biosorbent LPSP more favorable by pseudo-first-order kinetic model.

5.1.6.2 The Pseudo second-order model

The pseudo – second – order rate expression based on the sorption capacity of solid phase is generally expressed [141] as

$$dq_{t}/d_{t} = k_{2}(q_{e}-q_{t})^{2}$$
(5.1.5)

Where, k₂ is the rate constant of second order adsorption (g.mg⁻¹.min⁻¹), For the same boundary condition the integrated form of eqs (5.1.5) becomes

$$t/q_t = 1/k_2 q_e^2 + 1/q_e(t)$$
 (5.1.6)

where, the k_2 can be calculated from the slope and intercept of the plots of (t/q_t) versus t. The q_e values of calculated and experimental values for pseudo- second- order and correlation coefficient (r^2) values are presented in table.5.1.8.

5.1.7. Thermodynamic parameters

Thermodynamic parameters such as standard free energy (ΔG°), standard enthalpy change (ΔH°) and standard entropy change (ΔS°) were calculated by means of equilibrium constant change (K_{\circ}) with temperature (T). The free energy change can be verified by the following equation [142].

$$\Delta G^{\circ} = -RT \ln Ko$$
 (5.1.7)

Where,

 ΔG° = free energy change of sorption process (kJ/mol),

 K_0 = The equilibrium constant,

T = temperature in (K),

R = universal gas constant.

The free energy change may be represented in terms of enthalpy change of sorption as a function of temperature as follows

$$\Delta G^{\circ} = \Delta H - T \Delta S \tag{5.1.8}$$

The adsorption coefficient K_0 can be derived by combined and rearranging Eqs (5.1.7) and (5.1.8)

$$ln K_o = \Delta H^o / RT + \Delta S^o / R$$
 (5.1.9)

Where, ΔH° = Standard heat changes of the sorption, ΔS° = entropy change of sorption (KJ/mol). Thermodynamic parameter values are derived from the equation (5.1.8) for the adsorption of Cu (II) ions on LPSP and the values are represented in Table.5.1.9. The negative values of free energy changes (ΔG°) prove the spontaneous nature of sorption of Cu (II) on biosorbent LPSP and the positive values of ΔH° prove the sorption process of an endothermic nature. The positive values of ΔS° could be evidence for increased the adsorption at solid-solution interface during the sorption of Cu (II) metal ions on the biosorbent LPSP.

5.1.8. FTIR Spectrum of LPSP before and after adsorption of Cu (II) metal ions

The FTIR spectrum of LPSP before and after adsorption shows in figures-5.1.9. The stretching vibration of OH, NH, C=O, alkyl CH- and C-X groups were observed. The shifting frequencies Cu (II) ions are 3418, 2918, 1606, 778 and 904 cm⁻¹ respectively upon biosorption on LPJP biosorbent. The above mentioned fundamental frequencies of FTIR indicates clearly the complex nature of biosorbent used in the adsorption study.

5.1.9. X-Ray Diffraction of LPSP before and after adsorption of Cu (II) metal ions

The X-ray diffraction technique is a powerful technique to analyze the crystalline amorphous nature of the adsorbent material. The LPSP before and after

adsorption were recorded in figure-5.1.10. The intense main peak in before adsorption shows that the presence of highly organized crystalline nature of raw LPSP. After the adsorption of Cu (II) metal ions, the intensity of the main peak is slightly diminished and broadens. It reveals that the physical adsorption takes place on the upper layer of LPSP crystalline structure after adsorption of Cu (II) metal ions.

5.1.10. SEM Analysis for Copper (II) Ions on Adsorption

Scanning Electron Microscope (SEM) studies gives an idea about morphological property of the biosorbent (LPSP). The SEM images of unloaded and Cu (II) metal loaded LPSP are represents in figure-5.1.11. On unloaded image of LPSP have uneven and rough surface, it might be possible for loading Cu (II) metal ions on biosorbent (LPSP) surface. After the Cu (II) metal ions sorption, a significant change is viewed in the structure of biosorbent (LPSP) surface. It should be mentioned as a reason for sorption of Cu (II) metal ions. The biosorbent appears to have a rough surface and small pores likes new cavities like particles after the adsorption.

Table: 5.1.1 Effect of pH in Cu (II) ions adsorption, Time 50 min, Volume of Cu (II) solution 50 mL, Concentration of Cu (II) 150mg/L, Biosorbent Dose 200 mg and Temperature 30°C.

Initial pH	Removal Percentage of Copper
2	62.59
3	62.85
4	62.97
5	63.29
6	63.64
7	63.93
8	63.82
9	63.76
10	63.72

Table: 5.1.2 Effect of Biosorbent (LPSP) dose in Cu (II) ions adsorption, Time 50 min, pH 7, Volume of Cu (II) ions solution 50 mL, Concentration of Cu (II) 150mg/L and Temperature 30° C.

Biosorbent Dose	Removal Percentage of Copper
50	42.78
100	49.51
150	57.98
200	63.93
250	63.32

Table:5.1.3 Effect of Contact Time in Cu (II) ions adsorption, pH 7, Volume of Cu (II) solution 50 mL, Biosorbent Dose 200 mg, Concentration of Cu (II) 150mg/L and Temperature 30°C.

Contact Time	Removal Percentage of Copper
10	24.86
20	33.69
30	44.56
40	53.74
50	63.93
60	64.02
70	64.14
80	64.22

Table: 5.1.4 Effect of initial Concentration of Cu (II) ions in adsorption, pH 7, Volume of Cu (II) ions solution 50 mL, Biosorbent Dose 200 mg, Time 50 min and Temperature 30° C.

Initial Concentration of	Removal Percentage of
Copper (ppm)	Copper
50	64.12
100	64.07
150	63.93
200	61.29
250	59.73

Table: 5.1.5 Percentage of Cu (II) metal removal in various initial concentration on LPSP biosorbent

Ci		Removal %			
mg/L	30°C	35°C	40°C		
50	65.49	66.71	67.95		
100	64.37	65.59	66.49		
150	63.93	64.98	66.73		
200	61.29	62.69	65.27		
250	59.73	60.68	63.42		

Table: 5.1.6 Langmuir and Freundlich isotherm parameters for the adsorption of Cu (II) on LPSP

Temp.	Langm	nuir param	eters	Freundlich parameters		
(°c)	q _m (mg/g)	b (L/mg)	\mathbf{r}^2	$K_f \left(mg^{1-n} g^{-1} L^n\right)$	$n(mg^{1-n}g^{-1}L^n)$	\mathbf{r}^2
30°C	118.76	0.0923	0.995	2.5061	1.1287	0.962
35°C	200.83	0.0951	0.983	4.1020	1.1259	0.970
40°C	250.63	0.0614	0.994	5.3210	1.2689	0.974

Table: 5.1.7 Dimensionless Separation factor $(R_{\rm L})$ for the adsorption of Cu (II) on LPSP

(Ci)	Temperature °C			
	30°C	35°C	40°C	
50	0.2874	0.2796	0.3827	
100	0.1669	0.1570	0.2213	
150	0.1157	0.1089	0.1674	
200	0.0953	0.0905	0.1282	
250	0.0694	0.0673	0.1091	

Table: 5.1.8 Kinetics parameter for the adsorption of Cu (II) onto LPSP

Ci	Temp °C	Pseu	do first o	rder	Pseudo second order		
(mg/L)	remp 'C	q _e (n	1g/g)	\mathbf{r}^2	q _e (mg/g)		\mathbf{r}^2
(mg/L)		Cal.	Exp.	1	Cal.	Exp.	1
	30	45.09	46.06	0.9967	46.08	48.15	0.9787
50	35	45.88	46.85	0.9965	46.87	49.87	0.9775
	40	46.63	47.60	0.9959	47.62	49.99	0.9769
	30	89.17	90.14	0.9982	90.16	91.87	0.9795
100	35	89.19	91.16	0.9962	92.18	93.43	0.9772
	40	91.87	92.64	0.9954	92.86	93.97	0.9743
	30	127.30	128.07	0.9985	128.29	129.32	0.9881
150	35	128.03	129.10	0.9974	129.02	129.79	0.9874
	40	131.49	132.36	0.9939	132.48	133.59	0.9824
	30	154.97	155.60	0.9968	155.00	156.89	0.9818
200	35	158.09	169.02	0.9962	159.08	160.71	0.9882
	40	162.35	163.12	0.9959	163.34	164.45	0.9874
	30	175.55	176.32	0.9947	176.54	177.84	0.9762
250	35	180.27	181.14	0.9938	181.71	182.99	0.9751
	40	189.93	190.70	0.9931	190.92	191.97	0.9742

Table: 5.1.9 Thermodynamic parameters for the adsorption of Cu (II) on LPSP

(Ci)	ΔG ^o (KJ/mol)			ΔН°	ΔS°
(mg/L)	30°C	35°C	40°C	(KJ/mol)	(KJ/mol)
50	-4659.04	-5074.28	-5859.49	9.8915	48.1521
100	-4143.79	-4515.78	-4867.59	8.6931	41.5129
150	-3201.63	-3278.42	-3821.79	12.1809	49.5639
200	-2010.14	-2252.89	-4702.93	16.1418	59.7576
250	-1179.58	-1439.76	-3419.91	13.3653	47.8598

Table: 5.1.10 Comparative study of adsorbent capacity in Langmuir constant q_{max} (mg/g) of various biosorbent for Copper (II) ions.

Adsorbent	Adsorbent capacity (mg/g)	[Reference]
Pongamia pinnata leaf	0.495	[148]
Biomass ash	21.74	[149]
Ficus nootalensis Fruits	161.29	[150]
Drogon Fruit peel	92.593	[151]
Sorghum bicolor Agrowaste	4.149	[152]
Sargassum acinaram	34.96	[153]
Sugar cane bagasse	16.085	[154]
Robinia pseudoacacia pods	35.84	[155]
Algal Biomass	49.50	[156]
Aegle marmelos	23.14	[157]
Persimmon Leaf	19.42	[158]
LPSP	118.76	This study

Figure: 5.1.1 Effect of pH in Cu (II) ions adsorption, Time 50 min, Volume of Cu (II) solution 50 mL, Concentration of Cu (II) 150mg/L, Biosorbent Dose 200 mg and Temperature 30°C.

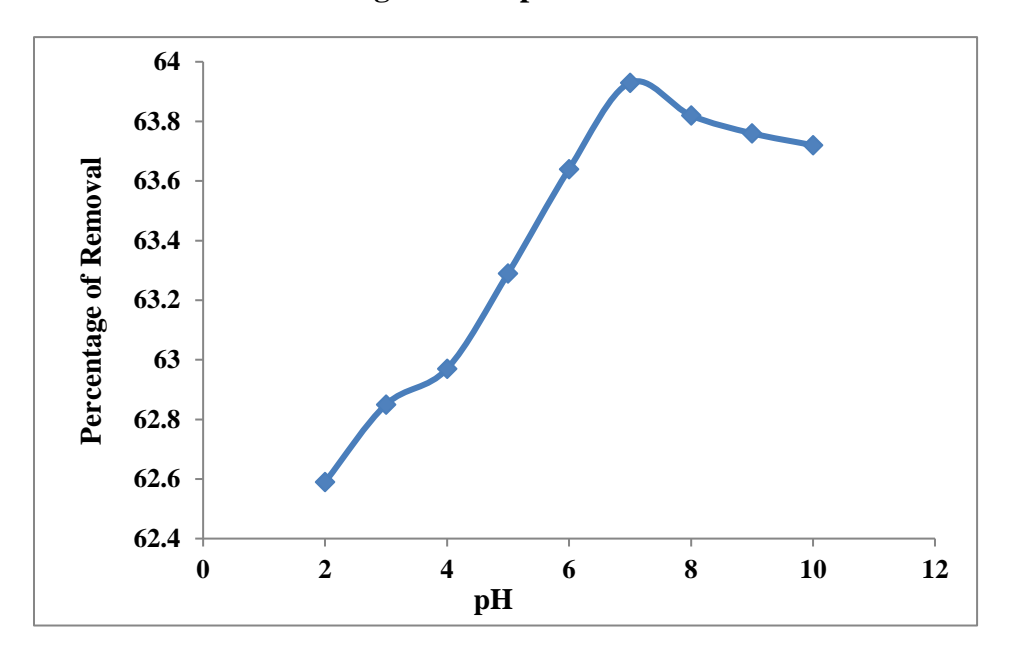


Figure: 5.1.2 Effect of Biosorbent (LPSP) dose in Cu (II) ions adsorption, Time 50 min, pH 7, Volume of Cu (II) ions solution 50 mL, Concentration of Cu (II) 150mg/L and Temperature 30°C.

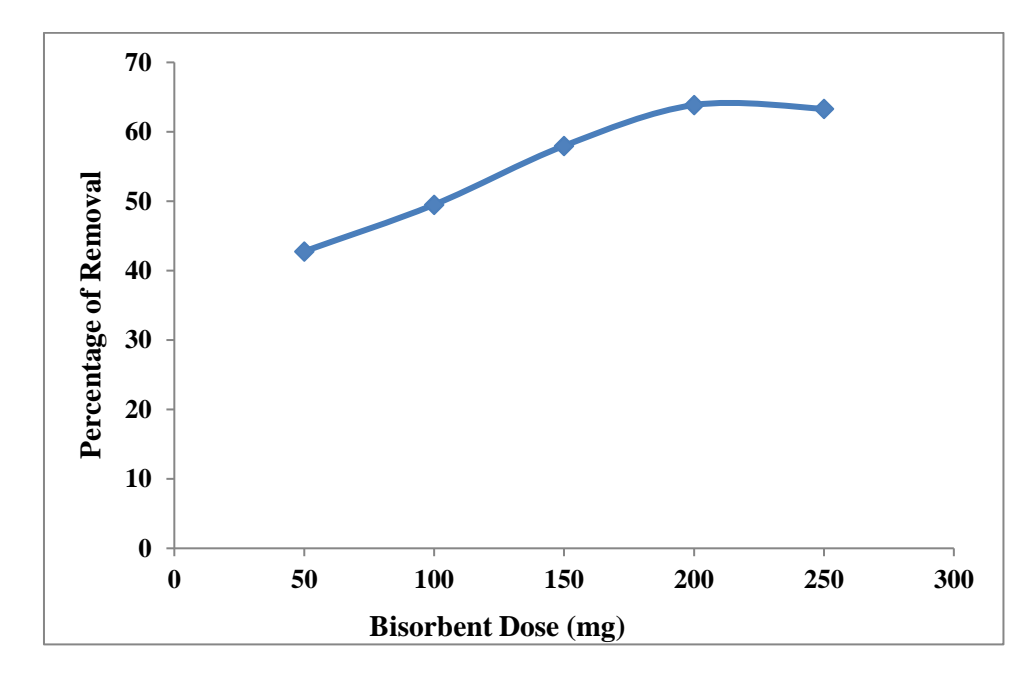


Figure: 5.1.3 Effect of Contact Time in Cu (II) ions adsorption, pH 7, Volume of Cu (II) solution 50 mL, Biosorbent Dose 200 mg, Concentration of Cu (II) 150mg/L and Temperature 30°C.

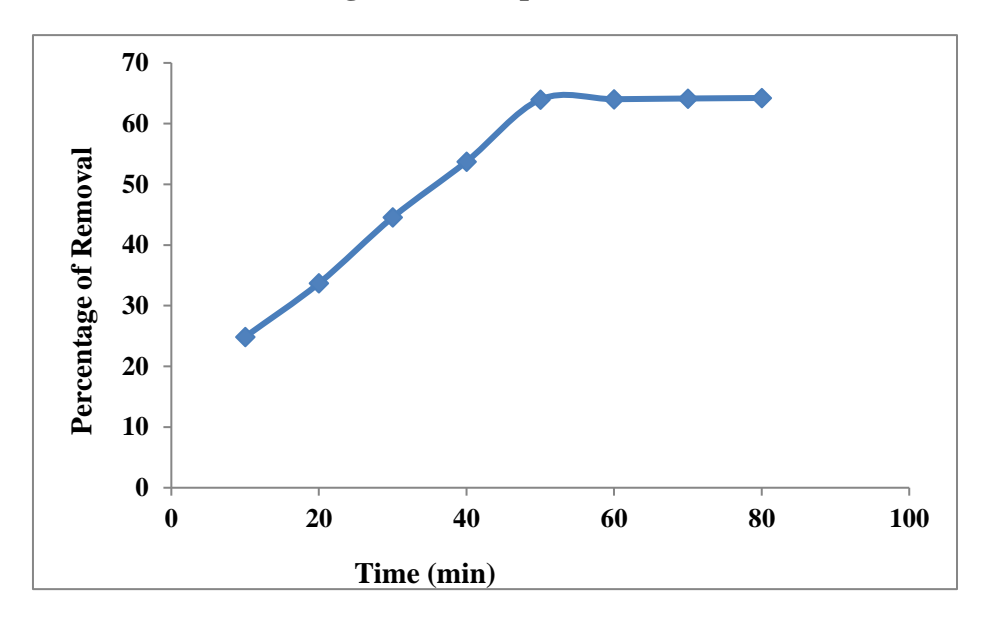


Figure: 5.1.4 Effect of initial Concentration of Cu (II) ions in adsorption, pH 7, Volume of Cu (II) ions solution 50 mL, Biosorbent Dose 200 mg, Time 50 min and Temperature 30°C.

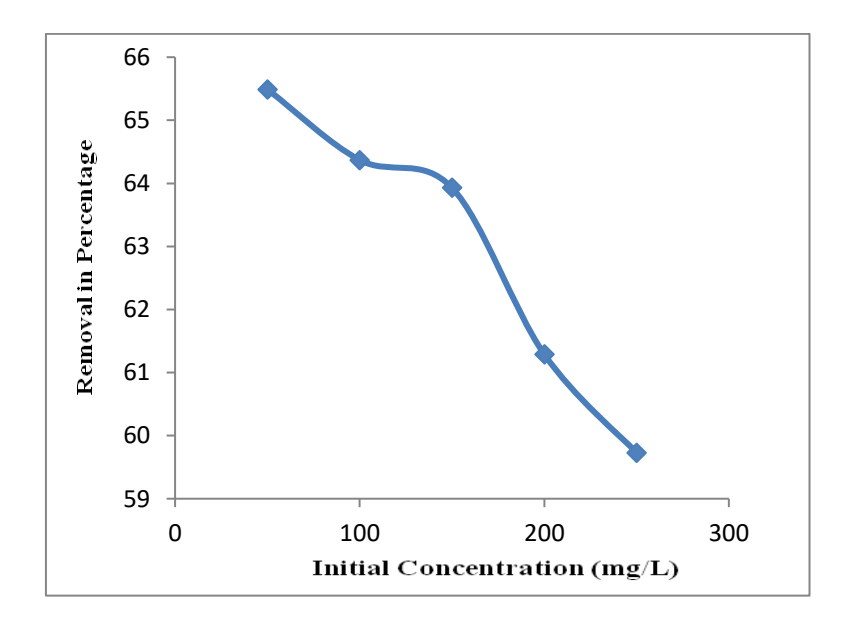
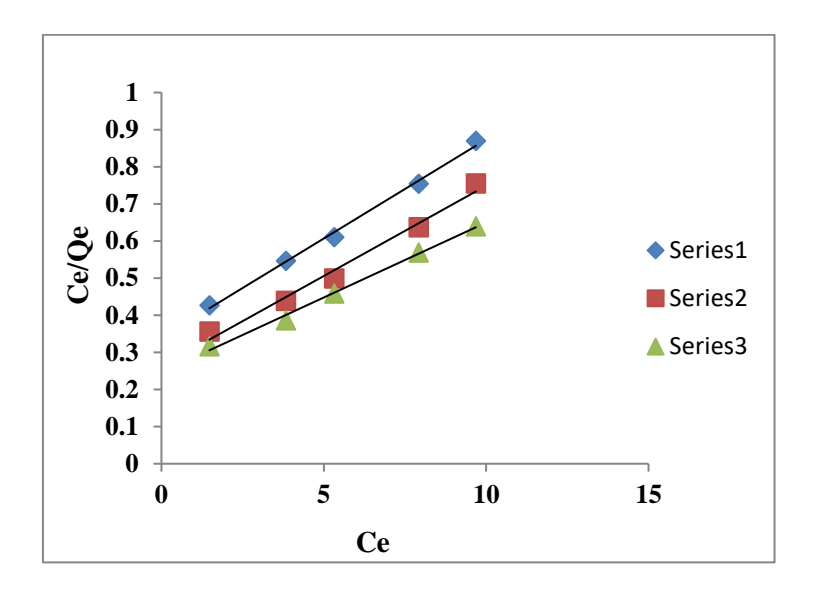


Figure: 5.1.5 Langmuir Isotherm plot for adsorption of Cu (II) metal Ions on

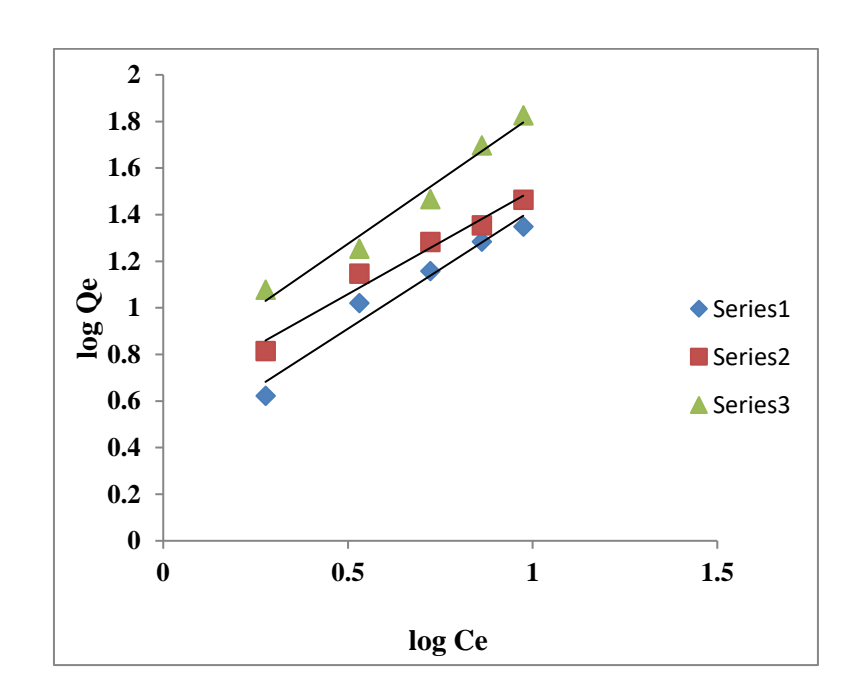
LPSP



30° C Series-1. 35° C Series-2. 40° C Series-3.

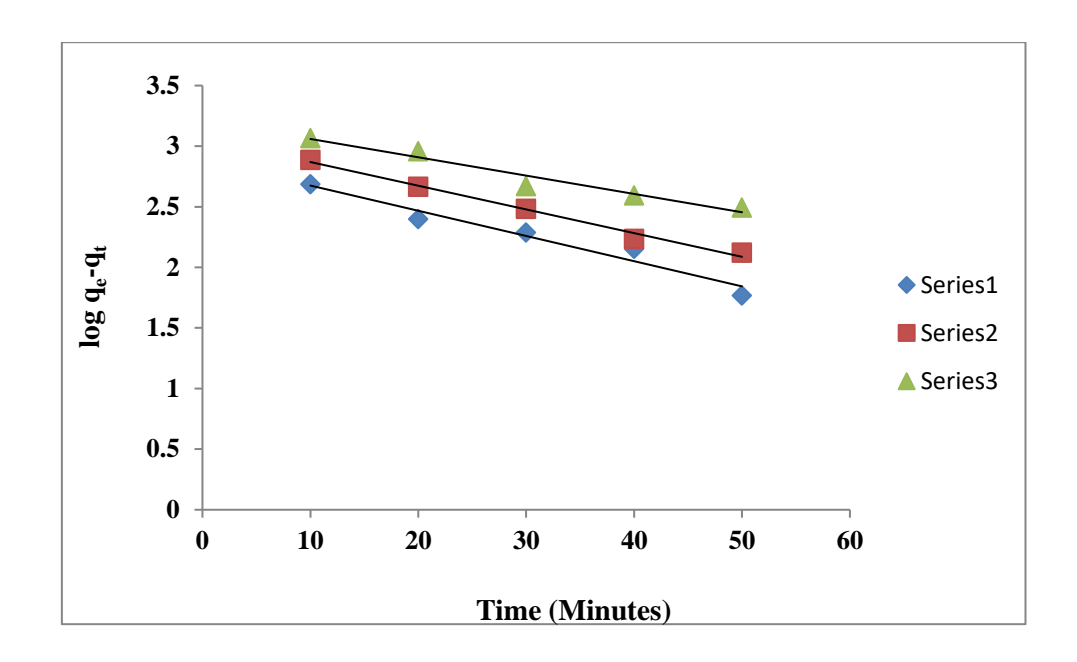
Figure: 5.1.6 Freundlich Isotherm plot for adsorption of Cu (II) metal Ions on

LPSP



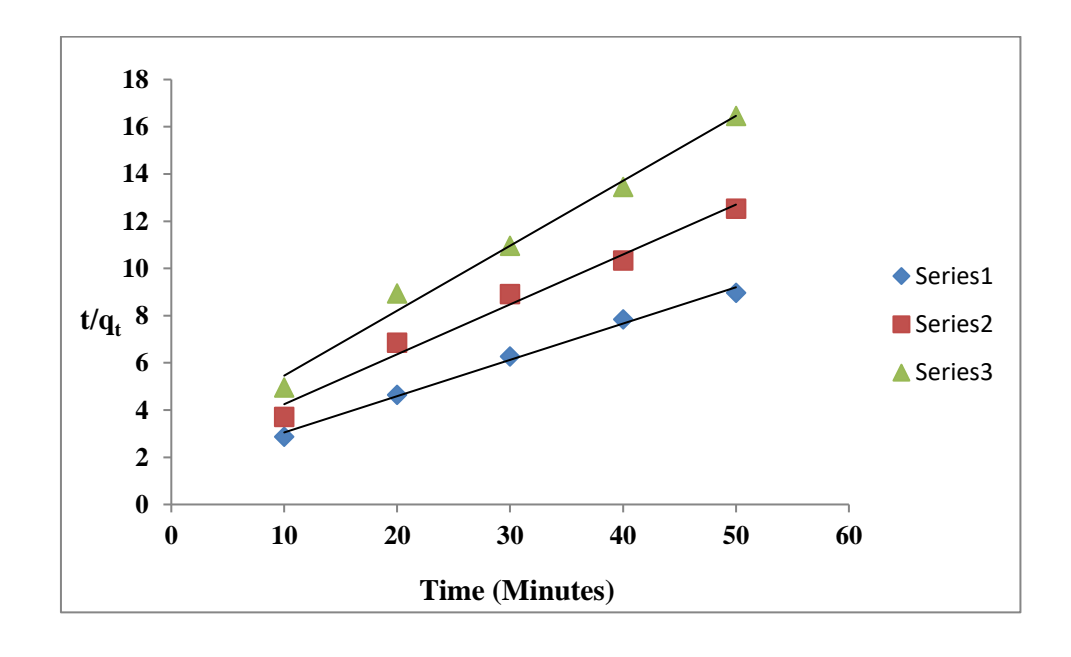
30° C Series-1. 35° C Series-2. 40° C Series-3.

Figure: 5.1.7 Pseudo first order plot for adsorption of Cu (II) metal Ions on LPSP



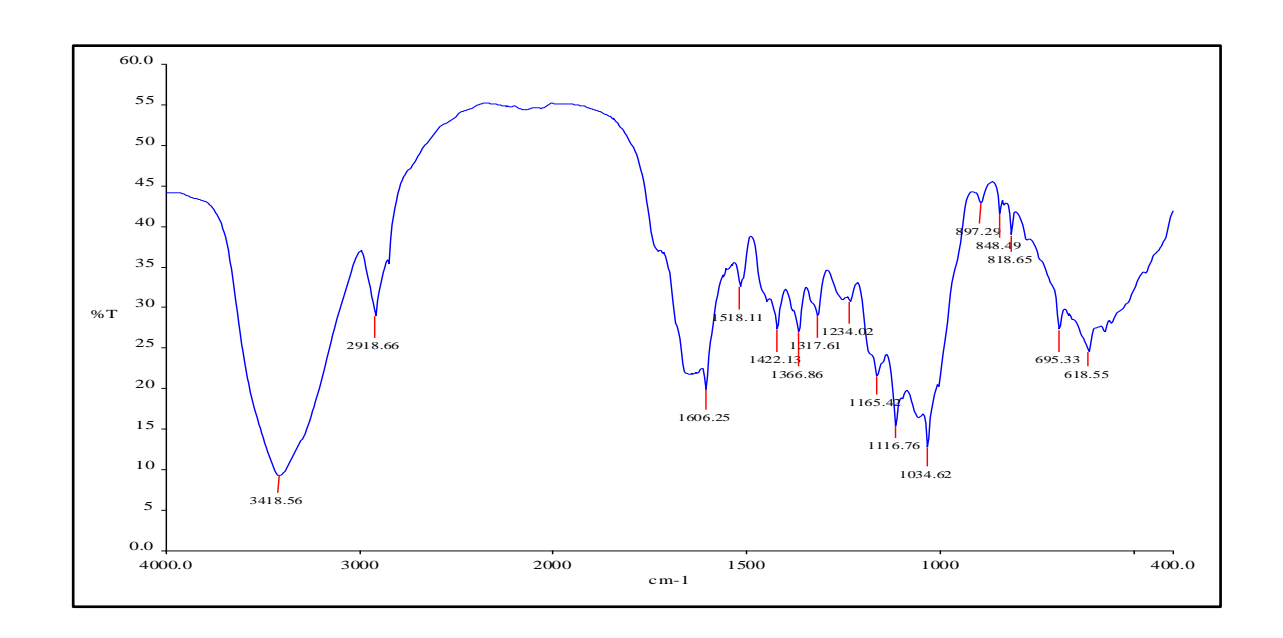
Series 1-100 ppm. Series 2-150 ppm. Series 3-200 ppm.

Figure: 5.1.8 Pseudo second order plot for adsorption of Cu (II) metal Ions on LPSP



Series 1-100 ppm. Series 2-150 ppm. Series 3-200 ppm.

Figure. 5.1.9. FTIR images of LPSP before and after adsorption of Cu (II) metal ions.



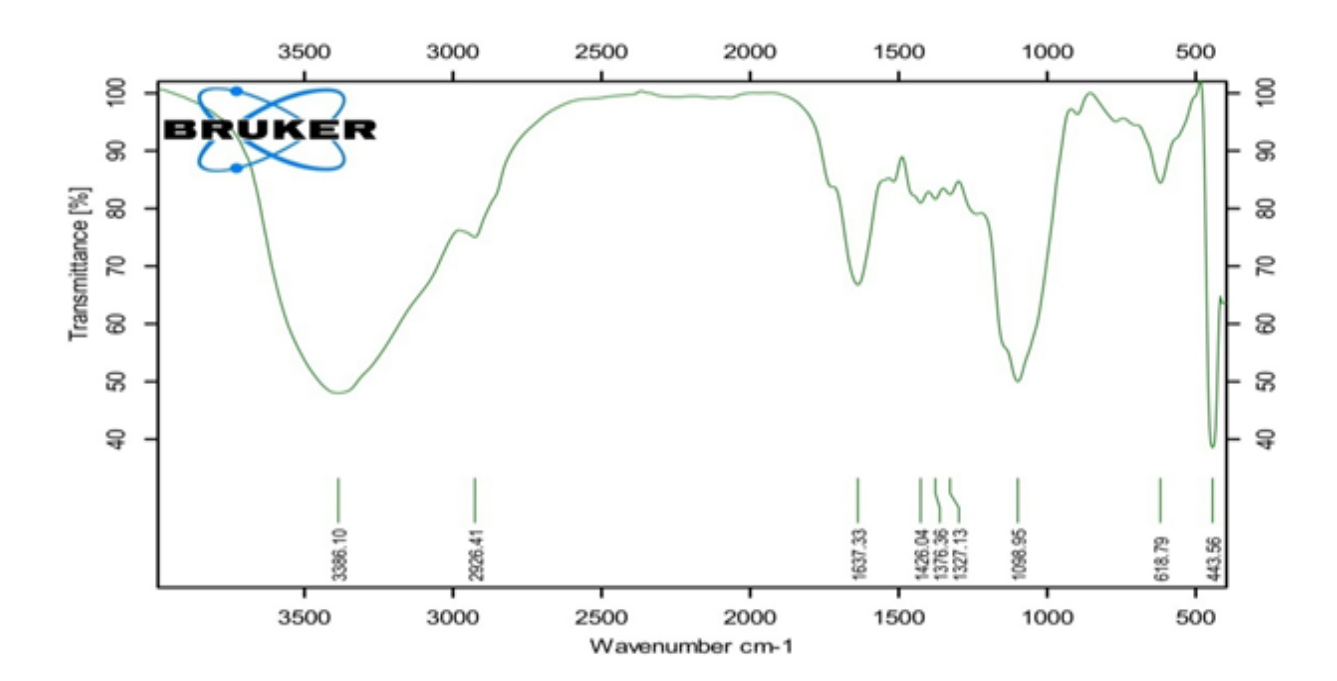
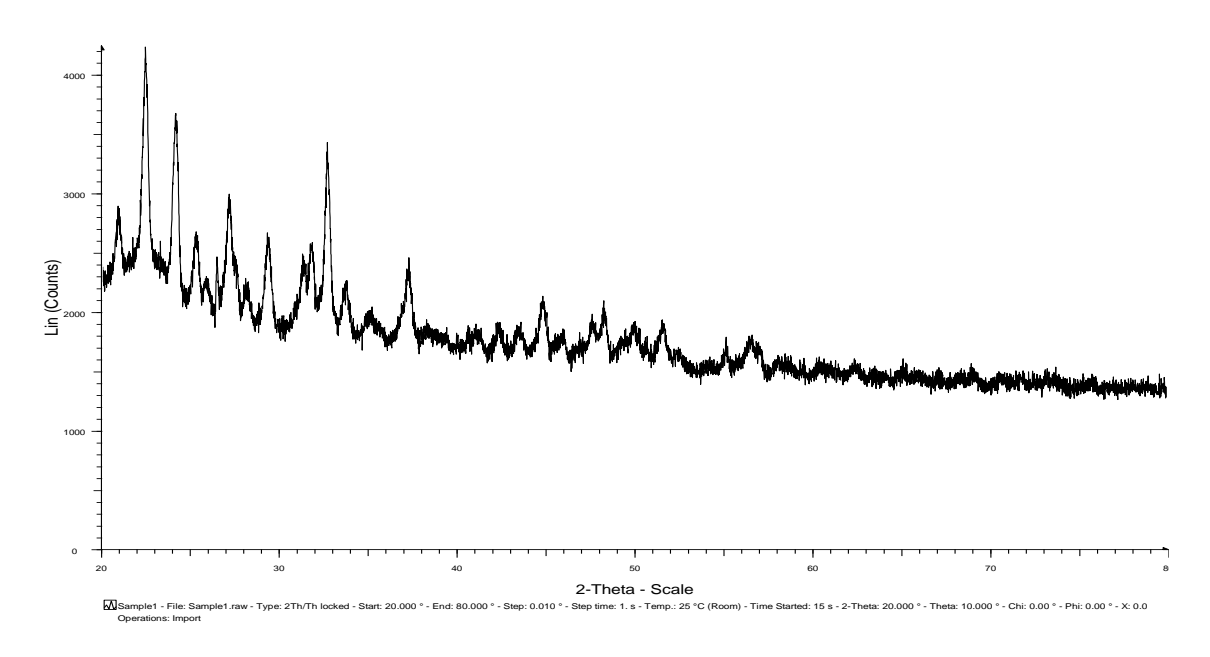


Figure: 5.1.10. XRD images of LPSP before and after adsorption of $Cu\ (II)$ metal ions.



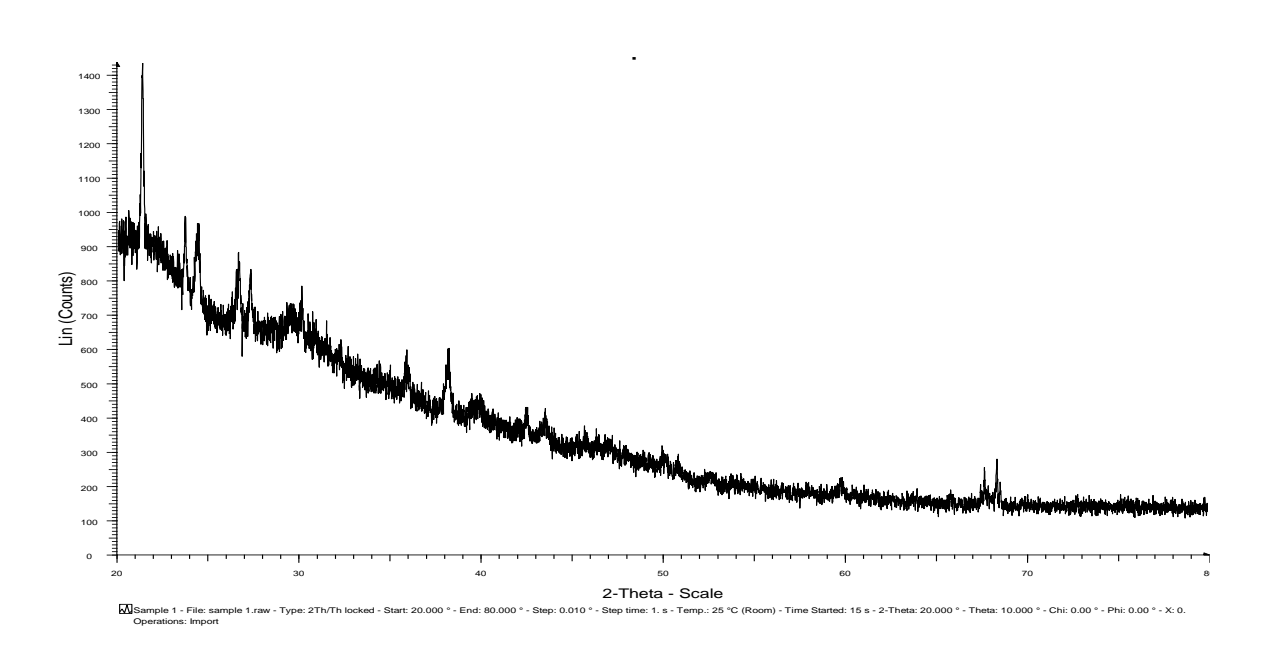
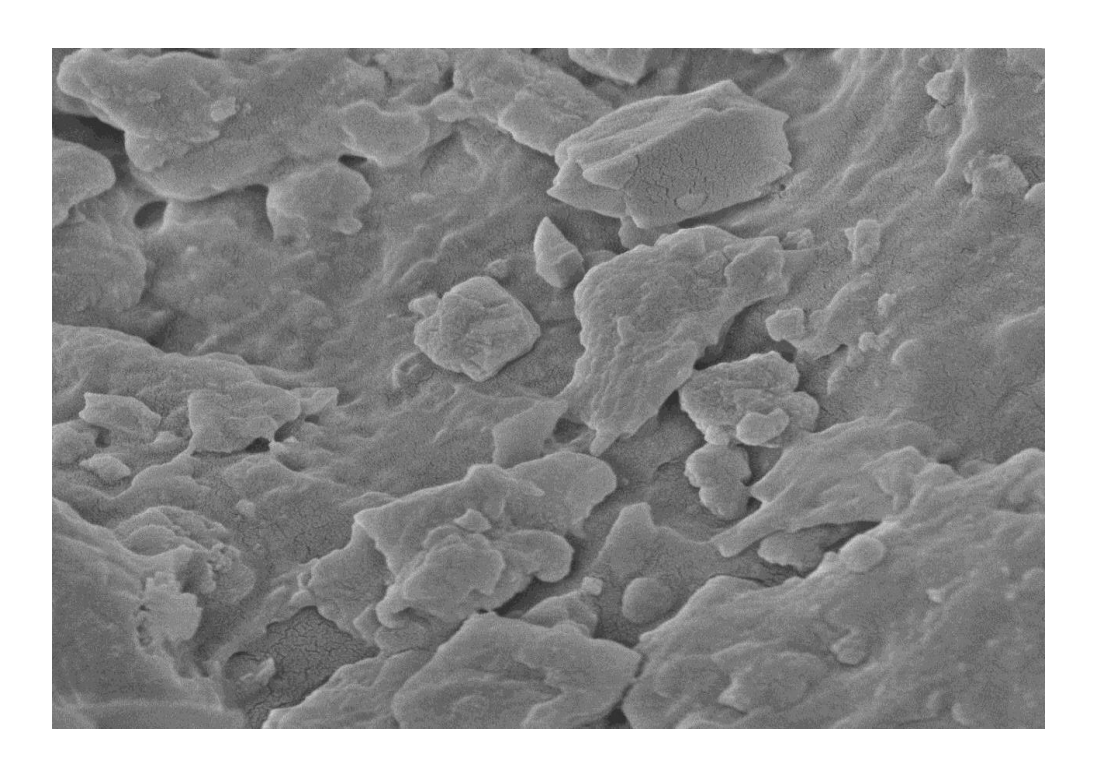
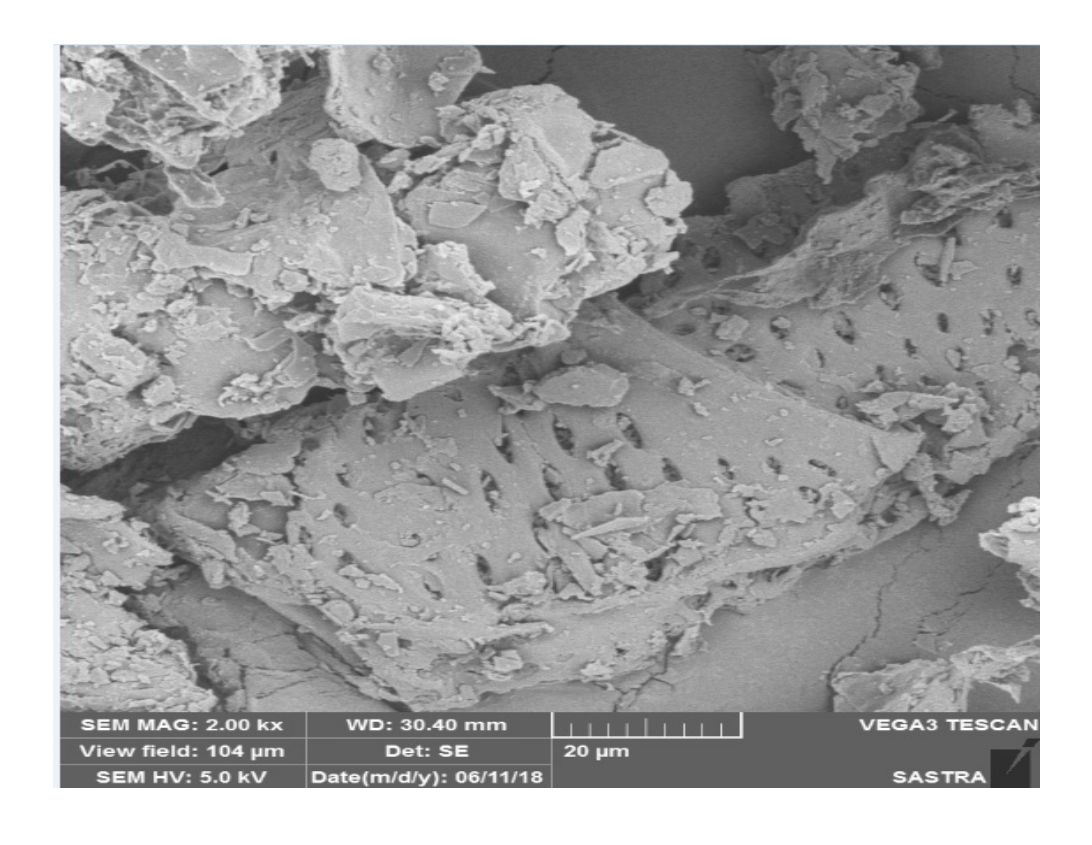


Figure. 5.1.11. SEM images of LPSP before and after adsorption of Cu (II) metal ions





5.2 REMOVAL OF CHROMIUM (VI) IONS FROM AQUEOUS SOLUTION USING LPSP

5.2.1 Effects of pH on Chromium (VI) ion adsorption

The effect of pH was conducted by varying the pH of the solution (2, 3, 4,5, 6, 7, 8, 9 and 10), initial concentration of Cr (VI) metal ion solution 150 (ppm), taction time 50 minutes, temperature 35°C, adsorbent dose 200 mg, 50 ml of Cr (VI) solution and agitation speed 360 rpm. The result shows in figure-5.2.1., and table-5.2.1. that at lower pH 3 maximum (60.59%) removal occurred. Hence, at higher pH 10 percentage of Cr (VI) slightly decrease to 59.27%. It may be due to the surface of biosorbent covered with different functional groups contains hydroxyl and alkyl groups with the increasing pH. The availability of functional group concentration increases which competes with Cr (VI). Therefore, the percentage removal of Cr (VI) slightly decreases at higher pH [159,160].

5.2.2 Effects of LPSP dose on Chromium (VI) ions adsorption

The adsorption of Cr (VI) onto LPSP was studied by varying the adsorbent dosage (50, 100, 150, 200, 250 and 300 mg), initial concentration of Cr (VI) metal ion solution 150 (ppm), temperature 35°C, taction time 50 minutes, 50 ml of Cr (VI) metal solution, agitation speed 360 rpm and pH 3. Figure-5.2.2 exhibits the retention of Cr (VI) ions against the dosage of biosorbent as shown in the graph, the adsorbent LPSP dosage increases while the adsorption of Cr (VI) ions also increases and then a certain value is reached. After a certain dose the adsorption was remains constant significantly and the stability of Cr (VI) on the biosorbent was attained at an adsorbent dose of 200 mg. At equilibrium the removal parentage of Cr (VI) becomes constant due to the saturation of the available adsorbent site on LPSP biosorbent [161].

5.2.3 Effects of taction time on Chromium (VI) ions adsorption

Effect of taction time is one of the main aspects to fix time for analyzes the various parameters. In this parameter, taction time varies like 10, 20, 30, 40, 50, 60, 70 and 80 minutes, Temperature 35°C, pH 3, adsorbent dose 200 mg, initial concentration of Cr (VI) ion solution 150 (ppm), 50 ml of Cr⁺⁶ solution and agitation speed 360 rpm are kept constant. Figure-5.2.3., and table-5.2.3 shows that the biosorbtion efficiency increases with increasing the taction time from 10 to 80 min. Maximum removal percentage for Cr (VI) ions was achieved up to 50 min after that did not change until 80 min. It may be due to that the a large number of surface area available on biosorbent in initial stage, there after it was slowed down later, because of the exhaustion of leftover surface area and repulsive forces between the bulk phase and the solute molecules [162].

5.2.4 Effects of various Concentrations on Chromium (VI) ions adsorption

In the effect of the initial concentration of Cr (VI) ions on the adsorption process varying the concentration likes 150, 200, 250, 300 and 350 ppm under the temperature 35°C, pH 3, agitation speed 360 rpm, time 50 minutes and 200 gm of adsorbent dose. The removal efficiency of the initial Cr (VI) ions concentration was obtained from the experimental data which are represented in figure-5.2.4., and table-5.2.4. The maximum removal possible in 150 ppm it clearly exhibits that the removal efficiency decreases with increasing initial concentration of Cr (VI) ion solution. It may be possible due to immediate saturation of limited obtainable biosorbent sites at higher concentration and the other hand at a lower concentration of Cr (VI) the removal efficiency achieved maximum due to the ratio of available surface sites of biosorbent to the number of moles of Cr (VI) ions [163].

5.2.5 Effects of temperature on Chromium (VI) ions adsorption

Temperature is a great impact factor in the adsorption process. In this experiment temperatures changed from 20 to 45°C, initial concentration of Cr (VI) ion 150 (ppm), under pH 3, agitation speed 360 rpm, taction time 50 minutes and 200 gm of adsorbent dose. In various adsorption experiments, the percentage of removal efficiency is increases when the temperature increases. The changes of removal efficiency of LPSP adsorption for the removal of Cr (VI) as a function of temperature shows in figure-5.2.5., and table-5.2.5., Just as in the previous reports, the Cr (VI) metal ions removal efficiency is slowly improved with the increased temperature of adsorption. However, the changes of temperature had small effect on LPSP adsorption Cr (VI). The percentage removal efficiency was increased only by 4.19% while temperatures changed from 20 to 45°C. Cr (VI) mobility increases at higher temperatures which leads to penetration of the harmful substances into the internal voids of LPSP particles. Thus, the removal efficiency was progressed with increasing the adsorption temperature. However, by further increases in temperature, the presence of inside vacant site pores was almost packed and thereafter the removal efficiency remains stable. The optimization process of the temperature effect was informed to us that continuance increases of the temperature do not bring any important changes in the process of adsorption [164].

5.2.6 Adsorption Isotherm Models

The adsorption isotherm specifies that how adsorbate molecules partitioned between adsorbent and liquid phase at equilibrium as a role of adsorbate concentration. In this learning, equilibrium studies were carried out to understand the character of the

adsorbent of Cr (VI) onto LPSP at equilibrium conditions by considering Langmuir and Freundlich adsorption isotherm models.

5.2.6.1. Langmuir isotherm model

The Langmuir isotherm model was studied about saturated monolayer formation for solute on the surface of the adsorbent in adsorption process [136]. The linear form of Langmuir isotherm model used in the term

$$C_e/q_e = 1/q_m K_L + C_e/q_m$$
 (5.2.1)

 C_e = Equilibrium constant for Cr (VI) metal ions (mg / L),

q_e = Amount of Cr (VI) metal ions adsorbed at equilibrium (mg/g),

q_m = Constant related to maximum adsorption capacity (mg/g),

 K_L = Langmuir constant related to energy of adsorption.

The equation for the linear plot of C_e/q_e against C_e should be a straight line. It indicates that adsorption follows the Langmuir adsorption isotherm model. The constant q_m can be derived from slope and intercept of the plot and the values are shown in table-5.2.7 and figure-5.2.6. It demonstrates that the Langmuir isotherm model fitted well for the chosen biosorbent and adsorbate system with respect to $r^2 = 0.972$ for 35°C. Furthermore, q_{max} of the LPSP is 91.24 (mg/g) was compared with the previous studies and q_{max} values were represented in Table-5.2.11.

The important characteristics of a Langmuir isotherm can be explained in terms of a dimensionless separation factor, R_L [165] which is defined by the following equation:

$$R_L = 1 / 1 + (q_{max} \times K_L)C_o$$
 (5.2.2)

Where, C_0 is the highest initial concentration and the value of separation factor, R_L represents the type of isotherm and nature of the adsorption process. Recognizing

the R_L values as the adsorption can be unfavorable ($R_L>1$); linear ($R_L=1$); favorable ($0 < R_L < 1$) or irreversible ($R_L=0$) [166]. Hence, as the R_L value nearer to zero, the adsorption will be done better. In this experimental study, the R_L value 0.1976 is indicates that favorable adsorption.

The Langmuir adsorption isotherm exhibited that it was fitted well due to high r^2 ($r^2 = 0.972$) value. The results stated that the nature of adsorption was a monolayer, which means a formation of Cr (VI) molecules in single layer on the LPSP adsorbent surface [167]. It was suggesting that the equilibrium adsorption of Cr (VI) onto LPSP might be best demonstrated with the Langmuir isotherm, because of the correlation between experimental and calculated values along with regression factors are in good agreement with Langmuir isotherm, it was exhibited that Cr (VI) was most favorably adsorbed by LPSP.

5.2.6.2 Freundlich Isotherm

The metal ions distribution between the liquid and solid phases can be illustrated by Freundlich isotherm model [139]. It best describes the adsorption onto heterogeneous surface. The common equation for the Freundlich isotherm model is represented as

$$\log q_e = \log k_f + 1/n \log C_e$$
 (5.2.3)

Where,

q_e = Amount of Cr (VI) ions adsorbed on per unit weight of biosorbent (mg/g),

 K_f = Freundlich constant, which is correlated to calculate of adsorption capacity (mg/g).

1/n = Sorption intensity (mg/L).

C_e = Equilibrium concentration for Cr (VI) metal ions (mg/L).

Linear plots drawn between log q_e against log C_e . The values of K_f and 1/n can be derived from the intercept and slope respectively and their values are exhibited in table-5.2.7. When 1/n values lies in between 1 to 10, the linearity of Freundlich plot 'n' values suggests that beneficial adorption for Cr (VI) on the biosorbent (LPSP) surface. These parameters have been determined from a plot log q_e v_s log C_e from the figure-5.2.7. Thus the values of K_f and 'n' were found as 4.1836 and 1.532 respectively at 35° C with r^2 of 0.965.

5.2.7 Kinetic Study

The Kinetics of adsorption studies have been carried out to illustrate adsorption mechanism and diffusion. The generated data had tested by Pseudo first order and Pseudo second order kinetics equation in order to determine the rate of the chromium ion adsorption on the LPSP, which controls the equilibrium time.

5.2.7.1. The Pseudo first-order model

The possibility of adsorption data obtained from Legergran pseudo first-order rate of equation can be described by the following equation:

$$dq_t/d_t = k_1(q_e-q_t)$$
 (5.2.4)

Where,

 k_1 is the rate constant for first order adsorption (g.mg⁻¹.mn⁻¹),

qe is Cr (VI) adsorbed at equilibrium per unit mass of the sorbent (mg/g),

qt is Cr (VI) adsorbed (mg/g).

The combined form of above equation becomes

$$\log (q_e - q_t) = \log(q_e) - (k_{1/2.303})t$$
 (5.2.5)

Figure-5.2.8 represents a plot log $(q_e - q_t)$ verses (t) represents a straight line of slope $(k_{1/2.303})$ and an intercept of log $(q_e)[140]$. The q_e calculated and experimental values given in table-5.2.9.

5.2.7.2. The Pseudo second-order model

This adsorption kinetic model equation developed as pseudo – second – order rate of equation representation is based on the sorption capacity of solid phase is commonly expressed [141] as

$$dq_t/d_t = k_2(q_e - q_t)^2$$
 (5.2.6)

Where, k₂ is the rate constant for pseudo second order adsorption (g.mg⁻¹.min⁻¹), For the same boundary condition the integrated form of above equation becomes

$$t/q_t = 1/k_2 q_e^2 + 1/q_e(t)$$
 (5.2.7)

Where, the k_2 can be calculated by the slope and intercept of the plots of (t/q_t) versus time (t) in figure-5.2.9. The pseudo-second-order adsorption capacity (q_e) values and correlation coefficient (r^2) values have represented in table-5.2.9.

The reasonable degree of conformity between the calculated values and experimental values has been found in the pseudo-first-order model compared with pseudo-second-order model. The correlation coefficient (r^2) for the adsorption of Cr (VI) was found to be very high ($r^2 = 0.986$) in pseudo-second-order model with q_e 46.56 mg/g. It was indicates that, the adsorption capacities (q_e) is very nearer to the calculated adsorption capacity, hence the pseudo-second-order model fitted for sorption of Cr (VI) ions on biosorbent (LPSP).

5.2.8 Thermodynamic parameters

Thermodynamic parameters such as standard free energy (ΔG°), standard enthalpy change (ΔH°) and standard entropy change (ΔS°) were calculated by means of equilibrium constant change (K_{o}) with temperature (T). The free energy change can be verified by the following equation [142].

$$\Delta G^{\circ} = -RT \ln Ko$$
 (5.2.8)

Where,

 ΔG° = The free energy change of sorption process (kJ/mol),

 K_o = The equilibrium constant,

T = The temperature in (K),

R = The universal gas constant.

The free energy change may be represented in terms of enthalpy change of sorption as a function of temperature as follows

$$\Delta G^{\circ} = \Delta H - T \Delta S \tag{5.2.9}$$

The adsorption coefficient K_o can be derived by combined and rearranging Eqs (5.2.8) and (5.2.9)

$$\ln K_0 = \Delta H^{\circ} / RT + \Delta S^{\circ} / R$$
 (5.2.10)

Where,

 ΔH° = The standard heat changes of the sorption(KJ/mol),

 ΔS° = The entropy change of sorption (KJ/mol).

The standard enthalpy and entropy changes values are calculated from the slope and intercept of linear plot lnK_o versus 1/T. Thermodynamic parameter values are derived from the equation (5.2.8) for the adsorption of Cu (II) ions on LPSP and the values are represented in table.5.2.10. The negative values of free energy changes prove

the spontaneous nature of sorption of Cu (II) on biosorbent LPSP and the positive values of ΔH° prove the sorption process of an endothermic nature. The positive values of ΔS° could be evidence for increased randomness at solid–solution interface during the sorption of Cr (VI) metal ions on the biosorbent LPSP.

5.2.9. FT-IR spectrum of LPSP before and after adsorption of Cr (VI) metal ions

The FTIR spectrum analysis provides information about the changes in functional groups on biosorbent (LPSP), the spectra of LPSP before and after the Cr (VI) metal ions adsorption represents in the figure-5.2.10. The FTIR spectrum of biosorbent displays a number of adsorption peaks range between of 400-4000 cm⁻¹, which clearly shows that only a complex nature for LPSP biosorbent. The band at 3418 cm⁻¹ representing –OH groups, the band at 2918 cm⁻¹ corresponding to C-H stretching, the band around at 1606 cm⁻¹ could be assigned to the C=O stretching, the band at 1518 cm⁻¹ and at 1422 cm⁻¹ indicating as CH₂ vibration, the band at 1034 cm⁻¹ indicating C-O stretching. Amongst these adsorption peaks predominantly bonded –OH groups, C=O stretching and carboxyl groups were involved in Cr (VI) ions biosorption [168, 169].

5.2.10. X-Ray Diffraction of LPSP before and after adsorption of Cr (VI) metal ions

The X-ray diffraction (XRD) technique is a powerful technique to analyze the crystalline amorphous nature of the adsorbent material. The LPSP before and after adsorption were recorded as given in figure-5.2.11. The intense main peak in LPSP before adsorption shows that the presence of highly organized crystalline nature for raw LPSP. After the adsorption of Cr (VI) metal ions, the intensity of the main peak is slightly diminished and broadens. This is means that the physical adsorption takes place on the upper layer of LPSP crystalline structure after adsorption of Cr (VI) metal ions.

5.2.11. SEM Analysis for LPSP before and after adsorption of Cr (VI) metal ions

Scanning Electron Microscope (SEM) studies provides the information about morphological property of the biosorbent (LPSP) shows in figure-5.2.12. The SEM image of unloaded LPSP material is represents the irregular and rough surface. After the Cr (VI) metal ions loaded on biosorbent (LPSP) surface, a significant change is viewed in the surface of biosorbent (LPSP). This property should be mentioned as a reason for sorption of metal ions. The biosorbent appears to have small pores like new cavities due to effective adsorption takes place.

Table-5.2.1 Effects of pH for Chromium (VI) ion on adsorption, Time 50 min, Volume of Cr (VI) ions solution 50 mL, Concentration of Cr (VI) 150 mg/L, Biosorbent Dose 200 mg and Temperature 35°C.

pН	Removal Percentage
2	60.43
3	60.59
4	60.51
5	60.47
6	60.31
7	59.98
8	59.67
9	59.49
10	59.27

Table-5.2.2. Effects of LPSP dose for Chromium (VI) ions on adsorption, Time 50 min, pH 7, Volume of Cr (VI) ions solution 50 mL, Concentration of Cr(VI) ions solution 150mg/L and Temperature 35°C.

LPSP Dose (mg)	Removal Percentage
50	39.46
100	45.42
150	54.65
200	60.59
250	60.01
300	60.01

Table-5.2.3. Effects of taction time for Chromium (VI) ions on adsorption, Biosorbent dose 200 mg, pH 7, Volume of Cr (VI) ions solution 50 mL, Concentration of Cr (VI) ions solution 150mg/L and Temperature 35°C.

Taction Time (min)	Removal Percentage
10	21.56
20	30.39
30	41.26
40	50.44
50	60.59
60	60.59
70	60.59
80	60.59

Table-5.2.4. Effects of various Concentrations of Chromium (VI) ions on adsorption, Biosorbent dose 200 mg, Time 50 min, pH 7, Volume of Cr (VI) ions solution 50 mL, and Temperature 35°C.

Concentrations of Chromium (ppm)	Removal Percentage
150	60.59
200	58.22
250	56.63
300	54.16
350	53.28

Table-5.2.5. Effects of various Temperature for Chromium (VI) ions on adsorption, Concentrations of Chromium (VI) ions solution 150 mg/L, Biosorbent dose 200 mg, Time 50 min, pH 7, and Volume of Cr (VI) ions solution 50 mL.

Temperature °C	Removal Percentage
20	56.74
25	59.16
30	60.59
35	60.59
40	60.59
45	60.59

Table: 5.2.6 Percentage of Cr (VI) metal removal in various initial concentration on LPSP biosorbent

Ci	Removal %		
mg/L	30°C	35°C	40°C
50	63.87	64.57	67.74
100	61.42	62.39	65.19
150	59.83	60.59	63.93
200	57.29	58.22	62.76
250	55.34	56.63	61.88

Table: 5.2.7 Langmuir and Freundlich isotherm parameters for the adsorption of ${\rm Cr}\,({\rm VI})$ on ${\it LPSP}$

Temp.	Langmuir parameters		Freundlich parameters			
(°C)	q _m (mg/g)	b (L/mg)	\mathbf{r}^2	$K_f (mg^{1-n} g^{-1} L^n)$	$n(mg^{1\text{-}n}g^{\text{-}1}L^n)$	\mathbf{r}^2
30°C	88.79	0.0893	0.973	2.1587	1.5552	0.962
35°C	91.24	0.0895	0.972	4.1836	1.5320	0.965
40°C	99.82	0.0889	0.978	5.3703	1.6713	0.974

Table: 5.2.8 Dimensionless separation factor (RL) for the adsorption of Cr (VI) ions on LPSP

(C _i)	Temperature °C				
	30°C	35°C	40°C		
50	0.2629	0.2812	0.3251		
100	0.1597	0.1873	0.2192		
150	0.1274	0.1976	0.1772		
200	0.0948	0.1102	0.1148		
250	0.0784	0.0985	0.1188		

Table:5.2.9 Kinetic parameters for the adsorption of Cr (VI) ions on LPSP

C.		Pseu	do first o	rder	Pseud	o second	order
C _i (mg/L)	Temp °C	q _e (mg/g)		\mathbf{r}^2	qe (mg/g)		\mathbf{r}^2
(IIIg/L)		Cal.	Exp.	1	Cal.	Exp.	
	30	31.10	32.14	0.9778	32.59	32.98	0.9956
50	35	33.89	34.85	0.9722	34.56	33.28	0.9955
	40	35.64	36.92	0.9748	36.55	36.25	0.9948
	30	61.18	62.85	0.9769	62.96	62.63	0.9965
100	35	63.20	64.79	0.9758	64.81	63.85	0.9943
	40	69.18	70.23	0.9753	68.94	68.47	0.9947
	30	92.61	93.96	0.9834	93.26	94.20	0.9947
150	35	93.10	94.14	0.9650	95.19	95.69	0.9902
	40	94.52	95.61	0.9829	96.75	96.34	0.9936
	30	122.72	123.59	0.9835	122.78	122.47	0.9987
200	35	125.13	126.66	0.9874	124.86	124.52	0.9972
	40	128.64	127.32	0.9859	128.54	128.59	0.9982
	30	152.56	154.29	0.9754	153.62	154.25	0.9959
250	35	155.26	156.72	0.9782	155.86	155.67	0.9967
	40	158.94	159.54	0.9748	159.71	159.86	0.9989

Table: 5.2.10. Thermodynamic parameters for the adsorption of $Cr\ (VI)$ ions on LPSP

(C _i)	ΔG° (KJ/mol)		ΔН°	ΔS°	
(mg/L)	30°C	35°C	40°C	(KJ/mol)	(KJ/mol)
50	-4558.02	-4972.22	-5758.46	9.7284	46.3241
100	-4042.44	-4416.74	-4766.57	8.5354	41.8927
150	-3101.53	-3176.38	-3720.75	12.1627	45.2632
200	-1910.16	-2150.68	-4601.89	14.1549	44.2379
250	-1069.68	-1337.62	-3418.27	13.7353	43.5485

Table-5.2.11. Comparative study of adsorbent capacity for Cr (VI) metal ions on Langmuir constant q_{max} (mg/g) by various biosorbent.

Adsorbent	Adsorbent capacity (mg/g)	[Reference]
Saw dust	20.70	[170]
S. quadricuada	12.00	[171]
Ficus auriculate leaves powder	13.33	[172]
Banana peel	10.42	[173]
Moringa stenopetala seed powder	09.70	[174]
Trametes versicolor polyporus	45.10	[175]
Sargassum dentifolium	41.20	[176]
Rhizopus sp.	09.95	[177]
Gooseberry seed	19.23	[178]
Laplap purpureus stem powder	91.24	This study

Figure: 5.2.1. Effects of pH for Chromium (VI) ion on adsorption, Time 50 min, Volume of Cr (VI) ions solution 50 mL, Concentration of Cr (VI) ions solution 150 mg/L, Biosorbent Dose 200 mg and Temperature 35°C.

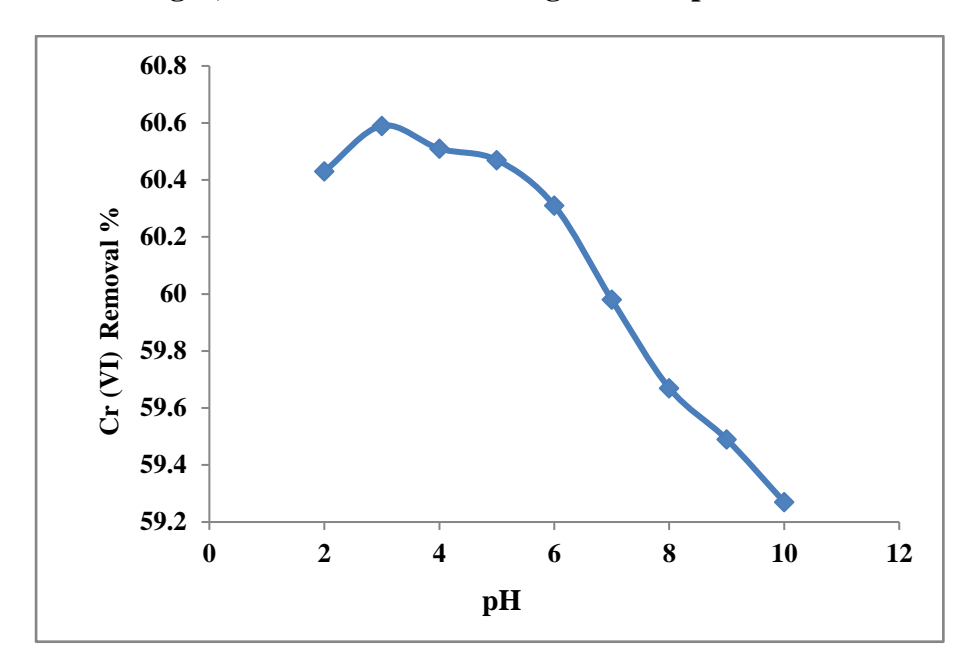


Figure: 5.2.2. Effects of Biosorbent (LPSP) dose for Chromium (VI) ions on adsorption, Time 50 min, pH 7, Volume of Cr (VI) ions solution 50 mL, Concentration of Cr(VI) ions solution 150mg/L and Temperature 35°C.

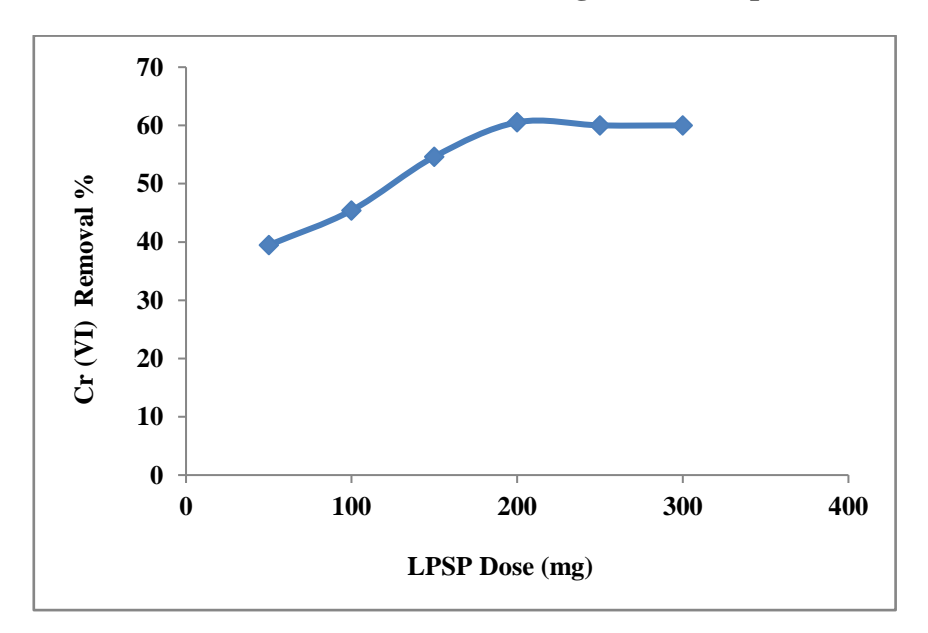


Figure: 5.2.3 Effects of taction time for Chromium (VI) ions on adsorption, Biosorbent dose 200 mg, pH 7, Volume of Cr (VI) ions solution 50 mL, Concentration of Cr(VI) ion solution 150mg/L and Temperature 35°C.

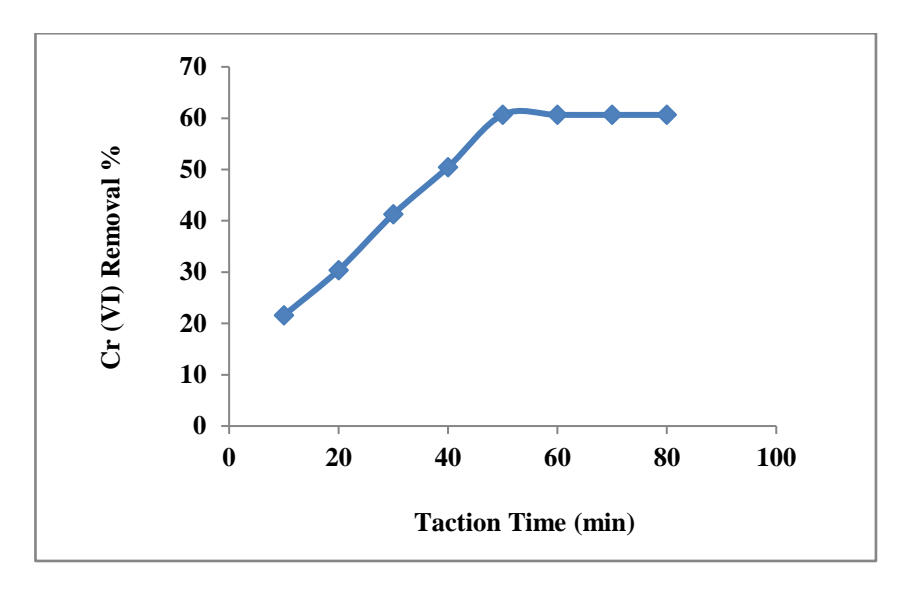


Figure: 5.2.4. Effects of initial Concentrations of Chromium (VI) ions solution on adsorption, Biosorbent dose 200 mg, Time 50 min, pH 7, Volume of Cr (VI) ions solution 50 mL, and Temperature 35°C.

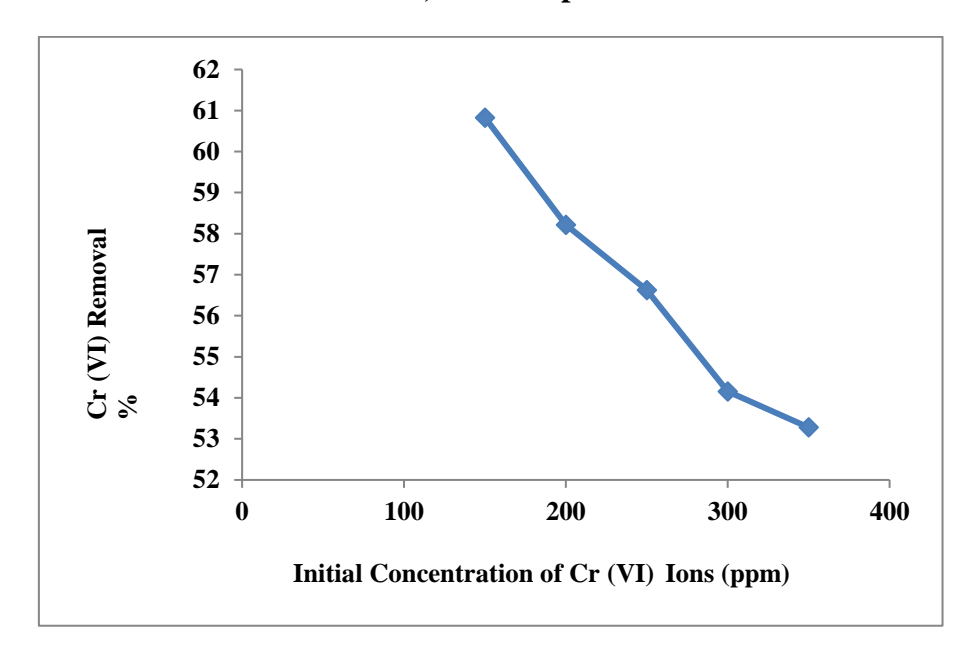


Figure: 5.2.5 Effects of Temperature for Chromium (VI) ions on adsorption,
Concentrations of Chromium (VI) ions 150 mg/L, Biosorbent dose 200 mg, Time
50 min, pH 7, and Volume of Cr (VI) ions solution 50 mL.

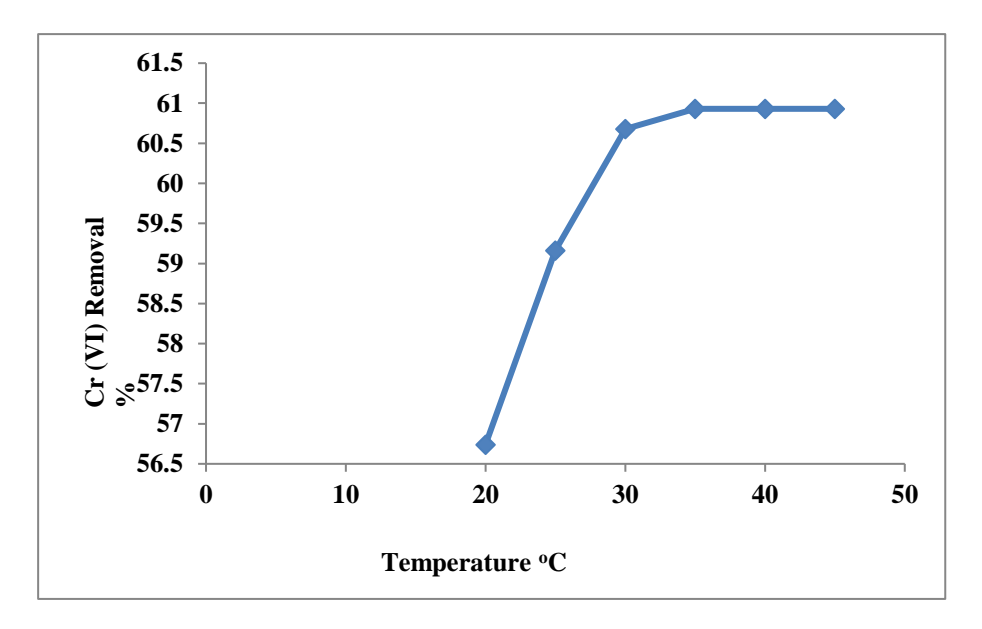


Figure : 5.2.6. Langmuir adsorption Isotherm plot for adsorption of Cr (VI) metal Ions on LPSP

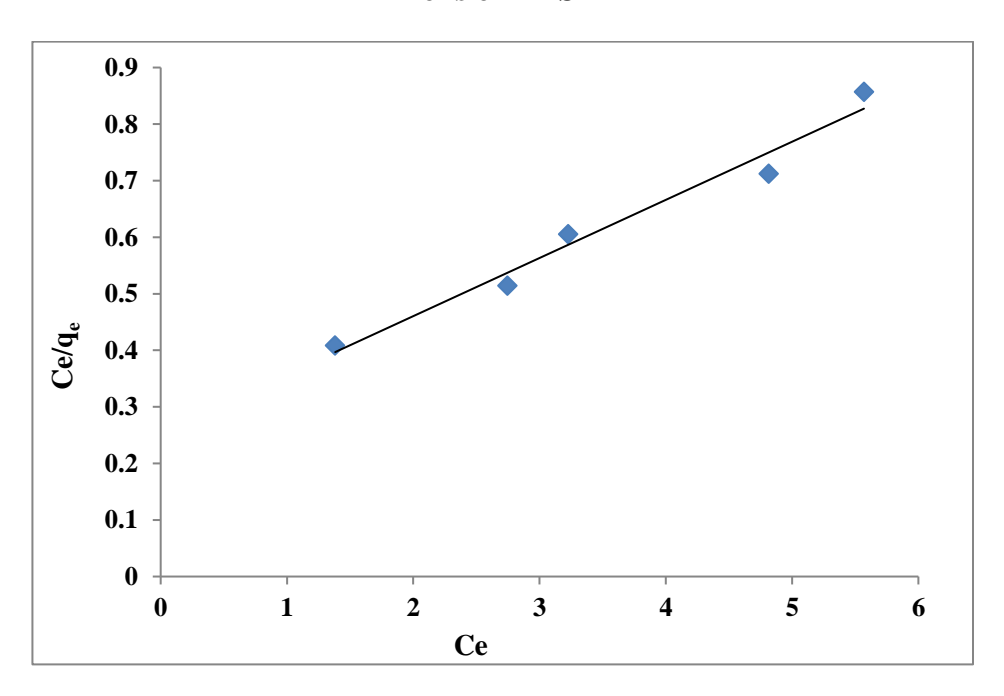


Figure : 5.2.7. Freundlich adsorption Isotherm plot for adsorption of Cr (VI) metal Ions on LPSP

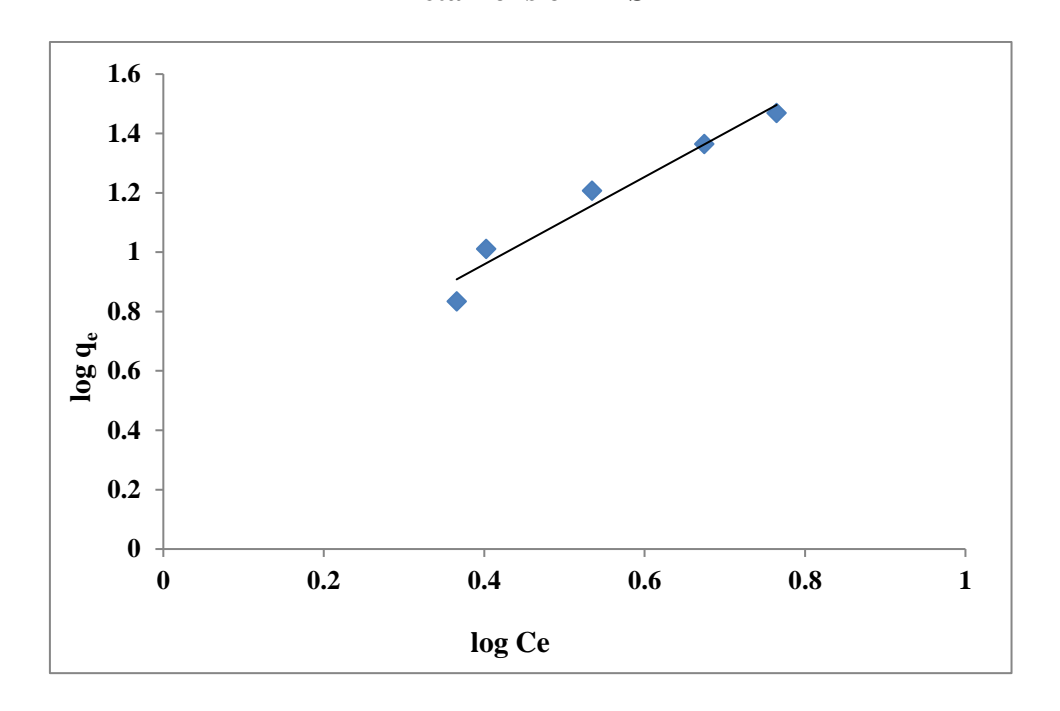
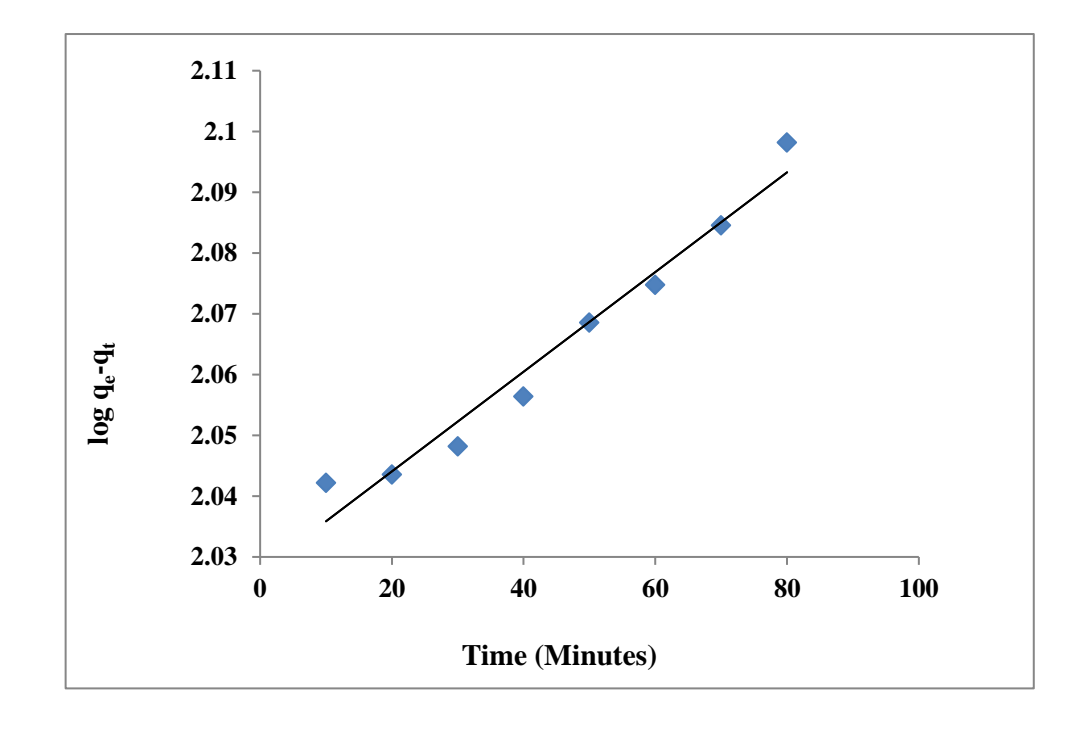


Figure : 5.2.8. Pseudo first order kinetic model plot for adsorption of Cr (VI) metal Ions on LPSP



 $\label{eq:Figure:5.2.9.Pseudo} \textbf{ second order kinetic model plot for adsorption of } \textbf{ Cr (VI)} \\ \textbf{ metal Ions on LPSP}$

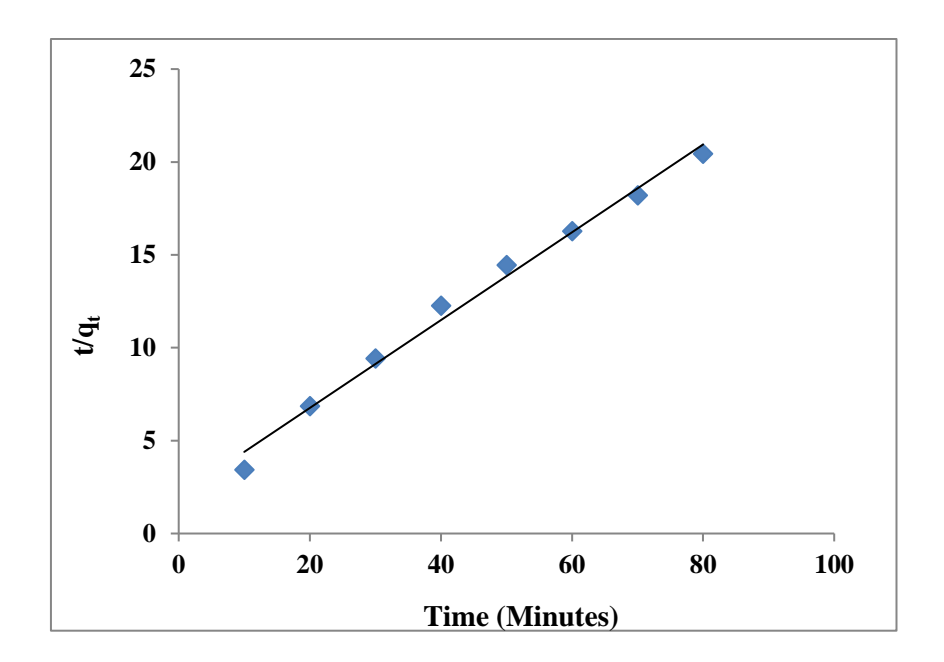
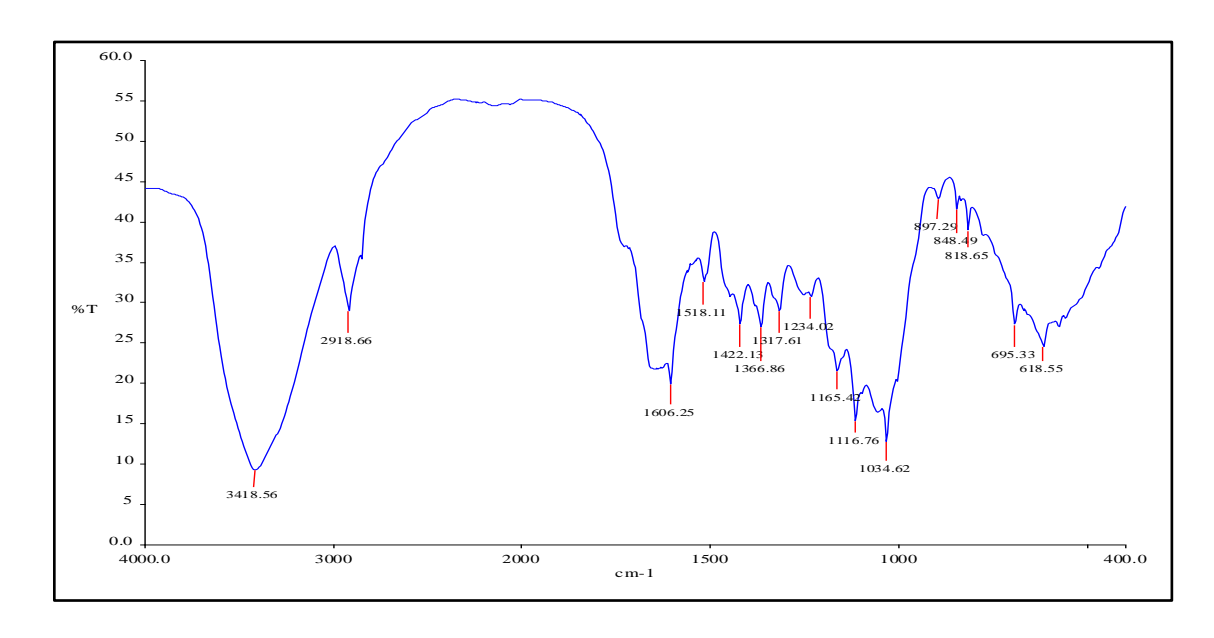


Figure : 5.2.10. FTIR analysis of LPSP before and after adsorption of Cr (VI) metal Ions



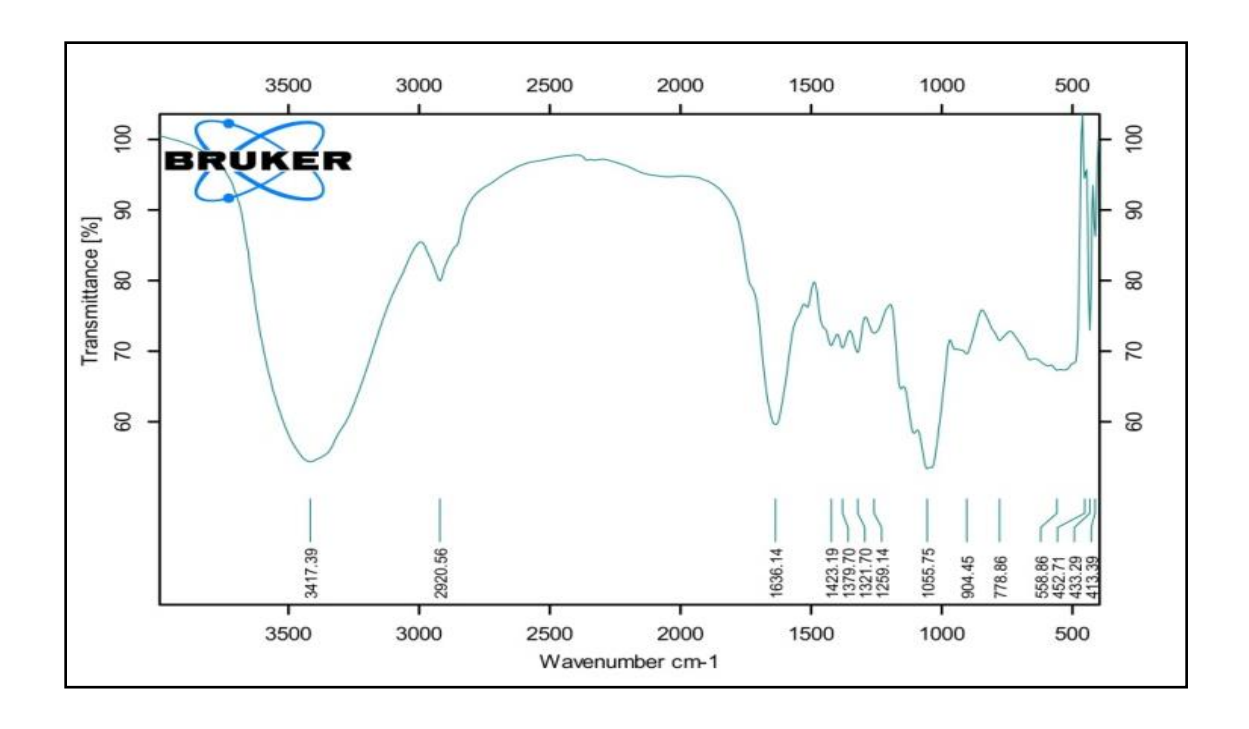
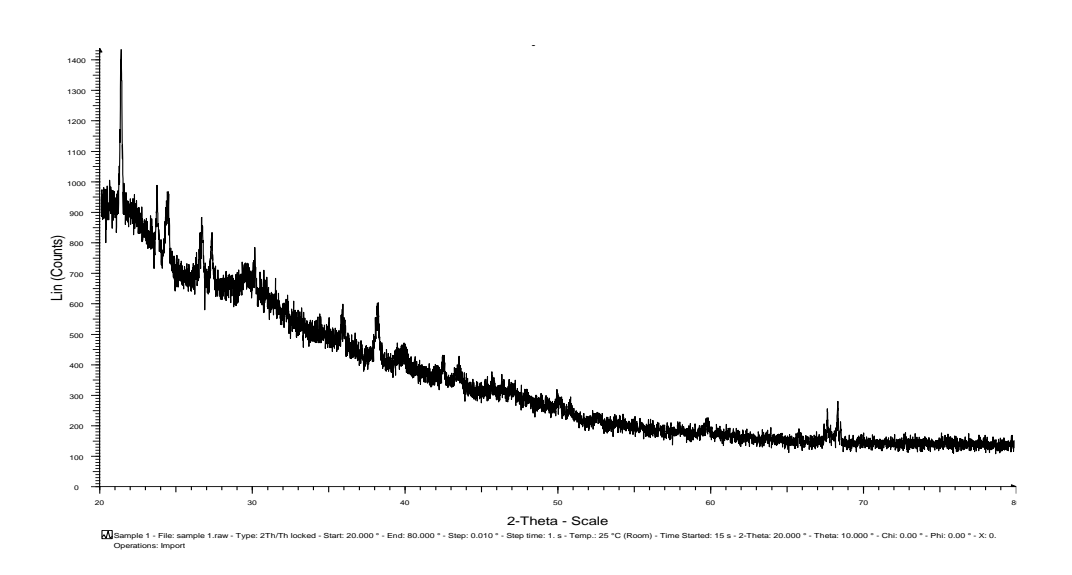


Figure: 5.2.11. XRD Pattern of LPSP before and after adsorption of Cr (VI) metal ions



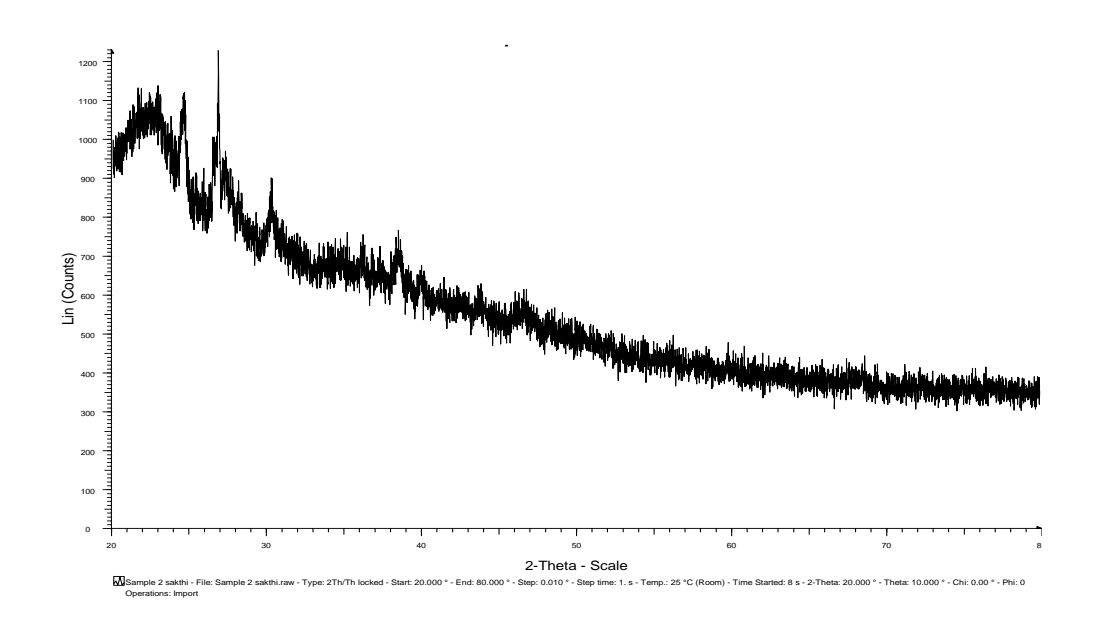
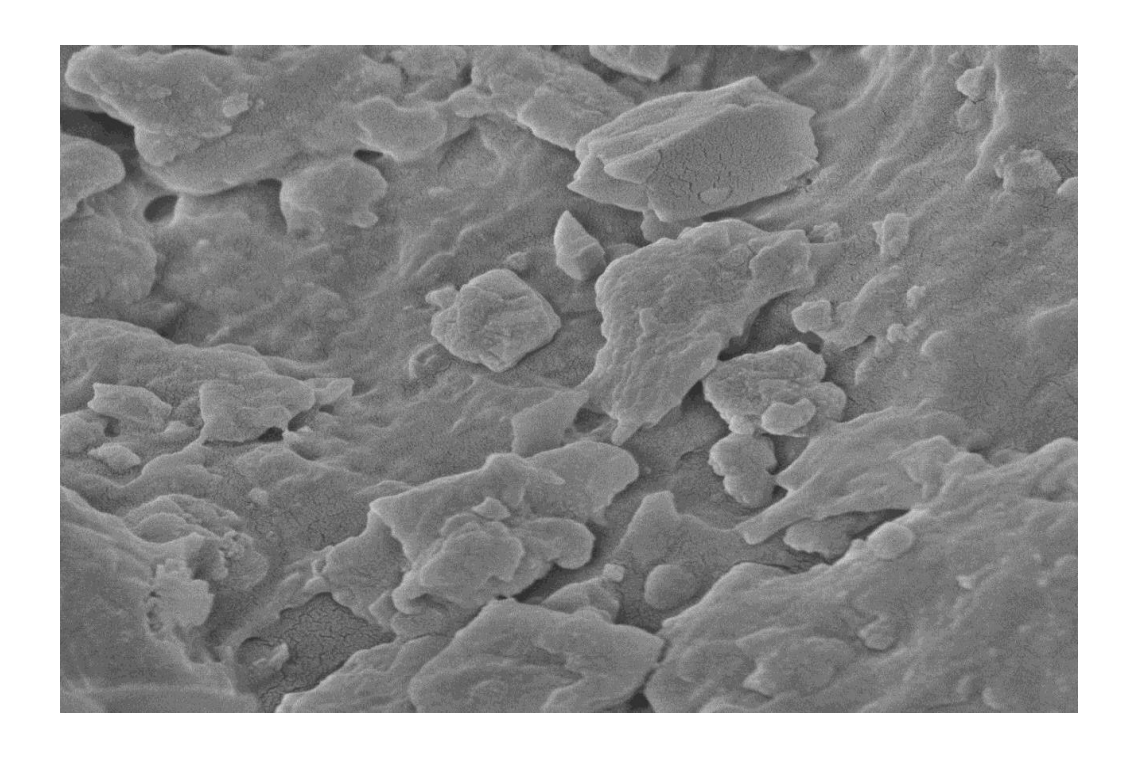
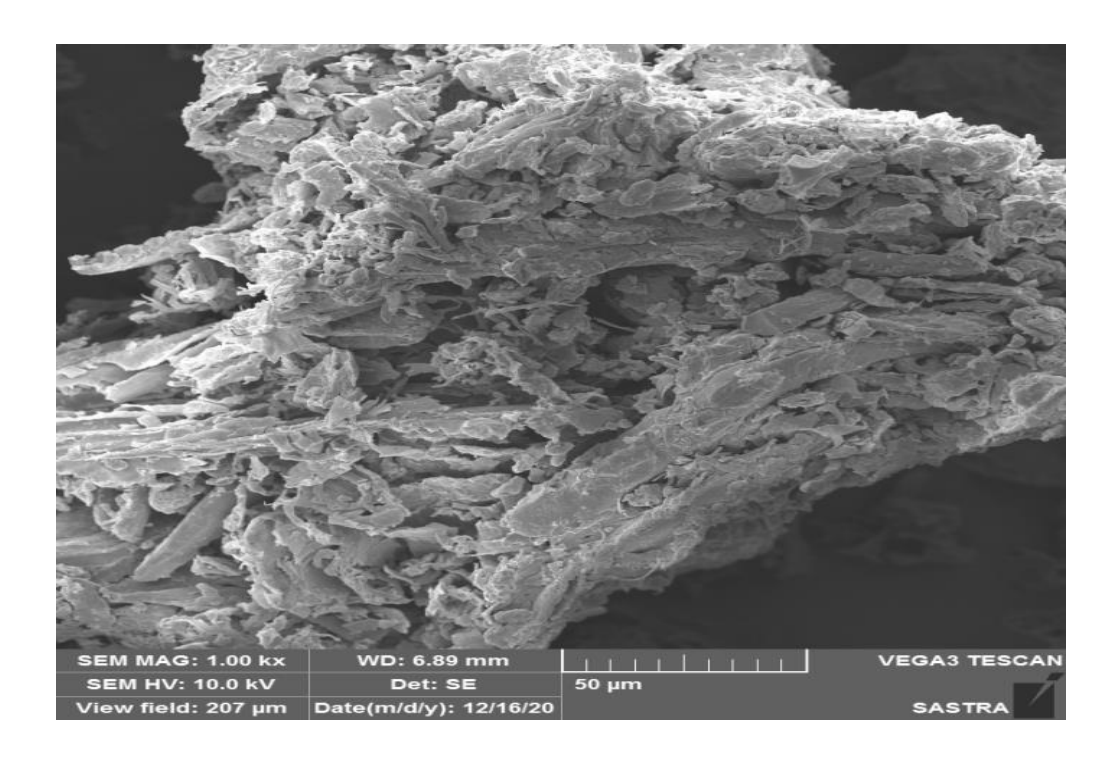


Figure: 5.2.12. SEM image of LPSP before and after adsorption of Cr (VI) metal ions





5.3. REMOVAL OF NICKEL (II) IONS FROM AQUEOUS SOLUTION USING LPSP

5.3.1 Effect of pH for Nickel (II) ions on adsorption

The effect of pH of the metal solution is the crucial factors that affecting the adsorption of metal ions on biosorbent (LPSP) surface. The adsorption capacity can be imputed at particular pH for the solution of heavy metals. (i.e. Pure ionic metal or metal hydroxyl). In addition, by reason of various functional groups on surface of the biosorbent, which develop to be as active sites for the binding of metal at a specific pH, the effect of pH on adsorption considerably changes. Consequently, when increase in pH may possibly leads to an increases or decreases on the adsorption, as a result various optimum pH values dependents upon the variety of adsorbent. The percentage for the removal of Ni (II) ions can study by the effect of pH, the pH of metal solutions were varied from pH 2 to pH 10 by addition with 1N HCl and/or 1N NaOH to the stock solution, agitation speed 360 rpm, volume of Ni (II) ions solution 50 mL, temperature 30°C, time 50 minutes, Ni (II)ions concentration 150 mg/L were constant. In lowered pH, the H⁺ ions compete with Ni (II) metal ions on the sites of biosorbent. In lowered pH, the overall charge on the particles surface of biosorbent becomes positive, hence the binding of positively charged Ni (II) metal ions reluctant to adsorbs on LPSP. On other way, When increasing the pH values from 2 to 7, the adsorption of Ni (II) ions increases may be caused by the negative charge increases on the biosorbent surface, which may be leads to increases the metal binding upto pH 7 after that pH>7 adsorption of Ni²⁺ ions are decreases due to availability of Ni (II) ions were reduced to occupation on the adsorption sites [179]. From the investigational results, the optimal pH for adsorption of Ni (II) ions is 7 shown in figure - 5.3.1., and table - 5.3.1.

5.3.2 Effect of Biosorbent dosage for Nickel (II) ions on adsorption

The biosorbent dose is one of the most important variables for metal uptake on adsorption. The effects of biosorbent weight was studied by varying from 50, 100, 150, 200 and 250 mg agitation speed 360 rpm, volume of Ni (II) ions solution 50 mL, pH 7, temperature 30°C, time 50 minutes, Ni (II) ions concentration 150 mg/L were constant. The biosorbent (LPSP) dosage have contacted on Ni (II) ions by the adsorption are showed in figure-5.3.2., and table – 5.3.2. It is demonstrates that when increasing the adsorbent dose the removal efficiency of Ni (II) ions also increases. This is may be attributed to increases large number of surface area for biosorbent in a fixed initial concentration of metal ion solution [180,181]. It was most possible for Ni (II) ions onto be adsorbed on adsorption sites and so the adsorption efficiency increased. Hence, the entire studies are carried by 200 mg of biosorbent dose.

5.3.3 Effect of contact time for Nickel (II) ions on adsorption

In the experimental study contact time is one of the main factors to fix time for analyzes the various parameters. Contact time likes 10, 20, 30, 40, 50, 60, 70 and 80 minutes, Temperature 30°C, pH 7, adsorbent dose 200 mg, initial concentration of Ni (II) ion solution 150 mg/L and agitation speed 360 rpm were kept constant. The percentage of removal and graphical representation are shows in table - 5.3.3 and figure-5.3.3. respectively. It was observed that the biosorbtion efficiency increased with increase in contact time from 10 to 80 min. Maximum removal percentage for Ni (II) ions were achieved up to 50 min after that remained constant until 80 min. It may be due to that the large number of surface area available on biosorbent in initial stage, there after it was slowed down later, because of the exhaustion of leftover surface area and repulsive forces between the bulk phase and the solute molecules [182].

5.3.4 Effect of Initial Concentration for Nickel (II) ions on adsorption

In the effect of initial concentration of Ni (II) ions on the adsorption process varying the concentration likes 50, 100, 150, 200 and 250 mg/L under the temperature 30°C, pH 7, agitation speed 360 rpm, time 50 minutes and 200 gm of adsorbent dose. The removal efficiency for effect of initial Ni (II) ions concentration was obtained from the experimental data which are represented in table-5.3.4 and figure-5.3.4. respectively. It clearly exhibits that when increasing initial Ni (II) ion concentration, the removal efficiency of Ni (II) ions decreases. As the ratio of adsorptive surface to metal ion concentration decreased with increasing metal ion concentration hence the metal ion removal was reduced. In lower concentration of Ni (II) ions, more number of binding sites available. But when the concentrations increasing, the number of Ni (II) metal ions competing for accessible binding sites in biosorbent increased [183].

5.3.5 Adsorption Isotherm Models

The adsorption isotherm specifies that how adsorbate molecules partitioned between adsorbent and liquid phase at equilibrium as a role of adsorbate concentration. In this learning, equilibrium studies were carried out to understand the character of the adsorbent of Ni (II) onto LPSP at equilibrium conditions by considering Langmuir and Freundlich adsorption isotherm models.

5.3.5.1. Langmuir isotherm model

The Langmuir isotherm model was studied about saturated monolayer formation for solute on the surface of the adsorbent in adsorption process [136]. The linear form of Langmuir isotherm model used in the term

$$C_e/q_e = 1/q_m K_L + C_e/q_m$$
 (5.3.1)

C_e = Equilibrium constant for Ni (II) metal ions (mg/L),

q_e = Amount of metal ions adsorbed at equilibrium (mg/g),

 q_m = Constant related to maximum adsorption capacity (mg/g),

 K_L = Langmuir constant related to energy of adsorption.

The equation for the linear plot of C_e / q_e against C_e should be a straight line. It shows that adsorption follows the Langmuir isotherm model. The constant q_m (124.79 mg/g) and 'b' (0.0826 L/mg) can be derived from slope and intercept of the plot and the values are shown in table-5.3.6 and figure-5.3.5. It reveals that the Langmuir isotherm model fitted well for the chosen biosorbent and adsorbate (Ni (II)) system with respect to r^2 = 0.991 at 30°C. Furthermore, q_{max} of the LPSP is 124.79 (mg/g) was compared with the previous studies and q_{max} values were represented in table-5.3.10.

The important characteristics of a Langmuir isotherm can be explained in terms of a dimensionless separation factor, R_L [165] which is defined by the following equation:

$$R_L = 1 / 1 + (q_{max} \times K_L)C_o$$
 (5.3.2)

Where C_0 is the highest initial concentration and the value of separation factor, R_L represents the type of isotherm and nature of the adsorption process. Recognizing the R_L values as the adsorption can be unfavorable ($R_L > 1$); linear ($R_L = 1$); favorable ($0 < R_L < 1$) or irreversible ($R_L = 0$) [166]. Hence, as the R_L values (Table 5.3.7) nearer to zero, the adsorption will be done better. The results stated that the nature of adsorption was a monolayer, which means a formation of Ni (II) molecules in single layer on the LPSP adsorbent surface [167]. It was suggesting that the equilibrium adsorption of Ni (II) onto LPSP might be best demonstrated with the Langmuir isotherm, because of

the correlation between experimental and calculated values along with regression factors are in good agreement with Langmuir isotherm, it was exhibited that Ni (II) was most favorably adsorbed by LPSP.

5.3.5.2 Freundlich Isotherm

The metal ions distribution between the liquid and solid phases can be illustrated by Freundlich isotherm model [139]. It best describes the adsorption onto heterogeneous surface. The common equation for the Freundlich isotherm model is represented as

$$\log q_e = \log k_f + 1/n \log C_e$$
 (5.3.3)

Where,

q_e = Amount of Ni (II) ions adsorbed on per unit weight of biosorbent (mg/g),

 K_f = Freundlich constant, which is correlated to calculate of adsorption capacity (mg/g).

1/n = Sorption intensity (mg/L).

C_e = Equilibrium concentration for Ni (II) metal ions (mg/L).

The values of K_f and 1/n can be derived from the intercept and slope of the linear plots of log q_e against log C_e , their values are exhibited in table-5.3.6. It was determined from graph drawn between plot log $q_e \, v_s \log C_e$ as represents in figure-5.3.6. Thus the values of K_f and 'n' were found for Ni (II) metal ions with r^2 values given in table-5.3.6. The r^2 value of Freundlich isotherm is less than Langmuir isotherm.

5.3.6 Kinetic Study

The Kinetics of adsorption studies have been carried out to illustrate adsorption mechanism and diffusion. The generated data had tested by Pseudo first order and Pseudo second order kinetics equation in order to determine the rate of the chromium ion adsorption on the LPSP, which controls the equilibrium time.

5.3.6.1. The Pseudo first-order model

The possibility of adsorption data obtained from Legergran pseudo first-order rate of equation can be described by the following equation:

$$dq_t/d_t = k_1(q_e-q_t)$$
 (5.3.4)

Where,

k₁ is the rate constant for first order adsorption (g.mg⁻¹.mn⁻¹),

qe is Ni (II) adsorbed at equilibrium per unit mass of the sorbent (mg/g),

q_t is Ni (II) adsorbed at equilibrium time (mg/g).

The combined form of above equation becomes

$$\log (q_e - q_t) = \log(q_e) - (k_{1/2.303})t$$
 (5.3.5)

Figure-5.3.7 represents a plot log $(q_e - q_t)$ verses (t) represents a straight line of slope $(k_{1/2.303})$ and an intercept of log $(q_e)[140]$. The reasonable degree of agreement between the calculated q_e values and experimental q_e values were found and show in table 5.3.8.

5.3.6.2. The Pseudo second-order model

This adsorption kinetic model equation developed as pseudo–second–order rate of equation representation is based on the sorption capacity of solid phase is commonly expressed [141] as

$$dq_t/d_t = k_2(q_e - q_t)^2$$
 (5.3.6)

Where,

k₂ is the rate constant for pseudo second order adsorption (g.mg⁻¹.min⁻¹), For the same boundary condition the integrated form of above equation becomes

$$t/q_t = 1/k_2 q_e^2 + 1/q_e(t)$$
 (5.3.7)

where, the k_2 can be calculated by the slope and intercept of the plots of (t/q_t) versus time (t) in figure-5.3.8. The pseudo-second-order adsorption capacity (q_e) values and correlation coefficient (r^2) values have represented in table-5.3.8.

The reasonable conformity between the calculated q_e and experimental q_e were found in the pseudo-second-order model compared with pseudo-first-order model. The correlation coefficient (r^2) for the adsorption of Ni (II) was found to be very high in pseudo-second-order model show in table-5.3.8 and it represents that, the adsorption capacities calculated (q_e) very nearer to the experimental (q_e), hence the pseudo-second-order model obeys the sorption of Ni (II) ions on biosorbent (LPSP).

5.3.7. Thermodynamic parameters

Thermodynamic parameters such as standard free energy (ΔG°), standard enthalpy change (ΔH°) and standard entropy change (ΔS°) were calculated by means of equilibrium constant change (K_{\circ}) with temperature (T). The free energy change can be verified by the following equation [142].

$$\Delta G^{\circ} = -RT \ln K_{o} \tag{5.3.8}$$

Where,

 ΔG° = free energy change of sorption process (kJ/mol),

 K_o = equilibrium constant,

T = temperature in (K),

R = universal gas constant.

The free energy change may be represented in terms of enthalpy change of sorption as a function of temperature as follows

$$\Delta G^{\circ} = \Delta H - T \Delta S \tag{5.3.8}$$

The adsorption coefficient K_0 can be derived by combined and rearranging Eqs (5.3.7) and (5.3.8)

$$\ln K_o = \Delta H^o / RT + \Delta S^o / R$$
 (5.3.9)

Where,

 ΔH° = standard heat changes of the sorption,

 ΔS° = entropy change of sorption (KJ/mol).

The standard enthalpy and entropy changes values are calculated from the slope and intercept of linear plot lnK_o versus 1/T. Thermodynamic parameter values are derived from the equation-5.3.9., for the adsorption of Ni (II) ions on LPSP and the values are represented in table.5.3.9. The negative values of free energy changes prove the spontaneous nature of sorption of Ni (II) metal ions on biosorbent LPSP and the positive values of ΔH^o prove the sorption process of an endothermic nature. The positive values could be evidence for increased randomness at solid-solution interface during the sorption of Ni (II) metal ions on the biosorbent LPSP.

5.3.8. FTIR Spectrum for LPSP on before and after adsorption of Ni (II) metal ions

The FTIR spectrum of LPSP before and after adsorption shows in figures-5.3.9 that the presence of hydroxyl, amino, carboxylic, carbonyl and alky CH- groups. The stretching vibration of OH, NH, C=O, alkyl CH- and C-X groups were observed. These shifted frequencies certain extent upon biosorption of Ni (II) ions. These are 3418, 2918, 1606, 778 and 904 cm⁻¹ respectively.

5.3.9. X-Ray Diffraction analysis for LPSP on before and after adsorption of Ni (II) metal ions

The X-ray diffraction technique is a important technique to analyze the crystalline amorphous nature of the adsorbent material. The LPSP before and after adsorption were recorded in figure - 5.3.10. The intense main peak in before adsorption shows that the presence of highly organized crystalline nature of raw LPSP. After the adsorption of Ni (II) metal ions, the intensity of the main peak is slightly diminished and broadens. It reveals that the physical adsorption takes place on the upper layer of LPSP crystalline structure after adsorption of Ni (II) metal ions.

5.3.10. SEM Analysis for LPSP on before and after adsorption of Ni (II) metal ions

Scanning Electron Microscope (SEM) studies provides the information about morphological nature of the biosorbent (LPSP). The SEM images of raw LPSP and Ni (II) metal loaded LPSP are represents in figure-5.3.11. SEM image of raw LPSP material is represents the uneven and rough surface and after that the Ni (II) metal ions loaded on biosorbent LPSP surface, it becomes significant change can viewed in the structure of biosorbent surface. This property indicated that sorption of Ni (II) metal ions on LPSP biosorbent.

Table: 5.3.1 Effect of pH for Ni(II) ions on adsorption, Time 50 min, Volume of Ni(II) ions solution 50 mL, Concentration of Ni(II) 150mg/L, Biosorbent Dose 200 mg and Temperature 30°C.

pН	Percentage of Removal
2	60.88
3	61.14
4	61.26
5	61.58
6	61.93
7	62.22
8	62.12
9	62.06
10	62.05

Table: 5.3.2 Effect of Biosorbent (LPSP) dose for Ni(II) ions on adsorption, Time 50 min, pH 7, Volume of Ni(II) ions solution 50 mL, Concentration of Ni(II) ions solution 150mg/L and Temperature 30°C.

Biosorbent dose (mg)	Percentage of Removal
50	41.07
100	47.81
150	56.27
200	62.22
250	61.72

Table: 5.3.3 Effect of Contact Time for Ni(II) ions on adsorption, pH 7, Volume of Ni(II) ions solution 50 mL, Biosorbent Dose 200 mg, Concentration of Ni(II) ion solution 150mg/L and Temperature 30°C.

Contact Time (min)	Percentage of Removal
10	23.15
20	31.98
30	42.85
40	52.03
50	62.22
60	62.31
70	62.43
80	61.11

Table: 5.3.4 Effect of Ni(II) ion solution Concentration, pH 7, Volume of Ni(II) ions solution 50 mL, Biosorbent Dose 200 mg, Time 50 min and Temperature 30°C.

Initial Concentration of Ni(II)	Percentage of	
(ppm)	Removal	
50	62.18	
100	61.56	
150	61.19	
200	59.57	
250	58.03	

Table: 5.3.5 Percentage of Ni(II) metal removal in various initial concentration on LPSP biosorbent

Ci	Removal %			
(mg/L)	30°C	35°C	40°C	
50	62.18	63.45	65.57	
100	61.56	62.49	64.51	
150	61.19	61.82	63.63	
200	59.57	60.69	61.47	
250	58.03	61.37	61.83	

Table: 5.3.6 Langmuir and Freundlich isother parameters for the adsorption of Ni(II) ions on LPSP biosorbent

Temp.	Langmi	uir Parame	eters	Freundlich Parameters			
(°C)	q _m (mg/g)	b (L/mg)	\mathbf{r}^2	$K_f (mg^{1-n} g^{-1} L^n)$	$n(mg^{1-n}g^{-1}L^n)$	\mathbf{r}^2	
30°C	124.79	0.0826	0.991	2.4183	1.1090	0.985	
35°C	182.62	0.0902	0.992	3.0171	1.3569	0.970	
40°C	194.48	0.992	0.994	5.6035	1.4016	0.984	

 $\label{eq:continuous_loss} Table: 5.3.7 \ Dimensionless \ separation \ factor \ R_L \ for \ adsorption \ of \ Ni(II) \ ions \ on \\ LPSP \ Biosorbent.$

Ci	Temperature °C			
(mg/L)	30°C 35°C 40°C			
50	0.2992	0.3124	0.3369	
100	0.1476	0.1912	0.2275	
150	0.1232	0.1572	0.1104	
200	0.0902	0.1180	0.0978	
250	0.0878	0.1088	0.0964	

Table: 5.3.8 Kinetic parameter for adsorption of Ni(II) ions onto LPSP Biosorbent

Ci		Pseu	Pseudo first order		Pseudo second order		
(mg/L)	Temp °C	qe (mg/g)		\mathbf{r}^2	q _e (mg/g)		\mathbf{r}^2
(Cal.	Exp.	•	Cal.	Exp.	-
	30	43.89	48.85	0.9757	45.78	46.62	0.9954
50	35	44.64	48.97	0.9746	46.64	47.50	0.9948
	40	44.98	49.99	0.9734	45.56	46.44	0.9933
	30	89.20	92.19	0.9747	89.20	92.18	0.9951
100	35	89.87	92.96	0.9736	91.78	92.54	0.9943
	40	90.32	93.29	0.9721	91.34	92.80	0.9937
	30	126.04	128.77	0.9852	128.16	128.40	0.9963
150	35	129.50	131.56	0.9844	131.42	131.38	0.9928
	40	133.91	132.96	0.9838	135.78	136.29	0.9918
	30	156.10	159.10	0.9822	158.16	159.22	0.9951
200	35	160.36	163.43	0.9818	162.37	163.32	0.9948
	40	163.76	166.78	0.9812	165.72	166.26	0.9938
	30	178.72	180.97	0.9752	180.68	180.56	0.9927
250	35	187.94	190.95	0.9740	189.88	190.78	0.9920
	40	190.06	193.30	0.9718	192.52	193.12	0.9919

Table:5.3.9 Thermodynamic parameter for adsorption of Ni(II) ions on LPSP

C _i	ΔG ^o (kJ/mol)			ΔH° (kJ/mol)	ΔS° (kJ/mol)
(8-)	30°C	35°C	40°C		
50	-4972.22	-5558.46	-5930.52	9.7918	47.5213
100	-4416.74	-4766.57	-5118.44	8.5834	42.4822
150	-3176.38	-4201.89	-4517.18	12.0820	46.6234
200	-2150.68	-3720.75	-3966.64	15.4184	55.5276
250	-1337.62	-3318.90	-2937.82	13.3432	44.6588

Table: 5.3.10.Comparative study of adsorbent capacity for Ni(II) metal ions on Langmuir constant q_{max} (mg/g) by various biosorbent.

Adsorbent	Adsorbent capacity (mg/g)	[Reference]
A.barbadensis Miller leaves powder	10.00	[184]
Trichoderma viride	47.60	[185]
Date seeds powder	41.00	[186]
Lotus stalk	31.45	[187]
Coconut desiccated meat	18.19	[188]
Rhizoclonium hookeri	81.70	[189]
Senna Alata Bark	83.39	[190]
Typha latifolia L.	55.55	[191]
Sawdust	12.50	[192]
LPSP	124.79	This study

Figure: 5.3.1 Effect of pH on adsorption of Ni(II) ions, Time 50 min, Volume of Ni(II) ions solution 50 mL, Concentration of Ni(II) ions solution 150mg/L,

Biosorbent Dose 200 mg and Temperature 30°C.

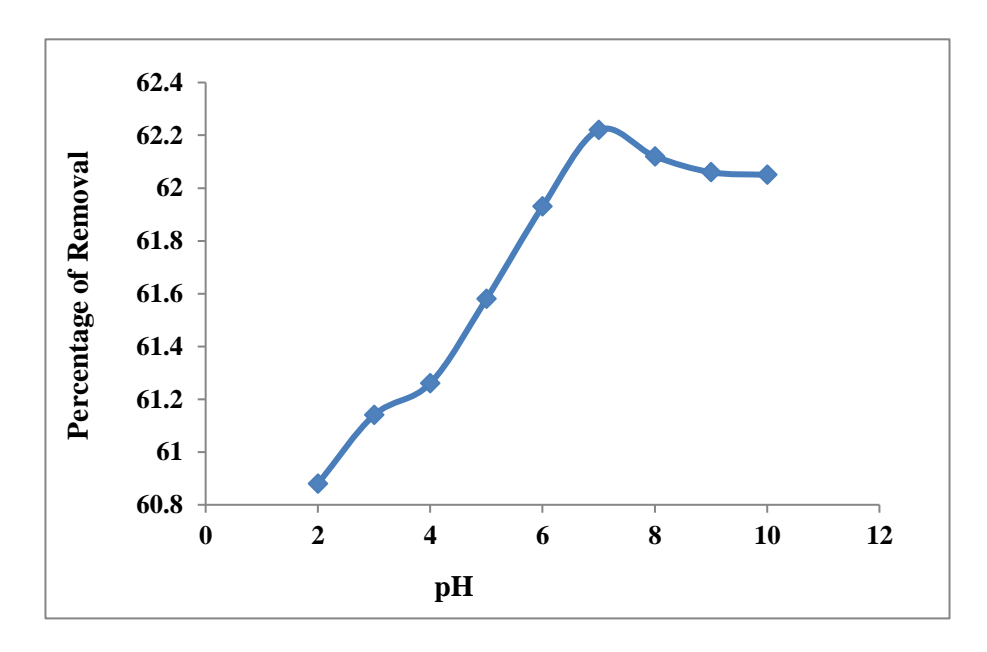


Figure: 5.3.2 Effect of Biosorbent dose (LPSP) on adsorption of Ni(II) ions solution, Time 50 min, pH 7, Volume of Ni(II) ions solution 50 mL, Concentration of Ni(II) ions solution 200mg/L and Temperature 30°C.

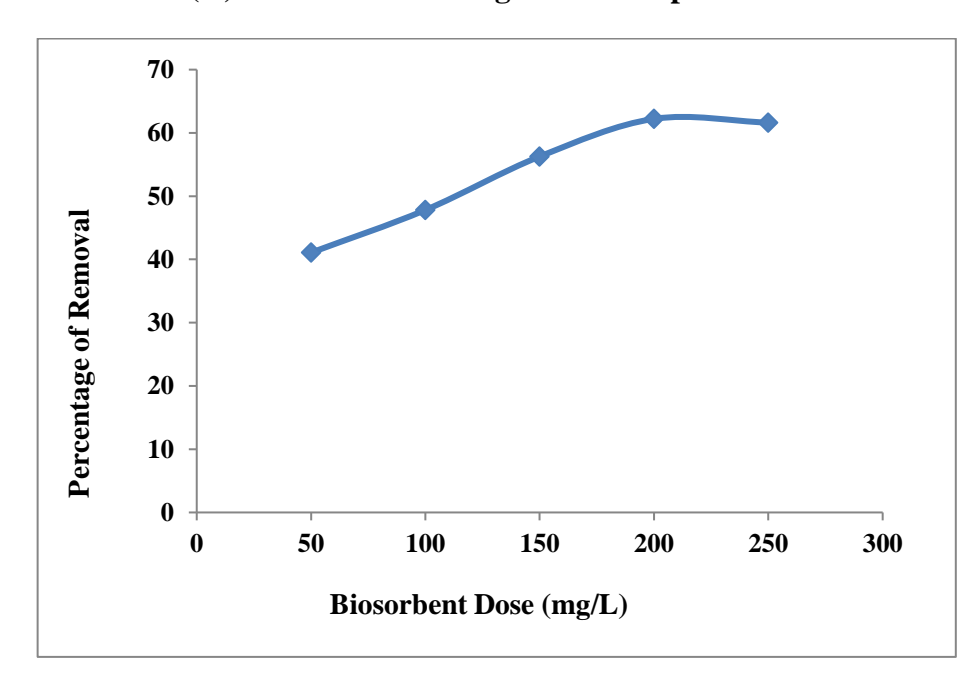


Figure: 5.3.3 Effect of Contact Time for Ni(II) ions solution on adsorption, pH 7, Volume of Ni(II) ions solution 50 mL, Biosorbent Dose 200 mg, Concentration of Ni(II) ions solution 200mg/L and Temperature 30°C.

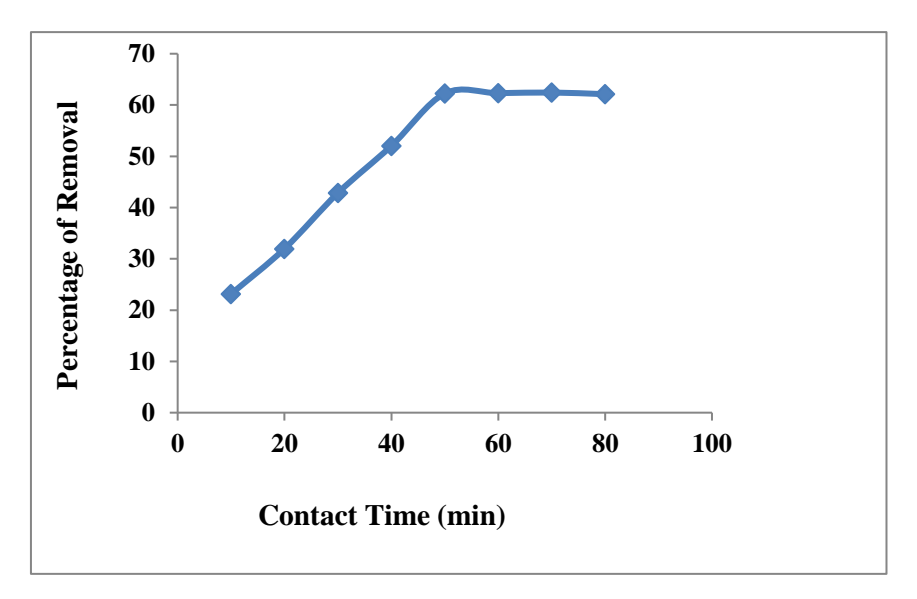


Figure: 5.3.4 Effect of initial Concentration for Ni(II) ions solution on adsorption, pH 7, Volume of Ni(II) ions solution 50 mL, Biosorbent Dose 200 mg, Time 50 min and Temperature 30°C.

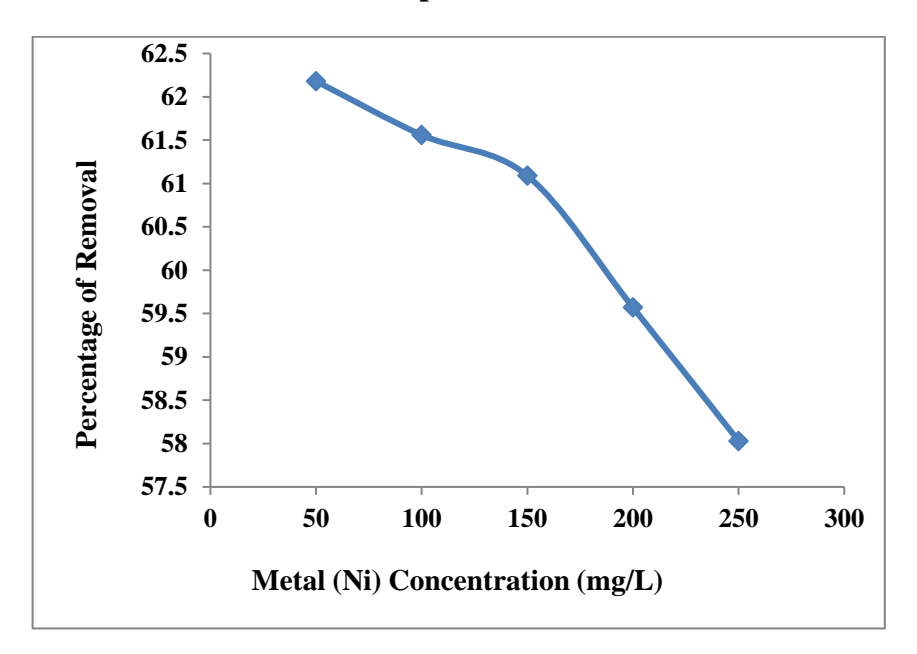
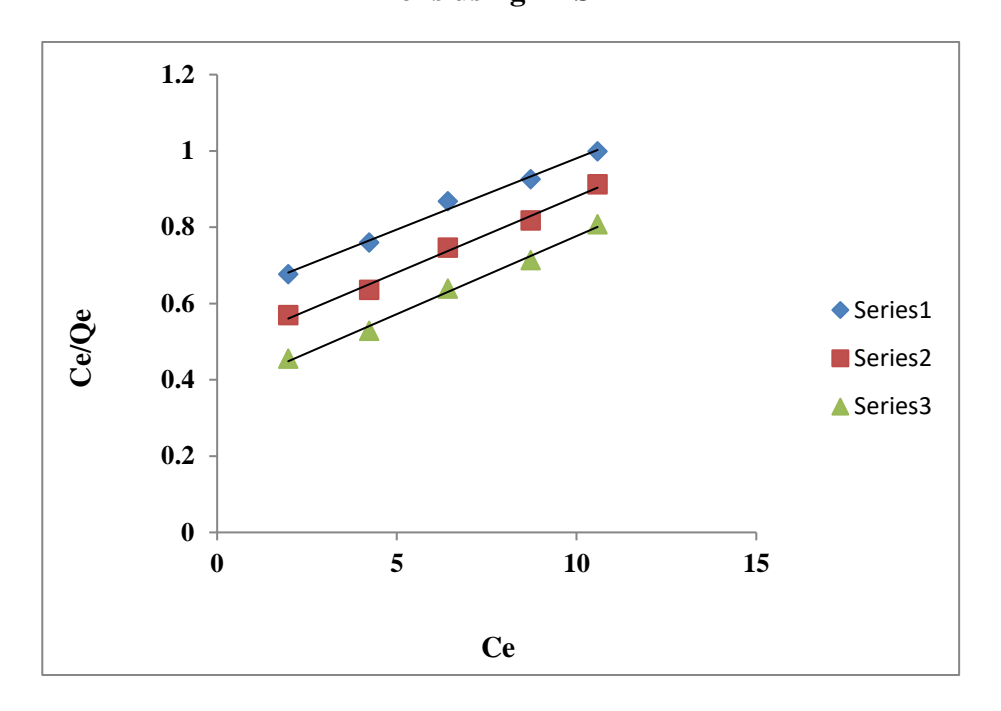
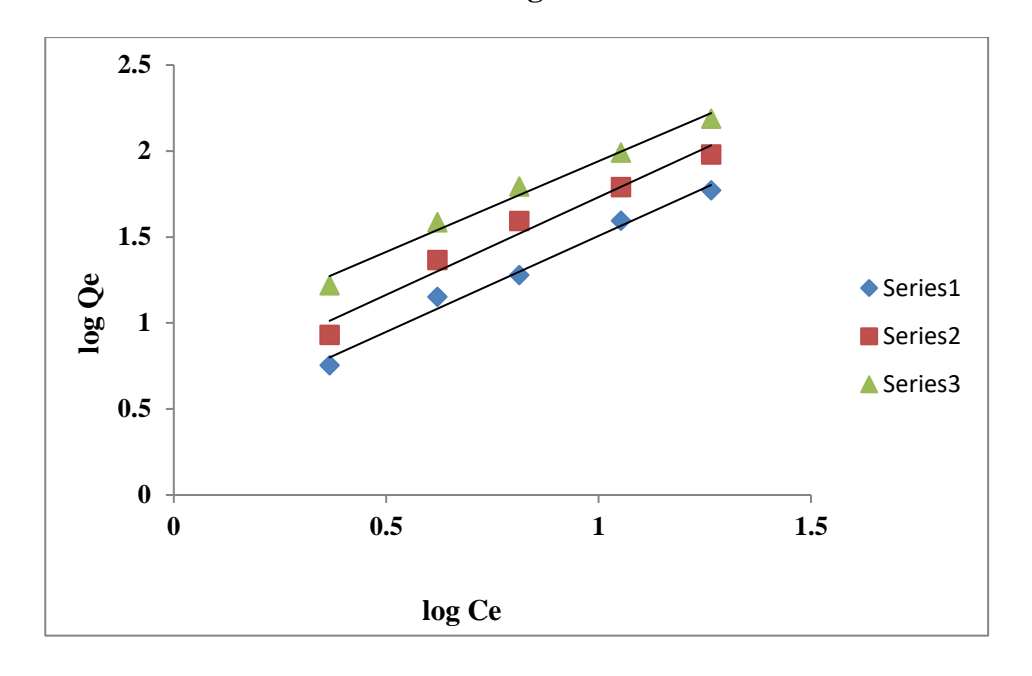


Figure: 5.3.5 Langmuir adsorption Isotherm model for removal of Ni(II) metal ions using LPSP



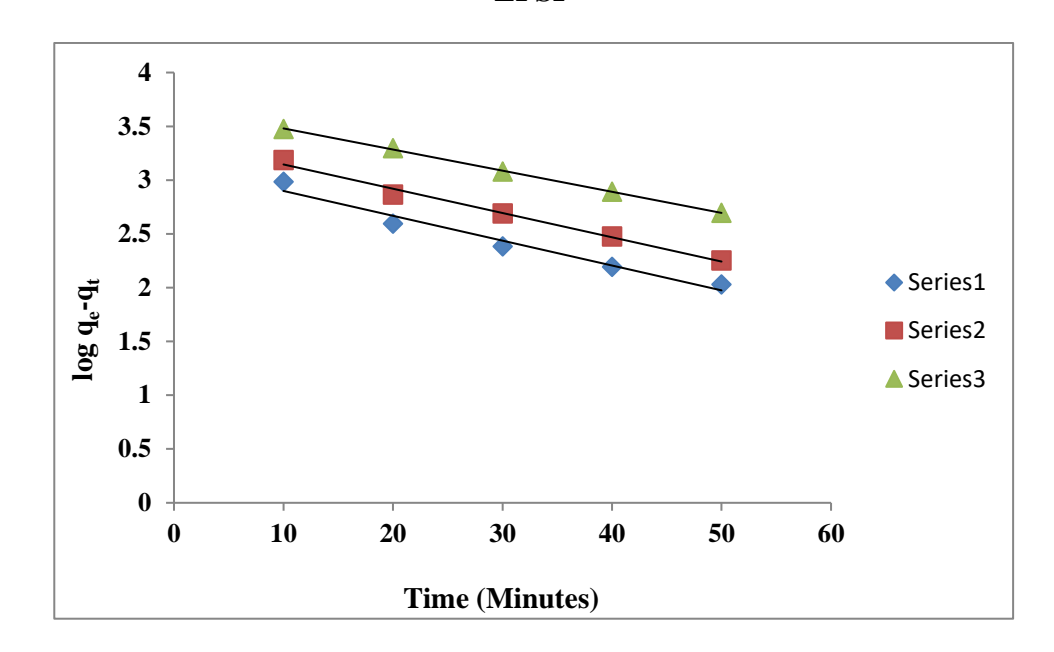
30°C Series-1. 35°C Series-2. 40°C Series-3.

 $\label{eq:Figure: 5.3.6} Freundlich adsorption Isotherm model for removal of Ni(II) metal \\ Ions using LPSP$



30°C Series-1. 35°C Series-2. 40°C Series-3.

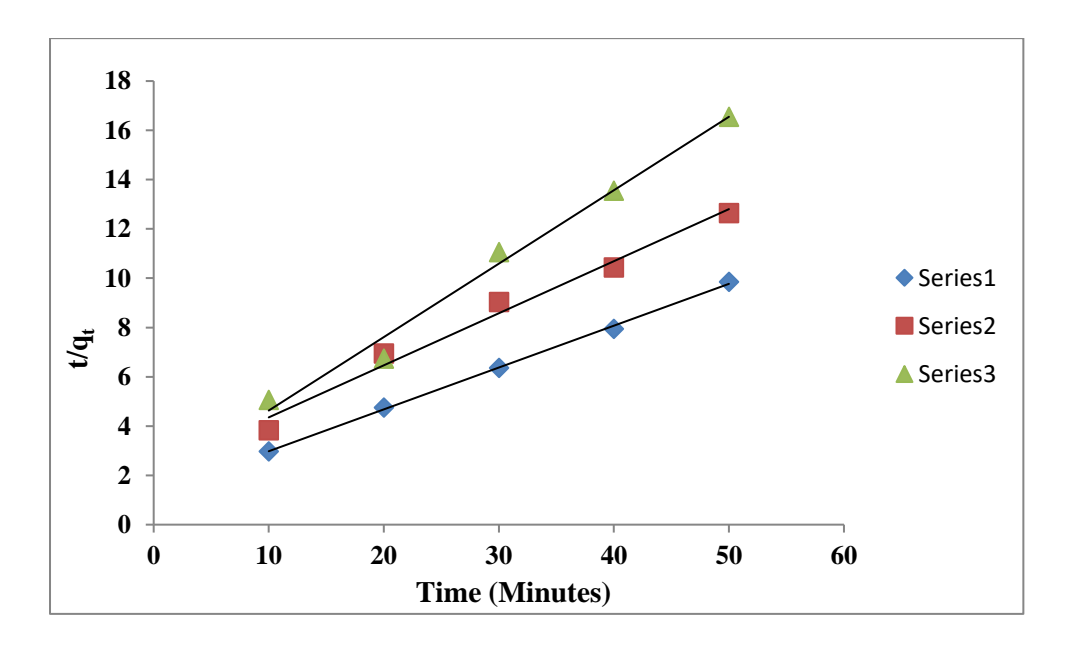
Figure: 5.3.7 Pseudo First order model for removal of Ni(II) metal Ions using LPSP



Series 1-100 ppm. Series 2-150 ppm. Series 3-200 ppm.

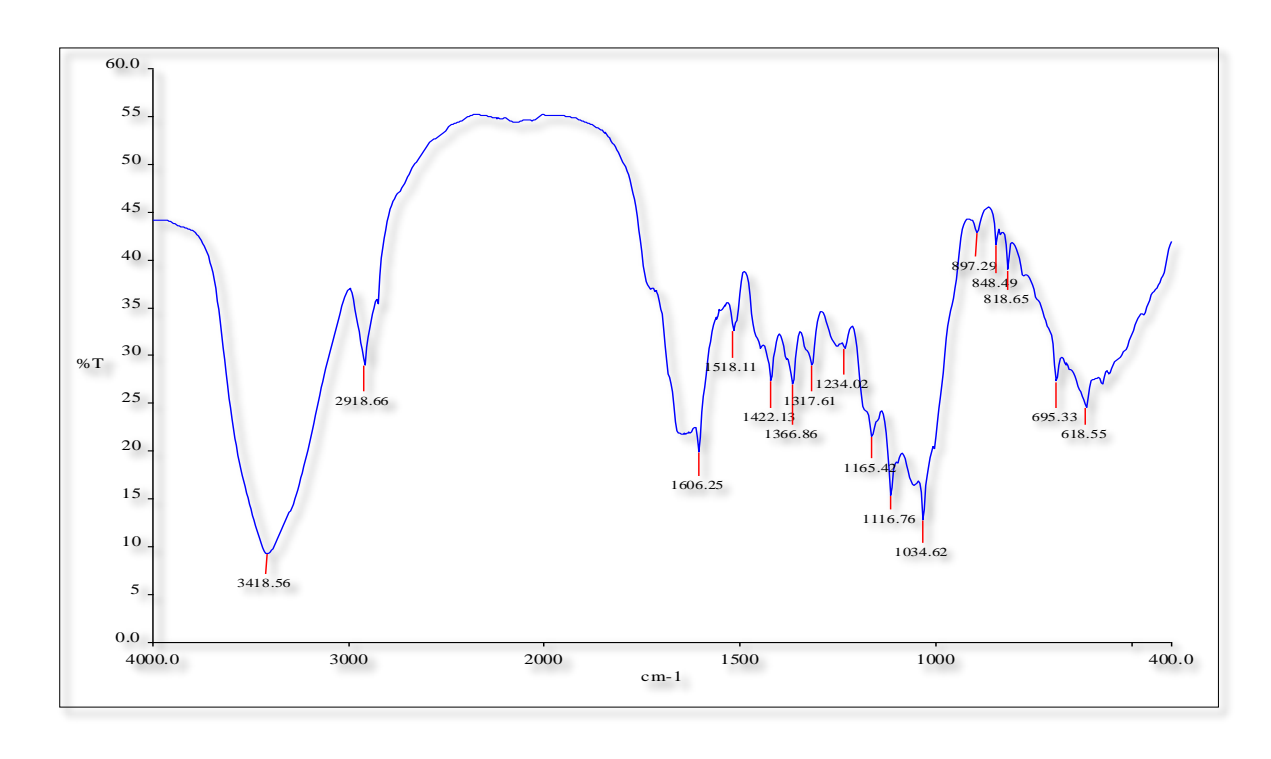
Figure: 5.3.8 Pseudo second order model for removal of Ni(II) metal Ions using

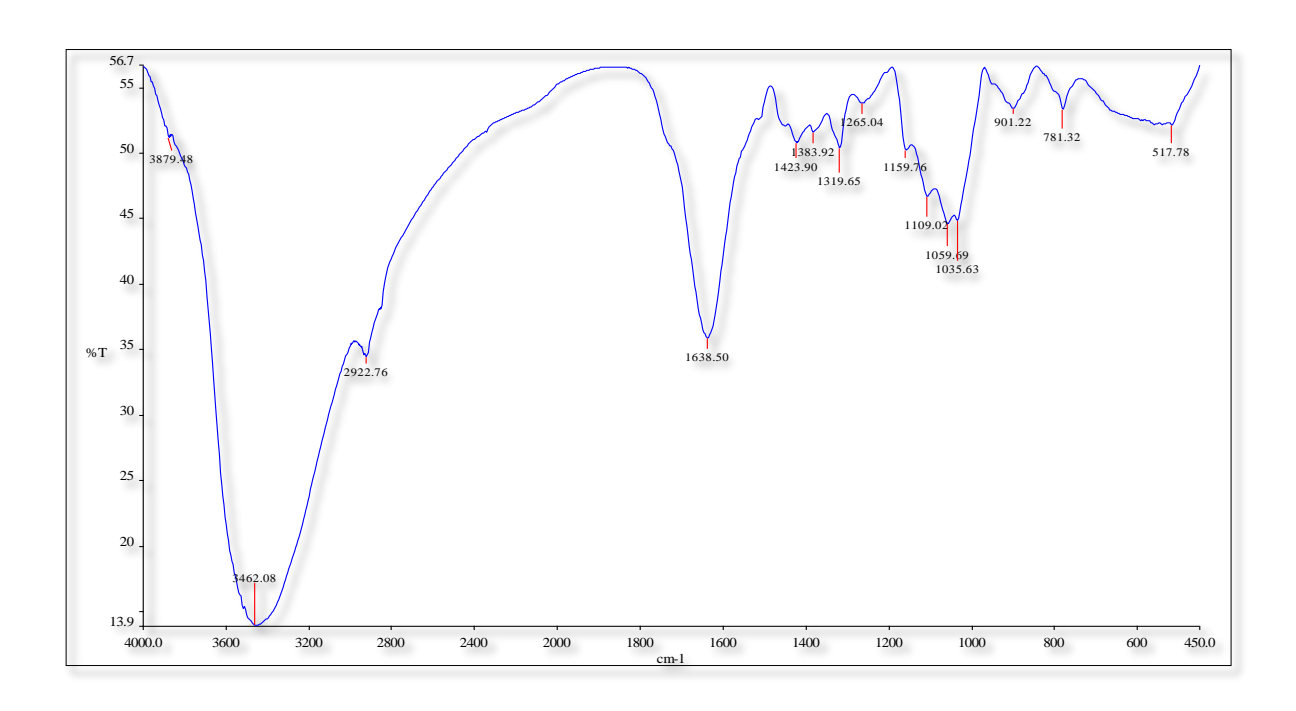
LPSP



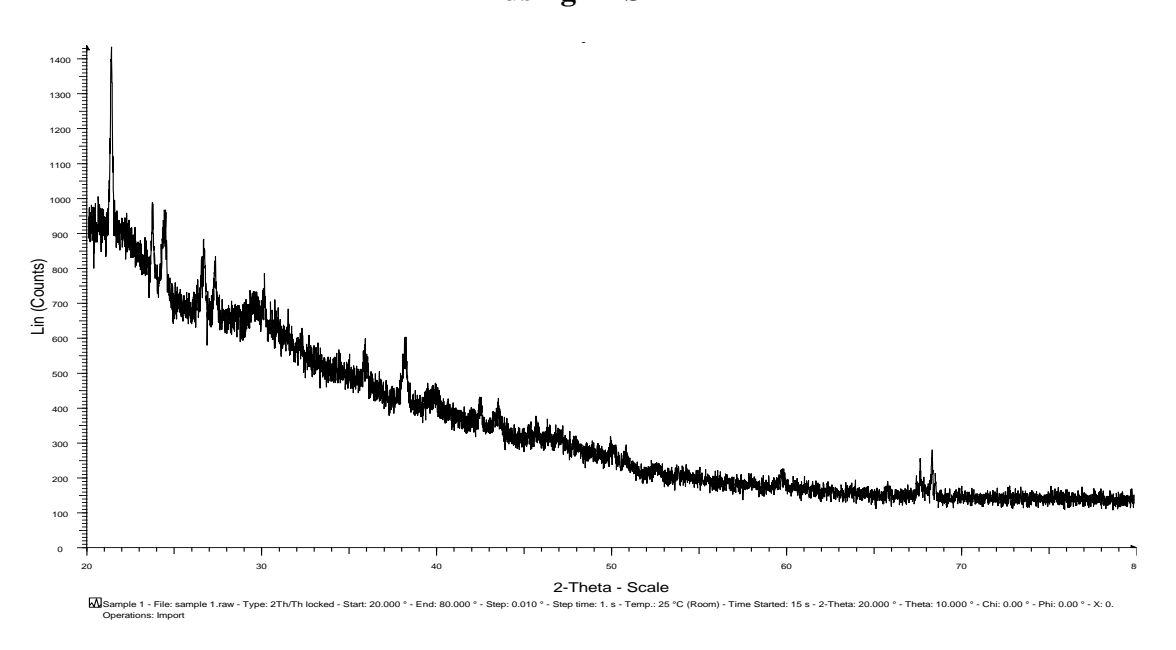
Series 1-100 ppm. Series 2-150 ppm. Series 3-200 ppm.

Figure: 5.3.9 FTIT Analysis for adsorption of Ni(II) metal ions on before and after using LPSP

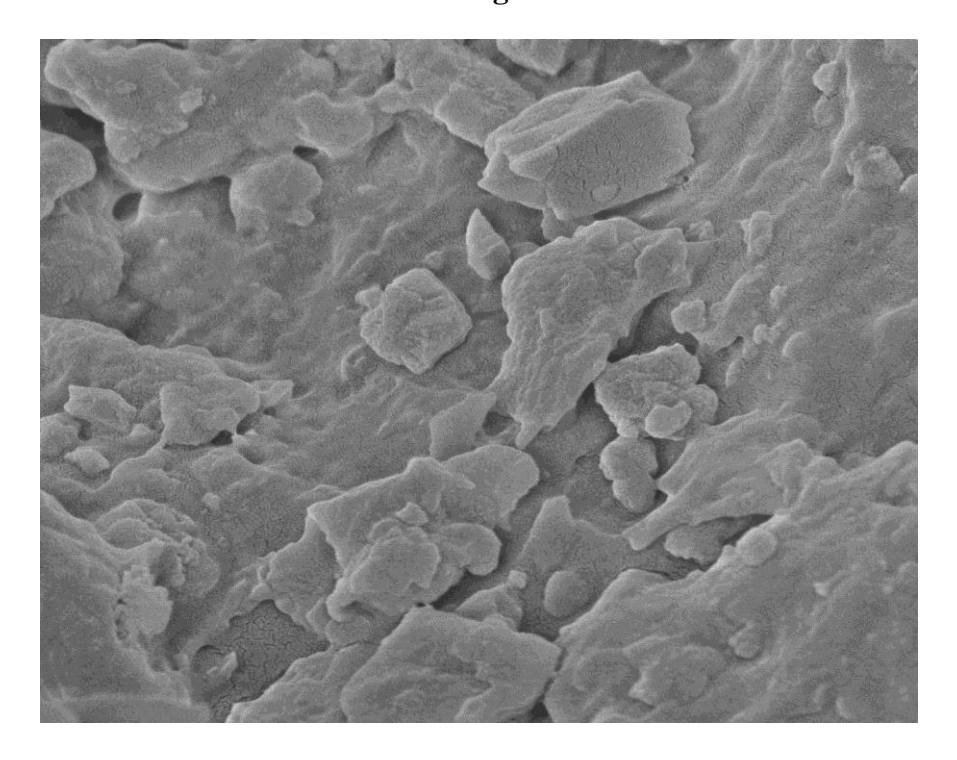


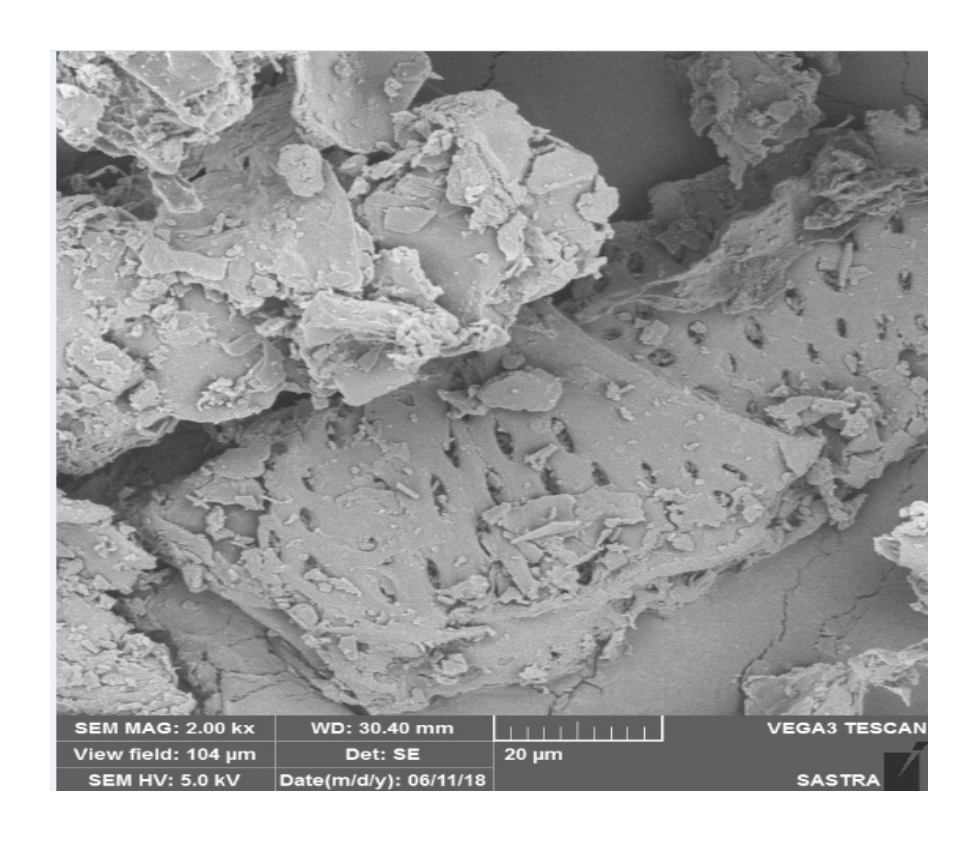


 $\label{eq:sigma} \textbf{Figure: 5.3.10 XRD Pattern for adsorption of Ni(II) metal ions on before and after} \\ \textbf{using LPSP}$



 $\label{eq:Figure: 5.3.11 SEM Analysis for adsorption of Ni(II) metal ions on before and \\ after using LPSP$





5.4 Removal of Bismark Brown R dye from aqueous solution using LPSP

5.4.1 Effect of pH for BBR dye from aqueous solution onto adsorption using LPSP

The pH of the aqueous solution of dye is the evidently main parameter for controlled the adsorption process. The experiments were completed with range of pH from 2 to 10, temperature is 30°C, contact time is 50 minutes, agitation speed is 360 rpm, initial dye concentration is 200 mg/L and the adsorbent dose is 300 mg. The results of the experiment are shown in the table-5.4.1. The graph has drawn between pH and BBR dye uptake is shown in the figure-5.4.1. The figure exhibits that the biosorbent contains polymers with more number of functional group, therefore the net charge on the biosorbent is more pH dependent [193]. When increasing the pH of the system while the number of negatively charged sites (OH-) also increases on biosorbent, due to increase in the hydroxyl ion concentration where as the number of positively charged sites (H⁺) also decreases [194]. Hence, at higher pH is most favors for the uptake of positively charged (cationic) dye due to the surface of the adsorbent gets more negatively charged by losing protons. Here the dye uptake occurs due to increased electrostatic force of attraction between surface of dye and adsorbent [195]. Therefore, dye uptake at lower pH decreases due to less number of negatively charged sites at the LPSP surface. The lower sorption of BBR dye at lower pH was maybe due to the presence of the large number of H⁺ ions competing with the cationic groups of the dye on sorption sites [196]. The maximum sorption was observed at pH 8 for BBR (cationic or positively charged dye) dye. The decrease in the biosorption of BBR dye after pH was insignificant.

5.4.2 Effect of biosorbent dose for BBR dye from aqueous solution onto adsorption using LPSP

The adsorbent dose was also studied for the removal of BBR dye from aqueous solution. The experiment was carried out with adsorbent dose is varied from 100 to 500 mg with other parameters are constant such as pH 8, initial dye concentration is 200 mg/L, temperature is 30°C, contact time is 50 minutes, agitation speed is 360 rpm. The results of the experiment are exhibited in table-5.4.2. The effect of biosorbent dosage for the removal of dye is shown in figure-5.4.2. The figure representing that adsorption was mostly complete with biosorbent from 100 to 300 mg. The adsorption of dye uptake increases with increase in dose of the adsorbent, because of increases the adsorption surface area and availability of adsorption sites [197]. Moreover, above the 300 mg of the adsorbent dose weight, did not show any significant for the removal of dye, hence, 300 mg biosorbent dose was preferred for following experiments.

5.4.3 Effect of contact time for BBR dye from aqueous solution onto adsorption using LPSP

The most essential factor in batch adsorption studies are the effect of contact time. In this study all of the parameter other than contact time 10 to 70 minutes, including temperature is 30°C, adsorbent dose is 300 mg, pH is 8, initial dye concentration is 200 mg/L and agitation speed is 360 rpm were kept permanent. The table-5.4.3 is exhibits the experimental data and the figure-5.4.3 shows efficiency of dye adsorption by effect of contact time. The time variant graph exhibits that in the preliminary stage of the dye adsorption is rapidly removed but while it reaches at equilibrium, it slows downward gradually. This is due to during the initial stage of adsorption process the availability of vacant surface sites and then a certain time period

the vacant sites of the adsorbent get occupied by dye molecules, as a result to form a repulsive force between the adsorbate on the adsorbent surface and bulk phases. The adsorption was takes place up to 50 minutes after that the equilibrium attainment, the percentage of adsorption of dye did not show any appreciable change with respect to time. This suggests that after equilibrium is attained, further treatment does not provide more removal [198]. In batch adsorption, the removal rate of the adsorbate in aqueous solution is mainly controlled by transport of dye molecules from the surrounding sites to the interior sites of the adsorbent particles [199]. The figure exhibited that a contact time of 50 minutes was sufficient to reach equilibrium and the adsorption no change with further increasing contact time, hence, the contact time has been preferred as 50 minutes for the continuous experiment.

5.4.4 Effect of Initial concentration for BBR dye from aqueous solution onto adsorption using LPSP

The experiment were carried out with a different concentrations of dye solution from 100 to 1000 mg/L and temperature is 30°C, adsorbent dose is 300 mg, pH is 8, contact time is 50 minutes, agitation speed is 360 rpm. The experimental data are shown in table-5.4.4 and the graphs were drawn between initial dye concentrations and dye uptake is shown in figure-5.4.4. The figure exhibits that the effect of initial dye concentration is highly depend upon the immediate relation between the available binding sites on an adsorbent surface and the concentration of dye [200]. Usually the dye removal percentage is decreases with increase in concentration of initial dye, which may be reason for the saturation of adsorption sites in the adsorbent surface and the adsorption ability increased with an increase in concentration of the dye. In low concentration there will be vacant active sites on surface of the adsorption and when the

initial dye concentration increases, the active sites not to be enough for adsorption of the dye molecules [201].

5.4.5 Adsorption Isotherm Studies

Adsorption of BBR dye onto LPSP was studied by the familiar isotherm equations namely, Langmuir and Freundlich models to explains that how the adsorbent interacts by the adsorbate. These are the most important physicochemical models in the description of adsorption process.

5.4.5.1. Langmuir Isotherm

Langmuir isotherm takes postulation that the sorption presents at particular homogeneous sites within the adsorbent. The common term for Langmuir equation is,

$$q_e = b \ q_{max} \ Ce/1 + bCe$$
 (5.4.1)

The linear structure of isotherm equation has written as,

$$1/q_e = (1/bq_{max}) (1/Ce) + (1/q_{max})$$
 (5.4.2)

 q_{max} = Saturation capacity of the adsorbent by maximum BBR dye uptake,

b = Energy of adsorption variable C_e and q_e respectively.

The constant q_{max} (17.59 mg/gm), 'b'(0.0185) and r^2 (0.9924) are the characters of Langmuir isotherm and can be determined from the Langmuir equation, a plot of $1/q_e$ Vs $1/C_e$ gives a straight line of a slope ($1/q_{max}$) and intercept $1/q_{max}$ as given in table-5.4.5 and figure-5.4.5. The high r^2 value represents that the Langmuir isotherm was fitted well. The linearity of the plot represents the application of Langmuir equation is supporting monolayer formation on the surface of the adsorption for BBR dye on LPSP biosorbent.

5.4.5.2. Freundlich Isotherm

Freundlich isotherm is an experimental equation based on a heterogeneous surface. The common form of Freundlich equation is,

$$q_e = k_f C_e^{1/n}$$
 (5.4.3)

The linear form of the equation is,

$$\log q_{e} = \log k_{f} + 1/n \log C_{e}$$
 (5.4.4)

The linear plot of log q_e versus log C_e got in this study which exhibits in figure-5.4.6., it can be utilized to find out the value of k_f (2.5379) and 'n' (1.0348) for adsorption of BBR dye by Freundlich adsorption isotherm at 30°C, values of K_f and 'n' given in table-5.4.5.

5.4.6 Kinetics Studies

Kinetic models were used to analyze the experimental data to explore about the potential rate controlling step and the mechanism of the adsorption such as the chemical reaction and mass transfer process. The transiting perform of batch adsorption process was studied by using pseudo first order and pseudo second order kinetic models.

5.4.6.1. Pseudo First order

The possibility of adsorption data following Lagergren pseudo-first-order kinetic is given by the linearized eq.

$$\log (q_e - q_t) = \log q_e - (k_1/2.303)t$$
 (5.4.5)

Where q_e (mg/g) and q_t (mg/g) refers to the amount of BBR dye adsorbed per unit weight of adsorbent at equilibrium and at time t, k_1 is the rate constant of

adsorption [18]. The sorption coefficient and the capacity of the equilibrium q_e can be determined from the linear plot of log $(q_e - q_t)$ versus time t from the figure-5.4.7. It was evidence that the linear plot exhibits the applicability of the Lagergran equation, q_e with correlation coefficient of r^2 is 0.9943 values were present at table-5.4.6 for BBR dye adsorption on LPSP biosorbent.

5.4.6.2. Pseudo Second order

This adsorption kinetic equation was developed by 'Ho', studied to give details about the sorption capacity, the pseudo second order model can be written as,

$$t/q_t = 1/k_2 q_e^2 + 1/q_e t$$
 (5.4.6)

Where, t is the constant time (min), q_e (mg/g) and q_t (mg/g) are the amounts of dye adsorbed at equilibrium and at any time, t [19].

If second order kinetics is applicable; the plot of t/q_t verses t should give a linear relationship (Figure-5.4.8). The q_e and r^2 values can be derived from the plot. The data values were reported in table-5.4.6. In Pseudo Second order, the calculated q_e very closer to the experimental q_e . It was seen that the pseudo-second-order model fitted very well and reporting a very high correlation coefficient of 0.9994 with q_e 126.35 mg/g for adsorption BBR dye on LPSP biosorbent.

5.4.5 FT-IR spectra of Laplap purpureus stems powder after BBR dye adsorption

The FTIR study provides the change in functional groups of biosorbent LPSP, spectra of the LPSP before and after the BBR dye adsorption shows in the figure-5.4.9. FTIR spectrum of native biosorbent revealed a number of absorption peaks with the range of 600-4000 cm⁻¹, which is only a sign of the complex chemical nature of this biosorbent. The aromatic compounds of the BBR dye molecule showed characteristic absorption peaks at 2995 cm⁻¹ due to aromatic OH stretching. The absorption band

appears at 1998 cm⁻¹ due to CH stretching of alkyl group. The absorption band at 3455 cm⁻¹ was due to NH stretching of amino group of dye molecule. The peaks appear at 1590 cm⁻¹, 1480 cm⁻¹ was due to C-N-C stretching. The absorption spectrum of biosorbent treated with dye solution showed evident changes with respect to that of native biosorbent. Amongst these changes were the broadening of the absorption bands between 3455 and 1480 cm⁻¹ which suggests the superposition of numerous peaks that appeared in these regions. The band appears at 1480 cm⁻¹ and 3455 cm⁻¹ due to the biosorbent binding with BBR dye molecule.

5.4.6 XRD Analysis for LPSP adsorbent before and after BBR dye on adsorption

The XRD pattern of LPSP before and after adsorption of BBR dyes are recorded in figure-5.4.10. The intense main peak shows the presence of a highly organized crystalline structure in unloaded LPSP. After the adsorption of BBR dye, the intensity of the highly organized peaks is slightly disappeared. This has been attributed to the adsorption of BBR dye on the upper layer of crystalline structure of the LPSP surface by means of physisorption.

5.4.7. Scanning Electron Microscope Analysis for BBR dye on LPSP before and after adsorption

Morphological characters of the biosorbent can be analyzed by Scanning Electron Microscope studies. It provides useful information about biosorbent. The SEM image of the raw LPSP biosorbent appears as a rough and uneven surface. This rough surface character must be considered as a reason for binding of BBR dye molecule. After the BBR was dye loaded on LPSP biosorbent, the SEM image is considerable changes were observed after loading of BBR dye in the LPSP biosorbent which shows in figure-5.4.11.

Table: 5.4.1 Effect of pH for BBR dye uptake, Time 50 min, Biosorbent dose 300 mg, Volume of BBR dye solution 50 mL, Initial dye concentration 200 mg/L and Temperature 30° C.

pН	Percentage of Removal
2	61.50
3	65.52
4	67.03
5	68.20
6	71.57
7	74.63
8	77.91
9	75.35
10	75.35

Table: 5.4.2 Effect of Biosorbent dose for BBR dye uptake, Time 50 min, pH 8, Volume of BBR dye Solution 50 mL, Initial dye concentration 200 mg/L and Temperature $30^{\circ}\mathrm{C}$

Adsorbent dose	Percentage of
(mg)	Removal
100	72.49
200	75.79
300	77.99
400	77.59
500	77.39

Table: 5.4.3 Effect of contact time for BBR dye uptake, pH 8, volume of BBR dye solution 50 mL, Biosorbent dose 300 mg, Initial dye concentration 200 mg/L and Temperature 30° C.

Time in(min)	Percentage of Removal
10	72.49
20	73.59
30	74.69
40	75.79
50	77.44
60	77.44
70	77.44

Table: 5.4.4 Effect of Initial dye concentration for BBR dye uptake, Time 50 min, pH 8, Volume of BBR dye Solution 50 mL, Biosorbent dose 300 mg and Temperature 30°C.

Percentage of Removal	
79.28	
77.99	
76.56	
76.25	
75.72	
75.46	
75.20	
73.80	
72.44	
71.78	

Table: 5.4.5 Langmuir and Freundlich model parameters

Temperature	Langmuir model			Freundlich model		
30° C	q _m (mg/g)	b (L/mg)	\mathbf{r}^2	$K_f (mg^{1-n} g^{-1} L^n)$	$n(mg^{1-n}g^{-1}L^n)$	\mathbf{r}^2
	17.59	0.0185	0.9924	2.5379	1.0348	0.9719

Table: 5.4.6 Pseudo-first-order and second order kinetic parameters

Ci	Temp.	Pseudo-first-order			Pseudo	-second-ord	er
(mg/L)	(°C)	Cal. Exp. r ²			Cal.	Exp.	\mathbf{r}^2
		$q_e (mg/g)$	q _e (mg/g)		$q_{e}\left(mg/g\right)$	$q_e (mg/g)$	
200	30	91.08	122.33	0.9943	111.17	126.35	0.9994

Figure: 5.4.1 Effect of pH for BBR dye uptake, Time 50 min, Biossorbent dose 300 mg, Volume of BBR dye solution 50 mL, Initial dye concentration 200 mg/L and Temperature 30°C.

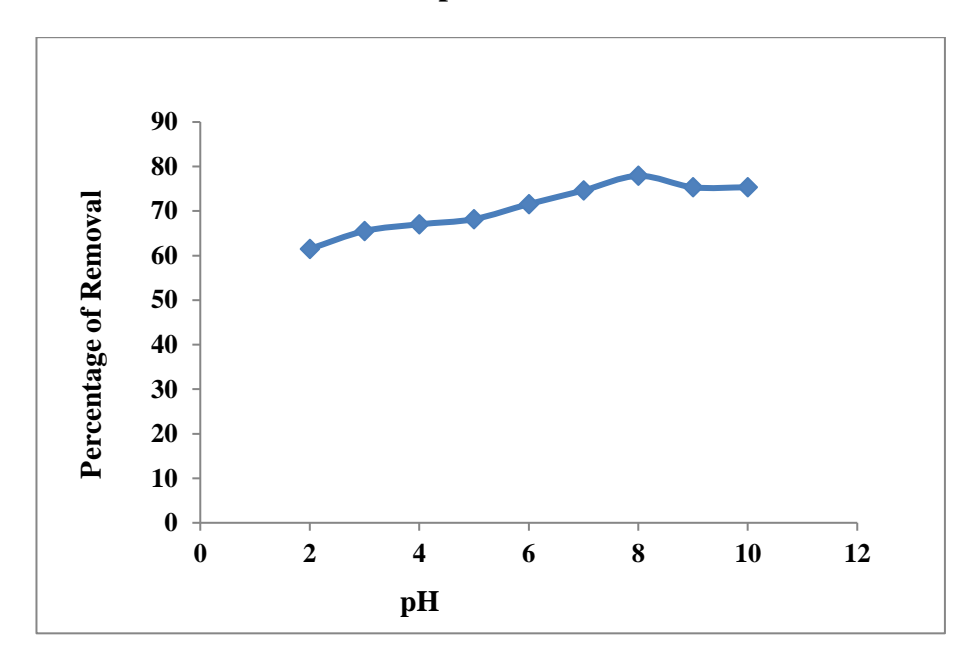


Figure: 5.4.2 Effect of Biosorbent dose for BBR dye uptake, Time 50 min, pH 8, Volume of BBR dye Solution 50 mL, Initial dye concentration 200 mg/L and Temperature 30°C.

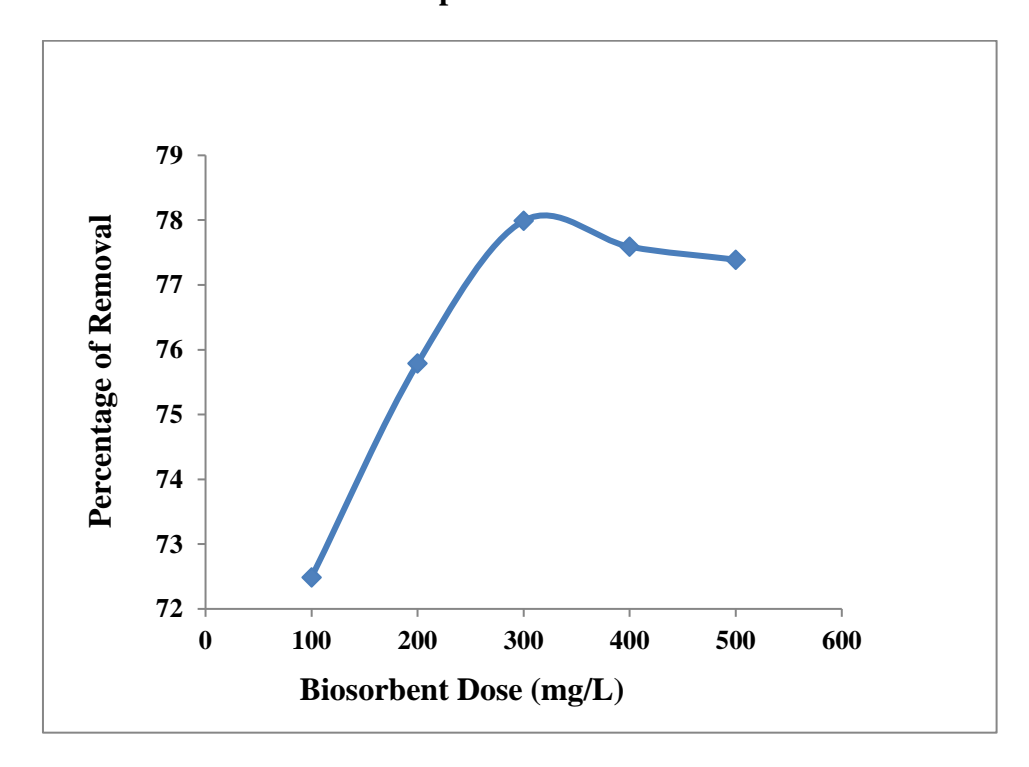


Figure: 5.4.3 Effect of contact time forBBR dye uptake, pH 8, volume of Solution 50 mL, Biosorbent dose 300 mg, Initial dye concentration 200 mg/L, Temperature 30°C.

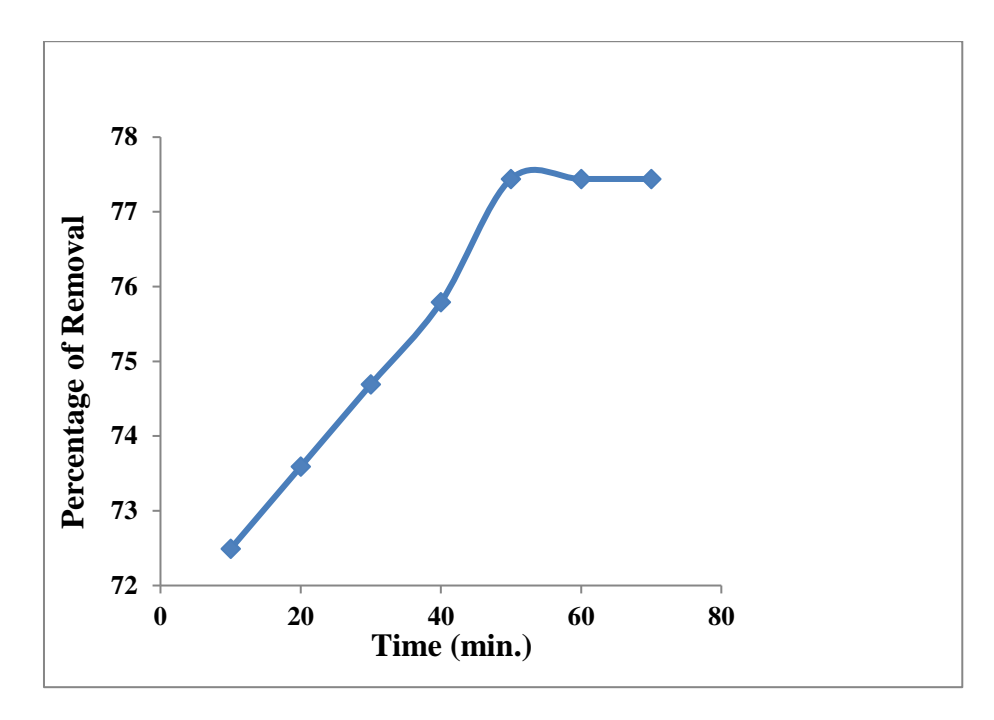


Figure: 5.4.4 Effect of Initial dye concentration for BBR dye uptake, Time 50 min, pH 8, Volume of Solution 50 mL, biosorbent dose 300 mg and Temperature 30° C.

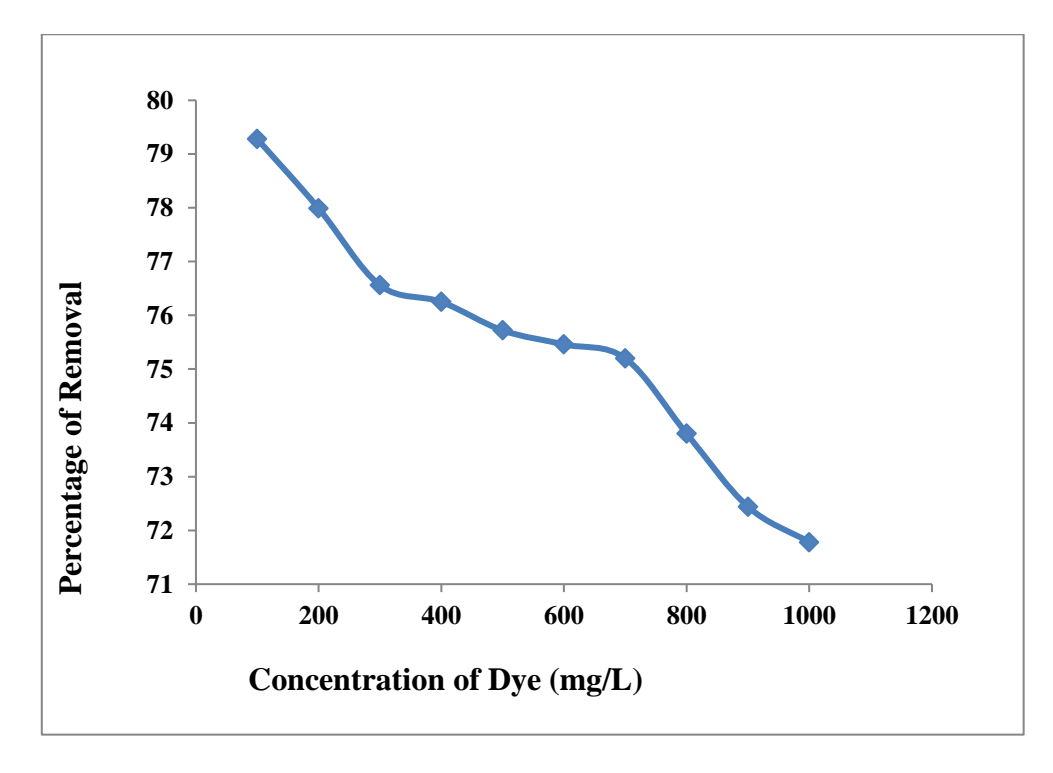


Figure: 5.4.5 Langmuir isotherm plot of Bismark Brown R dye using Laplap purpureus plant stem powder at 30°C.

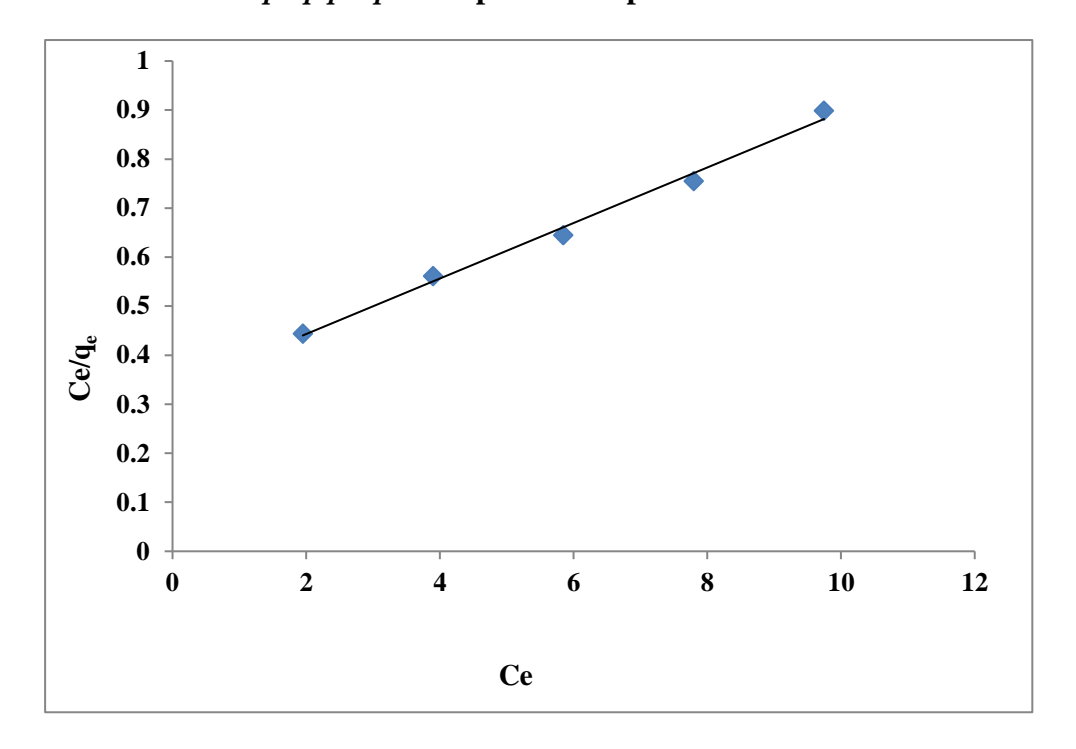


Figure: 5.4.6 Freundlich isotherm plot of Bismark Brown R dye using Laplap purpureus plant stem powder at 30°C.

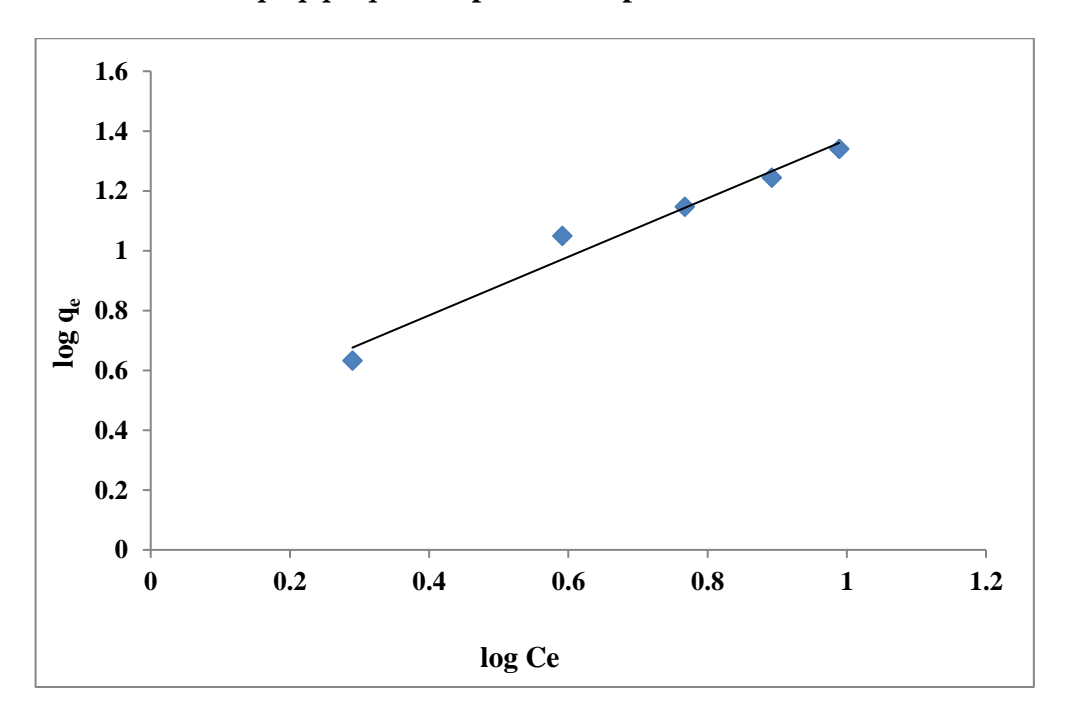


Figure: 5.4.7 Pseudo first order plot for adsorption of Bismark Brown R dye using *Laplap purpureus* plant stem powder.

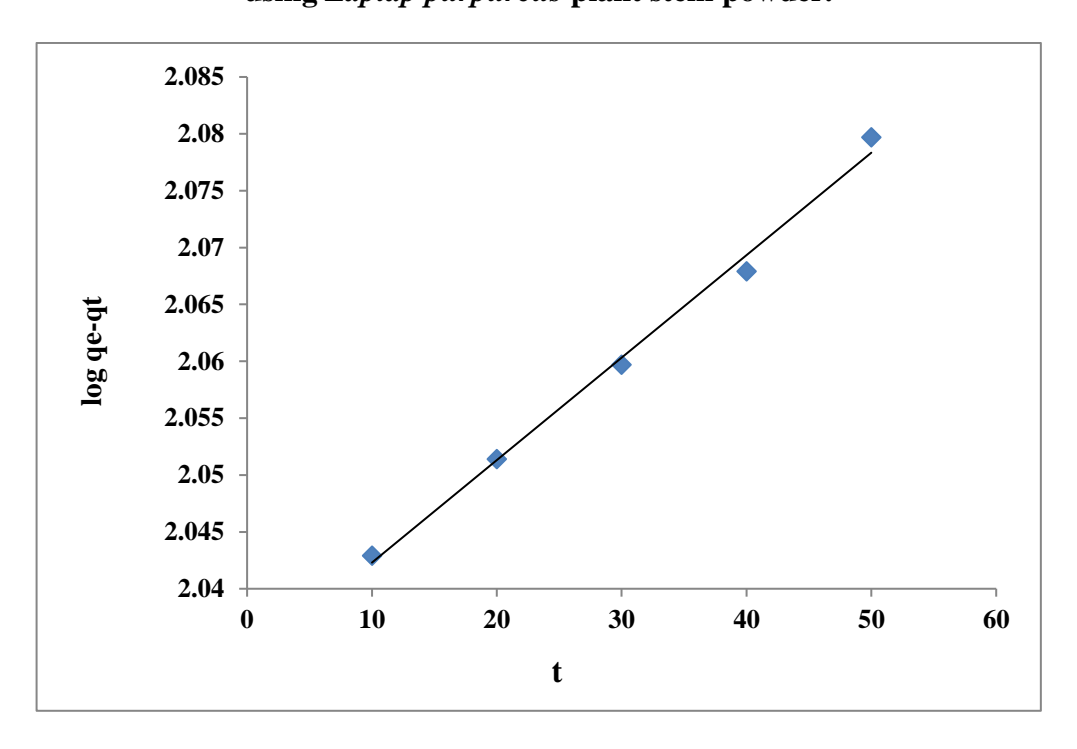


Figure: 5.4.8 Pseudo second order plot for adsorption of Bismark Brown R dye using *Laplap purpureus* plant stem powder.

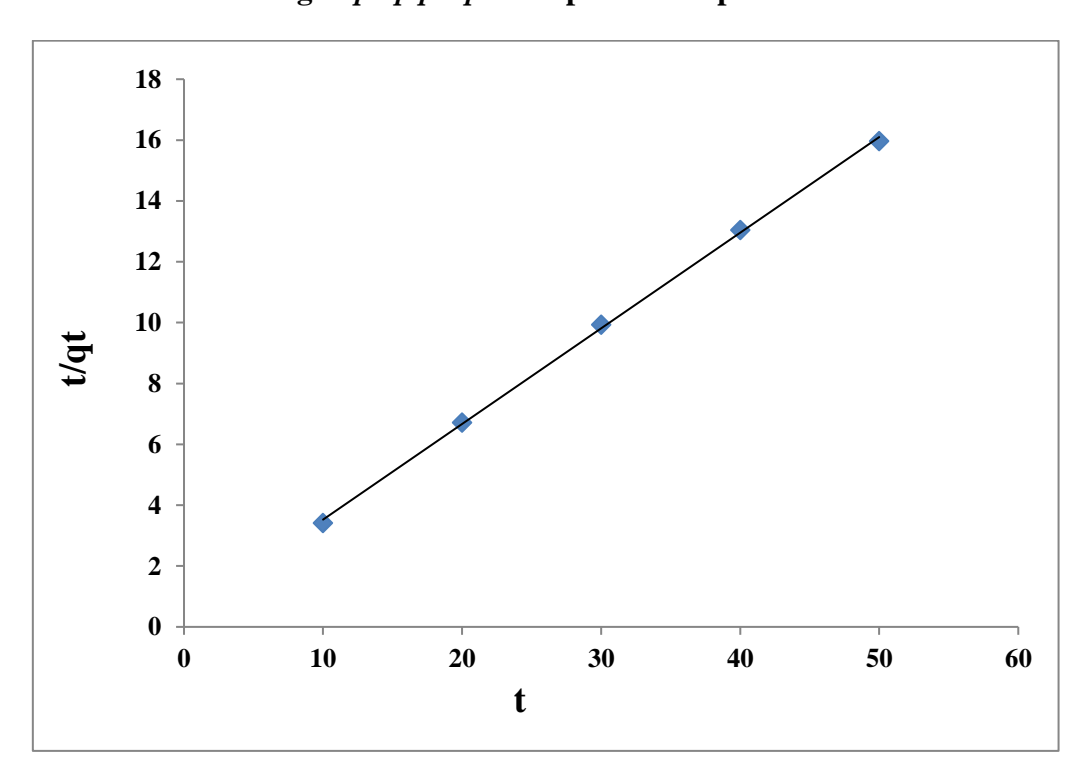
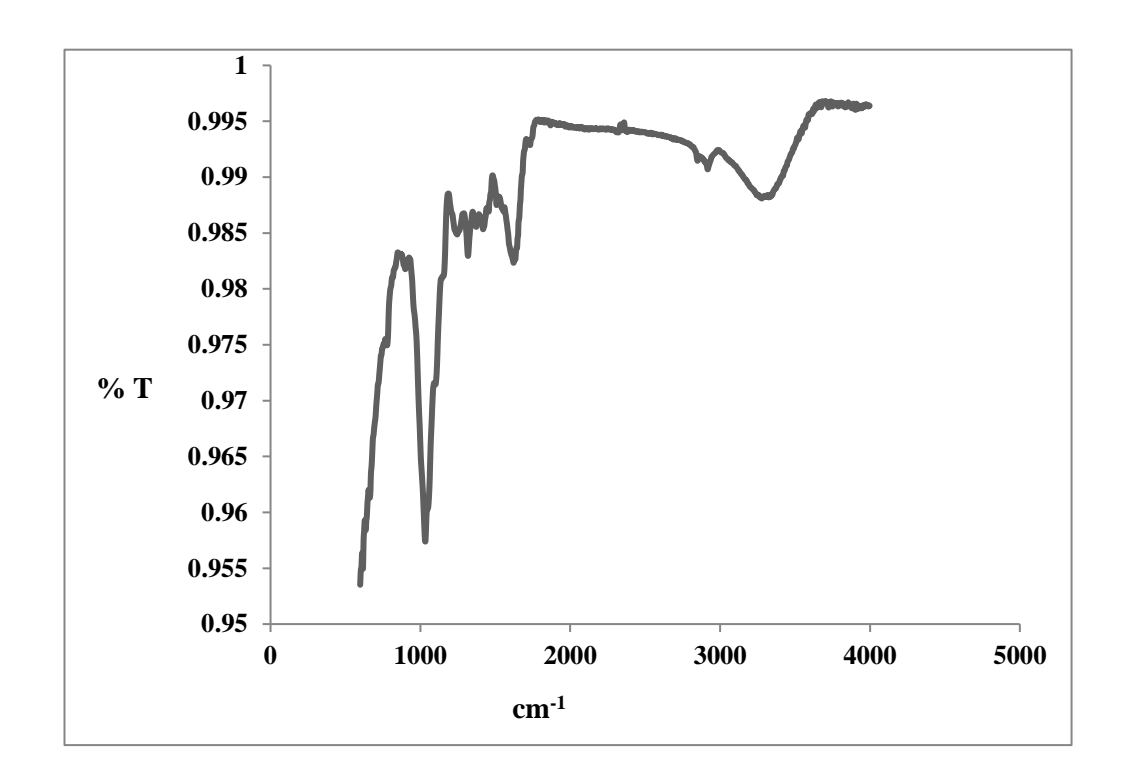


Figure: 5.4.9 FTIR images of before and after adsorption of Bismark Brown R dye using *Laplap purpureus* plant stem powder.



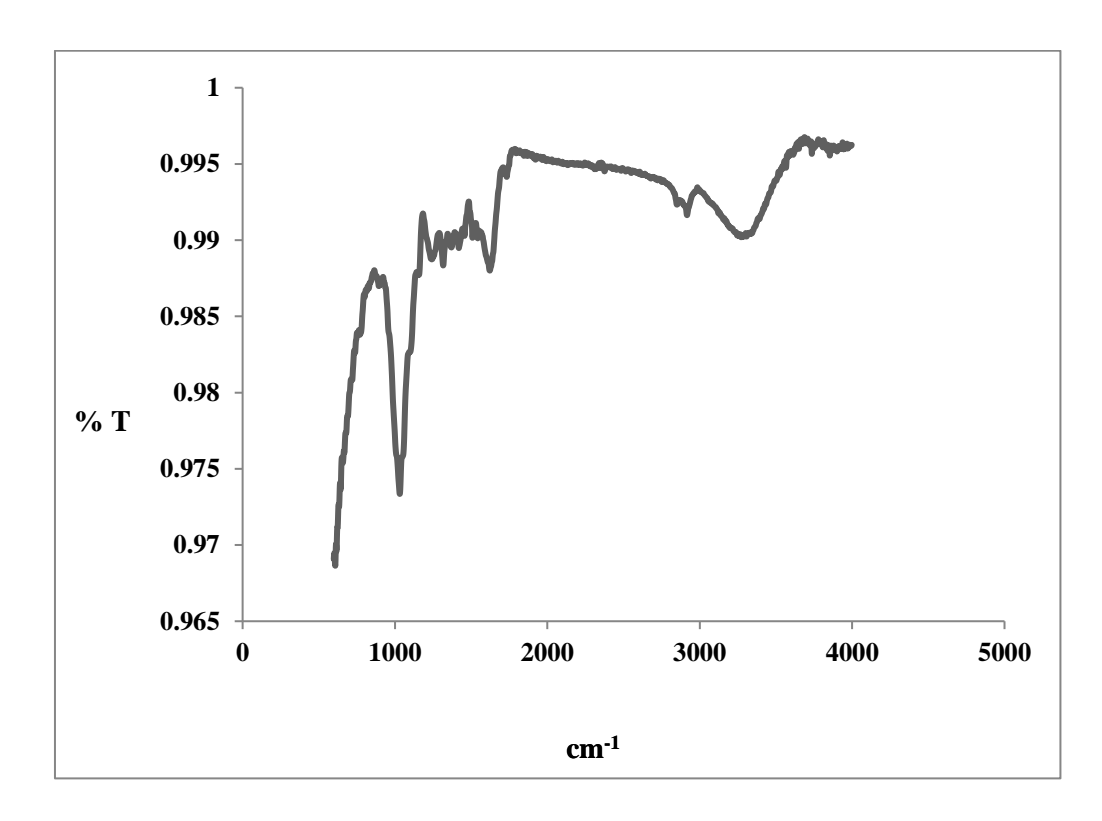


Figure: 5.4.10 XRD images of before and after adsorption of Bismark Brown R dye using *Laplap purpureus* plant stem powder.

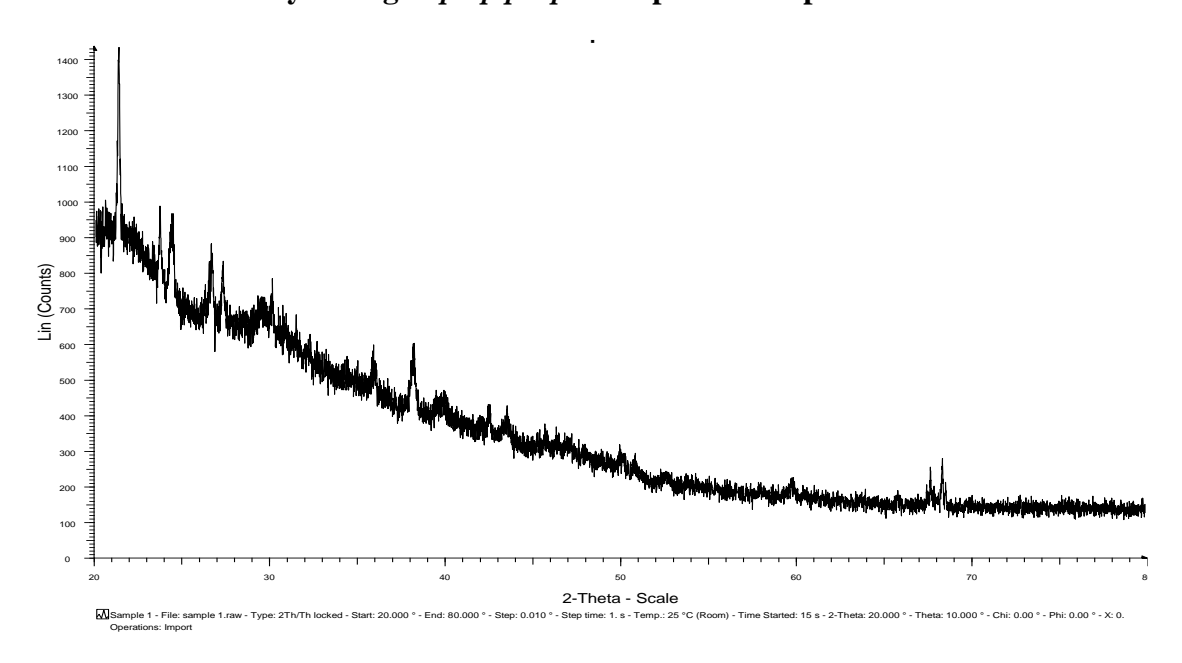
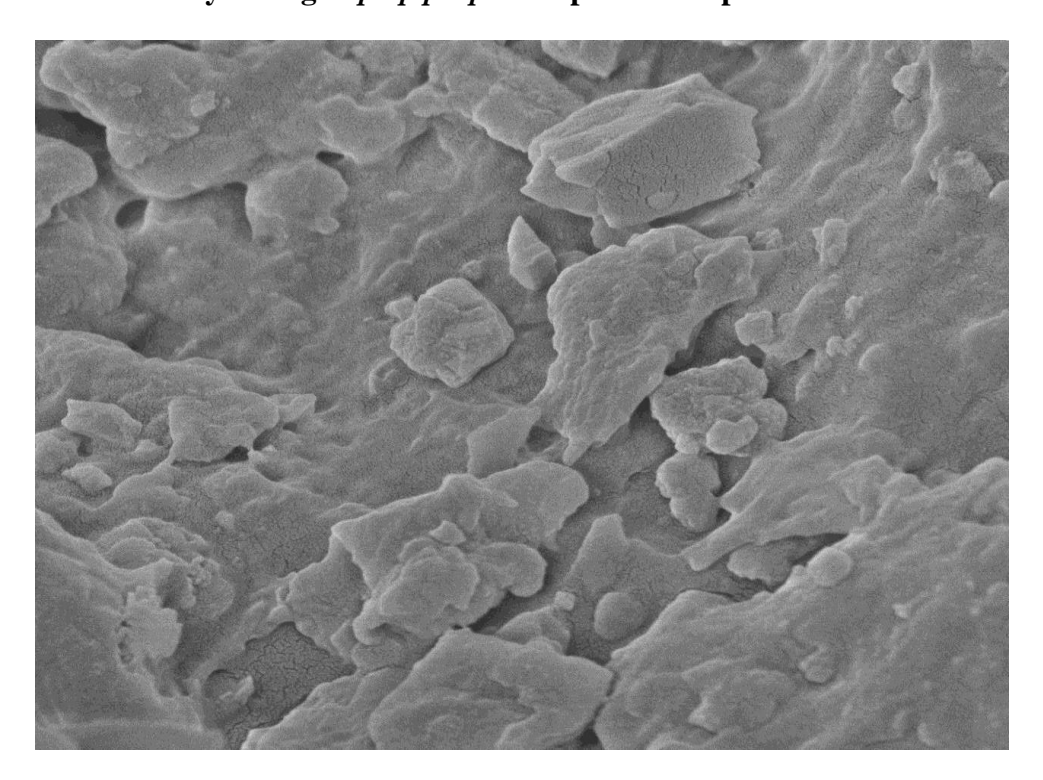
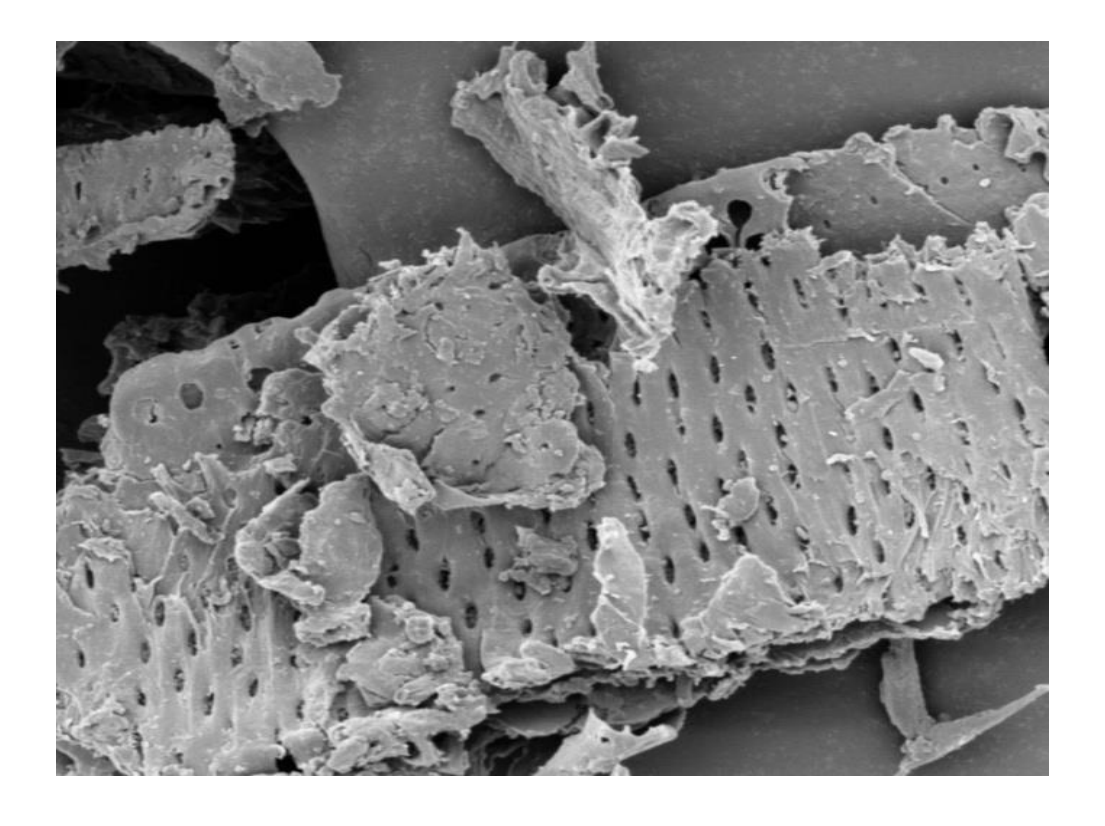


Figure: 5.4.11 SEM images of before and after adsorption of Bismark Brown R dye using *Laplap purpureus* plant stem powder.





5.5 Adsorption of Malachite Green dye on *Laplap purpureus* stems powder (LPSP)

5.5.1 Effect of pH on adsorption of Malachite Green dye

The effect of pH is the most important parameter to direct the adsorption process. The experiment was done with the pH range from 2 to 10, temperature 30°C, contact time 50 minutes, agitation speed 360 rpm, initial dye concentration 200 mg/L, and biosorbent dose 300 mg. The results of the experimentation are shown in the table-5.5.1., and figure-5.5.1. The biosorbent has posses polymers with more functional groups, hence, the net charge on the biosorbent is the most pH-dependent [193]. The effect of pH on adsorption can be explained on the basis of point zero charges (pHpzc), this is the point at pH-7, the net charge of the biosorbent is zero [202]. When pHpzc the surface of the biosorbent has negatively charged, the negatively charged LPSP surface is favorable for the adsorption of cationic MG dye from pH-7 up to pH-10. Thus, less adsorption occurs at lower pH from the lower pH-2 up to pH-7 for basic MG dye [203].

5.5.2 Effect of Biosorbent (LPSP) dose on adsorption of Malachite Green dye

The effect of biosorbent dosage also studied for the removal of MG dye in the form of a synthetic aqueous solution by the biosorbent dose varied from 100 to 500 mg amongst with the other parameters were constant which are pH 8, initial dye concentration 200 mg/L, temperature 30°C, contact time 50 minutes, agitation speed 360 rpm. The results of the experiment have given in table-5.5.2., and figure-5.5.2. The figure shows that most of the adsorption was completed with the biosorbent dose weight from 100 to 300 mg. The dye uptake increases by increasing the biosorbent dose due to increasing the number of availability of adsorption sites [204]. After the 300 mg of the biosorbent dose weight, the removal efficiency of dye was insignificant. Therefore, 300 mg biosorbent dose was favored for subsequent experiments.

5.5.3 Effect of contact time for adsorption of Malachite Green dye

In this parameter, the time varied from 10 to 70 minutes, temperature 30°C, biosorbent dose 300 mg, pH- 8, initial dye concentration 200 mg/L, and agitation speed 360 rpm had kept permanent. The experimental data were exhibited in table-5.5.3 and figure-5.5.3., shows the efficiency of dye adsorption for the effect of contact time. At the initial time of contact, the adsorption rapidly increases by the excess of vacant surface area on the biosorbent, and as the adsorption continues, the rate of adsorption decreases due to a decrease in surface area of the biosorbent [205]. The figure represented that the contact time of 50 minutes was enough to achieve equilibrium and the adsorption did not change by further increasing contact time. Therefore, the contact time has been favored as 50 minutes for the continuous experiment.

5.5.4 Effect of Initial concentration on adsorption of Malachite Green dye

The experimental study was done with various concentrations of MG dye solution from 100 to 1000 mg/L and temperature 30°C, biosorbent dose 300 mg, pH 8, contact time 50 minutes, agitation speed 360 rpm. The experiment data are shown in table-5.5.4., and figure-5.5.4. The figure exhibits that the percentage of removal is maximum at lower initial dye concentration and on the other hand the percentage of removal is minimum at a higher initial dye concentration. This represents that there is a fixed number of available binding sites per unit mass of the biosorbent surface. The number of the available binding sites is higher for low initial dye concentration compared with the high initial dye concentration. Therefore, most of the dye molecules were adsorb by biosorbent at low MG initial dye concentrations, hence, the percentage of dye removal is higher. Dye molecules contribute to binding with each other for a fixed number of available binding sites at higher MG initial dye concentration. So, a

few of the dye molecules cannot be adsorbed, as a result, the percentage of dye removal became lower [206, 207].

5.5.5Adsorption Isotherm

5.5.5.1 Langmuir Isotherm

The Langmuir isotherms models depend upon the postulation of monolayer adsorption on the surface of the adsorbent contain a limited number of adsorption sites of identical energies for adsorption. The general term for the Langmuir equation is,

$$qe = q_mbCe/(1+bCe)$$
 (5.5.1)

The linear term for Langmuir isotherm equation has written as,

$$Ce/qe = 1/bq_m + Ce/q_m$$
 (5.5.2)

Where,

qe = Adsorption density (mg/g) of Malachite Green dye at equilibrium,

Ce = Equilibrium concentration (mg/L) of Malachite Green dye in solution,

q_m = Maximum dye uptake corresponding to the saturation capacity of adsorbent (mg/g),

b = The Langmuir constant (L/mg) related to the energy of adsorption.

The constant q_m (36.52 mg/g) and 'b' (0.0493 L/mg) are the characters of the Langmuir isotherm and can be calculated from the Langmuir equation. In this study, a linear plot was obtained between Ce/qe Vs Ce which indicates that the adsorption process followed Langmuir adsorption isotherm (figure-5.5.5 and table-5.5.5). So, the linearity of the plots represents the purpose of the Langmuir equation, which fitted monolayer formation on the surface of the LPSP biosorbent in adsorption of MG dye due to high r^2 value (0.9893).

5.5.5.2 Freundlich Isotherm

The Freundlich isotherm is an experimental equation for a heterogeneous surface that occurs in the adsorption process. The general term for the Freundlich equation is,

$$qe = K_f Ce1/n$$
 (5.5.3)

Logarithmic form of the equation can be written as,

$$\ln qe = \ln K_f + (1/n) \ln Ce$$
 (5.5.4)

where, the intercept $\ln K_f$ is a measure of adsorption capacity and slope 'n' is the intensity of adsorption. The values of K_f (1.9764 mg^{1-n} g^{-1} L^n) and 'n' (1.0154 mg^{1-n} g^{-1} L^n) were calculated from intercept ($\ln K_f$) and slope (1/n) of plots drawn between $\ln qe$ vs $\ln Ce$ (Figure-5.5.6 and table-5.5.5). The variable qe and qe are dye adsorbed and the equal dye concentration in solution. If so, the 'n' value might be in the range of 1 to 10 (1.0154) pointing out beneficial adsorption, therefore the value of 'n' revealed that LPSP is considered as an effective biosorbent for the MG dye.

5.5.6. Adsorption Kinetic Studies

The Kinetic models were studied to examine the experimental data for investigation regarding the mechanism of the adsorption and potential rate-controlling steps such as the mass transfer process and the chemical reaction. The transiting work of the batch adsorption process was calculated by means of using pseudo-first-order and pseudo-second-order kinetic models of adsorption.

5.5.6.1 Pseudo First order

The linear form of Lagergren's pseudo-first-order kinetic model is represented by the following equation.

$$\ln (qe - qt) = \ln qe - K_1 t$$
 (5.5.5)

Where, qe (mg/g) and qt (mg/g) represents the amount of MG dye adsorbed per unit weight of adsorbent at equilibrium and at time t respectively, K_1 is the rate constant of adsorption.

The adsorption coefficient and the capacity of the equilibrium qe can be confirmed from the linear plot drawn between ln (qe-qt) vs 't' as shown in figure-5.5.7. It was indicated that the linear plot shows the possibility of the Lagergren equation, qe values were shown in table-5.5.6. The results revealed that the concentration of MG dye has no significant effect. The correlation coefficient of r² is 0.9833 with qe 114.42 mg/g.

5.5.6.2 Pseudo Second order

This adsorption kinetic model equation was developed by Ho and MacKay (1999), studied to give information about the adsorption capacity, the pseudo-second-order model can be written as,

$$t/qt = 1/K_2 qe^2 + 1/qet$$
 (5.5.6)

Where, K_2 is the rate constant of adsorption (g/mg min), t is the constant time (min), q_e (mg/g) and qt (mg/g) denote the amounts of MG dye adsorbed at equilibrium and at times respectively. If pseudo-second-order kinetics is applicable; the values of K_2 and q_e were calculated from intercept (1/ K_2 q_e^2) and slope (1/ q_e) of the plots of t/qt vs t have to give a linear relationship as given in figure-5.5.8., and qe and r^2 values can be obtained from the plots. These values were shown in table-5.5.6. It was exhibited that the calculated qe was very closer to experimental q_e , hence the pseudo-

second-order model fitted well and resulting high correlation coefficient of r^2 0.9977 with qe 122.74 mg/g for adsorption of MG dye on LPSP biosorbent.

5.5.7 FT-IR spectra of LPSP before and after adsorption of MG dye

The FTIR study provides the change in functional groups of biosorbent LPSP, spectrum of the LPSP before and after the MG dye adsorption shows in the figure-5.5.9. FTIR spectrum of native biosorbent revealed that a number of absorption peaks with the range of 600-4000 cm⁻¹, which is only a sign of the complex chemical nature of this biosorbent. The aromatic compounds of the MG dye molecule showed characteristic absorption peaks at 2995 cm⁻¹ due to aromatic OH stretching. The absorption band appears at 1998 cm⁻¹ due to CH stretching of alkyl group. The absorption band at 3455 cm⁻¹ was due to NH stretching of the amino group of the MG dye molecule. The peaks appear at 1590 cm⁻¹, 1480 cm⁻¹ was due to C-N-C stretching. The absorption spectrum of biosorbent treated with MG dye solution showed evident changes with respect to that of native biosorbent. Amongst these changes was the broadening of the absorption bands between 3455 and 1480 cm⁻¹ which suggests the superposition of numerous peaks that appeared in these regions. The band appears at 1480 cm⁻¹ and 3455 cm⁻¹ due to the biosorbent binding with the MG dye molecule.

5.5.8 Scanning Electron Microscope Analysis for LPSP before and after adsorption of MG dye

Morphological properties of the biosorbent have been analyzed by means of Scanning Electron microscope (SEM) studies, the images shows in figure-5.5.10. It provides information regarding the LPSP biosorbent before and after adsorption of MG dye. The SEM picture of the unloaded LPSP biosorbent seem as an uneven and rough surface. These uneven and rough surface properties must be well-thought-out as a reason for the binding of MG dye molecules on LPSP biosorbent. After the MG dye

loaded on the LPSP biosorbent, the SEM picture is great changes were obtained in the structure of the LPSP biosorbent. The biosorbent exhibits new shiny particles like an irregular surface and minute pores were appear after the adsorption process.

Table: 5.5.1 Effect of pH for MG dye adsorption, Time 50 min, Biosorbent weight 300 mg, Volume of dye solution 50 mL, Initial dye concentration 200 mg/L and Temperature 30°C.

pН	Percentage of Removal
2	60.47
3	63.53
4	66.89
5	68.07
6	71.47
7	74.43
8	74.81
9	75.05
10	75.97

Table: 5.5.2 Effect of Biosorbent dose on MG dye adsorption, Time 50 min, pH 8, Volume of dye Solution 50 mL, Initial dye concentration 200 mg/L and Temperature 30°C.

Adsorbent dose (mg)	Percentage of Removal
100	72.46
200	75.73
300	77.83
400	77.53
500	77.53

Table: 5.5.3 Effect of contact time on MG dye adsorption, pH 8, volume of dye Solution 50 mL, Biosorbent weight 300 mg, Initial dye concentration 200 mg/L, Temperature 30° C.

Time (min)	Percentage of Removal
10	72.39
20	73.53
30	74.59
40	75.73
50	76.03
60	75.97
70	75.94

Table: 5.5.4 Effect of Initial dye concentration on MG dye adsorption, Time 50 min, pH 8, Volume of dye Solution 50 mL, Biosorbent weight 300 mg and Temperature 30° C.

Concentration of	Percentage of
MG dye (ppm)	Removal
100	79.19
200	77.45
300	76.16
400	75.89
500	75.53
600	75.17
700	75.05
800	74.87
900	74.73
1000	74.69

Table: 5.5.5 Langmuir and Freundlich adsorption isotherm parameters for MG dye on LPSP

Temperature	Langmuir model		Freundlich model			
30°C	q _m (mg/g)	b (L/mg)	r ²	K _f (mg ¹⁻ⁿ g ⁻¹ L ⁿ)	n(mg ¹⁻ⁿ g ⁻¹ L ⁿ)	\mathbf{r}^2
	36.52	0.0493	0.9893	1.9764	1.0154	0.9700

Table: 5.5.6 Pseudo-first-order and Pseudo-second-order kinetic parameters for MG dye on LPSP

Ci	Temp.	Pseudo-First-Order			Pseud	do-Second-C	Order
mg/L	(°C)	Cal. Exp. r ²			Cal.	Exp.	r ²
		$q_e (mg/g)$	q _e (mg/g)		q _e (mg/g)	$q_e (mg/g)$	
200	30	90.32	114.42	0.9833	119.27	122.74	0.9977

Figure: 5.5.1 Effect of pH on adsorption of MG dye, Time 50 min, Biosorbent weight 300 mg, Volume of dye solution 50 mL, Initial dye concentration 200 mg/L and Temperature 30° C.

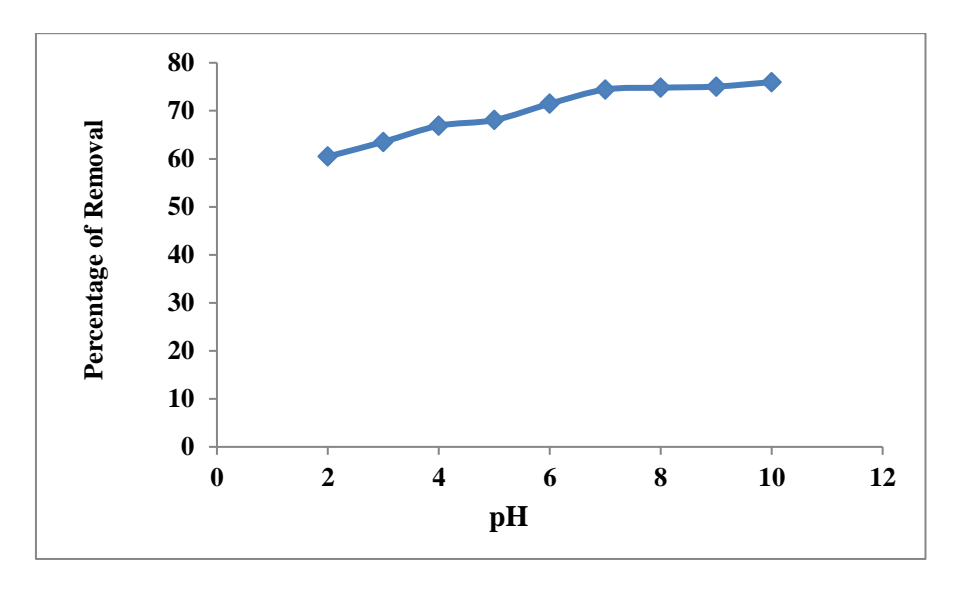


Figure: 5.5.2 Effect of Biosorbent dose on adsorption of MG dye, Time 50 min, pH 8, Volume of dye Solution 50 mL, Initial dye concentration 200 mg/L and Temperature 30°C.

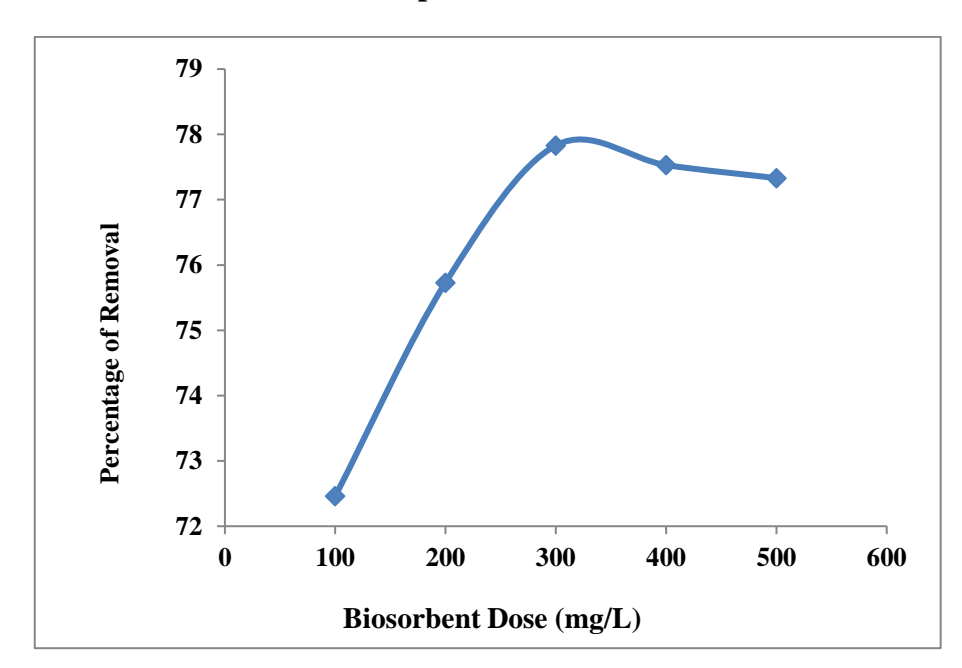


Figure: 5.5.3 Effect of contact time on adsorption of MG dye, pH 8, volume of dye Solution 50 mL, Biosorbent weight 300 mg, Initial dye concentration 200 mg/L, Temperature 30°C.

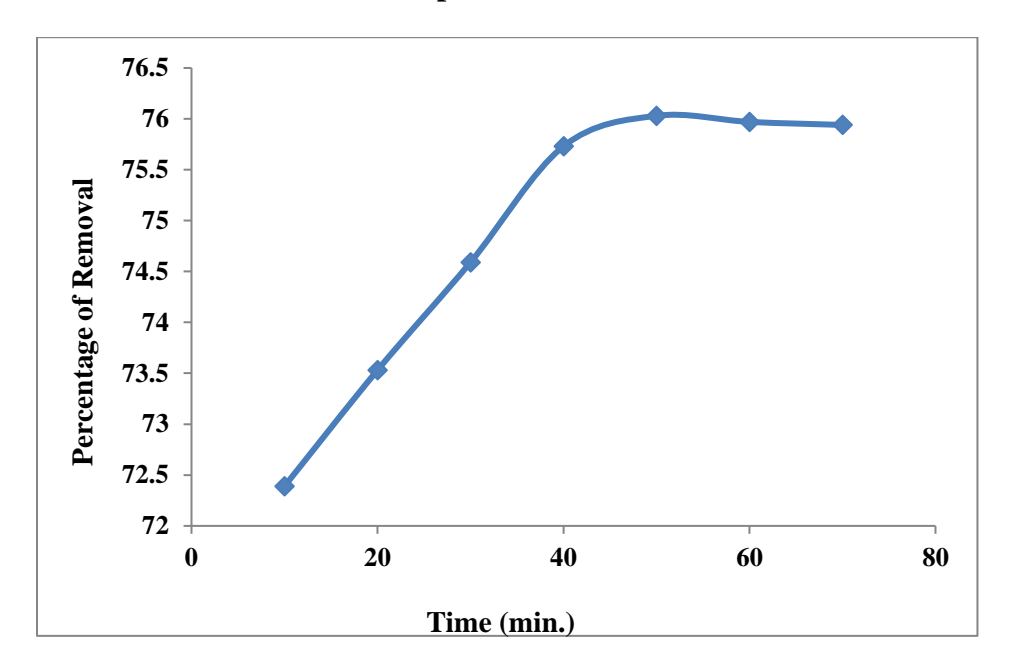


Figure: 5.5.4. Effect of Initial concentration on adsorption of MG dye, Time 50 min, pH 8, Volume of dye Solution 50 mL, Biosorbent weight 300 mg and Temperature 30°C.

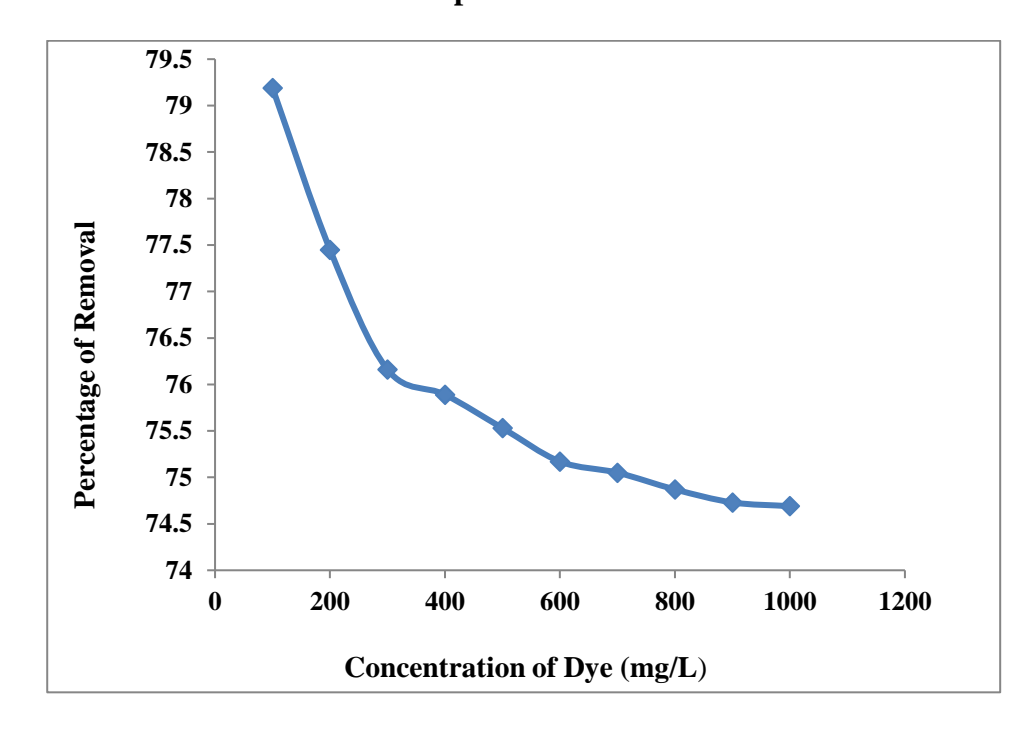


Figure: 5.5.5 Langmuir adsorption isotherm plot for Malachite Green dye using

Laplap purpureus plant stem powder.*

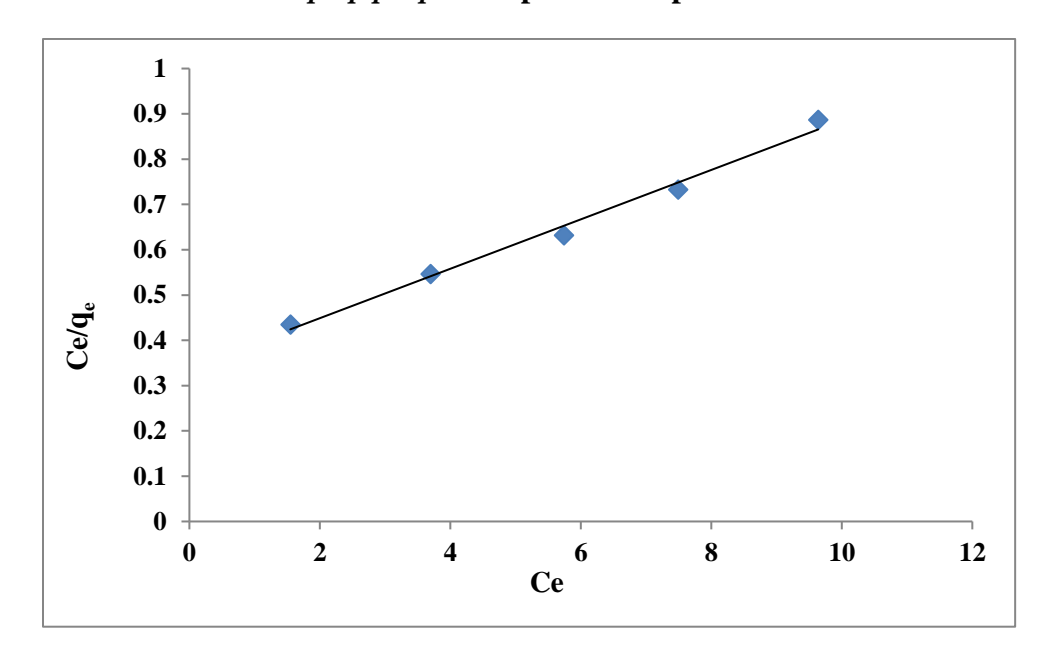


Figure: 5.5.6 Freundlich adsorption isotherm plot for Malachite Green dye using

Laplap purpureus plant stem powder.*

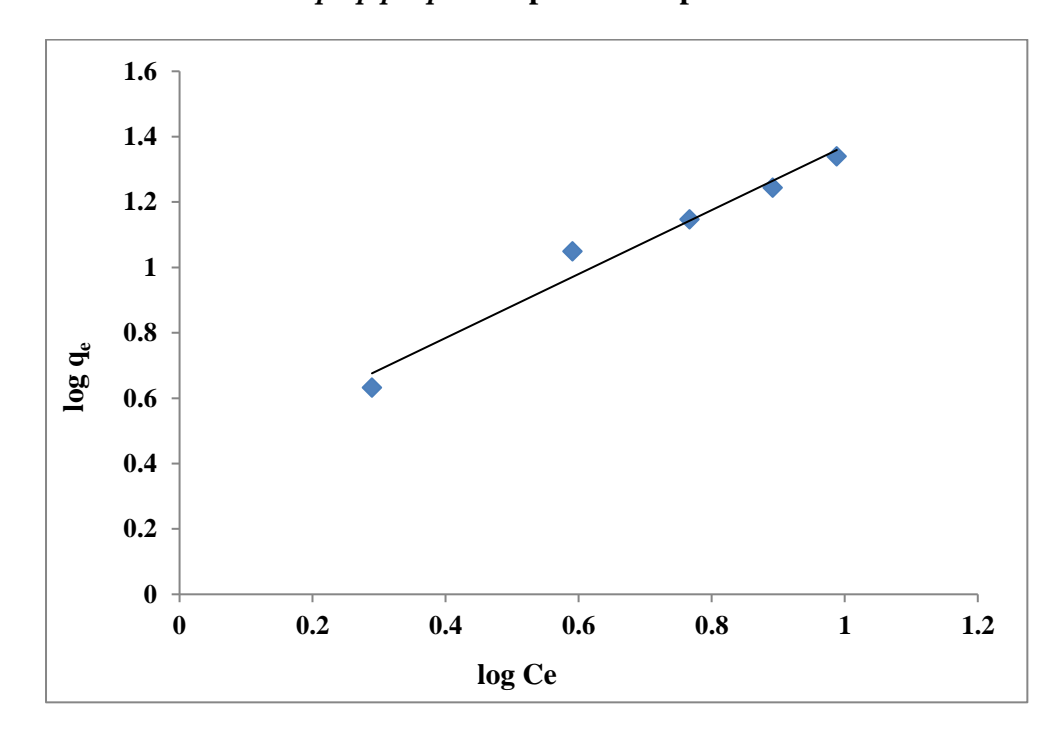


Figure: 5.5.7 Pseudo first order plot for Malachite Green dye using

Laplap purpureus plant stem powder.

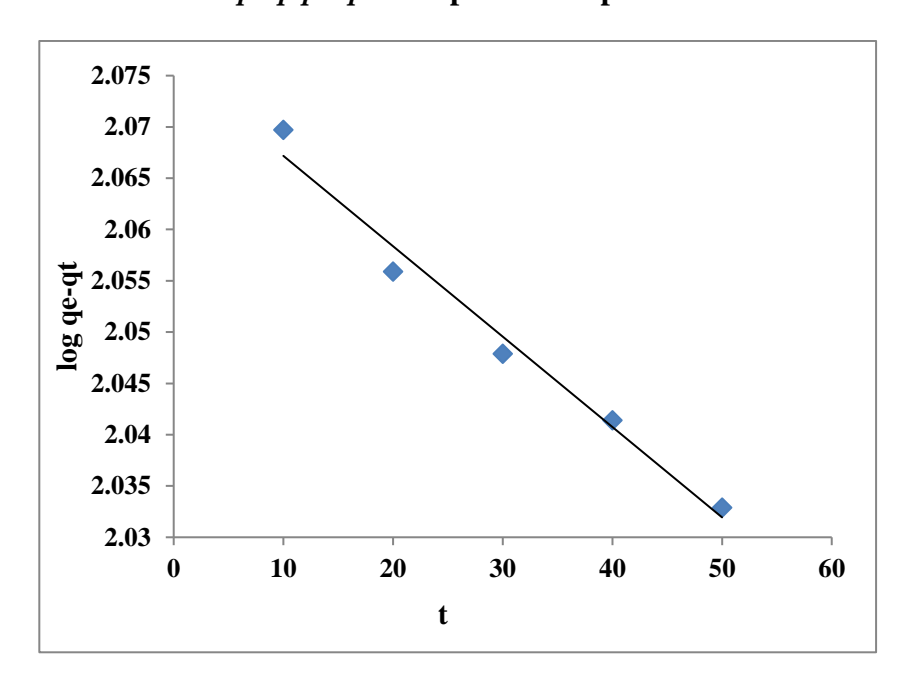


Figure: 5.5.8 Pseudo second order plot for Malachite Green dye using

Laplap purpureus plant stem powder.*

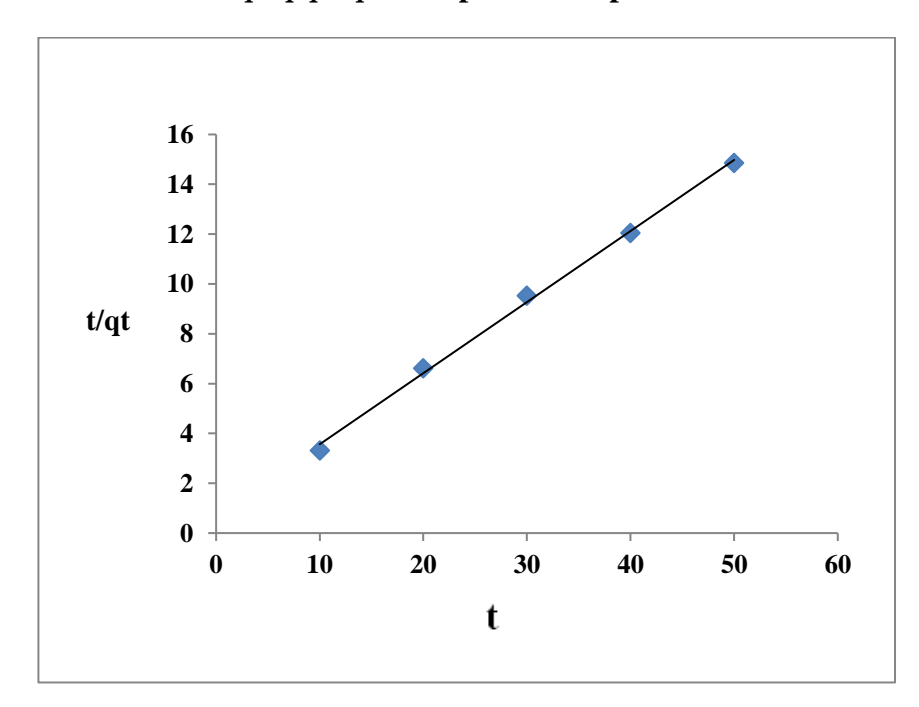
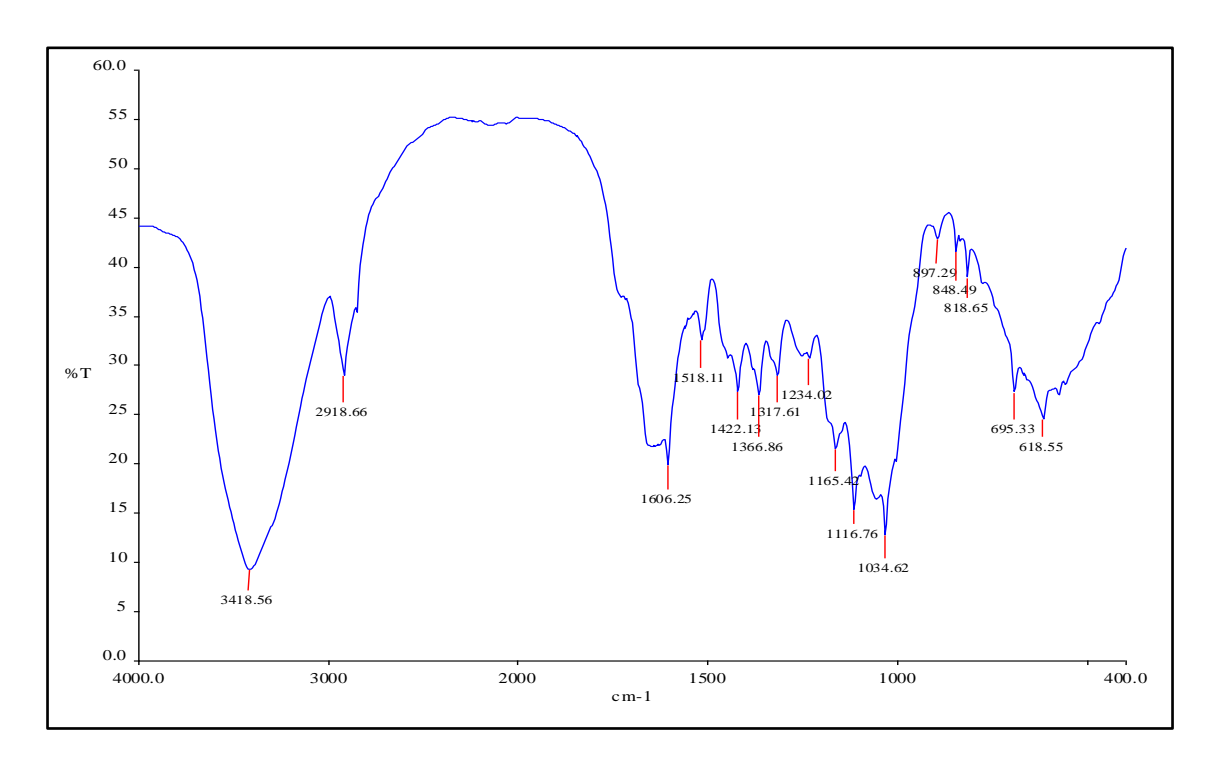
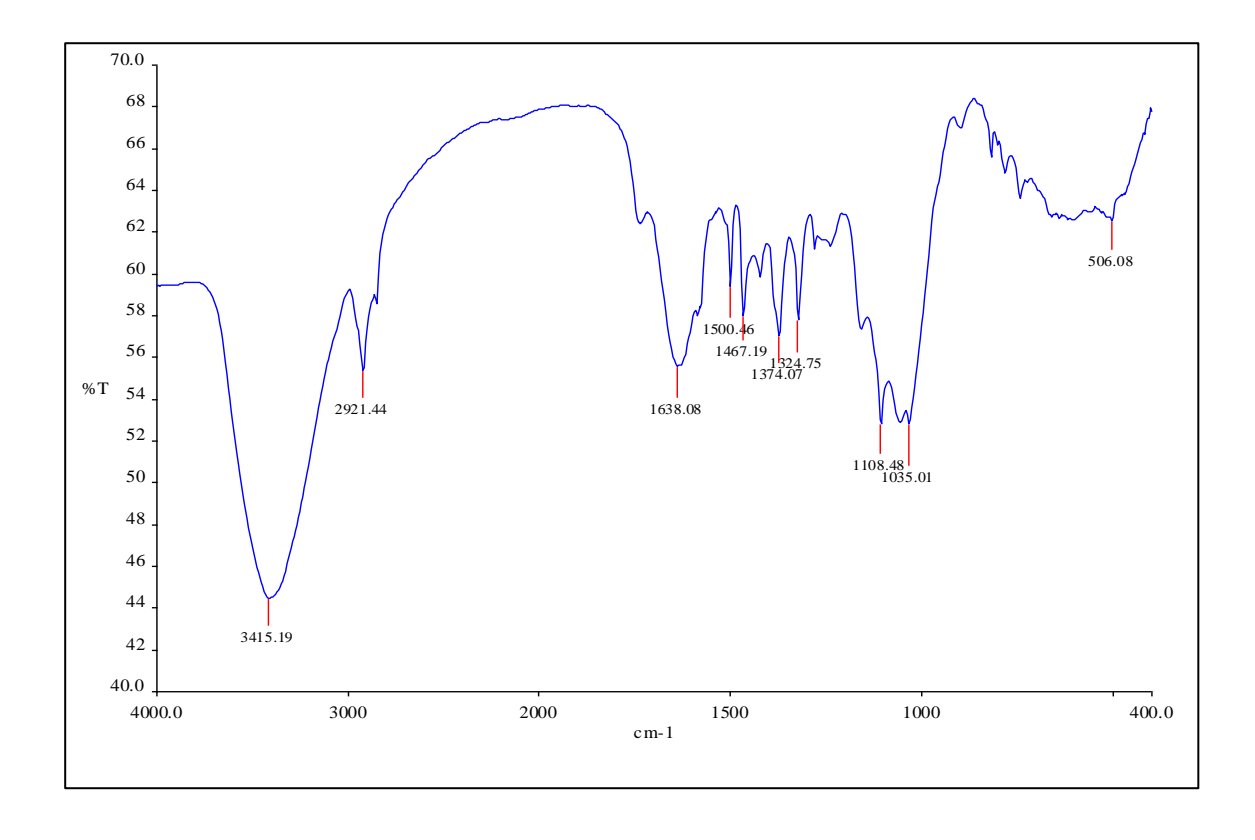
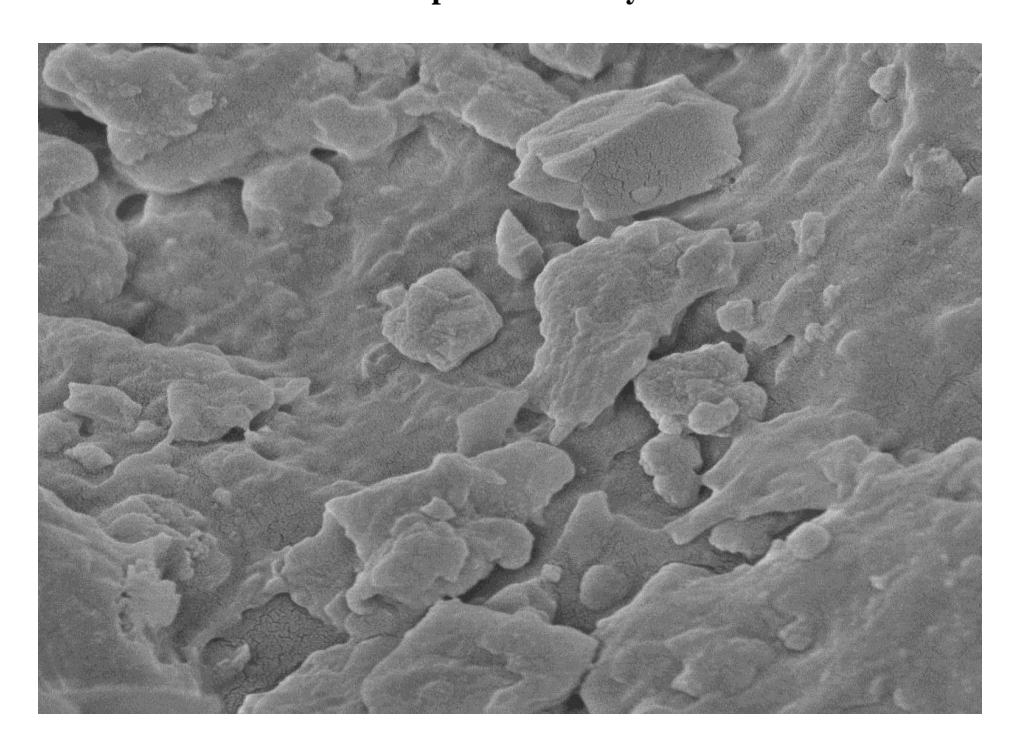


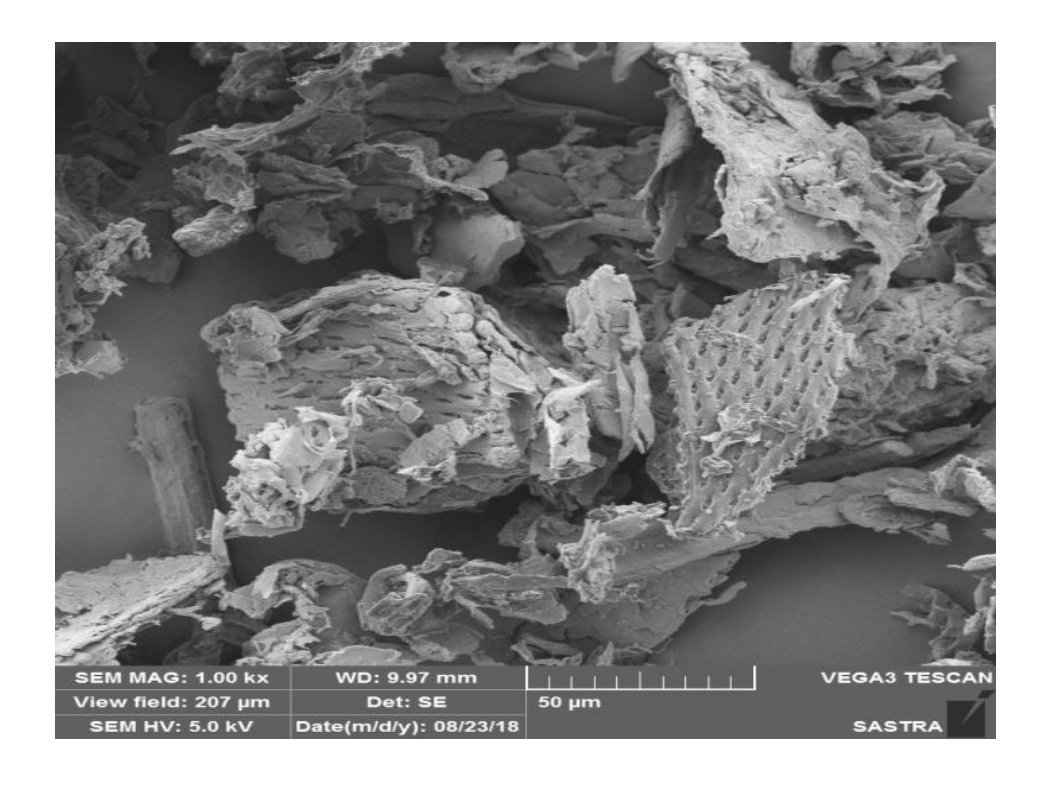
Figure: 5.5.9 FT-IR Analysis for LPSP before and after adsorption of MG dye





 ${\bf Figure: 5.5.10 \ Scanning \ Electron \ Microscope \ Analysis \ for \ LPSP \ before \ and \ after} \\ {\bf adsorption \ of \ MG \ dye.}$





5.6 Adsorption of Methyl Orange dye from aqueous solution using LPSP

5.6.1 Effect of pH for methyl Orange dye onto adsorption using LPSP

The pH values of Methyl Orange dye solutions are playing an important role that controlled the whole adsorption process. The experiments were done with pH range (2 to 10), temperature (30°C), contact time (30 minutes), agitation speed (360 rpm), initial dye concentration (200 mg/L) and the adsorbent dose is 300 mg. The table-5.6.1 is exhibits the experimental results. The figure-5.6.1 is exhibits the graph plotted between pH and dye removal efficiency. The figure shows that the biosorbent consists of polymers with many functional groups, so that the net charge on the biosorbent is also pH dependent [193]. The pH of the system increases while the number of negatively charged sites on the biosorbent (LPSP) surface also increases and thus when increases pH, the uptake of negatively charged dye (MO) decreases due to electrostatic repulsion between negatively charge of the dye (MO) and negative sites of the biosorbent (LPSP) [208]. At lower pH of acidic conditions, binding site of the adsorbent would be closely related to the H⁺ ions which act as bridging ligand between adsorbent surface and dye molecule (MO) [209]. Therefore, pH 3 is suitable for the higher adsorption of anionic dye (MO).

5.6.2 Effect of biosorbent dose for methyl orange dye onto adsorption using LPSP

The effect of adsorbent dose was also investigated for the removal of Methyl Orange dye from aqueous solutions. The experiments were carried out with adsorbent dose varied from (100 to 500 mg) with constant pH, initial dye concentration 200 mg/L, temperature (30°C), contact time (30 minutes), agitation speed (360 rpm). The table-5.6.2 is exhibits experimental results. The figure-5.6.2 is exhibits the graph plotted between biosorbent dose and dye removal efficiency. The figure is readily understood

that (MO) the dye uptake is increased with increase in dose of the adsorbent, because of the number of available adsorbent sites and the surface areas are increases. Hence, (MO) the dye removal efficiency is increases by increasing the adsorbent dose [210].

5.6.3 Effect of contact time for methyl orange dye onto adsorption using LPSP

The contact time is one of the most important factors in batch adsorption process. In this study contact time varies from 10 to 70 minutes, with temperature (30°C), adsorbent dose (300 mg), pH 3, initial dye concentration 200 mg/L, agitation speed (360 rpm) were kept constant. The table-5.6.3 exhibits experimental results. The figure-5.6.3 is the graph plotted between time and removal efficiency of dye. The rate of removal efficiency for MO dye on LPSP is increases at the starting of contact time (from 10 to 30 min) due to the large amount of surface area available for adsorption of dye and the capacity of the adsorbent became gradually exhausted with time since few remaining vacant surface sites became difficult to be occupied due to repulsive forces between the MO dye molecules on the solid surface and bulk phase [211].

5.6.4 Effect of Initial dye concentration for methyl orange dye onto adsorption using LPSP

The rate of adsorption is dependent on the initial amount of Methyl Orange dye concentration. The experiments were done with various concentration (100 to 1000 mg/L) and constant temperature (30°C), adsorbent dose (300 mg), pH 3, contact time (30 minutes), agitation speed (360 rpm). The table-5.6.4 exhibits the experimental results. The figure-5.6.4 is exhibits the graph plotted between initial dye concentration and dye removal efficiency. The rate of removal efficiency is decreases with increase in initial dye concentration of Methyl Orange dye at fixed biosorbent (LPSP) dose. In the case of lower concentrations, the ratio of initial number of dye molecules to the

available adsorption binding sites was low and subsequently more adsorption binding sites were available for the dye molecules, thus the removal percentage increased. However, at high concentrations, the ratio of initial number of available adsorption sites to dye molecules was low, thus the number of available adsorption binding sites becomes lower and subsequently the removal of dye decreased [212].

5.6.5 Adsorption Isotherm

5.6.5.1 Langmuir Isotherm

The Langmuir isotherms adsorption isotherm model is depends upon the postulation of monolayer of adsorption on surface of the adsorbent contain limited number of adsorption sites of identical energies for adsorption. The common expression for Langmuir equation is,

$$q_e = q_m b Ce/(1+bC_e)$$
 (5.6.1)

The linear structure of equation for Langmuir isotherm can be written as,

$$C_e/q_e = 1/bq_m + C_e/q_m$$
 (5.6.2)

Where,

q_e = Adsorption density (mg/g) of Methyl orange dye at equilibrium,

C_e = Equilibrium concentration (mg/L) of Methyl orange dye in solution,

 $q_{m} = Maximum \ dye \ uptake \ corresponding \ to \ the \ saturation \ capacity \ of \ adsorbent \ (mg/g),$

b = Langmuir constant (L/mg) related to energy of adsorption.

The constant q_m and 'b' are the characters of the Langmuir isotherm and can be calculated from the Langmuir equation. In this study, a linear plot was obtained from a graph drawn between C_e/q_e Vs C_e which indicates that the adsorption process followed Langmuir adsorption isotherm (figure-5.6.5 and table-5.6.5). So, that the linearity of the plots represents the purpose of Langmuir equation, which supports monolayer

formation on the surface of the LPSP biosorbent in adsorption due to high r^2 value (0.9859).

5.6.5.2 Freundlich model of adsorption Isotherm

Freundlich model of adsorption isotherm is an experimental equation for heterogeneous surface occurs on adsorption process. The common term for Freundlich equation is,

$$q_e = K_f Ce^{1/n}$$
 (5.6.3)

Logarithmic expression of equation can be written as,

$$\ln q_e = \ln K_f + (1/n) \ln C_e$$
 (5.6.4)

where, the intercept $\ln K_f$ is a measure of adsorption capacity and slope 'n' is the intensity of adsorption. The values of K_f and 'n' were calculated from intercept ($\ln K_f$) and slope (1/n) of plots drawn between $\ln q_e$ vs $\ln C_e$ (Figure-5.6.6 and table-5.6.5). The variable q_e and C_e are MO dye adsorbed and the equal dye concentration in solution. If so, the 'n' value might be in the range of 1 to 10 (0.4162) point out beneficial adsorption, but in the study 'n' value (0.4162) therefore the value of 'n' revealed that Freundlich model no significant effect for MO dye adsorbtion on LPSP biosorbent.

5.6.6. Adsorption Kinetic Studies

The Kinetic adsorption kinetic models were studied for examine the experimental values to investigate regarding the mechanism of the adsorption and potential rate controlling steps, such as mass transfer process and chemical reaction. The transiting work of batch adsorption process was calculated by means of using pseudo first order and pseudo second order kinetic models of adsorption.

5.6.6.1 Pseudo First order

The linear structure of equation for pseudo-first-order kinetic model is represented by the following equation.

$$\ln (q_e - q_t) = \ln q_e - K_1 t$$
 (5.6.5)

Where, q_e (mg/g) and q_t (mg/g) represents for the amount of dye adsorbed per unit weight of adsorbent at equilibrium and at time t respectively, K is the rate constant of adsorption.

The adsorption coefficient and the capacity of the equilibrium q_e can be confirmed from the linear plot drawn between $\ln (q_e - q_t)$ vs 't' as show in figure-5.6.7. It was indicated that the linear plot shows the possibility of the Lagergren equation, q_e values were shown in table-5.6.6. The correlation coefficient of r^2 is 0.9785 was revealed that the concentration of MO dye have no significant effect in pseudo first order.

5.6.6.2 Pseudo Second order

This adsorption kinetic model equation was developed by Ho and MacKay (1999), studied to give information about the adsorption capacity, the pseudo second order model can be written as,

$$t/q_t = 1/k_2 q_e^2 + 1/q_e t$$
 (5.6.6)

Where, k_2 is the rate constant of adsorption (g/mg min), t is the constant time (min), q_e (mg/g) and q_t (mg/g) denotes the amounts of dye adsorbed at equilibrium and at time 't' respectively. If pseudo second order kinetics is applicable; the values of k_2 and q_e were calculated from intercept (1/ k_2 q_e^2) and slope (1/ q_e) of the plots of t/ q_t vs t have to give a linear relationship as given in figure-5.6.8., and q_e and r^2 values can be obtained from

the plots. These values were shown in table-5.6.6. It was exhibit that the calculated q_e very closer to experimental q_e , and also r^2 value 0.9994 hence pseudo-second-order model fitted well for adsorption of MO dye on LPSP.

5.6.7 FT-IR spectra of LPSP before and after adsorption of methyl orange dye

The FTIR study provides the change in functional groups of biosorbent LPSP. The spectrum of LPSP before and after the MO dye adsorption shows in the figure-5.6.9. The FTIR spectrum of native biosorbent revealed a number of absorption peaks with that range of 600-4000 cm⁻¹, which is only a sign of the complex chemical nature of this biosorbent. The aromatic compounds of the MO dye molecule showed characteristic absorption peaks at 2995 cm⁻¹ due to aromatic OH stretching. The absorption band appears at 1998 cm⁻¹ due to CH stretching of alkyl group. The absorption band at 3455 cm⁻¹ was due to NH stretching of amino group of dye molecule. The peaks appear at 1590 cm⁻¹, 1480 cm⁻¹ was due to C-N-C stretching. The absorption spectrum of biosorbent treated with dye solution showed evident changes with respect to that of native biosorbent. Amongst these changes were the broadening of the absorption bands between 3455 and 1480 cm⁻¹ which suggests the superposition of numerous peaks that appeared in these regions. The band appears at 1480 cm⁻¹ and 3455 cm⁻¹ due to the biosorbent binding with MO dye molecule.

5.6.8 XRD pattern analysis for LPSP before and after adsorption of methyl orange dye

The X-ray diffraction technique is a significant technique to study the crystalline amorphous nature of the adsorbent material. The LPSP before and after adsorption were recorded in figure-5.6.10. The intense main peak in unloaded LPSP shows that the presence of highly organized crystalline nature, and after the adsorption

of MO dye, the intensity of the main peak is slightly diminished and broaden. It means that the physical adsorption takes place on the upper layer of LPSP crystalline structure after adsorption of MO dye.

5.6.9. SEM Analysis for LPSP before and after adsorption of methyl orange dye

Scanning Electron Microscope (SEM) analysis shows information about surface morphological properties of the biosorbent (LPSP). The untreated LPSP image is represents the rough and uneven surface. It should be considered as a reason for sorption of MO dye molecules, after the sorption of MO dye on LPSP, a considerable change is observed in the surface structure of the adsorbent (LPSP). The adsorbent appears to have a coarse surface and pores containing novel cavities like particles later than the adsorption of MO dye (figure-5.6.11).

Table:5.6.1. Effect of pH in MO dye, Time 30 min, Adsorbent weight 300 mg, Volume of MO dye solution 50 mL, Initial dye (MO) concentration 200mg/L and Temperature 30°C.

pН	Removal Efficiency of MO in percentage
2	63.38
3	63.80
4	62.38
5	61.90
6	60.95
7	60.00
8	59.04
9	58.09
10	57.14

Table: 5.6.2. Effect of biosorbent (LPSP) dose in MO dye, Time 30 min, pH 3, volume of MO dye solution 50 mL, Initial dye (MO) concentration 200mg/L and Temperature 30° C.

Adsorbent dose	Removal Efficiency of		
(mg)	MO in percentage		
100	57.54		
200	59.43		
300	62.26		
400	63.20		
500	63.72		

Table: 5.6.3. Effect of contact time in MO dye, pH 3, volume of MO dye solution 50 mL, Initial dye (MO) concentration 200mg/L and Temperature 30°C.

Time (min)	Removal Efficiency of MO				
	in percentage				
10	60.37				
20	61.32				
30	62.83				
40	62.73				
50	62.68				
60	62.66				
70	62.66				

Table: 5.6.4. Effect of Initial dye concentration in MO dye, pH 3, Time 30 min, volume of MO dye solution 50 mL and Temperature 30°C.

Initial Dye Concentration	Removal Efficiency of MO in Percentage		
(mg/L)			
100	63.72		
200	63.20		
300	61.11		
400	60.00		
500	59.64		
600	57.75		
700	55.93		
800	55.00		
900	53.71		
1000	52.45		

Table: 5.6.5 Langmuir and Freundlich model parameters for MO dye

Temperature	Langmuir model			Freundlich model		
30° C	$q_m (mg/g)$	b (L/mg)	\mathbf{r}^2	$K_f(mg^{1\text{-}n}g^{\text{-}1}L^n)$	$n(mg^{1-n}g^{-1}L^n)$	r ²
	12.22	0.0177	0.9859	1.0427	0.4162	0.8924

Table: 5.6.6 Pseudo-first-order and second order kinetic parameters for $$\operatorname{MO}$$ dye

		Pse	Pseudo-first-order			Pseudo-second-order		
C _i (mg/L)	Temp. (° C)	Cal. q _e (mg/g)	Exp. q _e (mg/g)	r ²	Cal. q _e (mg/g)	Exp. qe (mg/g)	r ²	
200	30	17.214	18.345	0.9785	18.132	18.345	0.9994	

Figure: 5.6.1. Effect of pH in MO dye, Time 30 min, Adsorbent weight 300 mg, Volume of MO dye solution 50 mL, Initial dye (MO) concentration 200mg/L and Temperature 30°C.

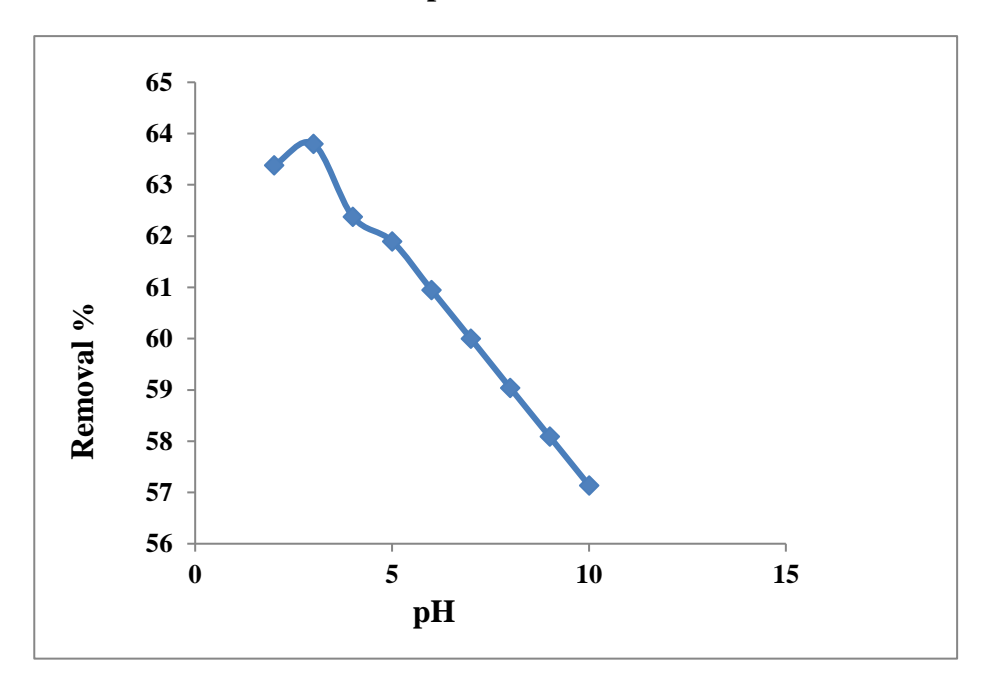


Figure: 5.6.2 Effect of biosorbent (LPSP) dose in MO dye, Time 30 min, pH 3, volume of MO dye solution 50 mL, Initial dye (MO) concentration 200mg/L and Temperature 30°C.

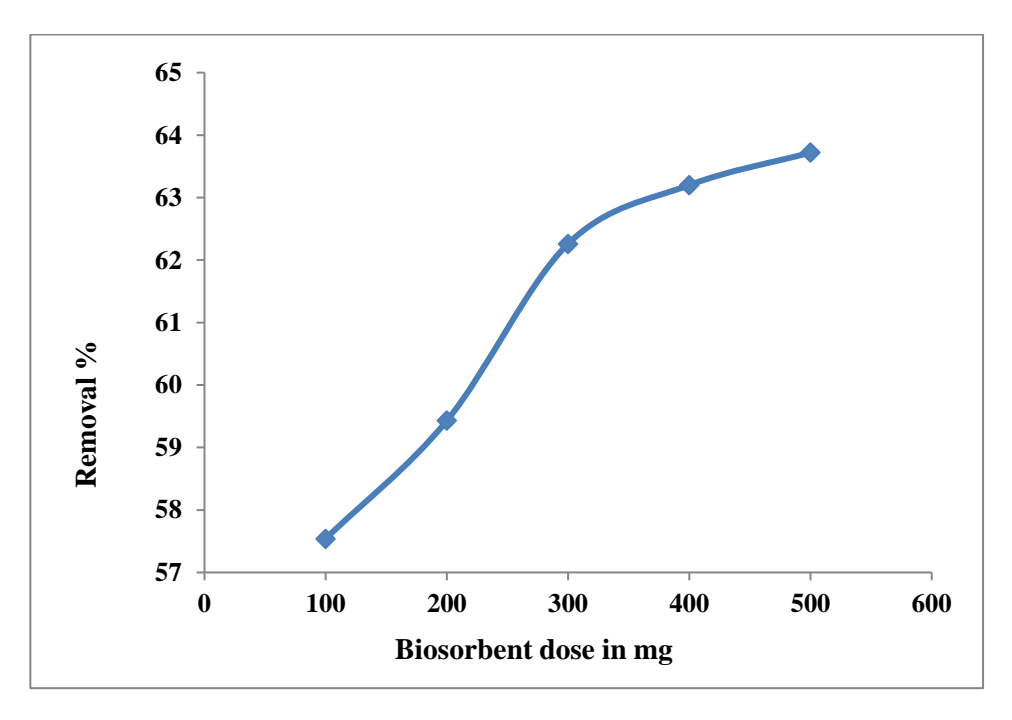


Figure: 5.6.3 Effect of contact time in MO dye, pH 3, volume of MO dye solution 50 mL, Initial dye (MO) concentration 200mg/L and Temperature 30°C.

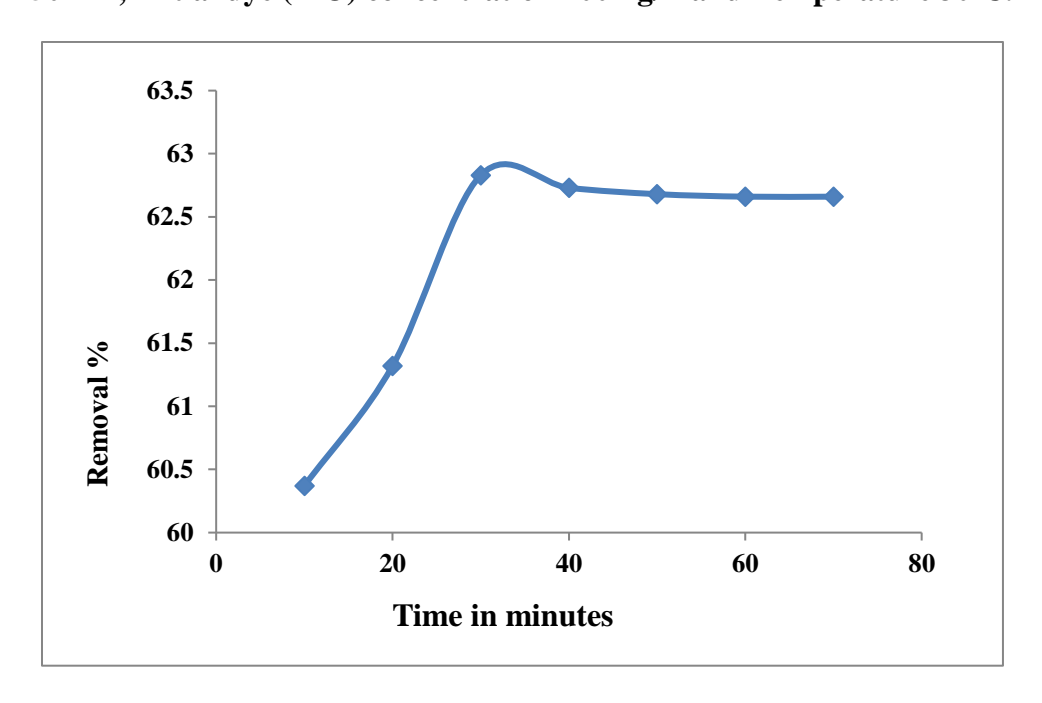


Figure: 5.6.4 Effect of Initial dye concentration in MO dye, pH 3, Time 30 min, volume of MO dye solution 50 mL and Temperature 30°C.

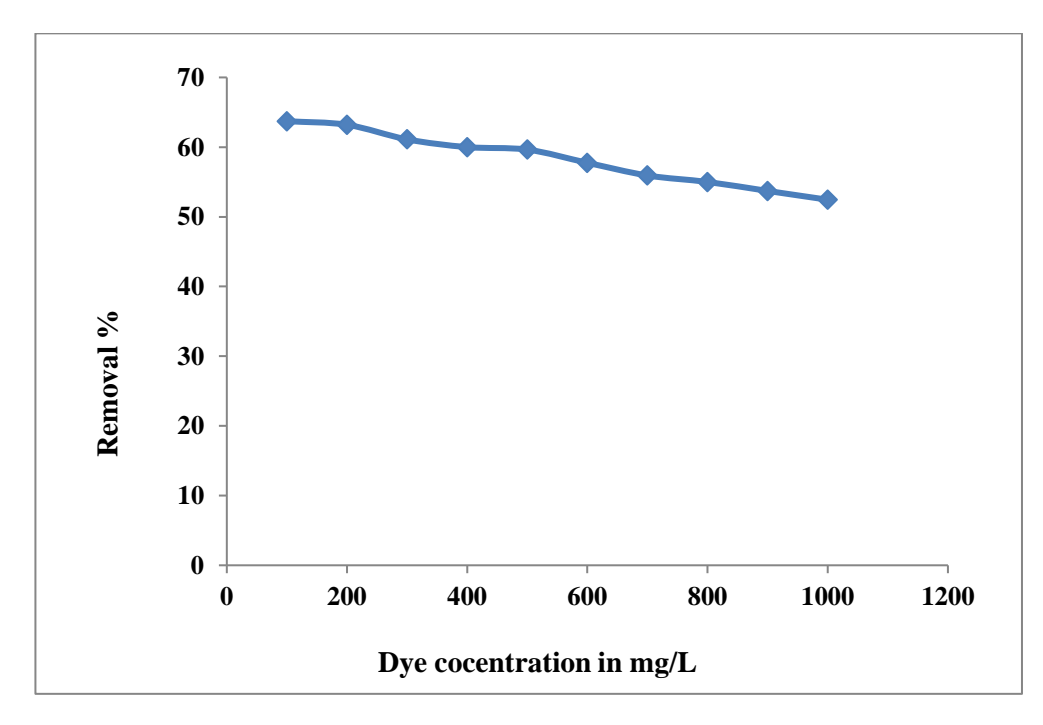


Figure: 5.6.5 Langmuir isotherm plot for Methyl Orange dye using *Laplap purpureus* plant stem powder.

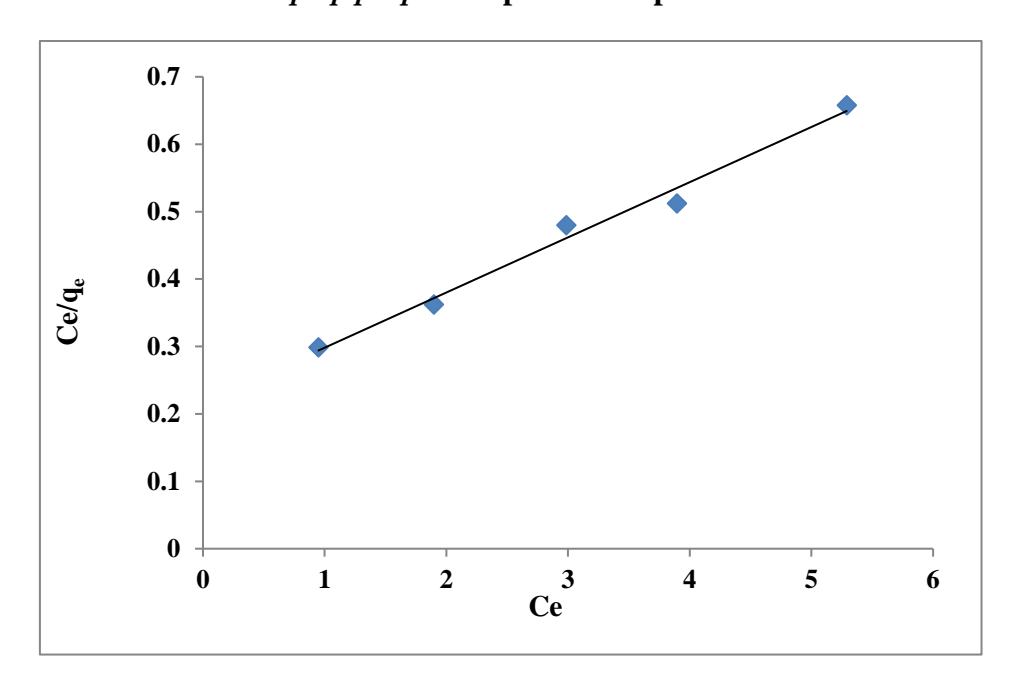


Figure: 5.6.6 Freundlich isotherm plot for Methyl Orange dye using *Laplap purpureus* plant stem powder.

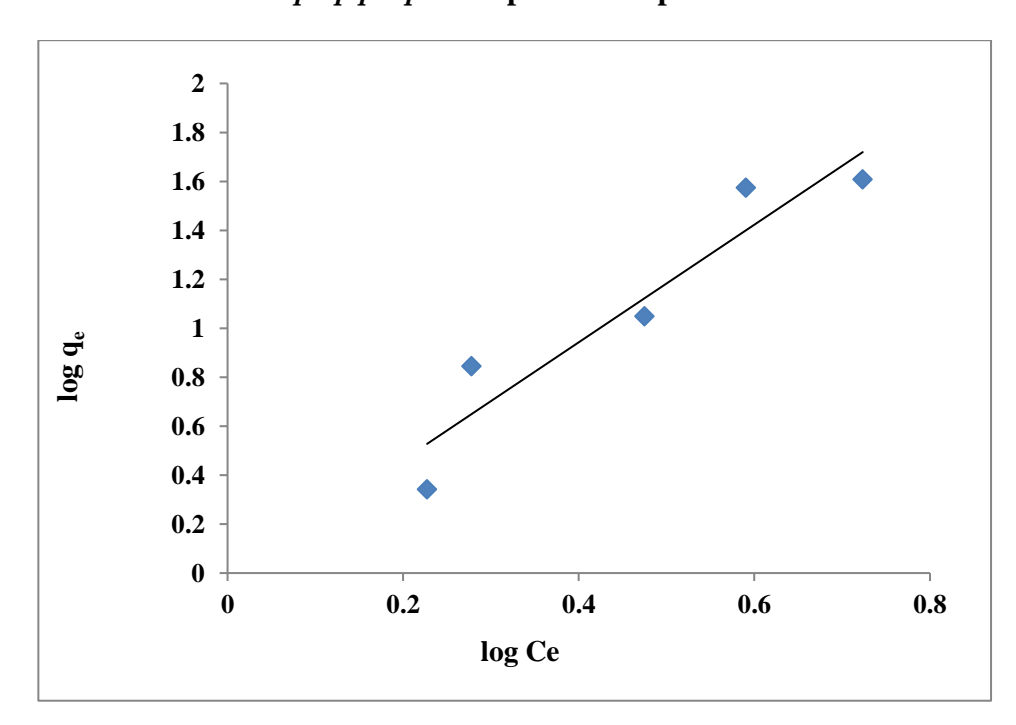


Figure: 5.6.7 Pseudo first order plot for Methyl Orange dye using

Laplap purpureus plant stem powder.

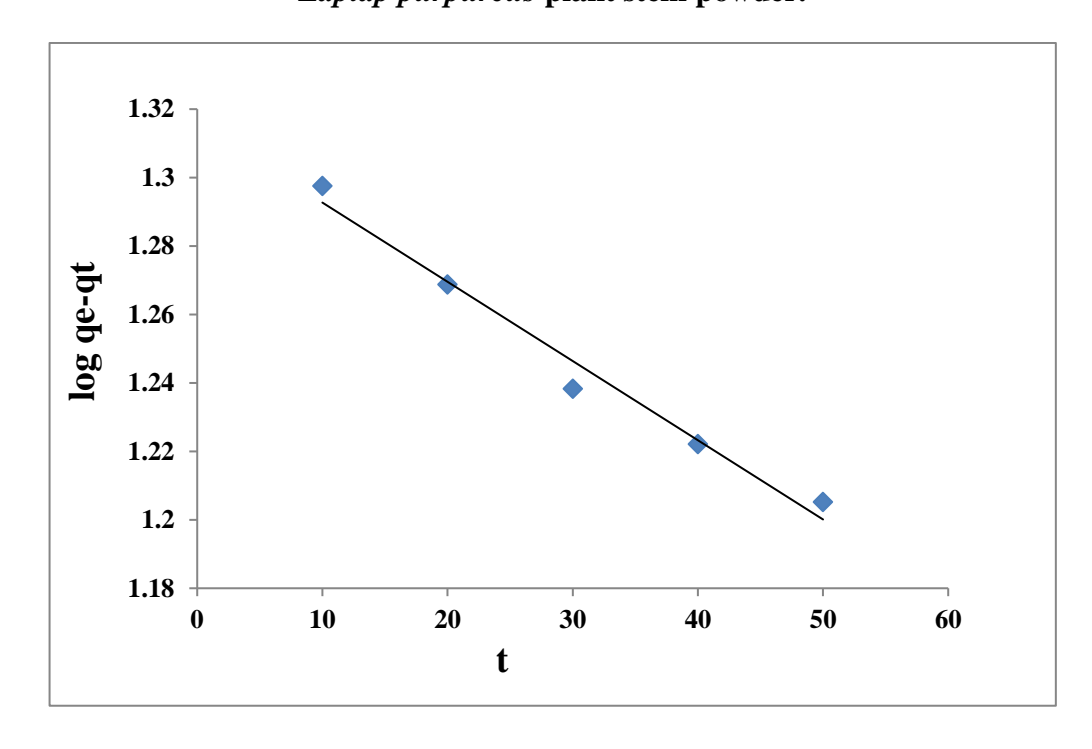
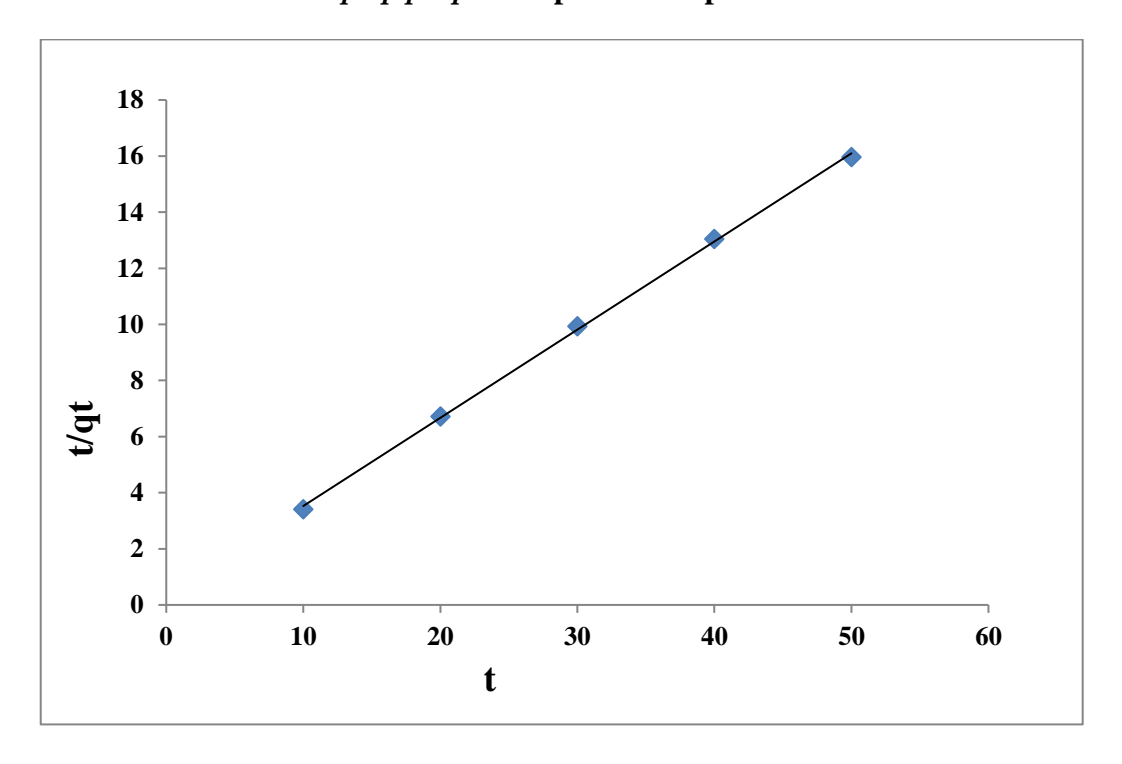
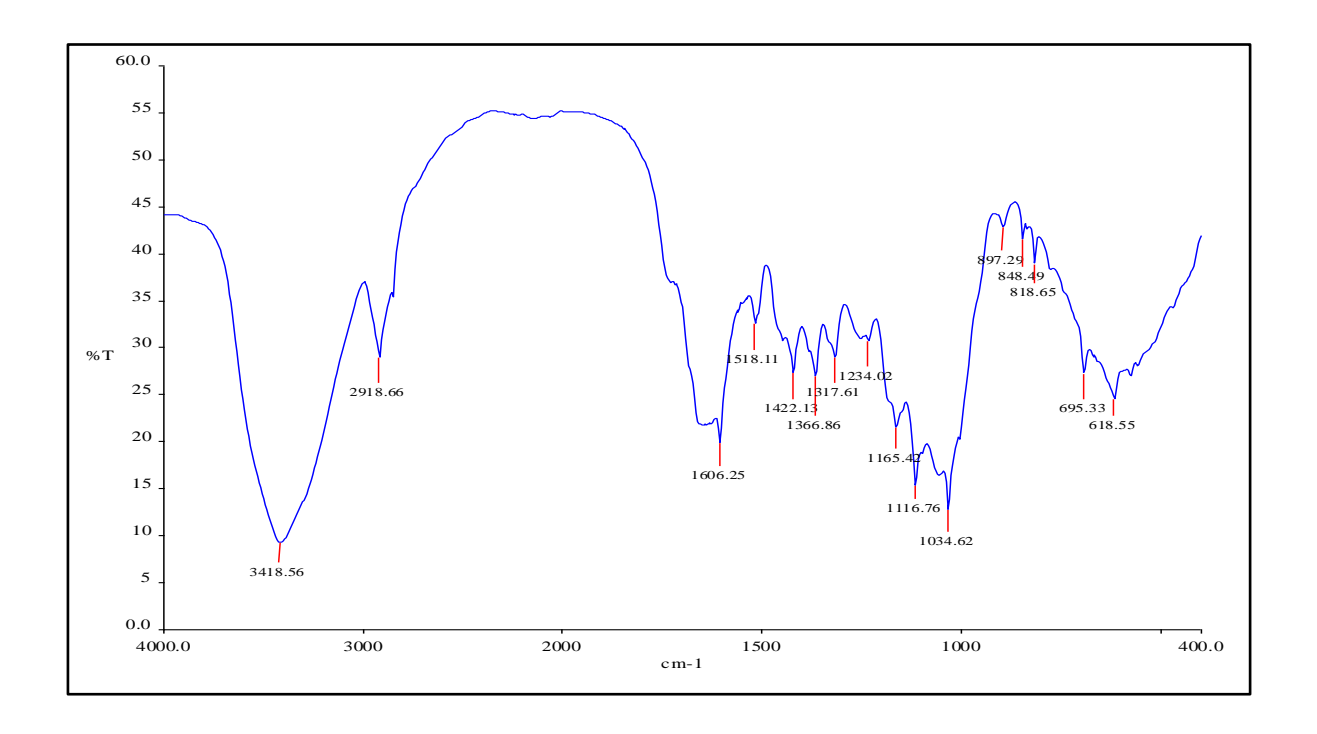
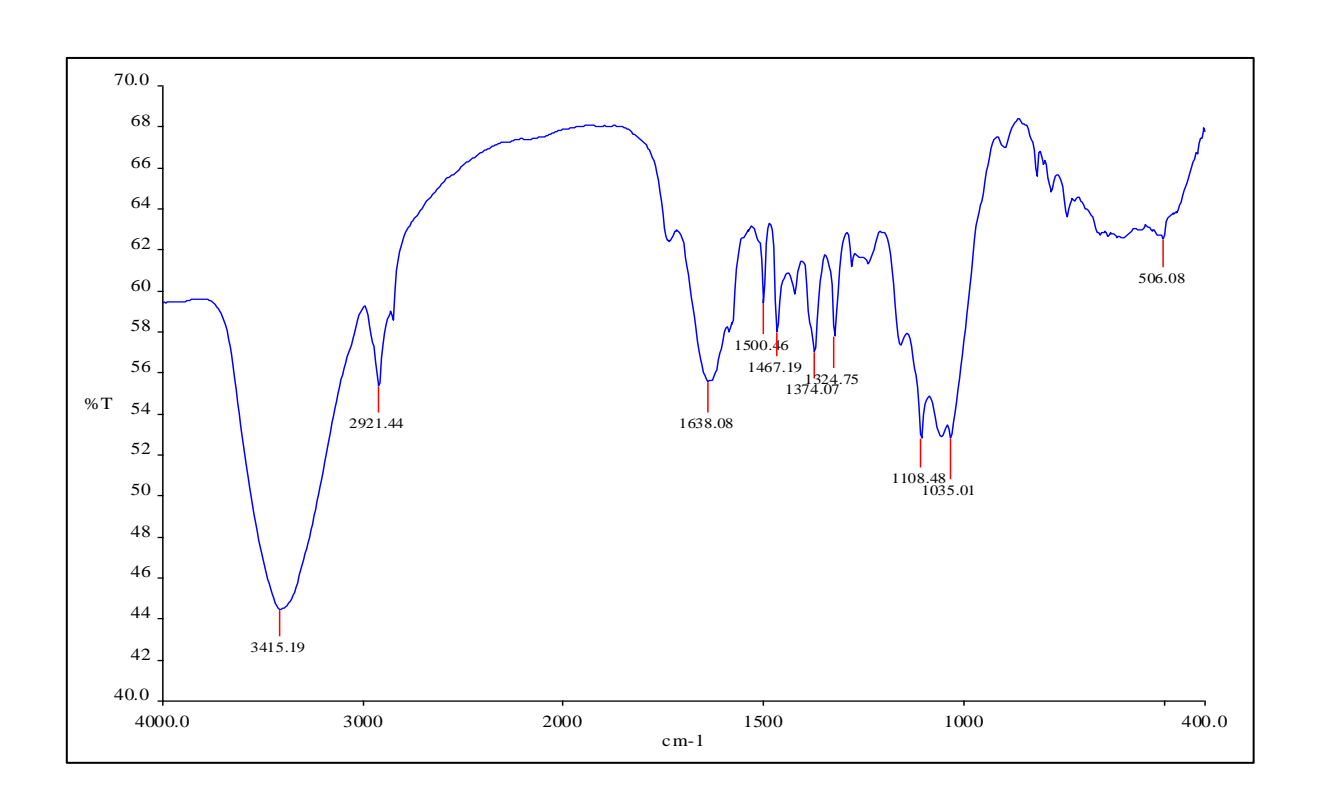


Figure: 5.6.8 Pseudo second order plot for Methyl Orange dye using Laplap purpureus plant stem powder.

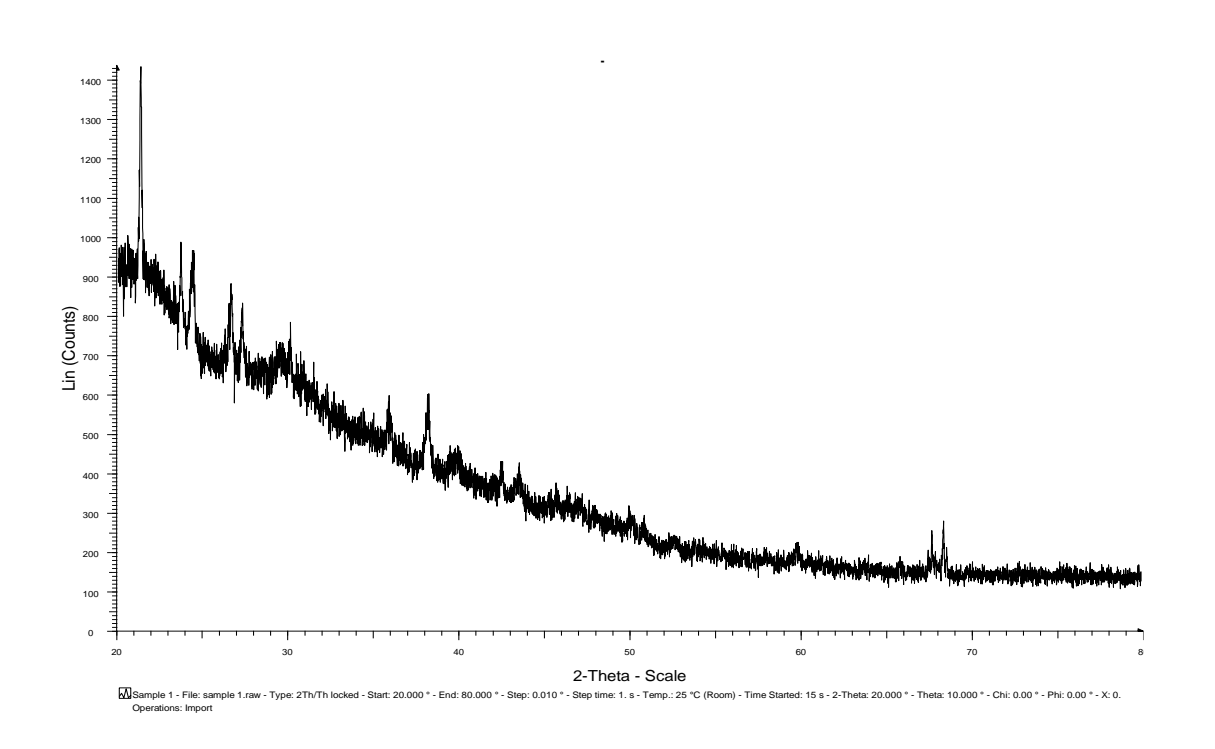


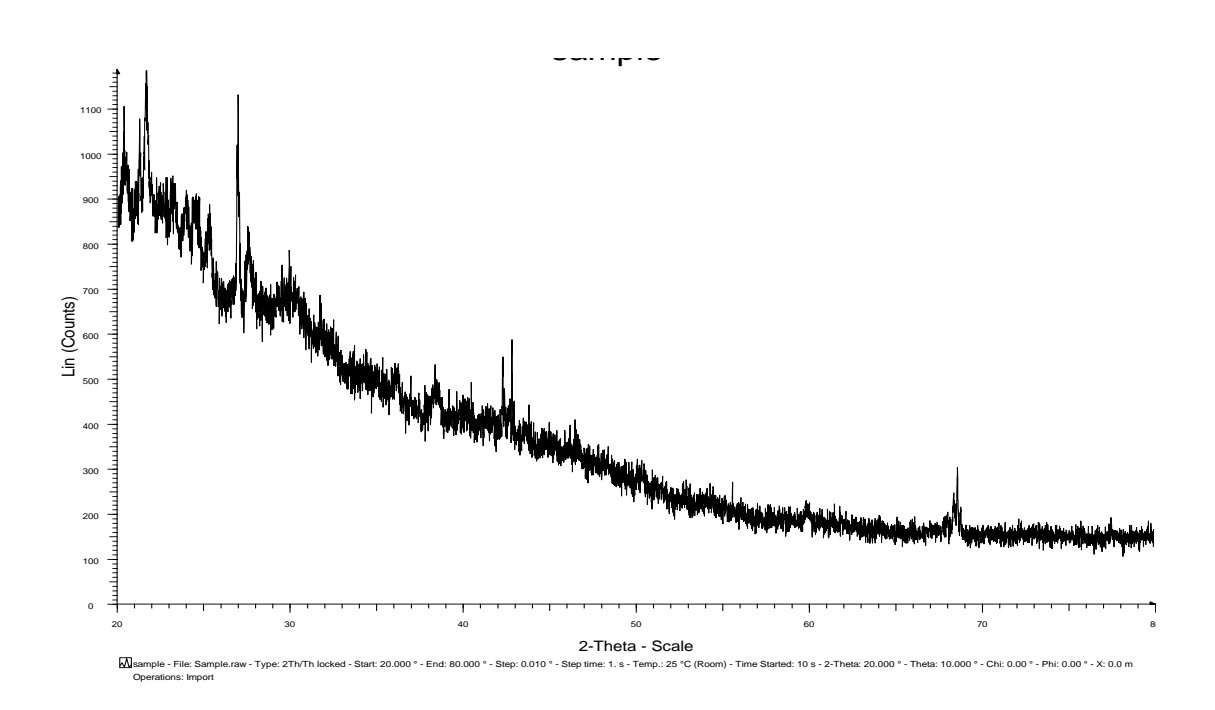
5.6.9 FT-IR Analysis for LPSP before and after adsorption of MO dye



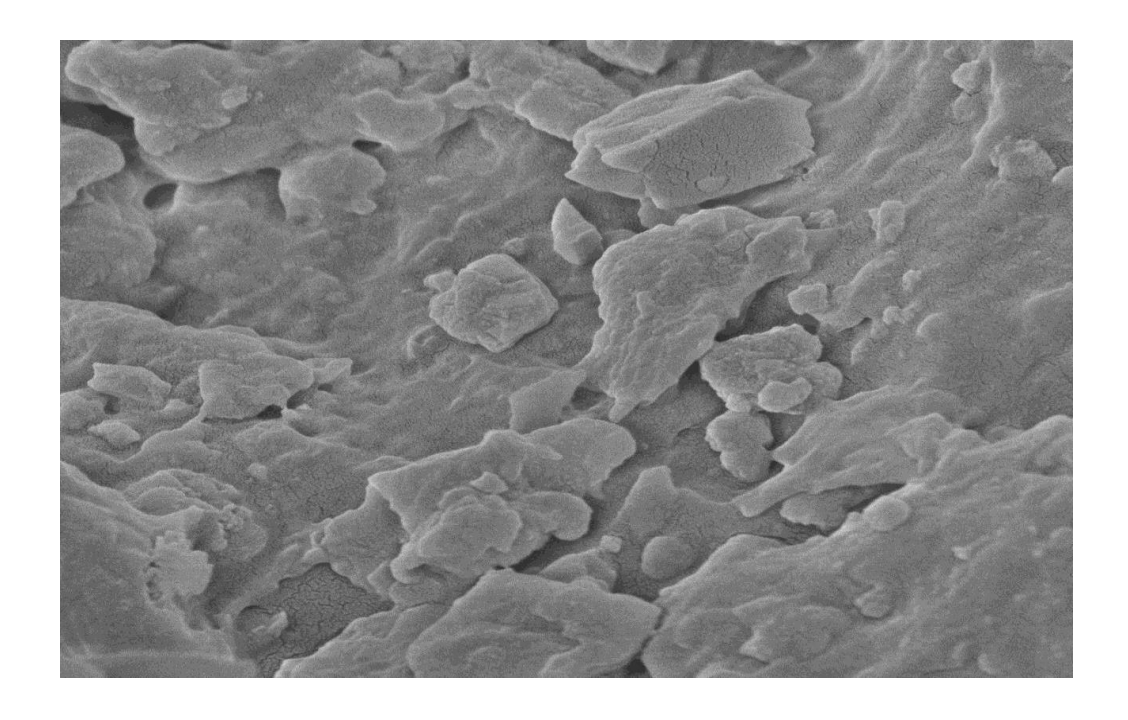


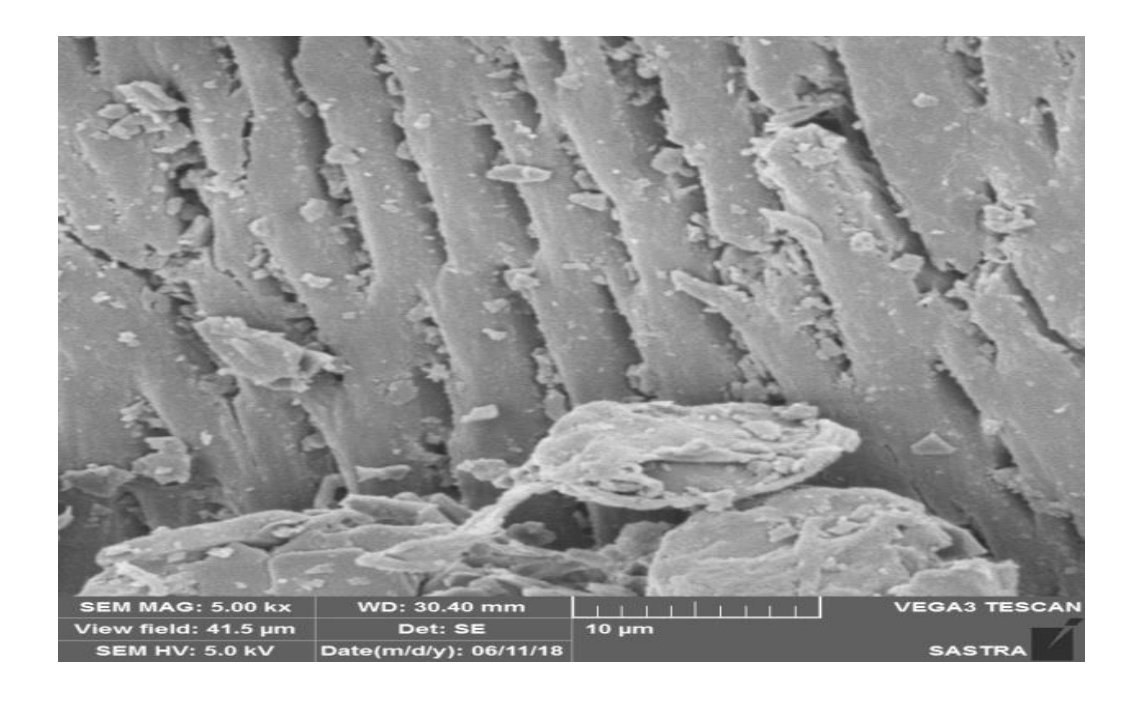
Figurer: 5.6.10 XRD pattern for LPSP before and after adsorption of MO dye





Figurer: 5.6.11 SEM Analysis for LPSP before and after adsorption of MO dye





CHAPTER - VI

SUMMARY AND CONCLUSION

In the present investigation, analysis on the equilibrium, kinetic and thermodynamic aspects of the adsorption of metal ions, such as, Cu (II), Cr (VI), and Ni (II) and dyes namely, BBR, MG, and MO by chosen adsorbent LPSP. The different parameters pertaining to the adsorption at equilibrium were determined in order to establish the behavior of the adsorption process using LPSP, batch experiments were carried out to examine the effective of adsorbent dose and adsorbent concentration in the removal of metal ions and dyes.

The pH of the system is major parameter in the adsorption process. The pH at which the optimum adsorption occurred at Cu(II)-7, Cr(VI)-3, Ni(II)-7, BBR dye-8, MG dye-8 and MO dye-3 due to electrostatic interaction in all system.

The maximum adsorption capacity for the prepared biosorbent LPSP could be determined quantitatively by the Langmuir and Freundlich adsorption isotherm. For evaluating the parameters related with the adsorption process, the equilibrium data for the adsorption of Cu(II). Cr(VI), Ni(II), BBR dye, MG dye and MO dye stains onto LPSP was examined in various concentrations and temperatures. The equilibrium parameter R_L values derived from Langmuir adsorption isotherm study were in between 0 to 1 and the 'n' values from Freundlich adsorption isotherm in between 1 to 10 indicated that the biosorption process are favorable for the adsorption system.

Afore mentioned adsorption isotherms Langmuir and Freundlich were evaluated in the heavy metal/dye removal process found that they are well fitted with the all the adsorption system. The equilibrium biosorption is best correlated with Langmuir

adsorption isotherm model compared with Freundlich adsorption isotherm model and the Langmuir model suggests monolayer adsorption of metals/dyes onto LPSP. The suitability of Langmuir adsorption isotherm for Cu(II), Cr(VI), Ni(II), BBR-dye, MG-dye and MO-dye onto LPSP is confirmed by the high r² values obtained in this study. The applicability of Freundlich adsorption isotherm suggest that the adsorption of Cu(II), Cr(VI), Ni(II), BBR-dye, MG-dye and MO-dye onto LPSP may be complex in nature.

The values of maximum bisorption capacity (q_m) obtained from Langmuir adsorption isotherm infers that LPSP is effective in adsorption and prefers the adsorption in the sequence.

$$Ni(II) > Cu(II) > Cr(VI) > MG dye > BBR dye > MO dye$$

The high value of K_f reveals that the LPSP have good affinity towards heavy metals/dyes in the process of adsorption and the adsorption limit was found and arranged in the order K_f values.

$$Cr(VI) > BBR dye > Cu(II) > Ni(II) > MG dye > MO dye$$

The variation in the adsorption capacity for each adsorbate may be due to the factors like as adsorbate ionic charge, adsorbate size, adsorbate shape, pore volume, pore shape and surface characteristic of the adsorbent.

Kinetics of sorption process onto LPSP was evaluated with the linearised form of the pseudo first order and pseudo second order models. The best kinetic model was determined by comparing the calculated adsorption capacity at equilibrium $(qe_{(cal)})$ values from the respective kinetic models with the experimentally determined adsorption capacity $(qe_{(exp)})$.

The calculated values $(qe_{(cal)})$ were closer to the experimental values $(qe_{(exp)})$ with high regression coefficient (r^2) in pseudo-first-order only for Cu(II) metal ions, and other metal ions/dyes also having the calculated values $(qe_{(cal)})$ were closer to the experimental values $(qe_{(exp)})$ with high regression coefficient (r^2) in pseudo-second-order. It clearly concluded that most of the metal ions/dyes were fitted for pseudo-second-order other than Cu(II) metal ions in this study.

Thermodynamic parameters are assessed utilizing the estimation of an equilibrium constant at various temperatures viz., 30°C, 35°C and 40°C, the estimation of ΔG° for Cu(II), Cr(VI) and Ni(II) metal ions onto LPSP were observed to be negative. While the estimation of ΔS° and ΔH° were positive.

The negative values of ΔG° demonstrated that the adsorption process was unconstrained with a high foundness for metals, the estimation of ΔG° was expanded with an increase in temperature, which proposes that the suddenness of adsorption corresponds to temperature. The positive estimation of ΔS° exhibits the increased disorderness at the solid-solution interface on the adsorption process and shows the affinity of adsorbent for adsorbate. The positive values of ΔH° revealed that the adsorption process is endothermic in nature. The magnitude of ΔH° for metal ions below 16 KJ/mol indicates that the adsorption occurred by the physisorption mechanism.

FTIR spectra confirm that the adsorption of metal ions/dyes (Cu(II), Cr(VI), Ni(II), BBR dye, MG dye, and MO dye) by either change in peak intensities of an adsorbent upon adsorption by the appearance or disappearance of additional peaks in the metal ions/dyes loaded adsorbent.

Amorphous nature of the adsorbent is revealed by its XRD patterns and also it was supported the physisorption mechanism.

The SEM images clearly represent that the maximum number of pores are present on the external surface of the adsorbent LPSP which are countable for the adsorption of metal ions/dyes onto the adsorbent.

This research work aimed to explore the utilization of agriculture waste as an adsorbent. Based on the experiment from the synthetic wastewater system, it could be concluded that the biosorbent LPSP prepared from the plant stem of *Laplap purpureus* is promising in terms of both economic and environmental aspects and could improve the adsorption for the removal of toxic heavy metal ions/dyes from wastewater system. Hence, the biosorbent LPSP can be used as a potential adsorbent for the removal of toxic heavy metal ions/dyes from industrial wastewater. Information reviewed is mainly focusing on the biosorption performance of such adsorbent and so interpretation and analysis of experimental data of the prepared biosorbent LPSP clearly indicated that LPSP has greater efficiency in the adsorption.

References

- 1. Kumar A, 2004. Water pollution: New Delhi, A.P.H publishing corporation: 199.
- 2. Singh S and Kumar M, 2006. Heavy metal load of soil, water and vegetables in periurban Delhi. *Environ. Monit. Assess.*, 120: 79-91.
- 3. Yesilada O, Asma D, and Cing S., 2003. Decolourization of textile dyes by fungal pellets. *Process Biochem.* 38: 933-938.
- 4. Yasemin B, Haluk A., 2006. A kinetic and thermodynamics study of methylene blue adsorption on Wheat Shell. *Desalination*. 194; 259-267.
- Ahalya N, Ramachandra TV and Kanamadi RD, 2005. Biosorption of Chromium
 (VI) from aqueous solutions by the husk of bengal gram (*Cicer arientinum*).
 Electronic Journal of Biotechnology (Online) 15 December 2005.
- 6. Fu Y and Viraraghavan T., 2001, Fungal decolourization of wastewaters: a review. *Bioresour. Technol.* 79, pp. 251–262.
- 7. Robinson T., Mcmullan G., Marchant R. and Nigam P, 2001. Remediation of dyes in textile effluent: a critical review on current treatment technologies with a proposed alternative. *Bioresour. Technol.* 77, pp. 247–255.
- 8. Sumathi S.and. Manju B.S, 2000, Uptake of reactive textile dyes by *Aspergillus foetidus*. *Enzyme Microbial*. *Technol*. 27, pp. 347–352.
- 9. Aksu Z and Tezer S., 2000. Equilibrium and kinetic modelling of biosorption of Remazol Black B by *R. arrhizus* in a batch system: effect of temperature. *Process Biochem.* 36, pp. 431–439.

- 10. O'Mahony T., Guibal E and. Tobin J.M, 2002. Reactive dye biosorption by *Rhizopus arrhizus* biomass. *Enzyme Microbial. Technol.* 31, pp. 456–463.
- 11. Tatsi, AA; Zouboulis, AI; Matis, KA; Samara, P; 2003. Coagulation-flocculation pretreatment of sanitary land fill leachates. *Chemosphere*. 53: 737-744.
- Rodrigues, A. C.; Boroski, M.; Shimada, N. S.; Garcia, J. C.; Nozaki, J.;
 Hioka, N., 2008. Treatment of Paper Pulp and Paper Mill Wastewater by
 Coagulation–flocculation Followed by Heterogeneous Photocatalysis. J.
 Photochem. Photobiol. A Chem. 194, 1.
- 13. Parson, S.; Jefferson, B., 2006. Introduction to Potable Water Treatment Processes; Blackwell Publishing, Ltd: UK.
- 14. Bratby, J., 2006. oagulation and Flocculation in Water and Wastewater Treatment; IWA Publishing: UK.
- Avramescu M, Gironès M, Borneman Z, Wessling M., 2008. Particle loaded hollow-fiber membrane absorbers for lysozyme separation. *J Membr Sci* 322(2): 306–313.
- 16. Zheng G, Ye H, Zhang Y, Li H, Lin L, Ding X., 2014. Removal of heavy metal in drinking water resource with cation-exchange resins (Type 110-H) mixed PES membrane adsorbents. *J Hazard Toxic Radioact Waste* 19(2):1–6.
- Bishop P.L and Breton R.A., 1893. Treatment of Electroless Copper Plating Wastes, Proc. 38th Purdue Industrial Conference 38: 473-480.
- Kanamadi R. D, Ahalya N and Ramachandra T.V., 2006. Biosorption of Heavy metals by low cost Adsorbent. *Technical Report*: 112.

- 19. Brandt, R. K., Hughes, M. R., Bourget, L. P., Truszkowska, K. and Greenler, R. G., 1993. The interpretation of CO adsorbed on Pt/SiO₂ of two different particle-size distributions, *Sur. Sci.*, 286 (1-2), 15-25.
- Cussler, E. L., 1997. Diffusion: Mass Transfer in Fluid Systems (2nd ed.), New York, Cambridge University Press, 308-330.
- Henderson, A. P., Seetohul, L. N., Dean, A. K., Russell, P., Pruneanu, S. and Ali, Z., 2009. A novel isotherm, Modelling Self-Assembled Monolayer Adsorption and Structural Changes, Langmuir, 25 (2), 931-938.
- Mrvcic J, Stanzer D, Solic E, Stehlik-Tomas V., 2012. Interaction of lactic acid bacteria with metal ions: Opportunities for improving food safety and quality.
 World Journal of Microbiology and Biotechnology. 28:2771-2782.
- 23. Davis TA, Volesky B, Mucci A. A review of the biochemistry of heavy metal biosorption by brown algae. *Water Research*. 2003;37:4311-4330.
- 24. Chojnacka K.,2010. Biosorption and bioaccumulation—the prospects for practical applications. *Environment International*. 36:299-307.
- Chojnacka K., 2009. Biosorption and Bioaccumulation in Practice. UK: Nova Science Publishers; p. 137.
- 26. Park D, Yun Y-S, Park JM., 2010. The past, present, and future trends of biosorption. *Biotechnology and Bioprocess Engineering*. 15:86-102.
- 27. Tsezos M, Remoundaki E, Hazikioseyian A., 2006. Biosorption -principles and applications for metal immobilization from waste-water streams. *In: Proceedings of EU-Asia Workshop on Clean Production and Nanotechnologies; Seoul*; pp. 23-33.

- 28. Santhi.T, Manonmani. S, Smitha. T, and Mahalakshmi. K., 2009. Adsorption of Malachite Green from aqueous solution onto a waste aqua cultural shell powders (Prawn waste): Kinetic study. *Rasayan J. Chem.* 2(4), 813-824.
- 29. Akazdam S, Chafi M, Yassine W, Sebbahi L, Gourich B, Barka N., 2017. Decolourization of Cationic and Anionic Dyes from Aqueous Solution by Adsorption on Naoh Treated Eggshells: Batch and Fixed Bed Column study using Response Surface Methodology. *Journal of Materials and Environmental Sciences*. 8(3), 784-800.
- 30. Javed Iqbal, Feroza Hamid Wattoo, Muhammad Hamid Sarwar Wattoo, Rukhsana Malik, Syed Ahmad Tirmizi, Muhammad Imran., 2011. Adsorption of acid yellow dye on flakes of chitosan prepared from fishery wastes. *Arabian Journal of Chemistry*. 4, 389-395.
- 31. Rais Ahmad, Rajeev Kumar, Shaziya Haseeb., 2012. Adsorption of Cu²⁺ from aqueous solution onto iron oxide coated eggshell powder: Evaluation of equilibrium, isotherms, kinetics, and regeneration capacity. *Arabian Journal of Chemistry*. 5; 353-359.
- 32. Ayjan Dawlet, Dilnur Talip, Hong Yu Mi, MaLiKeZhaTi., 2013. Removal of mercury from aqueous solution using sheep bone charcoal. (2013 ISEST), *Procedia Environmental Sciences* 18(2013); 800-808.
- 33. Rifaqat Ali Khan Rao, Kashifuddin M., 2016. Adsorption studies of Cd(II) on ball clay: Comparison with other natural clays. *Arabian Journal of Chemistry*, 9; S1233-S1241.

- 34. Mahammedi Fatiha, Benguella Belkacem., 2016. Adsorption of methylene blue from aqueous solutions using natural clay. *J. Mater. Environ. Sci.* 7(1), 285-292.
- Fortunate Phenyo Sejie, Misael Silas Nadiye-Tabbiruka., 2016. Removal of Methyl Orange (MO) from Water by adsorption onto Modified Local Clay (Kaolinite). *Physical Chemistry*. 6(2); 39-48.
- 36. Fethi Kooli, Liu Yan, Rawan Al-Faze, Awath Ai-Sehimi., 2015. Removal enhancement of basic blue 41 by brick waste from an aqueous solution. *Arabian Journal of Chemistry*. 8; 333-342.
- 37. Congwei Zhong, Dong Hoon Lee, Jin Hwi kim, Joo-Hyon Kang., 2021.
 Adsorption of dissolved copper and zinc on sand and iron oxide-coated sand
 (IOCS) for urban storm water treatment: effects of pH, chlorine, and sulfate.
 Desalination and Water Treatment. 219; 319-326.
- 38. Visa M, Andronic L, Duta A., 2015. Fly ash-TiO₂ nanocomposite material for multi-pollutants wastewater treatment. *J Environ Manag*. 150:336-43.
- 39. Ralph, J., Lundquist, K., Brunow, G., Lu, F. Kim, H., Schatz, P. F., Marita, J. M., Hatfield, R.D., Ralph, S.A., Christensen, J.H., Boerjan, W., 2004. Lignins: Natural polymers from oxidative coupling of 4-hydroxyphenylpropanoids. *Phytochem Rev.*, 3, 29–60.
- 40. Henry Nowicki., 2016. The basics of activated carbon adsorption. Wastewater.
- 41. Zhong. Q. Q, Yue. Q. Y, Li. Q, Gao. B. Y, Xu., 2014. Removal of Cu (II) and Cr (VI) from wastewater by an amphoteric sorbent based on cellulose-rich biomass. Carbohydr. *Polym.* 11, 788-796.

- 42. Caroll. D. O, Sleep. B, Krol. M, Boparai. H, Kocur. C., 2013. Nanoscale zero valent ion and bimetallic particles for contaminated site remediation. *Adv. Water Resour.* 51. 104-122.
- 43. Wang. D, Kang. J, Liu. H, Qu. J., 2009. Preparation of organically functionalized silica gel as adsorbent for copper ion adsorption. *J. Environ. Sci.* 21. 1473-1479.
- 44. Cai. X, Gao. Y, Sun. Q, Chen. Z, Megharaj. M, Naidu. R., 2014. Removal of co-contaminants Cu (II) and nitrate from aqueous solution using kaolin Fe/Ni nanoparticles. *Chem. Eng. J.* 244, 19-26.
- 45. Aksu. Z. Z, Isoglu. I. A., 2005. Removal of Copper (II) ions from aqueous solution by biosorption onto agricultural waste sugar beet pulp. Process. *Biochem.* 40, 3031-3044.
- 46. Demirbas. A., 2008. Heavy metal adsorption onto agro-based waste materials. *J. Hazard. Mater.* 175, 117-125.
- 47. Weng. X, Jin. X, Lin. J, Naidu. R, Chen. Z., 2016. Removal of mixed contaminants Cr (VI) and Cu (II) by green synthesized iron based nanoparticles. *Ecol. Eng.* 97, 32-39.
- 48. Wyllie. J., 1957. Copper poisoning at a cocktail party. *Am. J. Public Health*. 47, 617.
- 49. Spitalny. K. C, Brondum. J, Vogt. R. L, Sargent. H. E, Kappel. S. 1984. Drinking water-induced intoxication in a Vermont family. *Pediatrics*. 74, 1103-1106.
- Knobeloch. L, Ziarnik. M, Howard. J, Theis. B, Farmer. D, Anderson. H,
 Proctor. M., 1994. Gastrointestinal upsets associated with ingestion of coppercontaminated water. *Environ. Health. Prospect.* 102, 958-961.

- 51. Abdel-Jawad. M, Al-Shammari. S, Al-Sulaimi.J., 2002. Non- Conventional treatment of treated municipal wastewater for reverse osmosis. *Desalination*. 142(1), 11-18.
- 52. Kazakis. N, Kantiranis. N, Kalaitzidou. K, Kaprara. E, Mitrakas. M, Frei. R, Vargemezis. G, Vogiatzis. D, Zouboulis. A and Filippidis. A., 2018. Environmentally available hexavalent Chromium in soils and sediments impacted by dispersed fly ash in Sarigkiol basin (Northern Greece). *Environ. Pollut.* 235. 632-641.
- 53. Quitelas. C, Rozha. Z, Silva. B, Fonseca. B, Figueiredo. H, Tavares. T., 2009. Removal of Cd (II), Cr (VI), Fe (III) and Ni (II) from aqueous solutions by an E-coli biofilm supported on kaolin. *Chem. Eng. J.* 149. 319-324.
- 54. Abdel Al-Rub. F, Kandah. M, Aldabaibeh. N., 2002. Nickel removal from aqueous solutions using sheep manure wastes. *Eng. Life. Sci.* 2, 111-116.
- 55. Karimi. M, Shojaei. A, Nematollahzadeh. A, Abdekhodaie. M.J., 2012. Column study of Cr (VI) adsorption onto modified silica-polyacrylamide microspheres composite. *Chem. Eng. J.* 210, 280-288.
- 56. Samani. M.R, Borghei. S.M, Olad. A, Chaichi. M.J., 2010. Removal of Chromium from aqueous solutions using polyaniline-poly ethylene glycol composite. *J. Hazard. Mater.* 184, 248-254.
- 57. Gode. F and Pehlvan. E., 2005. Removal of Cr(VI) from aqueous solution by two Lewitit- anion exchange resins. *J. Hazard. Mater.* B119, 175-182.

- 58. Ahalya. N, Kanamadi. M.D, Ramachandra. T.V., 2006. Biosorption of Iron (III) using the husk of *Cicer arientinum*. *Indian Journal of Chemical Technology*. 13, 122-127.
- 59. Ahalya. N, Ramachandra. T.V., 2002. Restoration of wetlands-feasibility aspects of biological restoration and biodiversity-Feb 15-16, in Kongunadu Arts and Science College, Coimbatore, India.
- 60. Raji. C and Anirudhan. T.S., 1998. Batch Cr(VI) Removal by Polyacrylamide-grafted Sawdust: Kinetics and Thermodynamins. *Water Res.* 32(12). 3772-3780.
- 61. Lazaridis. N.K, Asouhidou. D.D., 2003. Kinetics of sportive removal of Chromium (VI) from aqueous solutions by Calcined Mg-Al-CO₃ hydrotalcite. *Water Res.* 37, 2875-2882.
- 62. Bhatnagar. A, Minocha. A. K., 2010. Biosorption optimization of nickel removal from water using *Punica granatum* peel waste. *Colloid Surface* B, 76, 544-548.
- 63. Jaafarzadeh. N, Mengelizadeh. M, Jalil. A, Takdastan. N, Alavi. N, Niknam. N., 2016. Removal of zinc and nickel from aqueous solution by chitosan and polyaluminium chloride. *International Journal of Environmental Engineering*. 5 (1), 16.
- 64. Vieira. M.G.A, Neto. A.F.A, Gimenes. M.L, da Silva. M.G.C., 2010. Sorption kinetics and equilibrium for the removal of nickel ions from aqueous phase on calcined Bofe bentonite clay. *J. Hazard. Mater.*, 177, 362-371.
- 65. Hernandez-Rodriguez. M, Yperman. J, Caeleerb. R, Maggen. J, Dadi. D, Gryglewicz. G, derBruggen. B.V, Hernandez. J.F, Otero-Calvis. A., 2018.

- Adsorption of Ni (II) on spent coffee and coffee husk based activated carbon. *J. Env. Chem. Eng.* 6, 1161-1170.
- 66. Jia. Y.F, Xiao. B, Thomas. K. M., 2002. Adsorption of metal ions on nitrogen surface functional groups in activated carbons. *Langmuir*. 18 (2), 470-478.
- 67. Aman. T., Kazi. A. A, Sabri. M.U., Bano. Q., 2008. Potato peels as solid waste for the removal of heavy metal copper (II) from waste water/industrial effluent. *Colloids Surf.*, B. 63, 116-121.
- 68. Boujelben. N, Bouzid. J, Elouear. Z. 2009. Adsorption of nickel and copper onto natural iron oxide-coated sand from aqueous solutions: study in single and binary systems. *J. Hazard. Mater.*, 163 (1), 376-382.
- 69. Katsou. E, Malamis. S, Haralambous. K.J, Loizidou. M., 2010. Use of ultrafiltration membranes and aluminosilicates for nickel removal from industrial wastewater. *J. Membr. Sci.*, 360, 234-249.
- 70. Alandis. N.M, Aldayel. O.A, Mekhemer, W.K, Hefne. J.A, Jokhab. H.A., 2010. Thermodynamic and kinetic studies for the adsorption of Fe (II) and Ni (II) ions from aqueous solution using Natural Bentonite. *J. Dispers. Sci.*, 31, 1526-1534.
- 71. Kasprzak. K.S, Sunderman. F.W, Salnikow. K., 2003 Nickel carcinogenesis.

 Mutat. Res. Fund. Mol. M. 533, 67-97.
- 72. Sole. G.M, Chipman. J.K., 1986. The mutagenic potency of chrysoidines and Bismark Brown dyes. *Carcinogenesis*. 7 (11), 1921-1923.
- 73. Manogari. R, Daniel. D, Krastanov. A., 2008. Ecol. Eng. Environ. Protect. 1, 30-35.

- 74. Xavier. A, Sathya. R, Gandhirajan. J, Nagarathnam. R., 2011. Dynamic study of Adsorption for the removal of Bismark Brown-Using Activated Carbons. *Material Science Forum.* 67, 187-204.
- 75. Zhang. J, Li. Y, Zhang. C, Jig. Y., 2008. Adsorption of malachite green from aqueous solution onto carbon prepared from *Arundo donax* root. *Journal of Hazard. Mater.* 150. 774-782.
- 76. Mital. A., 2006. Adsorption Kinetics of removal of a toxic dye, Malachite Green from waste water by using hen feathers. *Journal of Hazard. Mater.* B113. 196-202.
- 77. Hu ZG, Zhang. J, Chan WL, Szeto YS., 2006. The sorption of acid dye onto chitosan nanoparticle. *Polymer*. 47, 5838-42.
- 78. Kumar. A, Prasad. B, Mishra IM., 2008. Adsorption removal of acrylonitrile by commercial grade activated carbon: kinetics equilibrium and thermodynamics. *Journal of Hazard Mater.* 152, 589-600.
- 79. Kuntari, Dessyntha Anggiani Priwidyanjati., 1911. Adsorption of malachite Green Dye from Aqueous solution on the Bamboo Leaf Ash. Development of Chemical Education in 21st Century. *AIP Conf. Proc.* 020011-1-020011-7.
- 80. Hameed. B.H, El-Khaiary. M.I., 2008a. Batch removal of malachite green from aqueous solutions by adsorption on oil palm trunk fibre: Equilibrium isotherm and kinetic studies. *Journal of Hazard Material*. 154, 237-244.
- 81. Bulut. E, Ozacar. M, Sengil. I.A., 2008. Adsorption of malachite green onto bentonite: equilibrium and kinetic studies and process design. *Micropor*. *Mesopor*. *Master*. 115, 234-246.

- 82. Sudova. E, Machova. J, Srobodova. Z, Vesely. T., 2007. Negative effects of malachite green and possibilities of its replacement in the treatment of fish eggs and fish: a review. *Vet. Med.* 12, 527-539.
- 83. Hameed. B.H, El-Khaiary. M.I., 2008. Equilibrium, Kinetics and Mechanism of malachite green adsorption on activated carbon prepared from bamboo by K₂CO₃ activation and subsequent gasification with CO₂. *Journal of Hazard. Mater.* 157, 344-351.
- 84. Santhi. T, Manonmani. S, Smitha. T., 2010. Removal of malachite green from aqueous solution by activated carbon prepared from the epicarp of *Ricinus communis* by adsorption. *Journal of Hazard. Mater.* 179, 178-186.
- 85. Mittal. A, Malviya. A, Kaur. D, Mittal. J and Kurup. L., 2007. Studies on the adsorption kinetics and isotherms for the removal of Methyl Orange from wastewaters using waste materials. 148, 229-240.
- 86. Chen. S, Zhang. J, Zhang. C, Yue. Q, Li. Y and Li. E., 2010. Equilibrium and Kinetic studies of methyl orange and methyl violet adsorption on activated carbon derived from *Phragmites australis*. *Desalination*. 252. 149-156.
- 87. Haddadian. Z, Mohammad. A.S, Zurina. Z.Z, Ahmadun. F.R, Mohammad. H.I.S., 2013. Removal Methyl Orange from Aqueous Solutions Using Dragon Fruit (*Hylocereusundatus*) Foliage. *Chemical Science Transactions*. 2(3), 900-910.
- 88. Benjah-bmm27 (2007), File: Methyl-Orange -2D-Skeletal. Png. From Wikipedia, the free encyclopedia. Accessed 6th October, 2020.

- 89. Kucukosmanoglu. M, Gezici. O, Ayar. A., 2006. The adsorption behaviors of methylene blue and methyl orange in a diaminoethane sporopollenin-mediated column system. Sep. *Purif. Technol.* 52, 280-287.
- 90. Chung. K.T, Stevens. S. E, Cerniglia. C. E., 1992. The reduction of azo dyes by the intestinal microflora, Crit. Rev. *Microbiol.* 18, 175-190.
- 91. Chung. K.T., 1983. The significance of azo-reduction in the mutagenesis and carcinogenesis of azo dyes. Mutat. Res./Rev. Genet. *Toxicol*. 114, 269-281.
- 92. Mamatha. M, Aravinda H.B, Puttaih E.T, Manjappa. S., 2013. Factors and Kinetics Involved in Adsorption of copper from aqueous and Waste water onto *Pongamia pinnata. International Journal of Innovative Research in Science*, *Engineering and Technology*. 2 (4), 1091-1098.
- 93. Ju Okali, Ibe Ezuma., 2014. Adsorption Studies of heavy Metals by Low-Cost Adsorbents. *J. Appl. Sci. Environ. Manage*. 18 (3). 443-448.
- 94. Brahmaiah. T, Spurthi. L, Chandrika. K, Ramanaiah. S and Sai Prasad. K. S., 2015. Kinetics of heavy metal (Cr and Ni) Removal from the Wastewater by using Low Cost Adsorbent. World Journal of Pharmacy and Pharmaceutical Sciences. 4 (11), 1600-1610.
- 95. Rehab M. Ali, Hesham A. Hamad, Mohamed M. Hussein, Gihan F. Malash., 2016. Potential of using green adsorbent of heavy metal removal from aqueous solutions: Adsorption Kinetics, isotherm, thermodynamic mechanism and economic analysis. *Ecological Engineering*. 91, 317-332.
- 96. Sadeek A. Sadeek, Nabel A. Negm, Hassan H. H. Hefni, Mostafa M. Abdel Wahab., 2015. Metal adsorption by agricultural biosorbents: Adsorption

- isotherm, kinetic and biosorbent chemical structures. *International Journal of Biological Macromolecules*. 81, 400-409.
- 97. Sami Guiza., 2017. Biosorption of heavy metal from aqueous solution using Cellulosic Waste Orange Peel. *Ecological Engineering*. 99. 131-140.
- 98. Fouad Krika, Noureddine Azzouze, Mohamed Chaker Ncibi., 2016. Adsoptive removal of cadmium from aqueous solution by cork biomass: Equlibrium, dynamic and thermodynamic studies. *Arabian Journal of Chemistry*. 9, S1077-S1083.
- 99. Abdunnaser Mohamed Etorki, Mahmoud El-Rais, Mohamed Tahher Mahabbis, Nayef Mohamed Moussa., 2014. Removal of some Heavy Metals from Wastewater by Using of Fava Beans. American Journal of Analytical Chemistry. 5, 225-234.
- 100. Cheraghi. E, Ameri. E, Moheb. A., 2015. Adsorption of Cadmum ions from aqueous solutions using sesame as a low-cost biosorbent: Kinetics and equilibrium studies. *Int. J. Environ. Sci. Techno.* 12, 2579-2592.
- 101. Gupta Vikal, Nisha, Ratnoo Pramila and Goyal Jyotsna., 2019. Adsorption analysis of Mn (VII) by Green Algae. *International Journal of Green and Herbal Chemistry*. Sec. A, 8(1). 192-198. (Dec. 2018-Feb.2019).
- 102. Mohamed Chiban, Gabriela Carja, Gabriela Lehutu and Fouad Sinan., 2016.

 Equilibrium and thermodynamic studies for the removal of As (V) ions from aqueous solutions using dried plants as adsorbents. *Arabian Journal of Chemistry*. 9, S988-S999.

- 103. Ali A. Al-Homaidan, Jamila A. Alabdullatif, Amal A. Al-Hazzani, Abdullah A. Al-Ghanayem, Aljawharah F. Alabbad.,2015. Adsorptive removal of Cadmium ions by Spirunina Platensis dry biomass. *Saudi Journal of Biological sciences*. 22, 795-800.
- 104. Mohamed M. Ghoneim, Hanaa S. El-Desoky, Khalid M. El-Moselhy, Adel Amer, Emad H. Abou El-Naga, Lamiaa I. Mohamedein, Ahmed E. Al-Prol., 2014. Removal of cadmium from aqueous solution using marine green algae, Ulva lactuca. *Egyptian Journal of Aquatic Research*. 40, 235-242.
- 105. Sadia Waseem, Muhammad Imran Din, Saira Nasir, Atta Rasool., 2014. Evaluation of *Acacia nilotica* as a non conventional low cost biosorbent for the elimination of Pb(II) and Cd(II) ions from aqueous solutions. *Arabian Journal of Chemistry*. 7, 1091-1098.
- 106. Fatima Ouadjenia-Marouf, Reda Marouf, Jacques Schott, Ahmed Yahiaoui., 2013. Removal of Cu(II), Cd(II) and Cr(II) ions from aqueous solution by dam silt. *Arabian Journal of Chemistry*. 6, 401-406, (2013).
- 107. Ali A. Ali-Homaidan, Hadeel J. Al-Houri, Amal A. Al-Hazzani, Gehan Elgaaly, Nadine M. S. Moubayed., 2014. Biosorption of copper ions from aqueous solutions by *Spirulina plantensis* biomass. *Arabian Journal of Chemistry*, 7, 57-62.
- 108. Hassan Rezaei., 2016. Biosorption of Chromium by using Spirulina sp. *Arabian Journal of Chemistry*. 9, 846-853.

- 109. Suresh Kumar Halnor., 2019. Low cost Adsorbent to Remove Heavy Metals from Aqueous Solution. *International Journal of Green and Herbal chemistry. Sec. A*, 8(1), 118-122. (Dec.2018-Feb.2019).
- 110. Akbar Esmaeili, Betsabe Saremnia, Mona Kalantari., 2015. Removal of mercury(II) from aqueous solutions by biosorption on the biomass of *Sargassum glaucescens* and *Gracilaria corticata*. *Arabian Journal of Chemistry*. 8, 506-511.
- 111. Khairia M. Al-Qahtani., 2016. Water purification using different waste fruit cortexes for the removal of heavy metals. *Journal of Taibah University for Science*. 10, 700-708.
- 112. Sfaksi. Z, Azzouz. N Abdelwahab. A., 2014. Removal of Cr(VI) from waste by cork waste. *Arabian Journal of Chemistry*. 7, 37-42.
- 113. Atul Kumar Kushwaha, Neha Gupta and Chattopadhyaya MC., 2014. Removal of cationic methylene blue and malachite green dyes from aqueous solution by waste materials of *Daucus carota*. *Journal of Saudi Chemical Society*, **18**:200-207.
- 114. Selvakumar A, Rangabhashiyam S, Biosorption of Rhodamine B., 2019. onto novel biosorbents from Kappaphycus alvarezi, *Gracilaria salicornia* and *Gracilaria edulis*. *Environmental Pollution*, **255**:113291. 1-12.
- 115. Neha Gupta, Atul K, Kushwaha., Chattopadhyaya MC., 2016. Application of Potato (Solanum tuberosum) plant wastes for the removal of methylene blue and malachite green dyes from aqueous solution. *Arabian Journal of Chemistry*, **9**:S707–S716.

- 116. Warda Hassan, Umar Farooq, Muhammad Ahmad, Makshood Athar, Misbahul Ain Khan., 2017. *Arabian Journal of Chemistry*, **10**:S1512-S1522.
- 117. Smitha T, Santhi T, Ashly Leena Prasad and Manonmani S., 2017. *Cucumis Sativus* used as adsorbent for the removal of dyes from aqueous solution. *Arabian Journal of Chemistry*, **10**:S244–S251.
- 118. Sumanjit Kaur, Seema Rani and Rakesh Kumar Mahajan., 2013. Adsorption Kinetics for the Removal of Hazardous Dye Congo Red by Biowaste materials as Adsorbents. *Journal of Chemistry*. Article ID 628582.
- 119. Sumanjit Kaur, Seema Rani and R.K Mahajan. 2016. Equilibrium, Kinetics and thermodynamics parameters for adsorptive removal of dye Basic Blue 9 by ground nut shells and Eichhornia. *Arabian Journal of Chemistry*. 9, S1464-S1477.
- 120. Etim UJ, Umoren SA and Eduok UM., 2016. Coconut coir dust as a low cost adsorbent for the removal of cationic dye from aqueous solution. *Journal of Saudi Chemical Society*, **20**:S67 S6.
- 121. Ashish S, Sartape, Aniruddha M, Mandhare, Vikas, V, Jadhav, Prakash D, Raut, Mansing A, Anuse, Sanjay S and Kolekar., 2017. Removal of malachite green dye from aqueous solution with adsorption technique using *Limonia acidissima* (wood apple) shell as low cost adsorbent. *Arabian Journal of Chemistry*, 10:S3229 S3238.
- 122. Muhammad Khairud Dahri, Muhammad Raziq Rahimi Kooh, and Linda B.L.Lim, 2017. Removal of methyl violet 2B from aqueous solution Using

- Casuarina equisetifolia Needle. Hindawi Publishing Corporation. ISNR Environmental Chemistry. Volume 2013; 1-8. Article ID 619819.
- 123. Somasekhara Reddy MC and Nirmala V., 2014. Bengal gram seed husk as an adsorbent for the removal of dyes from aqueous solutions column studies. *Arabian Journal of Chemistry*, **10**:S2406-S2416.
- 124. Sushmita Banerjee, M.C. Chattopadhyaya,, 2017. Adsorption Characteristics for the removal of a toxic dye, tartrazine from aqueous solutions by low cost agricultural by-products. *Arabian Journal of Chemistry*, **10**:S1629-S1638.
- 125. Adejumoke A. Inyinbor, Folahan A. Adekola and Gabriel A. Olatunji., 2015.
 Adsorption of Rhodamine B Dye from Aqueous Solution on *Irvingia gabonensis*Biomass: Kinetics and Thermodynamics studies. S. Afr. J. Chemistry. 68, 115-125.
- 126. Wycliffe Chisutia Wanyonyi, John Mmari, Paul Mwanza Shinundu., 2014.
 Adsorption of Congo Red Dye from Aqueous Solution Using Roots of Eichhornia crassipes: Kinetic and Equilibrium studies. Energy Procedia. 50, 862-869.
- 127. Kalaiselvi. D, Sangeetha. V, Basker. A and Saravanan. D., 2014. Sorption equilibrium, kinetics and thermodynamic studies of cationic dye from aqueous solution using herbal adsorbent developed from rhizome of *Acorus calamus*. *International Journal of Green and Herbal Chemistry*. Sec.A. Vol.3 (3), 950-965.
- 128. Satish Patil, Jeyesh Patil and Naseema Patel., 2015. Kinetics of adsorption of methylene blue from aqueous solutions using agricultural wastes. *International Journal of Green and Herbal Chemistry. Sec. A*, Vol.4(2), 259-273.

- 129. Binglu Zhao, Wei Xiao, Yu Shang, Huimin Zhu, Runping Han., 2017. Adsorption of light green anionic dye using cationic surfactant-modified peanut husk in batch mode. *Arabian Journal of Chemistry*. 10, S3595-S3602.
- 130. Zulkarnain Chaidir, Desvina Trio Sagita, Rahmiana Zein and Edison Munaf.,
 2015. Bioremoval of methyl orange dye using durian fruit (*Durio zibethinus*)
 Murr seeds as biosorbent. *Journal of Chemical and Pharmaceutical Research*. 7
 (1), 589-599.
- 131. Shaik Karimulla and K. Ravindhranath., 2014. Extraction of methyl orange dye from polluted waters using bio-sorbents derived from *Thedpesia populanea* and *Pongamia pinnata* plants. *Der Pharma Chemica*, 6 (4), 333-344.
- 132. Paul Egwuonwu DIM., 2013. Adsorption of Methyl Red and Methyl Orange using different tree bark powder. *Academic Research International*. 4 (1), 330-338.
- 133. Mashael Alshabanat, Rasmiah S. Al-Mufarij and Ghadah M. Al-Senani., 2016.
 Study on Adsorption of Malachite Green by Date Palm Fiber, *Oriental Journal of Chemistry*, 32(6), 3139-3114.
- 134. Xiuli Han, Jinyi Yuan, Xiaojian Ma., 2014. Adsorption of malachite green from aqueous solution onto lotus leaf: equilibrium, kinetic and thermodynamic studies, *Desalination and water Treatment*, 52, 5563-5574.
- 135. El-Khamsa Guechi, Oualid Hamdaoui., 2016. Sorption of malachite green from aqueous solution by potato peel: Kinetic and equilibrium modeling using non-linear analysis method, *Arabian Journal of Chemistry*, 9, S416-S424.

- 136. Langmuir I., 1918. The adsorption of gases plane surfaces of glass, mica and platinum. *J. Am. Soc.*, 579, 1361 1403.
- 137. Weber T W, Chakravorti. R.K., 1974. Pore and Solid diffusion models for fixed bed adsorbers. *J. Am. Inst. Chem. Eng.*, 20, 228.
- McKay G, Blair H S, Gardner J R., 1982. Adsorption of dyes on chitin.
 I. Equilibrium Studies. J. Appl. Polym. Sci. 27, 3043 3057.
- 139. Freundlich H., 1906. The dye adsorption is losungen (Adsorption in Solution)., *Z Phys. Chem.*,57, 385 470.
- 140. Doenmez, G., Aksu, Z., 2002. Removal of Chromium (VI) from Saline wastewaters by Dunaliella Speceis. *Process Biochemistry*, 38(5), 751-762.
- 141. Ho Y S and McKay G., 2000. The kinetic of sorption of divalent metal ions on to Sphagnum moss peat, Water Res. 34, 735 742.
- 142. Arivoli, S., 2007. Kinetic and thermodynamic studies on the adsorption of some metal ions and dyes on to low cost activated carbons, Ph.D., Thesis, Gandhigram Rural University, Gandhigram.
- 143. Tay C.C, Leiw H.H, Yong S.K, Surif S, Redzwan G, Abdul-Talib S., 2012.
 Cu (II) removal onto fungal derived biosorbents: Biosorption performance and the half saturation constant concentration approach. *International Journal of Research in Chemistry and Environment*. 2, 138-143.
- 144. Abdul Rahim A.R, Iswarya, Johari K, Shehzad N, Saman N, Mat H., 2021. Conversion of coconut waste into cost effective adsorbent for Cu(II) and Ni(II) removal from aqueous solutions. *Environmental Engineering Research*. 26, https://doi.org/10.4491/eer.2020.250.

- 145. Myalowenkosi I. Sabela, Kwanele Kunene, Suvardhan Kanchi, Nokukhanya M. Xhakana, Ayyappa Bathinapatla, Phumlane Mdluli, Deepali Sharma, Krishna Bisetty., . 2016. Removal of Copper (II) from wastewater using green vegetable waste derived activated carbon: An approach to equilibrium and kinetic study. Arabian Journal of Chemistry.
- 146. Ali A. Al-Homaidan, Hadeel J. Al-Houri, Amal A. Ali-Hazzani, Gehan Elgaaly, Nadine M. S. Moubayed., 2014. Biosorption of copper ions from aqueous solutions by Spirulina plantensis biomass. *Arabian Journal of Chemistry*. 7, 57-62.
- 147. M. Mamatha, H. B. Aravinda, E. T. Puttaiah, S. Manjappa., 2013. Factors and Kinetics Involved in Adsorption of Copper from Aqueous and wastewater into Pongamia pinnata. International Journal of Innovative Research in Science, Engineering and Technology. 2(4), 1091-1098.
- 148. A. Anitha, K. Kohilavani, R. Murugalakshmi., 2018. Removal of Copper (II) by Adsorption on Biomass Carbon Derived from Pongamia (*Pongamia pinnata*) Leaf. *International Journal of Applied Engineering Research*, 13(20): 14669-14674.
- 149. Lei Xu, Hongbiao Cui, Xuebo Zheng, Jiani Liang, Xiangyu Xing, Lunguang Yao, Zhaojin Chen and Jing Zhou., 2017. Adsorption of Cu²⁺ to biomass ash and its modified product. Water Science & Technology. Bonus Issue 1, pp 115-125.
- 150. Godfrey Musumba, Caroline Nakiguli, Cranmer Lumbanga, Paul Mukasa, Emmanuel Ntambi., 2020. Adsorption of Lead (II) and Copper (II) Ions from Mono Synthetic Aqueous Solutions using Bio-char from Ficus natalensis Fruits. Journal of Encapsulation and Adsorption Sciences. 10; 71-84.

- 151. Pongthipun Phuengphai, Thapanee Singjanusong, Napaporn Kheangkhun, Amnuay Wattanakornsiri., 2021. Removal of Copper (II) from aqueous solution using chemically modified fruit peels as efficient low-cost biosorbents. *Water Science and Engineering*. https://doi.org/10.1016/j.wes.2021.08.003.
- 152. Muhammad Salman, Rabia Rehman, Umar Farooq, Anum Tahir and Liviu Mitu., 2020. Biosorptive Removal of Cadmium (II) and Copper (II) Using Microwave-Assisted Thiourea-modified sorghum bicolor Agrowaste. *Journal of Chemistry*. Vol.2020, Article ID.8269643. https://doi.org/10.1155/2020/8269643, pp.1-11.
- 153. Deniz Uzunoglu, Nur Gurel, Nazim Ozkaya, Ayla Ozer., 2014. The single batch biosorption of copper (II) ions on *Sargassum acinatum*. *Desalination and Water Treatment*. 52; 1514-1523.
- 154. Huan-Ping Chao, Chung-Cheng Chang., 2012. Adsorption of Copper (II), Cadmium (II), Nickel (II) and Lead (II) from aqueous solution using biosorbents. *Adsorption*, 18: 395-401.
- 155. Mohammad W. Amer Rafat A. Ahmed . Akl M. Awwad., 2015. Biosorption of Cu (II), Ni (II), Zn (II) and Pb (II) ions from aqueous solution by *Sophora japonica* pods powder. *Int. J. Ind.Chem.* 6 : 67-75.
- 156. Al-Qdah, Eman Assirey. Biosorption of copper from wastewater by Algal Biomass. https://www.researchgate.net/publication/337561017.
- 157. Shakila H. Peli Thanthri, Kavitha H. Ranaweera, Bupani Asiri Perera., 2021.

 Adsorption study of Cu²⁺ Ions from aqueous solutions by Bael-Flowers (*Aegle marmelos*). *Biointerface Research in Applied Chemistry*. 11(4); 11891-11904.

- **158.** 11. Lee S.Y, Choi H.J., 2018. Persimmon leaf bio-waste for adsoptive removal of heavy metals from aqueous solution. *Journal of Environmental Management*. 209; 382-392.
- 159. Samuel MS, Shah S, Subramaniyan V, Qureshi T, Bhattacharya J, Pradeep Singh ND., 2018. Preparation of graphene oxide/chitosan/ferrite nanocomposite for Chromium (VI) removal from aqueous solution. *Int J Biol Macromol*. 119: 540–547.
- 160. Parlayici S, Eskizeybek V, Avci A, Pehlivan E., 2015. Removal of Chromium(VI) using activated carbon supported functionalized carbon nanotubes. *J Nanostuct Chem.* 5: 255–263.
- 161. Khan TA, Nazir M, Ali I, Kumar A., 2017. Removal of Chromium (VI) from aqueous solution using guar gum–nano zinc oxide biocomposite adsorbent. *Arab J Chem.* 10: 2388–2398.
- 162. R. Saravanane, T. Sundararajan, S. Sivamurthyreddy., 2002. Efficiency of chemically modified low cost adsorbents for the removal of heavy metals from wastewater: a comparative study", *Indian. J Env Health.* 44: 78–81.
- 163. Dehghani MH, Mohammadtaher M, Bajpai AK, Heibati B, Tyagi I, Asif M, Agarwal S, Gupta VK., 2015. Removal of Noxious Cr(VI) ions using single-walled carbon nanotubes and multivalued carbon nanotubes. *Chem Eng J.* 279: 344–352
- 164. D. Akltas, N. Dizge, H.C. Yatmaz, Y. Caliskan, Y. Ozay, A. Caputcu., 2017. The adsorption and Fenton behavior of iron rich Terra Rosa soil for removal of

- aqueous anthraquinone dye solutions: kinetic and thermodynamic studies, *Water Sci. Technol.* 76:3114–3125.
- 165. Samarghandi MR, Hadi M, Moayedi S, Askari FB., 2009. Two-parameter isotherms of methyl orange sorption by pinecone derived activated carbon. *Ira J Environ Health Science Eng.* 6: 285-294
- 166. Qada ENE, Allen SJ, Walker GM., 2006. Adsorption of Methylene Blue onto activated carbon produced from steam activated bituminous coal: A study of equilibrium adsorption isotherm. *Chem Eng J.* 124: 103-110.
- 167. Reyhaneh Saadi, Zahra Saadi, Reza Fazaeli and Narges Elmi Fard., 2015. Monolayer and multilayer adsorption isotherm models for sorption from aqueous media. *Korean Journal of Chemical Engineering*, 32(5): 787-799.
- 168. Malkoc, E., Nuhoglu, Y., 2006. Cr (VI) adsorption by waste acorn of Quercus ithaburensis in fixed beds: Prediction of break-through curves. *Chem. Eng. J.* 119: 61-68.
- 169. Hassan Rezaei., 2016. Biosorption of chromium by using *Spirulina* sp. *Arabian Journal of Chemistry*. 9: 846-853.
- 170. J.R. Memon, S.Q. Memon, M.I. Bhanger, A. El-Turki, K.R. Hallam, G.C. Allen., 2009. Banana peel: a green and economical sorbent for the selective removal of Cr(VI) from industrial wastewater, *Colloid Surf.* B 70: 232–237.
- 171. Kannan Pakshirajan & Alemayehu Netsanet Worku & Mike A. Acheampong & Henk J. Lubberding & Piet N. L. Lens., 2013. Cr(III) and Cr(VI) Removal from Aqueous Solutions by Cheaply Available Fruit Waste and Algal Biomass. *Appl Biochem Biotechnol*. 170:498–513.

- 172. Rengabhashiyam S, Selvaraje N., 2015. Adsorption remediation of hexavalent chromium from synthetic wastewater by a natural and ZnCl₂ activated *Sterculia guttata* shell. *J. Mol Liq.* 207: 39-49.
- 173. Serife Parlayici and Erol Pehlivan., 2019. Comparative study of Cr (VI) removal by bio-waste adsorbents: equilibrium, kinetics and thermodynamic. *Journal of Analytical Science and Technology*. 10:15.
- 174. Tolera Seda Badessa, Esayas Wakuma and Ali Mohammed Yimer., 2020.

 Bio-sorption for efective removal of Chromium(VI) from wastewater using

 Moringa stenopetala seed powder (MSSP) and banana peel powder (BPP). BMC

 Chemistry. 14:71. https://doi.org/10.1186/s13065-020-00724-z
- 175. <u>Eva Pertile</u>, Tomas Dvorsky, <u>Vojtech Vaclavik</u>, and Silvie Heviankova., 2021.

 Use of Different Types of Biosorbents to Remove Cr (VI) from Aqueous Solution. 11(3): 240. doi: <u>10.3390/life11030240</u>.
- 176. Husien S, Labena A, El-Belely EF, Mahmoud Hamada M, Hamouda Asmaa S., 2019. Adsorption studies of Hexavalent Chromium [Cr (VI)] on micro-scale biomass of *Sargassum dentifolium*, Seaweed, *Journal of Environmental Chemical Engineering*. doi: https://doi.org/10.1016/j.jece.2019.103444.
- 177. Martha A. Espinoza-Sancheza, Katiushka Arevalo-Ninoa, Isela Quintero-Zapataa, Ileana Castro-Gonzaleza, Veronica Almaguer-Cantua., 2019. Cr(VI) adsorption from aqueous solution by fungal bioremediation based using Rhizopus sp. *Journal of Environmental Management*. 251: 109595.
- 178. J. Aravind; G. Sudha; P. Kanmani; A.J. Devisri; S. Dhivyalakshmi;M. Raghavprasad., 2015. Equilibrium and kinetic study on chromium (VI)

- removal from simulated waste water using gooseberry seeds as a novel biosorbent. *Global J. Environ. Sci. Manage.*, 1(3): 233-244.
- 179. Hassan Pahlavanzadeh and Mahsa Motamedi., 2020. Adsorption of Nickel, Ni(II), in Aqueous Solution by Modified Zeolite as a Cation-Exchange Adsorbent. DOI:10.1021/acs.jced.9b00868 *J. Chem. Eng.* Data.
- 180. M.G.A. Vieira, A.F. Almeida Neto, M.L. Gimenes, M.G.C. da Silava., 2010. Sorption kinetics and equilibrium for the removal of nickel ions from aqueous phase on calcined Bofe bentonite clay, *J. Hazard. Mater.* 177, 362-371
- 181. M. Thirumavalavan, Y. Lai, J. Lee., 2011. Fourier transform infrared spectroscopic analysis of fruit peels before and after the adsorption of heavy metal ions from aqueous solution. *J Chem Eng Data* 56: 2249–2255.
- 182. R. Saravanane, T. Sundararajan, S. Sivamurthy reddy., 2002. Efficiency of chemically modified low cost adsorbents for the removal of heavy metals from wastewater: a comparative study", *Indian. J Env Hlth* 44: 78–81.
- 183. R. Gupta and Mohapatra., 2003. Microbial biomass: an economical alternative for removal of heavy metals from waste water, *Indian J. Exp. Biol.* 41, 945-966.
- 184. Shweta Gupta. Arinjay Kumar., 2019. Removal of nickel (II) from aqueous solution by biosorption on *A.barbadensis Miller* waste leaves powder. *Applied water Science*. 9:96: 1-11.
- 185. Effective Biosorption of Nickel (II) from Aqueous Solutions Using *Trichoderma* viride. Journal of Chemistry. Volume 2013, Article ID 716098, 1-7. http://dx.doi.org/10.1155/2013/716098.

- 186. Abubakr Elkhaleefa, Ismat H.Ali, Eid I.Brima, A.B. Elhag and Babikar Karama., 2020. Efficient Removal of Ni(II) from Aqueous Solutions by Date Seeds Powder Biosorbent: Adsorption Kinetics, Isotherm and Thermodynamics. 8, 1001; doi:10.3390/pr8081001.
- 187. Hui, L., Yuan, H., Sung, Y., Yang, T., Li, L. 2011. Adsorption behavior of Ni (II) on lotus stalks derived active carbon by phosphoric acid activation, *Desalination*, 268, 12-19.
- 188. Abdul Rahman Abdul Rahim, Iswarya, Khairiraihanna Johari, Nasir Shehzad, Norasikin Saman, Hanapi Mat., 2021. Conversion of coconut waste into cost effective adsorbent for Cu(II) and Ni(II) removal from aqueous solutions. *Environ. Eng. Res.* 26(4); 200250. https://doi.org/10.4491/eer.2020.250.
- 189. S. Suganya, A. Saravanan, P. Senthil Kumar, M. Yashwanthraj, P. Sundar Rajan and K. Kayalvizhi., 2017. Sequestration of Pb(II) and Ni(II) ions from aqueous solution using microalga *Rhizoclonium hookeri*: adsorption thermodynamics, kinetics, and equilibrium studies. *Journal of Water Reuse and Desalination*. 7(2);214-227.
- 190. M.Chidambaram, R. Sivakumar., 2019. Adsorption of Nickel (II) ion from Aqueous Solution by Adsorbent. A Journal of Composition Theory. XII(XII) 1108-1123.
- 191. Gholamreza Ebrahimzadeh Rajaei, Hossein Aghaie, Karim Zare, and Mehran Aghaie., 2012. Adsorption of Ni(II) and Cd(II) Ions from Aqueous Solutions by Modified Surface of *Typha latifolia* L. Root, as an Economical Adsorbent. *J. Phys. Theor. Chem.* 9 (3): 137-147.

- 192. Lahieb Faisal Muhaisen., 2017. Nickl ions removal from aqueous solutions using Sawdust at Adsorbent: Equilibrium, Kinetic and Thermodynamic studies.

 *Journal of Engineering and Sustainable Development. Vol. 21(3), 60-71.
- 193. Maurya NS, Mittal AK and Cornel P., 2006. Biosorption of dyes using dead macro fungi: Effect of dye structure, ionic strength and pH. *Biores. Technol*, **97**:512 521.
- 194. Iqbal MJ AM N., 2007. Adsorption of dyes from aqueous solution on activated charcoal. *Journal of Hazard. Mater*, **B139**:57-66.
- 195. Ponnusami V, Gunasekar V and Srivastava SN., 2009. Kinetics of methylene blue removal from aqueous solution using gulmohar (*Delonix regia*) plant leaf powder; multivariate regression analysis. *J. Hazard. Mater*, **169**:119 -127.
- 196. Hameed, B.H., 2008. Equilibrium and kinetic studies of methyl violet sorption by agricultural waste. *J. Hazard. Mater*, **154**: 204 212.
- 197. SenthilKumar, P., Ramalingam, S., Senthamarai, C., Niranjanaa, M., Vijayalakshmi, P., Sivanesan, S., 2010. Adsorption of dye from aqueous solution by cashew nut shell: studies on equilibrium isotherm, kinetics and thermodynamics of interactions. *Desalination*, **261**:52-60.
- 198. Sushmita Banerjee, M.C., 2017. Chattopadhyaya, *Arabian Journal of Chemistry*, **10**:S1629-S1638.
- 199. Ahmad, A., Rafatulla, M., Ibrahim, M.H., Hashim, R., 2009. Scavenging behavior of meranti sawdust in removal of Methylene Blue from aqueous solution. *J. Hazard. Mater*, **170**:357.

- 200. Salleh, M.A.M., Mohmoud, D.K., Karim, W.A., Idris, A., 2011. Cationic anionic dye adsorption by agricultural solid waste: a comprehensive review.

 Desalination, 280:1 13.
- 201. Kannan, N., Sundaram, M.M., 2001. Kinetics and mechanism of removal of methylene blue by adsorption on various carbons a comparative study. *Dyes and Pigments*, **51**:25 40.
- 202. El-Qada, E.N., Allen, S.J., Walker, G.M., 2006. Adsorption of methylene blue onto activated carbon produced from stream activated bituminous coal: a study of equilibrium adsorption isotherm. *Chem. Eng. J.* 124, 103-110.
- 203. Franca, A.S., Oliveira, L.S., Ferreira, M.E., 2009. Kinetics and equilibrium studies of methylene blue adsorption by spent coffee grounds. *Desalination*, 249, 267.
- 204. Gong, R., Jin, Y., Chen, F., Chen, J., Liu, Z., 2006. Enhanced malachite green removal from aqueous solution by citric acid modified rice straw. *Journal of Hazardous Materials*. 137, 865.
- 205. Yasemin Islek Coskun, Nur Aksuner, Jale Yanik, 2019. Sandpaper Wastes as Adsorbent for the removal of Brilliant Green and Malachite Green Dye. *Acta Chim. Slov.* 66, 402-413.
- 206. M. Auta, B.H. Hameed., 2013. Acid modified local clay beads as effective low-cost adsorbent for dynamic adsorption of methylene blue. *J. Ind. Eng. Chem.*
- 207. B.K. Nandi, A. Goswami, M.K. Purkait., 2009. Adsorption Characteristics of brilliant green dye on kaolin, 161, 387-395.

- 208. Binglu Zhao, Wei Xiao, Yu Shang, Huimin Zhu, Runping Han., 2017. *Arabian Journal of Chemistry*. 10 S3595-S3602.
- Edris Bazrafshan, Amin Allah Zarei, Hossein Nadi and Mohammad Ali Zazouli.,
 2014. *Indian Journal of Chemical Technology*. 21:105-113.
- 210. Sumanjit, Seema Rani, R.K. Mahajan., 2016. *Arabian Journal of Chemistry*. 9:S1464-S1477.
- 211. HA. Chanzu, JM. Onyari, PM. Shiundu., 2012. J. Polym. Environ. 20(3) 665-672.
- 212. Ruihua Huang, Qian Liu, Jie Huo and Bingchao Yang., 2017. *Arabian Journal of Chemistry*. 10: 24-32.



Journal of Advanced Scientific Research

ISSN
0976-9595
Research Article

Available online through http://www.sciensage.info

REMOVAL OF BISMARK BROWN R DYE FROM AQUEOUS SOLUTION BY LAPLAP PURPUREUS PLANT STEMS UTILIZED AS BIOSORBENT

G. Bharathidasan*¹, N. Mani¹, G. Vishnuvardhanaraj¹, K. Mohamed Faizal²

¹PG and Research Department of Chemistry, A.V.V.M. Sri Pushpam College, (Affiliated to Bharathidasan University), Poondi, Thanjavur (Dt), Tamil Nadu, India

²PG and Research Department of Chemistry, Khadir Mohideen College, (Affiliated to Bharathidasan University), Adirampattinam,
Thanjavur (Dt), Tamil Nadu, India

*Corresponding author: gpdasangee@gmail.com

ABSTRACT

Adsorption of dye utilizing biosorbent is an unusual method to remove the dye from industrial wastewater. Biosorbent arranged from *Laplap Purpureus* Stem Powder (LPSP) have been utilized as an adsorbent for the removal of Bismark Brown R dye from the aqueous solution. The biosorbent matter was analyzed by Scanning Electron Microscope (SEM) image and Fourier Transfer Infra Red (FTIR) spectroscopy. The batch adsorption experiment studies were carried out to evaluate various adsorbing effect of experimental parameters such as effect of pH, adsorbent dosage, equilibrium time and initial dye concentration. The data obtained from the experimental values were analyzed by Langmuir and Freundlich isotherm model. The adsorption kinetic studies were also analyzed by pseudo first order and pseudo second order models. The result reveals that the removal efficiency of biosorbent (LPSP) is very better for the Bismark Brown R dye from made up aqueous solution.

Keywords: Adsorption, Laplap purpureus, Biosorbent, Bismark Brown R, Isotherms, Kinetics

1. INTRODUCTION

Environmental pollution arises due to the release of industrial effluents are a main distress in growing countries. Generally, unused or partially used industrial effluents are being discharged directly to the natural ecosystem. This industrial effluents act as chief water pollutants. The most of the important category of pollutants derived from dyes, which are organic in nature and they are in the industrial effluents discharged from various industries like food, pharmaceutical, textiles, cosmetics, paper, leather, rubber and plastics. Man-made dyes are being produced on large amount than the natural dyes and are regularly used in textile industries. Due to their wide-ranging of applications, the man-made dyes can cause serious environmental problems and severe health risks. The dyes may be discharged into the water bodies is toxic to aquatic species as well as human beings, due to the presence of an aromatic or heavy metal in their structure. The contamination of dye in water is causes many healthiness troubles such as nausea, hemorrhage, ulceration and etc [1-2]. The various dye removal methods are using for purification of industrial effluents including oxidation, coagulation, floatation,

filtration biological adsorption, membrane and treatment. In the above all the methods the adsorption technique appears to have significant possible for the removal of dye from textile industrial effluents [3]. Adsorption technique is better in simplicity of design, low cost, easy to handle and insensitivity to toxic material. A huge number of suitable adsorbents such as activated carbon, polymeric resins and a variety of low cost adsorbents like non modified or modified cellulosic biomass, bacterial biomass have been studied [4]. Detection of a potential dye adsorbent should be in good concurrence with its dye binding capability, its requirements and limits with respect to environmental factors. The conversion of agricultural wastes into valuable materials with negligible generating pollutants is a prominent challenge and suggested for an industrial sustainable development in order to defend the environment [4]. Hence, biosorption is a promising technique for pollutants removal from their solutions. The materials of biological sources are used as a sorbents to remove dyes from the aqueous solutions. These 'biosorbents' have a variety of functional groups that can complex with the dyes. Researcher in the field of biosorption proposes a number of advantages more than other techniques like the material can be find easily as byproducts, unreacted or waste materials can be reused, no need of cost for growth media, simple methods, requires low cost investment, the process is rapid, easy to operate, greener synthesis and free from the physiological restraint of living cells [5]. Nowadays a huge number of biosorbents have been utilized to removal of dyes, such as Daucus carota [6], Kappaphycus alvarezii, Gracilaria salicornia, Gracilaria edulis [7], Solanum tuberosum plant waste [8], Haloxylon recurvum stem [9], Cucumis sativus fruit peel [10], Coconut coir dust [11], wood apple shell [12], Casuarina equisetfolia Needle [13], Bengal gram seed husk [14] Saw dust [15]. The effectiveness of adsorption process mostly depends on investment cost and removal ability of adsorbents used. agricultural waste materials are getting much more consideration as adsorbents due to its low cost and wide range of availability for the removal of dyes from textile industrial effluents. The objectives of present study were to evaluate the sorption characteristics of Laplap purpureus stem powder (LPSP), under suitable conditions used for the removal of dye from aqueous solution.

2. MATERIALS AND METHODS

2.1. Preparation of adsorbent

The Laplap purpureus plant stems were received from locality home garden later than harvest at Sevvaypatti village, Karambakudi (T.K), Pudukkottai (D.T), Tamil Nadu -614 614, India. The stems were chops into small segments, systematically washed with tap water to eliminate dirt and then further washed with distilled water and after then dried in direct sun light for five days. The dried Laplap purpureus plant stems were ground as very fine powder in a domestic grinder and sieving to separate the particles size of $<90~\mu m$ by using manual experimental (Jayant Test Sieves) sieves. These separated Laplap purpureus stem powdered (LPSP) particles were kept in good conditioned air tight plastic bottle for use in adsorption studies.

2.2. Preparation of Adsorbate

Bismark Brown R dye having molecular formula $C_{21}H_{26}Cl_2N_8$ was selected as the adsorbate. The Himedia grade of Bismark Brown R dye was used. The concentration of 1g/L stock solution of dye was prepared by precisely weighed Bismark Brown R dye dissolving in double distilled water. The experimental dye solution was obtained by diluting the stock solution in precise proportions to required initial dye concentrations. 4-[5-

(2,4-Diamino-5-methylphenyl) diazenyl-2-methylphenyl] diazenyl-6-methylbenzol-1, 3-diamine is the IUPAC name of the Bismark brown R dye. The structure of Bismark Brown R is shown in fig. 1. [16-17].

$$H_2N$$
 H_3C
 $N=N$
 $N=N$
 $N=N$
 CH_3
 CH_3

Fig. 1: Structure of Bismark Brown R Dye

2.3. Data Analyzing Methods

2.3.1. Adsorption Isotherm Studies

Adsorption isotherm is one of the most important physicochemical models in the description of adsorption process. It explains that how the adsorbent interacts by the adsorbate. Therefore it is essential in optimal the use of the adsorbent. The experimental data were tested by the familiar isotherm equations namely, Langmuir and Freundlich models.

2.3.1.1. Langmuir Isotherm

Langmuir isotherm takes postulation that the sorption presents at particular homogeneous sites within the adsorbent. The common term for Langmuir equation is,

$$q_e = b q_{max} Ce/1+bCe$$

The linear structure of isotherm equation has written as,

$$1/q_e = (1/bq_{max}) (1/Ce) + (1/q_{max})$$

 $q_{max}\!=\!\!Saturation$ capacity of the adsorbent by maximum dye uptake, b = Energy of adsorption variable C_e and q_e respectively.

2.3.1.2. Freundlich Isotherm

Freundlich isotherm is an experimental equation based on a heterogeneous surface. The common form of Freundlich equation is,

$$q_e = k_f C_e^{1/n}$$

and the linear form is, $\log q_e = \log k_f + 1/n \log C_e$ where the intercept $\log k_f$ is a measure of adsorption capacity and slope 1/n is the intensity of adsorption.

2.3.2. Kinetics Studies

Kinetic models were used to analyze the experimental data to explore about the potential rate controlling step and the mechanism of the adsorption such as the chemical reaction and mass transfer process. The transiting perform of batch adsorption process was studied by using pseudo first order and pseudo second order kinetic models.

2.3.2.1. Pseudo First order

The possibility of adsorption data following Lagergren pseudo-first-order kinetic is given by the linearized eq.

$$\log (q_e - q_t) = \log q_e - (k_1/2.303)t$$

Where q_e (mg/g) and q_t (mg/g) refers to the amount of dye adsorbed per unit weight of adsorbent at equilibrium and at time t, k_1 is the rate constant of adsorption [18].

2.3.2.2. Pseudo Second order

This adsorption kinetic model equation was developed by 'Ho', studied to give details about the sorption capacity, the pseudo second order model can be written as,

$$t/q_t = 1/k_2 q_e^2 + 1/q_e t$$

Where t is the constant time (min), q_e (mg/g) and q_t (mg/g) are the amounts of dye adsorbed at equilibrium and at any time, t [19].

2.3.2.3. Batch Experiment

Adsorption experiments of dye solution were carried by treated with 500 mg of adsorbent dose and introducing 50 mL of stock solution of dye. The various parameters were performed like effect of pH, effect of adsorbent dose, effect of contact time and effect of initial dye concentration. After that the preferred times of treatment, the experimental samples were drained to remove the adsorbent and then adsorption progress was observed by using lambda 35 **UV**-visible Spectrophotometer at 420 nm is the wave length for maximum absorbance of λ_{max} for Bismark Brown R dye.

3. RESULTS AND DISCUSSION

3.1. Effect of pH for dye solution onto adsorption

The pH of the aqueous solution of dye is the evidently main parameter for controlled the adsorption process. The experiments were completed with range of pH from 2 to 10, temperature is 30°C, contact time is 50 minutes, agitation speed is 360 rpm, initial dye concentration is 200 mg/L and the adsorbent dose is 300 mg. The results of the experiment are shown in the table 1. The graph has drawn between pH and BBR dye uptake is shown in the fig. 2. The figure shows that the biosorbent contains polymers with more number of functional group; therefore the net charge on the biosorbent is more pH dependent [20]. When increasing the pH of the system while the number of negatively charged sites (OH) also increases on biosorbent, due to increase in the hydroxyl

ion concentration where as the number of positively charged sites (H⁺) also decreases [21]. Hence, at higher pH is most favors for the uptake of positively charged (cationic) dye due to the surface of the adsorbent gets more negatively charged by losing protons. Here the dye uptake occurs due to increased electrostatic force of attraction between surface of dye and adsorbent [22]. Therefore, dye uptake at lower pH decreases due to less number of negatively charged sites at the LPSP surface. The lower sorption of BBR dye at lower pH was maybe due to the presence of the large number of H⁺ ions competing with the cationic groups of the dye on sorption sites [23]. The maximum sorption was observed at pH 8 for BBR (cationic or positively charged dye) dye. The decrease in the biosorption of BBR dye after pH was insignificant.

Table 1: Effect of pH on dye uptake, Time 50 min, Biosorbent dose 300 mg, Volume of the solution 50 mL, Initial dye concentration 200 mg/L and Temperature 30⁸C

рН	Percentage of Removal
2	61.50
3	65.52
4	67.03
5	68.20
6	71.57
7	74.63
8	77.91
9	75.35
10	75.35

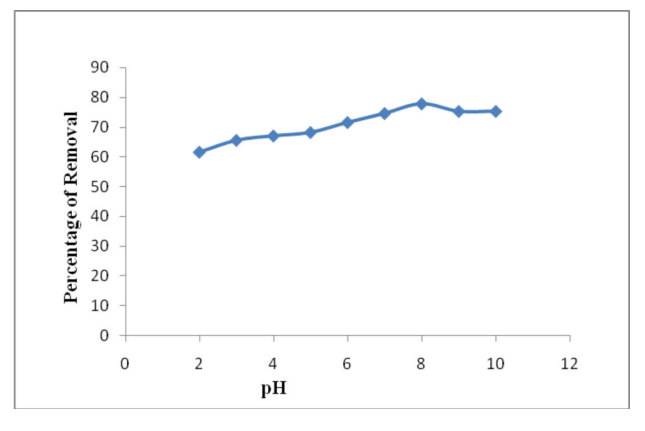


Fig. 2: Effect of pH on dye uptake, Time 50 min, Biossorbent dose 300 mg, Volume of the solution 50 mL, Initial dye concentration 200 mg/L and Temperature $30^{\,8}$ C

3.2. Effect of biosorbent dose for dye solution onto adsorption

The adsorbent dose was also studied for the removal of BBR dye from aqueous solution. The experiment was carried out with adsorbent dose is varied from 100 to 500 mg with other parameters are constant such as pH 8, initial dye concentration is 200 mg/L, temperature is 30°C, contact time is 50 minutes, agitation speed is 360 rpm. The results of the experiment are shown in table -2. The effect of biosorbent dosage for the removal of dye is shown in fig. 3. The figure representing that adsorption was mostly complete with biosorbent from 100 to 300 mg. The adsorption of dye uptake increase with increase in dose of the adsorbent, because of increases the adsorption surface area and availability of adsorption sites [24]. Moreover, above the 300 mg of the adsorbent dose weight, did not show any significant for the removal of dye, hence, 300 mg biosorbent dose was preferred for following experiments.

Table 2: Effect of Biosorbent dose on dye uptake, Time 50 min, pH 8, Volume of Solution 50 mL, Initial dye concentration 200 mg/L and Temperature 30⁸ C

Adsorbent dose (mg)	Percentage of Removal
100	72.49
200	75.79
300	77.99
400	77.59
500	77.39

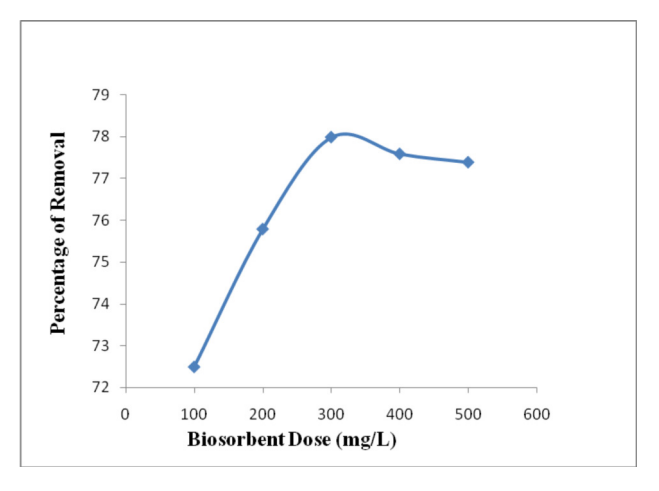


Fig.3: Effect of Biosorbent dose on dye uptake, Time 50 min, pH 8, Volume of Solution 50 mL, Initial dye concentration 200 mg/L and Temperature 30 °C

3.3.Effect of contact time for dye solution onto adsorption

The most essential factor in batch adsorption studies are the effect of contact time. In this study all of the parameter other than contact time 10 to 70 minutes, including temperature is 30°C, adsorbent dose is 300 mg, pH is 8, initial dye concentration is 200 mg/L and agitation speed is 360 rpm were kept permanent. The table 3 is exhibits the experimental data and the fig. 4 shows efficiency of dye adsorption by effect of contact time.

Table 3: Effect of contact time on dye uptake, pH 8, volume of solution 50 mL, Biosorbent dose 300 mg, Initial dye concentration 200 mg/L, Temperature 30 °C

Time in(min)	Percentage of Removal
10	72.49
20	73.59
30	74.69
40	75.79
50	77.44
60	77.44
70	77.44

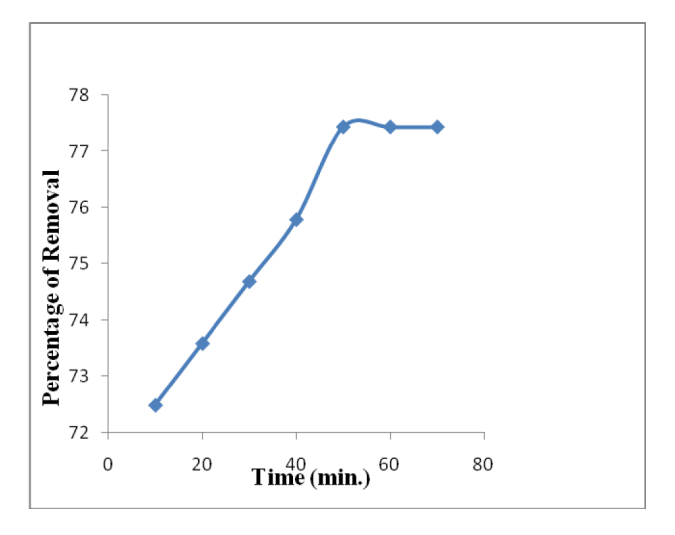


Fig. 4: Effect of contact time on dye uptake, pH 8, volume of Solution 50 mL, Biosorbent dose 300 mg, Initial dye concentration 200 mg/L, Temperature 30 °C

The time variant graph exhibits that in the preliminary stage of the dye adsorption is rapidly removed but while it reaches at equilibrium, it slows downward gradually. This is due to during the initial stage of adsorption process the availability of vacant surface sites and then a

certain time period the vacant sites of the adsorbent get occupied by dye molecules, as a result to form a repulsive force between the adsorbate on the adsorbent surface and bulk phases. The adsorption was takes place up to 50 minutes after that the equilibrium attainment, the percentage of adsorption of dye did not show any appreciable change with respect to time. This suggests that after equilibrium is attained, further treatment does not provide more removal [15]. In batch adsorption, the removal rate of the adsorbate in aqueous solution is mainly controlled by transport of dye molecules from the surrounding sites to the interior sites of the adsorbent particles [25]. The figure exhibited that a contact time of 50 minutes was sufficient to reach equilibrium and the adsorption no change with further increasing contact time, hence, the contact time has been preferred as 50 minutes for the continuous experiment.

3.4.Effect of Initial dye concentration for dye solution onto adsorption

The experiment were carried out with a different concentrations of dye solution from 100 to 1000 mg/L and temperature is 30°C, adsorbent dose is 300 mg, pH is 8, contact time is 50 minutes, agitation speed is 360 rpm. The experimental data are shown in table 4 and the graphs were drawn between initial dye concentrations and dye uptake is shown in figure 5.

Table 4: Effect of Initial dye concentration on dye uptake, Time 50 min, pH 8, Volume of Solution 50 mL, Biosorbent dose 300mg and Temperature 30⁸ C

Initial dye	Percentage of Removal
concentration (ppm)	G
100	79.28
200	77.99
300	76.56
400	76.25
500	75.72
600	75.46
700	75.20
800	73.80
900	72.44
1000	71.78

The figure exhibits that the effect of initial dye concentration is highly depend upon the immediate relation between the available binding sites on an adsorbent surface and the concentration of dye [26].

Usually the dye removal percentage is decreases with increase in concentration of initial dye, which may be reason for the saturation of adsorption sites in the adsorbent surface and the adsorption ability increased with an increase in concentration of the dye. In low concentration there will be vacant active sites on surface of the adsorption and when the initial dye concentration increases, the active sites not to be enough for adsorption of the dye molecules [27].

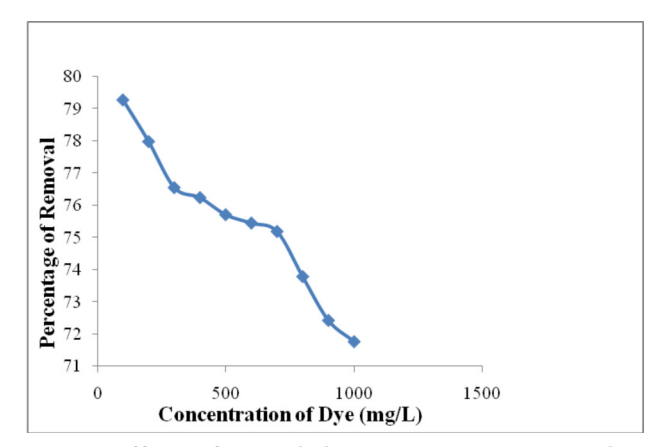


Fig. 5: Effect of Initial dye concentration on dye uptake, Time 50 min, pH 8, Volume of Solution 50 mL, biosorbent dose 300 mg and Temperature 30⁸C

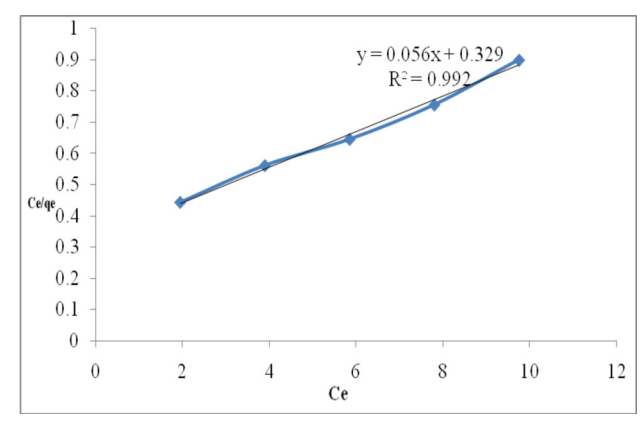


Fig. 6: Langmuir isotherm plot of Bismark Brown R dye using *Laplap purpureus* plant stem powder

3.5. Adsorption Isotherm Models

The constant q_{max} and b are the characters of Langmuir isotherm and can be determined from the Langmuir equation, a plot of $1/q_e$ Vs $1/C_e$ gives a straight line of a slope $(1/q_{max})$ and intercepts $1/q_{max}$. So that the data matching with Langmuir isotherm. The linearity of the plot represents the application of Langmuir equation is supporting monolayer creation on the surface of the

adsorption. The variable from Freundlich equation, q_e and C_e are dye adsorbed and the equal dye concentration in solution. Langmuir and Freundlich plots were here using the tables 5 and their plots were shown in fig. 6 and fig. 7 respectively.

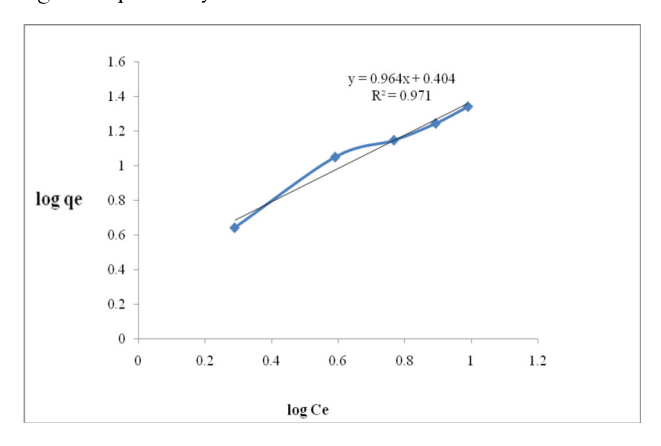


Fig. 7: Freundlich isotherm plot of Bismark Brown R dye using *Laplap purpureus* plant stem powder

3.6. Kinetic Models

The sorption coefficient and the capacity of the equilibrium $q_{\rm e}$ can be determined from the linear plot of log $(q_{\rm e}\!-\!q_{\rm t})$ versus time t from the fig. 5. It was evidence that the linear plot exhibits the applicability of the Lagergren equation; $q_{\rm e}$ values were present at table 6. The results represented that the concentration of dye has no significant effect. The correlation coefficient of r^2 is 0.9943. If second order kinetics is applicable; the plot of t/q_t verses t should give a linear relationship (Fig. 9). The $q_{\rm e}$ and r^2 values can be derived from the plots. The data values were reported in Table 6.

It was seen that the pseudo-second-order model fit very well and reporting a very high correlation coefficient of 0.9994 with $q_{\rm e}$ 126.35.

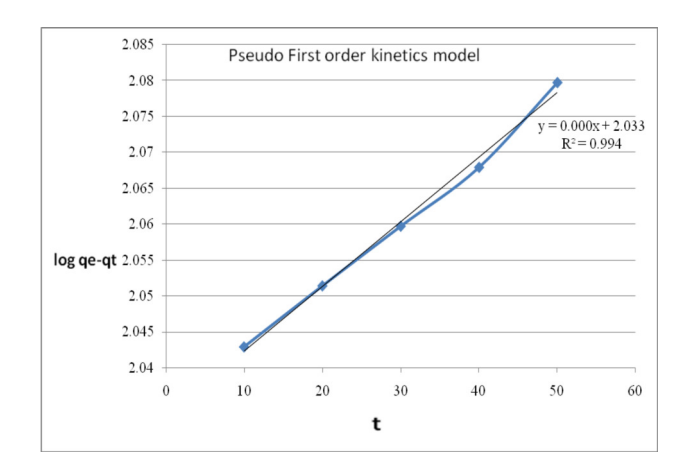


Fig 8: Pseudo first order kinetic model

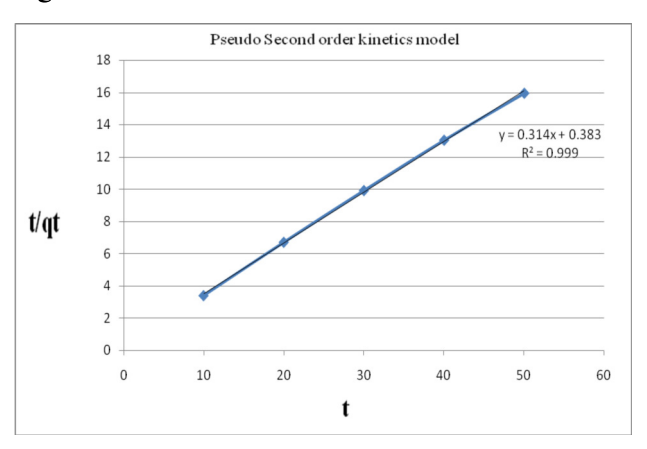


Fig. 9: Pseudo second order kinetic model.

Table 5: Langmuir and Freundlich model parameters

Temperature	Langmuir model			Frei	ındlich model	
30° C	$qm(mg/g)$ $b(L/mg)$ r^2		$Kf (mg^{1-n}g^{-1}L^n)$	$n(mg^{1-n}g^{-1}L^n)$	\mathbf{r}^2	
	17.59	0.0185	0.9924	2.5379	1.0348	0.9719

Table: 6 Pseudo-first-order and second order kinetic parameters

Pseudo-first-order			Pso	eudo-second	l-order
$q_e(mg/g)$			$q_e(mg/g)$		
Theo.	Exp.	\mathbf{r}^2	Theo.	Exp.	\mathbf{r}^2
91.08	122.33	0.9943	111.17	126.35	0.9994

3.7.SEM Analysis

Morphological characters of the biosorbent can be analyzed by Scanning Electron Microscope (SEM) studies. It provides useful information about biosorbent. The SEM image of the raw LPSP biosorbent appears as the rough and uneven surface. This rough surface

character must be considered as a reason for binding of BBR dye molecules. After the BBR dye loaded on LPSP biosorbent, the SEM image is considerable changes were observed in the structure of the biosorbent. The biosorbent appears as irregular surface and pores includes novel shiny particles after the adsorption process.

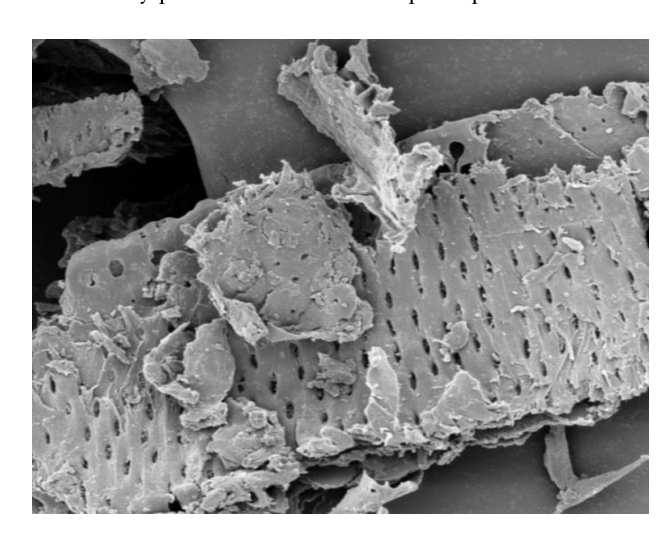


Fig. 10: SEM images of Raw LPSP and BBR dye Loaded LPSP

3.8. FTIR of LPSP

The FTIR study provides the change in functional groups of biosorbent LPSP, spectra of the LPSP before and after the BBR dye adsorption shows in the figure 11a and 11b.

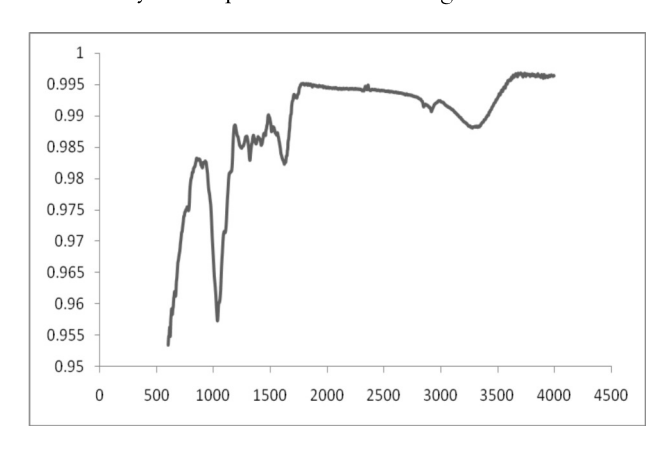


Fig. 11a: FTIR spectra of unloaded LPSP

FTIR spectrum of native biosorbent revealed a number of absorption peaks with the range of 600-4000 cm⁻¹, which is only a sign of the complex chemical nature of this biosorbent. The aromatic compounds of the dye molecule showed characteristic absorption peaks at 2995 cm⁻¹ due to aromatic OH stretching. The absorption band at 1998 cm⁻¹ was due to CH stretching of alkyl group.

The absorption band at 3455 cm⁻¹ was due to NH stretching of amino group of dye molecule. The peaks appear at 1590 cm⁻¹, 1480 cm⁻¹ was due to C-N-C stretching. The absorption spectrum of biosorbent treated with dye solution showed evident changes with respect to that of native biosorbent. Amongst these changes were the broadening of the absorption bands between 3455 and 1480 cm⁻¹ which suggests the superposition of numerous peaks that appeared in these regions. The band at 1480 cm⁻¹ and 3455 cm⁻¹ were due to the biosorbent binding with BBR dye molecule.

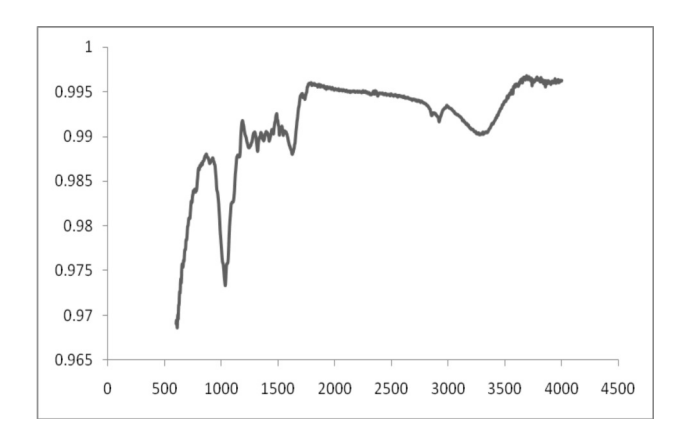


Fig.11b: FTIR spectra of loaded LPSP

4. CONCLUSION

The results observed that the biosorbent received from locally home garden as costless material, Laplap purpureus plant stem powder (LPSP) have deserved in adsorption ability with respect to the removal of Bismark Brown R dye in the form of its aqueous solution. The conclusion made from the present studies shows that LPSP is an apt material for dye adsorption. pH, Adsorbent dose, Equilibrium time and Initial dye concentration are more favorable for the dye removal efficiency of the adsorbent. It was concluded that the sorption process is pH dependent and the upper limit adsorption capacity of BBR dye is at pH 8. The optimal dose weight was 300 mg. The best possible time was noted to be 50 min. and with 77.44% BBR dye removal efficiency. Present result shows that Langmuir model is better fit than Freundlich model for the adsorption equilibrium data. In the examined concentration range 50 to 250 mg/L, the results also reveals that, it follows pseudo second order than pseudo first order kinetic model. SEM and FT-IR spectral characterization clearly reveals that the adsorption of BBR dye onto biosorbent LPSP. Therefore, LPSP can be utilized for removal of BBR dye in the form of aqueous solution.

5. ACKNOWLEDGEMENT

The authors are thankful to the Secretary and Correspondent of A.V.V.M. Sir Pushpam College (Autonomous), Poondi-613 503 and Khadir Mohideen College, Adirampattinam, Thanjavur (Dt), Tamil Nadu, India, for encouragement to do this study.

6. REFERENCES

- Yesilada O, Asma D, Cing S. Process Biochem, 2003; 38:933-938.
- 2. Yasemin B, Haluk A. Desalination, 2006; **194**:259-267.
- 3. Wang S, Zhu ZH. Dyes and Pigments, 2007; 75:306-314
- 4. Santhi T, Manonmani S. *Bioresources.com*, 2010; **5(1)**:419-437.
- 5. Farooq U, Kozinski JA, Khan MA, Athar M. *Biores*. *Technol*, 2010; **101**:5043-5053.
- 6. Kushwaha AK, Gupta N, Chattopadhyaya MC. *Journal of Soudi Chemical Society*, 2014; **18**:200-207.

- 7. Selvakumar A, Rangabhashiyam S. *Environmental Pollution*, 2019; **255**:113291.
- 8. Gupta N, Kushwaha AK, Chattopadhyaya MC. *Arabian Journal of Chemistry*, 2016; **9**:S707-S716.
- 9. Warda Hassan, Umar Farooq, Muhammad Ahmad, Makshood Athar, Misbahul Ain Khan. *Arabian Journal of Chemistry*, 2017; **10**:S1512-S1522.
- 10. Smitha T, Santhi T, Ashly Leena Prasad, Manonmani S. *Arabian Journal of Chemistry*, 2017; **10**:S244-S251.
- 11. Etim UJ, Umoren SA, Eduok UM. *Journal of Saudi Chemical Society*, 2016; **20**:S67-S76.
- 12. Sartape AS, Mandhare AM, Jadhav VV, Raut PD, Anuse MA, Kolekar SS. *Arabian Journal of Chemistry*, 2017; **10**:S3229-S3238.
- 13. Muhammad Khairud Dahri, Muhammad Raziq Rahimi Kooh, Linda BLLim. *ISNR Environmental Chemistry*, 2013; 1-8.
- 14. Somasekhara Reddy MC, Nirmala V. *Arabian Journal of Chemistry*, 2014; **10**:S2406-S2416.
- 15. Sushmita Banerjee, Chattopadhyaya MC. *Arabian Journal of Chemistry*, 2017; **10**:S1629-S1638.
- 16. Verma VK, Mishra AK. *Global NEST Journal*, 2010; **12 (2)**:PP190-196.
- 17. Ahmed M, Kamil, Firas H, Abdulrazak, Ahmed F, Halbus and Falah H. Hussein. *Journal of Environment Analytical Chemistry*, 2014; 1:1.
- 18. Lagergren S, Svenska BK. Vetenskapsakademiens. Handlinger, 1982; **24:1**:1898.
- 19. Ho YS. Scientometrics, 2004; **59(1)**:171-177.
- 20. Maurya NS, Mittal AK, Cornel P. *Biores. Technol*, 2006; **97**:512-521.
- 21. Iqbal MJ AM N. Journal of Hazard. Mater, 2007; **B139**:57-66.
- 22. Ponnusami V, Gunasekar V, Srivastava SN. *J. Hazard. Mater*, 2009; **169**:119-127.
- 23. Hameed BH. J. Hazard. Mater, 2008; 154:204-212.
- 24. SenthilKumar P, Ramalingam S, Senthamarai C, Niranjanaa M, Vijayalakshmi P, Sivanesan, S. *Desalination*, 2010; **261**:52-60.
- 25. Ahmad A, Rafatulla M, Ibrahim MH, Hashim R. J. *Hazard. Mater*, 2009; **170**:357.
- 26. Salleh MAM, Mohmoud DK, Karim WA, Idris A. *Desalination*, 2011; **280**:1-13.
- 27. Kannan N, Sundaram MM. *Dyes and Pigments*, 2001; **51**:25-40.



Journal of Advanced Scientific Research

ISSN
0976-9595
Research Article

Available online through http://www.sciensage.info

REMOVAL OF CHROMIUM (VI) IONS FROM AQUEOUS SOLUTION BY USING LAPLAP PURPUREUS (DOLICHOS BEAN) PLANT STEMS AS BIOSORBENT

G. Bharathidasan*1, G. Vishnuvardhanaraj1, K. Mohamed Faizal2, N. Mani1, D. Tamilvendan3

¹PG and Research Department of Chemistry, A.V.V.M. Sri Pushpam College (Autonomous), (Affiliated to Bharathidasan University),
Poondi, Thanjavur (Dt), Tamil Nadu, India

²PG and Research Department of Chemistry, Khadir Mohideen College, (Affiliated to Bharathidasan University),
Adirampattinam, Thanjavur (Dt), Tamil Nadu, India

³Department of Chemistry, NIT, Tiruchirappalli, Tamil Nadu, India

*Corresponding author: gpdasangee@gmail.com

ABSTRACT

The main intention of the present work is to explore the removal effectiveness of Cr^{+6} ions from their aqueous solutions by adsorption method using *Laplap purpureus* stem powder (LPSP) as a biosorbent. The most important purpose of research is to analyze the batch mode of adsorption performance such as influences of pH, the dosage of biosorbent, taction time, concentration of Cr^{+6} ions solution, and temperature. The data obtained from the experiment results were studied by means of both Langmuir and Freundlich adsorption isotherm models. The pseudo-first-order and pseudo-second-order models have been analyzed to examine the kinetic models of adsorption. The adsorption isotherm models and kinetic study of analysis were divulged that an adsorption method was most favored for the Langmuir isotherm model. This investigation exhibits that the pseudo-second-order model plays an important responsibility in the adsorption mechanism to remove Cr^{+6} ions. The biosorbent (LPSP) has better adsorption ability and also the removal of competence for Cr^{+6} ions from its aqueous solution.

Keywords: Adsorption, Biosorbent, Laplap purpureus stem powder (LPSP), Kinetics, Langmuir, Freundlich.

1. INTRODUCTION

Environmental pollution arises due to rapid increasing of industries, which leads to deposition of excessive heavy metal on the earth surface [1]. Heavy metal stress is a most important concern against to all living things and major sources of heavy metal pollution derive from mining, smelting and other chemical industries [2, 3]. Especially, Chromium has been used enormously in various industries like textiles, metal finishing work, electroplating technique, leather tanning, production of stainless steel, preparation of chromate, dyes making for plastics, wood and manufacturing of paint, pigments and chemicals [4]. Chromium is one of the heavy metals in the top 16 metals that have ruinous effects on human beings [5]. Chromium metal exists in the form of its trivalent (Cr⁺³) or hexavalent (Cr⁺⁶) in the environment. The species of Chromium metal act as highly toxic in the biological system like carcinogen, teratogen and mutagen [6, 7]. Especially, the oxidation state of Chromium⁺⁶ has more poisonous character than Chromium⁺³ to human health [8]. The hexavalant Chromium is almost quite

soluble in water over the entire range of pH, hence it easily contaminates the environment [9]. It causes liver damage, edemas, pulmonary congestion, skin allergies and cancer on human beings by prolonged exposure of Chromium metal species, but the recommended limits of chromium in potable water is 0.05 mg/L [10]. Even though, Chromium (III) metal is needed 50-200 mg per day to the human body for the utilization of fat, protein and sugar [11]. Therefore, the removal of harmful heavy metal chromium from industrial waste is a significant one in the world to guard our surroundings. An Ordinary technique like chemical precipitation, reduction, ion exchange, evaporation, membrane process and adsorption are applied for the elimination of hazardous heavy metals from industrial effluents. Particularly, the adsorption process proposes preferable uses such as low operational cost, minimizing the chemical apply or biological sludge, high rate of removal performance to heavy metals from metal aqueous solutions, retrieval of biosorbents, the possibility of metal regeneration and eco friendly [12]. The mechanism of surface sorption is mainly dependent upon physiochemical interactions in between metals and the surface of biosorbent and they are active appreciably more than assumed in equilibrium models [13]. The physicochemical phenomenon during the adsorption process is rapid and reversible [14]. As a final point, the adsorption method is proficient to removal of heavy metal from its metal aqueous solutions by preparation of low-cost and eco-friendly bio-sorbent. In recent years most of the researchers had studied a variety of bio-adsorbents. In the present work, the adsorption of Cr⁺⁶ ions from its aqueous solution with the biosorbent prepared from Laplap purpureus plant stems powder (LPSP) was studied. The adsorption kinetic models and the equilibrium data were obtained by adsorption experiments and it was used to analyze the biosorbent sample. Consequently, the percentage of adsorption and quantities of adsorption to Cr⁺⁶ was calculated by using LPSP from the aqueous solution of chromium. The basic kinetic models like pseudo-first-order and pseudo-second-order models have been studied to exhibit the adsorption efficiency of Cr⁺⁶ ions in the adsorption process by using LPSP as a biosorbent.

2. MATERIAL AND METHODS

2.1. Adsorbent

The Laplap purpureus (Dolichos Bean) stems were obtained in the home garden after the harvest of bean fruits at Sevvaypatti village in Pudukkottai district, Tamil Nadu, India. The stems were cut into tiny pieces and systematically washed with tap water to remove unwanted dirt impurities and subsequently washed with distilled water and then dried in direct sunlight only for five days. After that, the stem pieces were ground as very fine powder using a domestic grinder and then stem powder was screened by manual experimental (Jayant Test Sieves) sieves in the size of $< 90 \mu m$. These separated Laplap purpureus stem powdered (LPSP) particles were stockpiled in a good-quality, conditioned air-tight plastic bottle for further use in biosorption studies [15]. There was no other chemical treatment for making adsorbent.

2.2. Batch adsorption studies

The effects of various parameters were studied for the removal of Cr⁺⁶ ions by *Laplap purpureus* stem Powder (LPSP). The AR grade of chemicals were used for experimental analysis at a high range of purity. The stock solution of the adsorbate consists of 1000 mg/L of Cr⁺⁶ metal ions solution prepared by dissolving the measured

quantity of K₂Cr₂O₇ in double-distilled water. The investigational stock solution was diluted for the required initial concentration. In each adsorption experiment, 50 ml of Cr⁺⁶ ion solution with a well-known concentration was an addition to 200 mg of Laplap purpureus stem powder (LPSP) in a 250 ml of stopper flask, the adsorption experimental procedure was conducted at 35°C, then the combination was stirred for 50 minutes in a mechanical shaker at pH 3. The pH values were altered with 1N HCl and in 1N NaOH solution. The samples were withdrawn from the mechanical shaker at the proper time period and then adsorbent was separated by filtration with the help of No.40 Whatman filter paper. The concentration of Cr+6 metal ion solutions was investigated before and after treatment of the experiment by a UV-visible Spectrophotometer (Systronics PC-based double beam Spectrophotometer 2202).

3. RESULTS AND DISCUSSION

3.1. Effects of pH on Chromium (VI) ion adsorption

The effect of pH was studied by varying the pH of the solution (2, 3, 4, 5, 6, 7, 8, 9 and 10), initial concentration of Cr⁺⁶ metal ion solution 150 (ppm), taction time 50 minutes, temperature 35°C, adsorbent dose 200 mg, 50 ml of Cr⁺⁶ solution and agitation speed 360 rpm. The results shown in fig.1 indicated that at lower pH 3 maximum (60.59%) removal occurred. Hence, at higher pH 10 percentage of Cr⁺⁶ slightly decreased to 59.27%. This may be owing to the surface of biosorbent covered with various functional groups containing hydroxyl and alkyl groups with the increasing pH. The availability of functional group concentration increases which competes with Cr⁺⁶. Therefore, the percentage removal of Cr⁺⁶ slightly decreases at higher pH [16, 17].

3.2. Effects of LPSP dose on Chromium (VI) ions adsorption

The adsorption of Cr^{+6} onto LPSP was studied by varying the adsorbent dosage (50, 100, 150, 200, 250 and 300 mg), initial concentration of Cr^{+6} metal ion solution 150 (ppm), temperature 35°C, taction time 50 minutes, 50 ml of Cr^{+6} metal solution, agitation speed 360 rpm and pH 3. Figure-2 exhibits the retention of Cr^{+6} ions against the dosage of biosorbent as shown in the graph, the adsorbent dosage increases while the adsorption of Cr^{+6} ions increases and then a certain value is reached. After a certain dose, the adsorption remained constant significantly and the stability of Cr^{+6} on the biosorbent

was attained at an adsorbent dose of 200 mg. At equilibrium, the removal percentage of Cr^{+6} became constant due to the saturation of the available adsorbent site on the biosorbent [18].

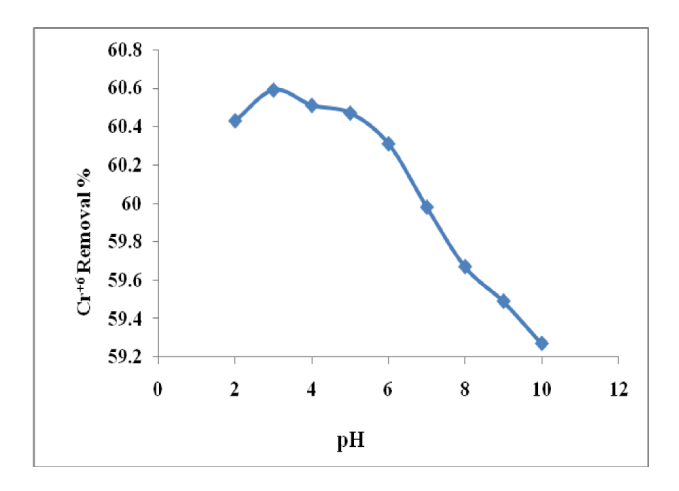


Fig. 1: Effects of pH on Chromium (VI) ion adsorption

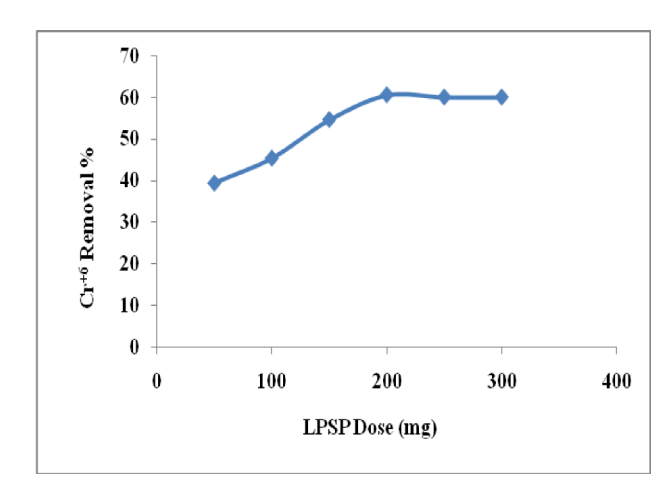


Fig. 2: Effects of LPSP dose on Chromium⁺⁶ ions adsorption

3.3. Effects of taction time on Chromium (VI) ions adsorption

The experimental study of taction time is one of the main factors to fix time for analyzes the various parameters. In this parameter, taction time varied like 10, 20, 30, 40, 50, 60, 70 and 80 minutes, Temperature 35°C, pH 3, adsorbent dose 200 mg, initial concentration of Cr⁺⁶ ion solution 150 (ppm), 50 ml of Cr⁺⁶ solution and agitation speed 360 rpm were kept constant. Figure-3 represented that the biosorbtion efficiency increased with increases in taction time from 10 to 80 min. Maximum removal

percentage for Cr⁺⁶ ions was achieved up to 50 min after that did not change until 80 min. It may be due to that the large number of surface area available on biosorbent in initial stage, there after it slowed down later, because of the exhaustion of leftover surface area and repulsive forces between the bulk phase and the solute molecules [19].

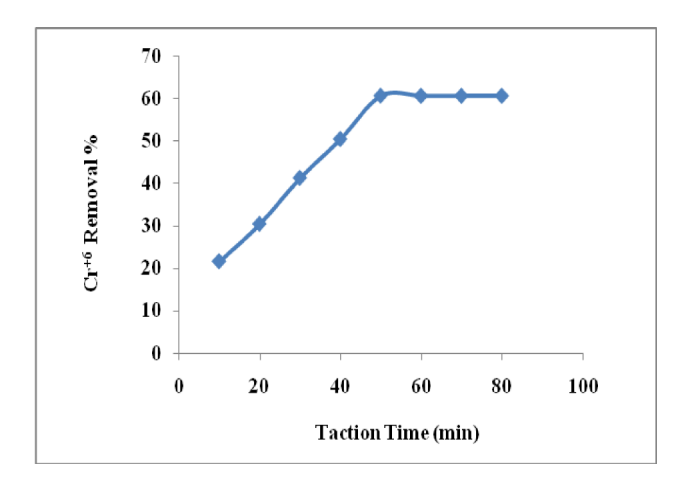


Fig. 3: Effects of taction time on Chromium (VI) ions adsorption

3.4. Effects of various Concentrations or Chromium (VI) ions adsorption

Concentration of the metal ion is an important factor in the adsorption process. In this parameter, the initial concentration varied likes as 150, 200, 250, 300 and 350 ppm and other parameters such as temperature 35°C, pH 3, agitation speed 360 rpm, time 50 minutes and 200 gm of adsorbent dose were kept constant. The removal efficiency of the initial Cr+6 ions concentration was obtained from the experimental data which are represented in Fig.4. The maximum removal was possible in 150 ppm which clearly exhibit that the removal efficiency decreases with increasing initial concentration of Cr⁺⁶ ion solution. It may be due to immediate saturation of limited obtainable biosorbent sites at higher concentration and the other hand at a lower concentration of Cr⁺⁶ the removal efficiency achieved maximum due to the ratio of available surface sites of biosorbent to the number of moles of Cr⁺⁶ ions [20].

3.5. Effects of temperature on Chromium (VI) ions adsorption

Temperature is a great impact factor in the adsorption process. In this experiment, temperatures changed from

20 to 45°C, initial concentration of Cr^{+6} ion 150 (ppm), under pH 3, agitation speed 360 rpm, taction time 50 minutes and 200 gm of adsorbent dose. In several adsorption experiments, the percentage of removal efficiency increases as the temperature increases. The changes in removal efficiency of LPSP adsorption for Cr^{+6} as a function of temperature is shows in Fig. 5.

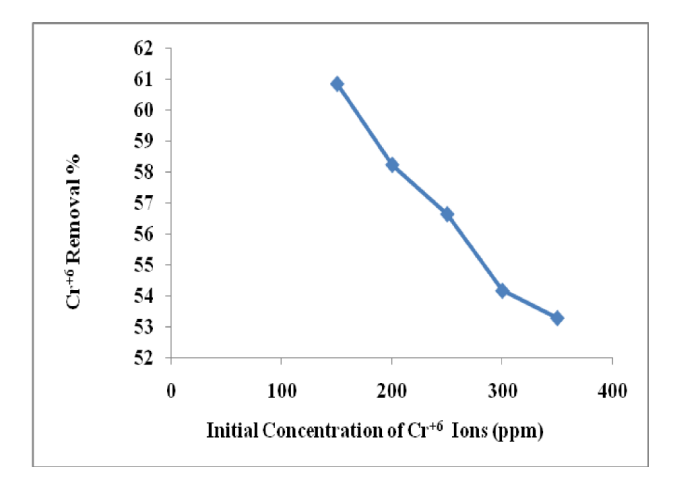


Fig. 4: Effects of various Concentrations on Chromium (VI) ions adsorption

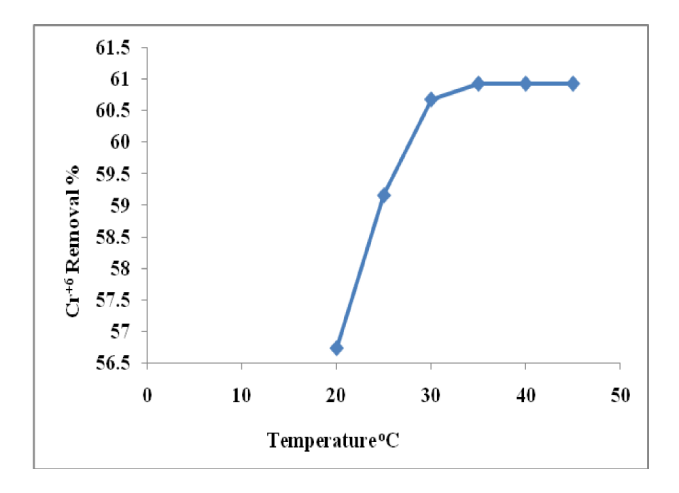


Fig. 5: Effects of Temperature on Chromium (VI) ions adsorption

Just as in the previous reports, the Cr^{+6} metal ions removal efficiency is slowly improved with the increased temperature of adsorption. However, the changes of temperature had small effect on LPSP adsorption Cr^{+6} . The percentage removal efficiency was increased only by 4.19% while temperatures changed from 20 to 45°C. Cr^{+6} mobility increases at higher temperatures which leads to penetration of the harmful substances into the

internal voids of LPSP particles. Thus, the removal efficiency was progressed with increasing the adsorption temperature. However, by further increase in temperature, the presence of inside vacant site pores was almost packed and thereafter the removal efficiency remains stable. The optimization process of the temperature effect was informed to us that continuance increases of the temperature do not bring any important changes in the process of adsorption [21].

3.6. Adsorption Isotherm Models

The adsorption isotherm specifies that how adsorbate molecules partitioned between adsorbent and liquid phase at equilibrium as a role of adsorbate concentration. In this learning, equilibrium studies were carried out to understand the character of the adsorbent of Cr⁺⁶ onto LPSP at equilibrium conditions by considering Langmuir and Freundlich adsorption isotherm models.

3.6.1. Langmuir isotherm model

The Langmuir isotherm model studied about saturated monolayer formation for solute on the surface of the adsorbent in adsorption process [22]. The linear form of Langmuir isotherm model used in the term

$$C_e/q_e = 1/q_m K_L + C_e/q_m$$

 $C_{\rm e}$ = Equilibrium constant for metal ions (mg / L), $q_{\rm e}$ = Amount of metal ions adsorbed at equilibrium (mg/g), $q_{\rm m}$ = Constant related to maximum adsorption capacity (mg/g), K_L = Langmuir constant related to energy of adsorption.

The equation for the linear plot of C_e / q_e against C_e should be a straight line. It shows that adsorption obeys the Langmuir isotherm model. The constant q_m can be derived from slope and intercept of the plot and the values are shown in table 1 and fig.6. It demonstrates that the Langmuir isotherm model fitted well for the chosen biosorbent and adsorbate system with respect to r^2 = 0.972. Furthermore, q_m of the LPSP is 91.24 (mg/g) was compared with the previous studies and q_m values were represented in table 2.

The important characteristics of a Langmuir isotherm can be explained in terms of a dimensionless separation factor, R_L [23], which is defined by the following equation:

$$R_L = 1 / 1 + (q_{max} \times K_L)C_o$$

Where C_o is the highest initial concentration and the value of separation factor, R_L represents the type of isotherm and nature of the adsorption process. Recognizing the R_L values as the adsorption can be unfavorable ($R_L > 1$); linear ($R_L = 1$); favorable ($0 < R_L < 1$)

or irreversible (R_L =0) [24]. Hence, as the R_L value nearer to zero, the adsorption will be done better. In this experimental study, the R_L value 0.1976 (Table 1) favourable adsorption.

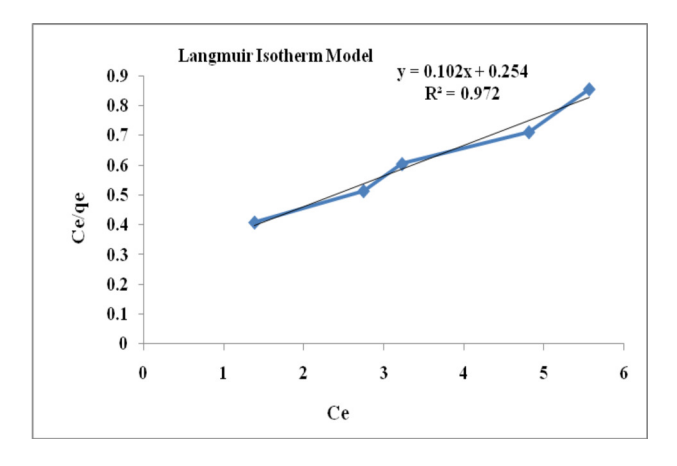


Fig. 6: Langmuir adsorption Isotherm Model

3.6.2. Freundlich Isotherm

The metal ions distribution between the liquid and solid phases can be illustrated by Freundlich isotherm model [25]. It best describes the adsorption onto heterogeneous surface. The common equation for the Freundlich isotherm model is represented as

$$\log q_e = \log k_f + 1/n \log C_e$$

Where, q_e = Amount of Cr^{+6} ions adsorbed on per unit weight of biosorbent (mg/g), K_f = Freundlich constant, which is correlated to calculate of adsorption capacity (mg/g). 1/n = Sorption intensity (mg/L) and C_e = Equilibrium concentration (mg/L). Linear plots of log q_e against log C_e . The values of K_f and 1/n can be derived from the intercept and slope respectively and their values

are exhibited in table 1. When 1/n lies in between 1 to 10 values, the linearity of Freundlich plot suggests the favorable adorption for Cr^{+6} on the biosorbent surface. These parameters have been determined from a plot $logq_e\ v_s\ logC_e\ (Fig.7)$. Thus the values of K_f and n were found as 4.1836 and 1.532 respectively at 35°C with r^2 of 0.965.

The Langmuir adsorption isotherm exhibited that it has fitted well due to high r^2 (r^2 =0.972) value compared with Freundlich adsorption isotherm model. The results stated that the nature of adsorption was a monolayer, which means a formation of Cr^{+6} molecules in single layer on the LPSP adsorbent surface [26]. It was suggesting that the equilibrium adsorption of Cr^{+6} onto LPSP might be best demonstrated with the Langmuir isotherm, because of the correlation between experimental and calculated values along with regression factors are in good agreement with Langmuir isotherm, it was exhibited that Cr^{+6} was most favorably adsorbed by LPSP.

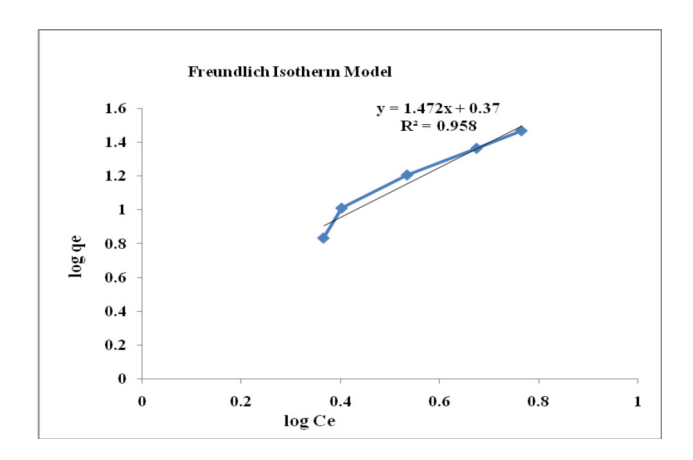


Fig. 7: Freudlich adsorption Isotherm Model

Table 1: Langmuir and Freundlich model parameters

C_{i}	Langmuir Model			Freundlich Model			
150	Temp °C	$q_m(mg/g)$	$R_L (L/mg)$	\mathbf{r}^2	$K_f(mg^{1-n}g^{-1}L^n)$	n (mg ¹⁻ⁿ g ⁻¹ L ⁿ)	\mathbf{r}^2
130	35°C	91.24	0.1976	0.972	4.1836	1.532	0.965

Table 2: Comparative study of adsorbent capacity in Langmuir constant q_{max} (mg/g) of various biosorbent

Adsorbent	Adsorbent capacity (mg/g)	[Reference]
Saw dust	20.70	[27]
S. quadricuada	12.00	[28]
Ficus auriculate leaves powder	13.33	[29]
Banana peel	10.42	[30]
Moringa stenopetala seed powder	09.70	[31]
Trametes versicolor polyporus	45.10	[32]
Sargassum dentifolium	41.20	[33]
Rhizopus sp.	09.95	[34]
Gooseberry seed	19.23	[35]
Laplap purpureusstem powder	91.24	This study

3.7. Kinetic Study

The Kinetics of adsorption studies have been carried out to illustrate adsorption mechanism and diffusion. The generated data had tested by Pseudo first order and Pseudo second order kinetics equation in order to determine the rate of the chromium ion adsorption on the LPSP, which controls the equilibrium time.

3.7.1. The Pseudo first-order model

The possibility of adsorption data obtained from Legergren pseudo first-order rate of equation can be described by the following equation:

$$dq_t/d_t = k_1(q_e - q_t)$$

Where, k_1 is the rate constant for first order adsorption $(g.mg^{-1}.mn^{-1})$, q_e is Cr^{+6} adsorbed at equilibrium per unit mass of the sorbent (mg/g), q_t is Cr^{+6} adsorbed (mg/g). The combined form of above equation becomes $\log (q_e - q_t) = \log(q_e) - (k_{1/2.303})t$

Fig. 8 represents a plot log $(q_e - q_t)$ verses (t) represents a straight line of slope $(k_{1/2.303})$ and an intercept of log (q_e) [36].

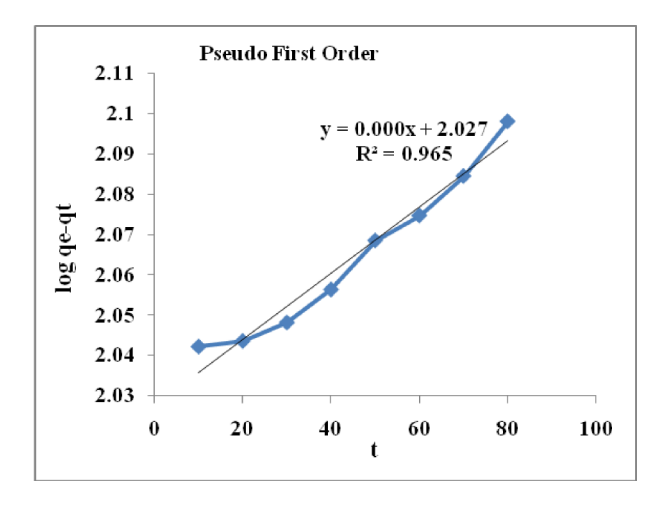


Fig. 8: Pseudo First Order Kinetic Model

3.7.2. The Pseudo second-order model

This adsorption kinetic model equation developed as pseudo second-order rate of equation representation is based on the sorption capacity of solid phase is commonly expressed as:

$$dq_t/d_t = k_2(q_e-q_t)^2$$

Where, k₂ is the rate constant for pseudo second order adsorption (g.mg⁻¹.min⁻¹), For the same boundary condition the integrated form of above equation becomes

$$t/q_t = 1/k_2 q_e^2 + 1/q_e(t)$$

where, the k_2 can be calculated by the slope and intercept of the plots of (t/q_t) versus time (t) (fig. 9). The pseudo second-order adsorption capacity (q_e) values and correlation coefficient (r^2) values are represented in table 3. The reasonable degree of conformity between the calculated data values and experimental data values have been found in the pseudo-first-order model compared with pseudo-second-order model. The correlation coefficient (r^2) for the adsorption of Cr^{+6} was found to be very high $(r^2=0.986)$ in pseudo-second-order model with q_e 46.56. This value represents that, the adsorption capacities (q_e) is nearer to the calculated adsorption capacity, hence the pseudo-second-order model obeys the sorption of Cr^{+6} ions on biosorbent (LPSP).

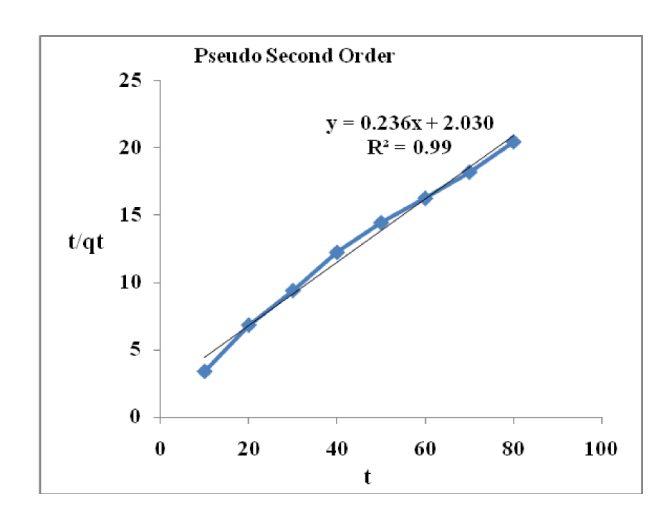


Fig. 9: Pseudo Second Order Kinetic Model

3.8. FT-IR spectrum

The FTIR spectrum analysis provides information about the changes in functional groups on biosorbent (LPSP), the spectra of LPSP before and after the Cr⁺⁶ metal ions adsorption are represented in the fig. 10 and 11. The FTIR spectrum of biosorbent displays a number of adsorption peaks range between of 400-4000 cm⁻¹, which clearly shows only a complex of chemical nature for this biosorbent. The band at 3418 cm⁻¹ representing -OH groups, the band at 2918 cm⁻¹ corresponding to C-H stretching, the band around at 1606 cm⁻¹ could be assigned to the C=O stretching, the band at 1518 cm⁻¹ and at 1422 cm⁻¹ indicating as CH₂ bonding vibration, the band at 1034 cm⁻¹ indicating C-O stretching. Amongst these adsorption peaks predominantly bonded -OH groups, C=O stretching and carboxyl groups were involved in Cr⁺⁶ ions biosorption [37, 38].

Table 3: Pseudo-first-order and Pseudo-second-order kinetic parameters

	_	Pseudo first order			Pseudo second order		
$\mathbf{C_i}$	Temp°C	\mathbf{q}_{e}		m ²	\mathbf{q}_{e}		2
	-	Theo.	Exp.	1	Theo.	Exp.	1
150	35°C	43.10	47.14	0.965	45.19	46.56	0.990

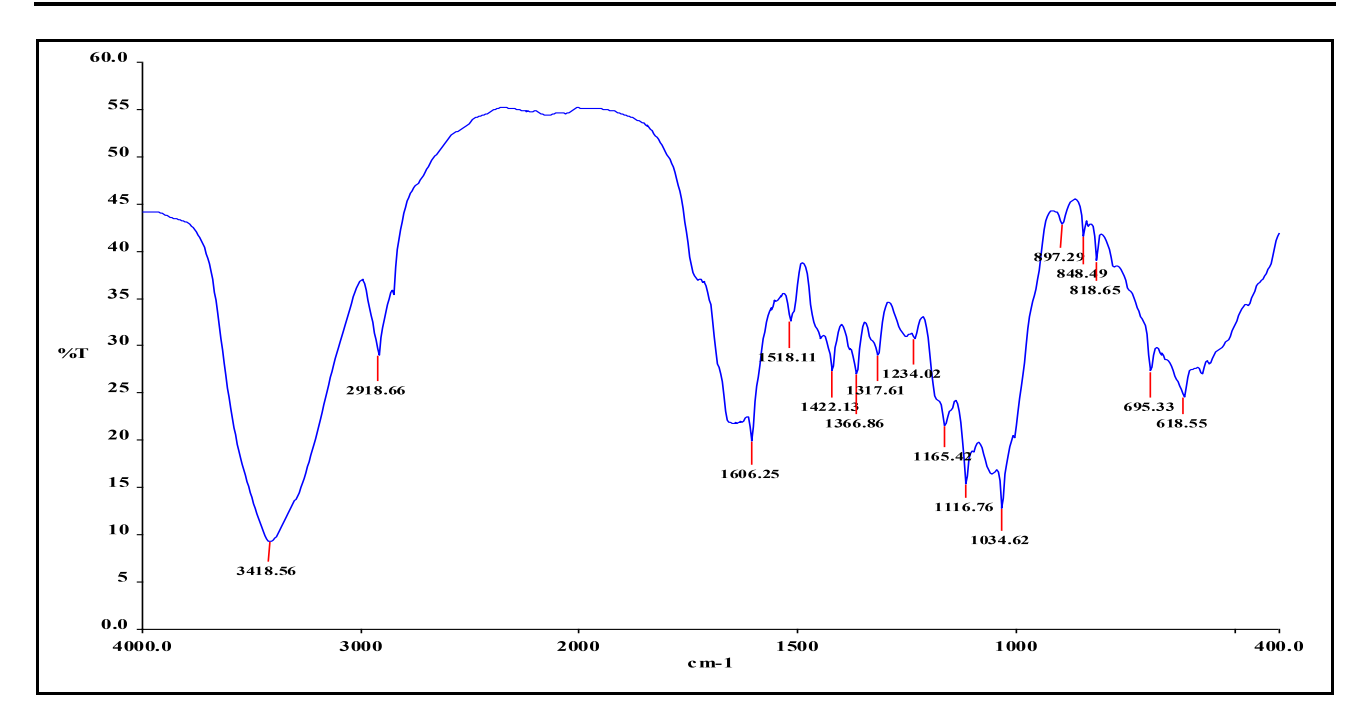


Fig. 10: FTIR spectra of Laplap purpureus stems powder before adsorption

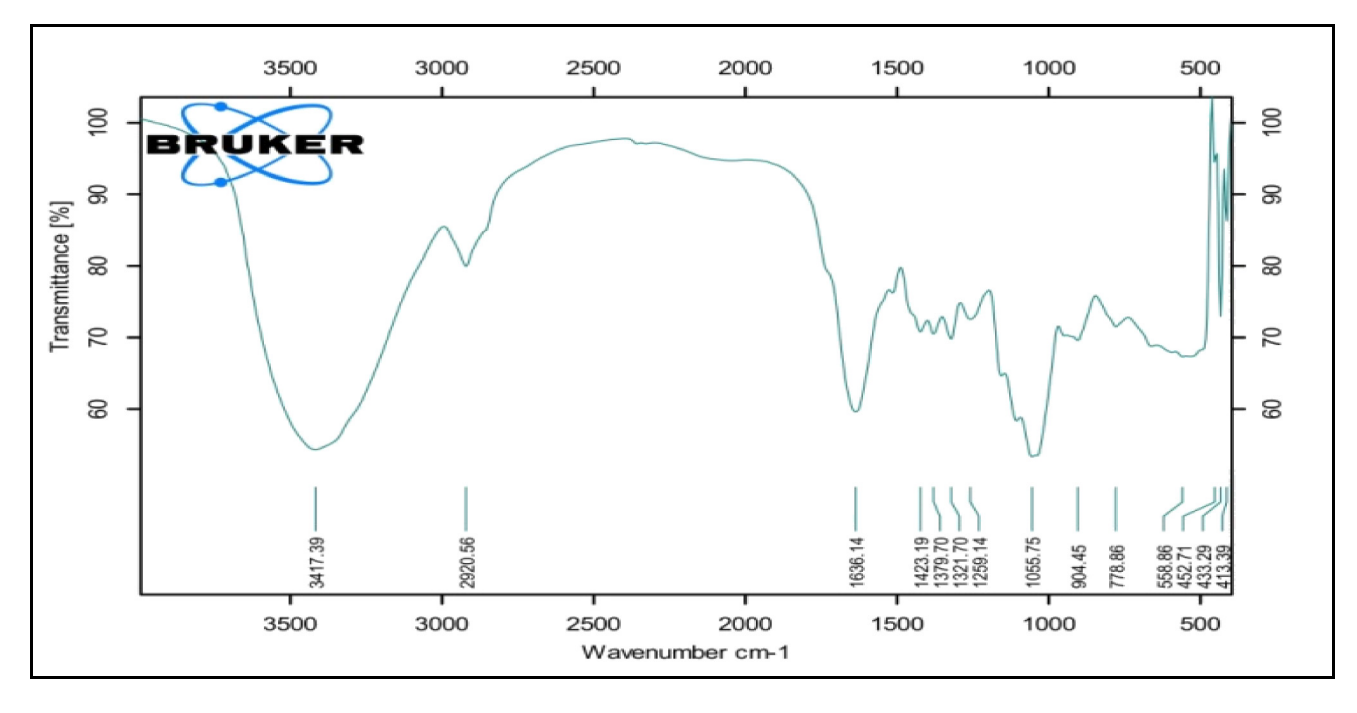


Fig. 11: FTIR spectra of Laplap purpureus stems powder after adsorption

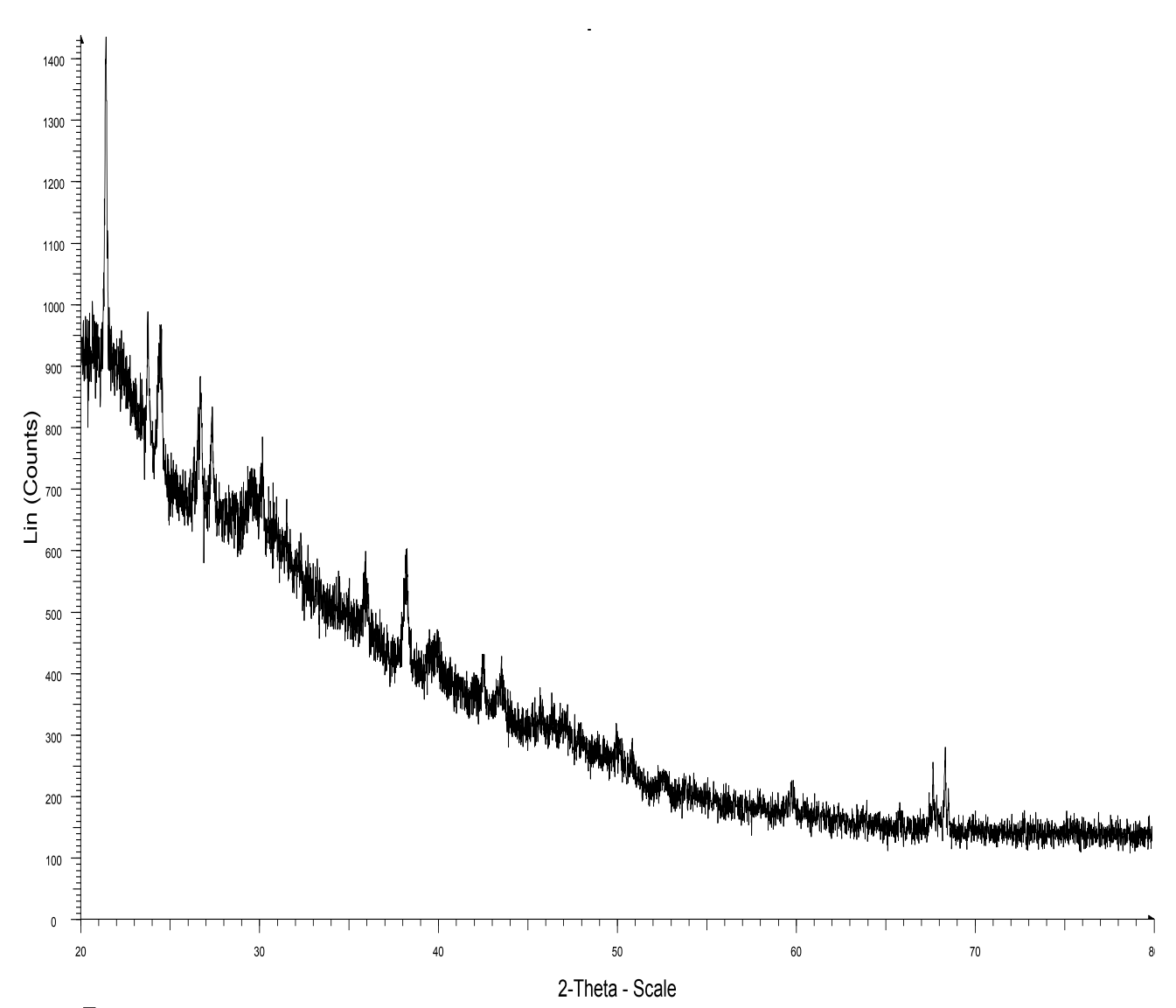
Journal of Advanced Scientific Research, 2021; 12 (3): Aug-2021

3.9. X-Ray Diffraction of LPSP

The X-ray diffraction (XRD) technique is a powerful technique to analyze the crystalline amorphous nature of the adsorbent material. The LPSP before and after adsorption were recorded in Fig.12 (sample 1) and 13 (sample 2) respectively. The intense main peak (Fig.12) shows that the presence of highly organized crystalline nature of raw LPSP. After the adsorption of Cr⁺⁶ metal ions (Fig.13), the intensity of the main peak is slightly diminished and broadens. This is means that the physical adsorption takes place on the upper layer of LPSP crystalline structure after adsorption of Cr⁺⁶ metal ions.

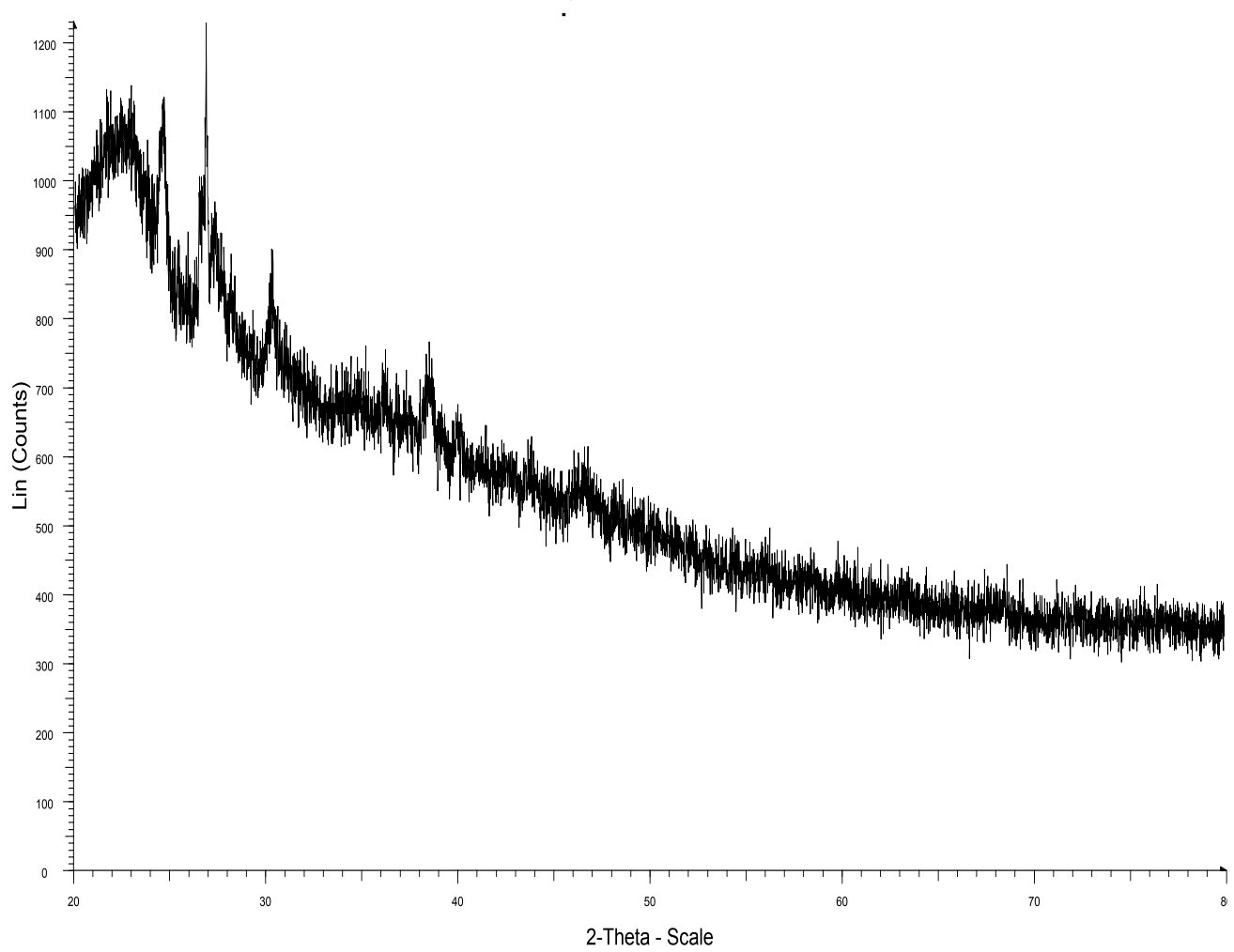
3.10. SEM Analysis for Cr⁺⁶ Ions on Adsorption

Scanning Electron Microscope (SEM) studies provides the information about morphological property of the biosorbent (LPSP). Fig.14 is SEM image of unloaded LPSP material which represents the irregular and rough surface. The Fig.15 is SEM image of Cr⁺⁶ metal ions loaded on biosorbent (LPSP) surface. After the Cr⁺⁶ ions sorption, a significant change is viewed in the surface of biosorbent (LPSP). This property should be mentioned as a reason for sorption of metal ions. The biosorbent appears to have small pores like new cavities due to effective adsorption takes place.



Wample 1 - File: sample 1.raw - Type: 2Th/Th locked - Start: 20.000 ° - End: 80.000 ° - Step: 0.010 ° - Step time: 1. s - Temp.: 25 °C (Room) - Time Started: 15 s - 2-Theta: 20.000 ° - Theta: 10.000 ° - Chi: 0.00 ° - Phi: 0.00 ° - X: 0.00 ° - Theta: 10.000 ° - Chi: 0.00 ° - Chi: 0.00 ° - Chi: 0.00 ° - Chi: 0.00 ° - Phi: 0.00 ° - X: 0.00 ° - Chi: 0.0

Fig. 12: XRD Pattern of Laplap purpureus stems powder before adsorption



Sample 2 sakthi - File: Sample 2 sakthi raw - Type: 2Th/Th locked - Start: 20.000 ° - End: 80.000 ° - Step: 0.010 ° - Step time: 1. s - Temp:: 25 °C (Room) - Time Started: 8 s - 2-Theta: 20.000 ° - Theta: 10.000 ° - Chi: 0.00 ° - Phi: 0 Operations: Import

Fig. 13: XRD patteren of Laplap purpureus stems powder after adsorption

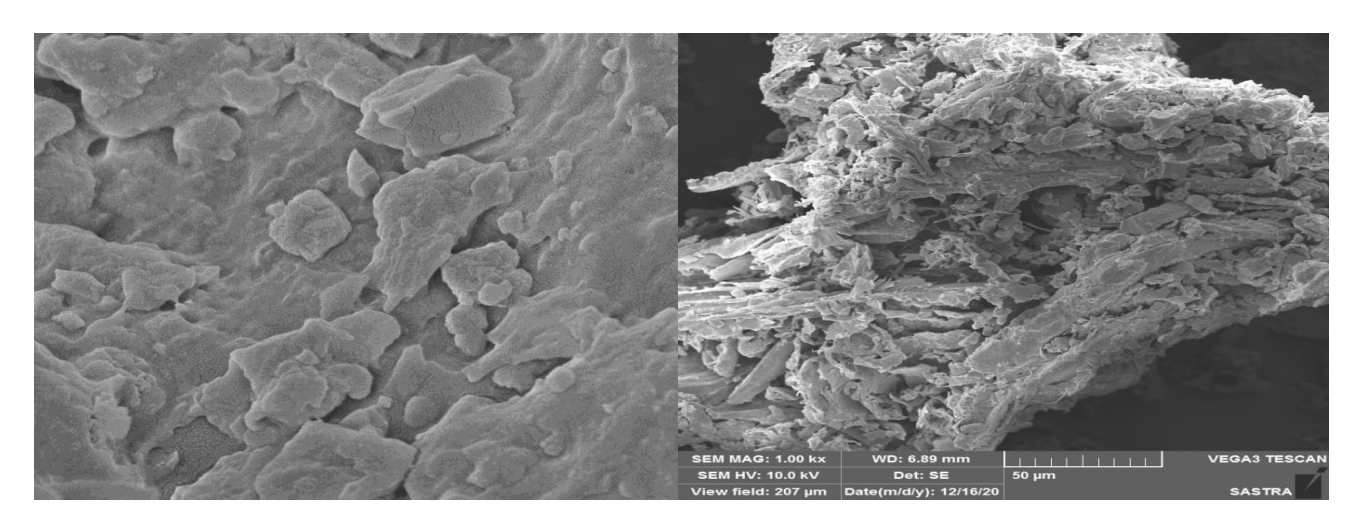


Fig. 14: SEM image before adsorption

Fig. 15: SEM image after adsorption

Journal of Advanced Scientific Research, 2021; 12 (3): Aug-2021

4. CONCLUSION

The results demonstrated that Laplap purpureus stem powder (LPSP) is an efficient biosorbent for the removal of Cr⁺⁶ ions from its aqueous solution. The present study investigated that biosorbent is an essential alternate for the adsorption of Cr⁺⁶ metal ions. The percentage of removal efficiency was dependent upon pH, biosorbent dose, taction time, initial Cr⁺⁶ ions concentration and temperature of the system. It was concluded that the optimum biosorption phenomenon occurred at pH 3, the optimal dose was 200 mg, the suitable taction time was noted to be 50 minutes, reasonably acceptable Cr+6 ion concentration was 150 ppm and the best adsorption temperature was 35°C. The adsorption equilibrium better fitted with Langmuir isotherm model compared with Freudlich isotherm model. The adsorption kinetic process was found to be better fitted with pseudo-second-order model than pseudo-first-order. The SEM, FTIR and XRD spectral analysis clearly exhibited the biosorption of Cr⁺⁶ ions on biosorbent LPSP. Therefore, LPSP may be used as a cheap biosorbent for removal of Cr⁺⁶ metali ons.

5. ACKNOWLEGEMENT

The authors are thankful to the Secretary and Correspondent of A.V.V.M Sri Pushpam College (Autonomous), Poondi-613 503 and Khadir Mohideen College, Adirampattinam, Thanjavur (Dt), Tamil Nadu, India, for encouragement to do this study.

6. REFERENCES

- 1. Bhattacharya A, Gupta A, Kaur A, Malik D. *Water Sci Technol.*, 2019; **79(3)**:411-424.
- Raga Sudha N, Varaprasad D, Manivannan N, Mathivanan N, Veera Bramhachari P, Chandra-sekhar. Journal of Advanced Scientific Research, 2021; 12(2) Suppl 1:206-210.
- 3. Sun C, Li W, Xu Y, Hu N, Ma J, Cao W, et al. *Aquatic Technology*, 2020; **224**: 105504.
- 4. Abdel-Jawad M, Al-Shammari S, Al-Sulaimi J. *Desalination*. 2002; **142(1)**:11-18.
- 5. Wang Q, Song J, Sui M. Energy Pro., 2011; 5:1104-1108.
- 6. Abdel Al-Rub. F, Kandah. M, Aldabaibeh. N. *Eng. Life. Sci.*, 2002; **2**:111-116.
- 7. Karimi M, Shojaei A, Nematollahzadeh A, Abdekhodaie MJ. *Chem. Eng. J.*, 2012; **210**:280-288.
- 8. Samani MR, Borghei SM, Olad A, Chaichi MJ. *J. Hazard. Mater.*, 2010; **184**:248-254.
- Gode F, Pehlvan E. J. Hazard. Mater., 2005; B119: 175-182.

- 10. Raji C, Anirudhan TS. Water Res., 1998; **32(12)**: 3772-3780.
- 11. Lazaridis NK, Asouhidou DD. *Water Res.*, 2003; **37**:2875-2882.
- Ahluwalia SS, Goyal D. Bioresour. Technol., 2007; 98:2243-2257.
- 13. Flouty R, Estephane G. J. Environ. Manage, 2012; 111:106-114.
- 14. Darnall DW, Greene B, Hosea M, McPherson RA, Henzl M, Alexander MD, In: Thompson, R. (Ed.), Litho Ltd. Whitstable, Kent, 1986; PP. 1-24.
- 15. Akbar Esmaeili, Betsabe Saremnia, Mona Kalantari. *Arabian Journal of Chemistry*, 2015; **8**:506-511.
- Samuel MS, Shah S, Subramaniyan V, Qureshi T, Bhattacharya J, Pradeep Singh ND. Int. J. Biol Macromol., 2018; 119:540-547.
- 17. Parlayici S, Eskizeybek V, Avci A, Pehlivan E. *J. Nanostuct. Chem.*, 2015; **5**:255-263.
- 18. Khan TA, Nazir M, Ali I, Kumar A. Arab. J. Chem., 2017; **10**:2388-2398.
- 19. Saravanane R, Sundararajan T, Sivamurthyreddy S. *Indian. J. Env Health.*, 2002; 44:78-81.
- 20. Dehghani MH, Mohammadtaher M, Bajpai AK, Heibati B, Tyagi I, Asif M, et al. *Chem. Eng J.*, 2015; 279:344-352.
- 21. Akltas D, Dizge N, Yatmaz HC, Caliskan Y, Ozay Y, Caputcu A. *Water Sci. Technol.*, 2017; **76**:3114-3125.
- 22. Langmuir I, J. Am. Soc., 1918; 30.579:1361-1403.
- 23. Samarghandi MR, Hadi M, Moayedi S, Askari FB. *Ira J. Environ Health Science Eng.*, 2009; **6**:285-294.
- 24. Qada ENE, Allen SJ, Walker GM. Chem. Eng. J., 2006; **124**:103-110.
- 25. Freundlich. Z Phys. Chem., 1906; 57:385-470.
- 26. Saadi R, et al. Korean Journal of Chemical Engineering, 2015; 32(5):787-799.
- 27. Memon JR, Memon SQ, Bhanger MI, El-Turki A, Hallam KR, Allen GC. *Colloid Surf.*, 2009; **B 70**: 232-237.
- 28. Kannan P, Alemayehu NW, Mike A, Acheampong HJ, Lubberding Piet Lens NL. *Appl. Biochem. Biotechnol.*, 2013; **170**:498-513.
- Rengabhashiyam S, Selvaraje N. J. Mol. Liq., 2015;
 207:39-49.
- 30. Serife Parlayici, Erol Pehlivan. *Journal of Analytical Science and Technology*. 2019; **10:15**.
- 31. Tolera Seda Badessa, Esayas Wakuma, Ali Mohammed Yimer. *BMC Chemistry*. 2020; **14:71**. https://doi.org/10.1186/s13065-020-00724-z
- 32. Eva Pertile, Tomas Dvorsky, Vojtech Vaclavik, Silvie Heviankova. *Life*, 2021; **11(3)**:240.
- 33. Husien S, Labena A, El-Belely EF, Mahmoud Hamada M, Hamouda Asmaa S. *Journal of Environmental*

- Chemical Engineering. 2019; doi: https://doi.org/10.1016/j.jece.2019.103444.
- 34. Martha A. Espinoza-Sancheza, Katiushka Arevalo-Ninoa, Isela Quintero-Zapataa, Ileana Castro-Gonzaleza, Veronica Almaguer-Cantua. *Journal of Environmental Management*, 2019; **251**:109595.
- 35. Aravind J, Sudha G, Kanmani P, Devisri AJ, Dhivyalakshmi S, Raghavprasad M. *Global J. Environ*.
- Sci. Manage., 2015; 1(3):233-244.
- 36. Doenmez G, Aksu Z. *Process Biochemistry*, 2002; **38(5)**:751-762.
- 37. Malkoc E, Nuhoglu Y. Chem. Eng. J., 2006; 119: 61-68
- 38. Hassan Rezaei. *Arabian Journal of Chemistry*, 2016; **9**:846-853.